

Universidade de São Paulo  
Instituto de Física

Explorando correlações iniciais: correlações  
internas de um ambiente e a estatística do calor  
entre sistemas correlacionados

Versão corrigida

Naim Elias Comar

Orientador: Prof. Dr. Gabriel Teixeira Landi

Tese de doutorado apresentada ao Instituto de Física  
como requisito parcial para a obtenção do título de  
Doutor em Ciências.

Banca Examinadora:

Prof. Dr. Gabriel Teixeira Landi - Orientador (Instituto de Física da USP)

Prof. Dr. Barbara Lopes Amaral (Instituto de Física da USP)

Prof. Dr. Fernando Antonio Nazareth Nicacio (Instituto de Física da UFRJ)

Prof. Dr. Frederico Borges de Brito (Instituto de Física de São Carlos/USP)

Prof. Dr. Nadja Kolb Bernardes (Departamento de Física da UFPE)

São Paulo  
2023



**FICHA CATALOGRÁFICA**  
**Preparada pelo Serviço de Biblioteca e Informação**  
**do Instituto de Física da Universidade de São Paulo**

Comar, Naim Elias

Explorando correlações iniciais: correlações internas de um ambiente e a estatística do calor entre sistemas correlacionados. São Paulo, 2023.

Tese (Doutorado) - Universidade de São Paulo. Instituto de Física. Depto. de Física dos Materiais e Mecânica.

Orientador: Prof. Dr. Gabriel Teixeira Landi.

Área de Concentração: Física.

Unitermos: 1. Informação quântica.

USP/IF/SBI-035/2023

University of São Paulo  
Physics Institute

Exploring initial correlations: internal  
environment correlations and the heat statistics  
between correlated systems

Corrected version

Naim Elias Comar

Supervisor: Prof. Dr. Gabriel Teixeira Landi

Thesis submitted to the Physics Institute of the  
University of São Paulo in partial fulfillment of the  
requirements for the degree of Doctor of Science.

Examining Committee:

Prof. Dr. Gabriel Teixeira Landi - Supervisor (Institute of Physics at USP)

Prof. Dr. Bárbara Lopes Amaral (Institute of Physics at USP)

Prof. Dr. Fernando Antonio Nazareth Nicacio (UFRJ Institute of Physics)

Prof. Dr. Frederico Borges de Brito (Physics Institute of São Carlos/USP)

Prof. Dr. Nadja Kolb Bernardes (Department of Physics at UFPE)

São Paulo  
2023



*“The best that most of us can hope to achieve in physics is simply to misunderstand at a deeper level.”*

— Wolfgang Pauli

Aos meus avós Cecília Sousa de Oliveira, Matilde Lizzul Comar, Kalil Abrahão Elias e Alcibiade Valerio Comar, *in memoriam*.

## *Agradecimentos*

Eu gostaria de dar os meus principais agradecimentos à minha mãe Sônia de Sousa Elias e ao meu pai Mário Vito Comar, pelo enorme suporte, amor e por terem feito possível tudo o que alcancei na vida. Um agradecimento muito especial também ao meu orientador, Gabriel Teixeira Landi, por ter me aceitado como seu orientando e ter sido um orientador extremamente atencioso, competente, compreensivo e principalmente muito entusiasmante pelo seu exemplo como cientista, estes quatro anos trabalhando juntos realmente me ensinaram muito sobre a Física em si e sobre a diversão e dificuldades em tentar expandir sua construção.

Quero agradecer às minhas irmãs Suyane Elias Comar e Temily Elias Comar por toda ajuda em momentos difíceis e também pelo companheirismo em todos os momentos. Muitos agradecimentos à Simone França Costa, por ser a melhor companheira que eu poderia imaginar e por ter me dado muito apoio, amor e paciência, principalmente no período de escrita. Obrigado às minhas tias Soila Elias, Solange Elias e Regina Martins pelo carinho de sempre e às minhas primas Simone, Jacqueline e Alexia, assim como suas famílias queridas que tenho no coração.

Quero agradecer muito também aos meus amigos, sem o apoio, alegria, descontração e companhia essencial deles, este trabalho não seria possível. Portanto, queria agradecer a Alexandre Santos, Ana Carolina Rainho, Ana Paula Sachelaride, André Santana de Araújo, Anielton Camargo, Arthur Cazon Vincoletto, Austin Ramsés Nascimento Silva, Bárbara Malheiros, Beatriz Nemezio Rainho, Bonifácio Lima, Brenda Bertotto Malabarba, Bruna Patrocínio, Bruna Shinohara de Mendonça, Caio Medonça Pimentel, Carla Estfani Lopes dos Santos, Catarina Pasta Aydar, Daniel Beltrão, Diego Spiering, Douglas Gomes, Ester Schulz, Fábio Chagas da Silva, Felipe Godoy, Felipe Sampaio, Fernando Augusto Joaquim, Fernando Freire, Flora Collins Benjamim, Francisca Crislane Vieira de Brito, Gabriel Petian, Gabriela de Oliveira, Gizelly Ayumi Yamamoto, Guilherme Coelho, Guilherme Nunes, Hanna Martins Morilhas, Henrique Berquó, Jader Rodrigues, João Carlos Juliano, José Augusto Padovese, José Eduardo Peres y Peres, Kian Shaikhzadeh Santos, Lavínia Helena Aune Ferreira, Léo Bindilatti, Lívia Lopes, Lucas Magno, Lucas Palhano, Lucas Pimenta, Luciano Barcelos, Macus Saad, Marcus Lemes, Moisés Medeiros, Nadia Soraya Linares Zepeda, Navid Portela Salehi, Nícolas Shildberg, Rafaela Geising, Riis Rhavia Assis Bachega, Roberto Baldijão, Roberto Parra, Rodrigo Frausino, Rodrigo Ramos, Rogério Camargo, Romulo Oliveira dos Santos, Rudá Pereira, Silvio Jonas da Silva Junior, Thandryus Augusto, Uric Bonatti Cardoso, Victor, William Santos, Williams Ribeiro, Xavier Júnior e a muitos outros amigos que não escrevi aqui por falta de memória no momento, mas que com certeza também me ajudaram muito neste caminho. Agradeço também às pessoas muito queridas que moraram comigo

---

neste período, Ana Camila Costa Esteves, Ana Flávia de Freitas Gutierrez, Aryella Faé Rabello, Brenda Bertotto Malabarba, Ewerton Igor de França Barros, Lucas Aguiar, Lucas Cagnotto de Moraes, Matheus Henry Przygocki, Melissa de Oliveira Guirelli e Rafael Patrick Marcelino Rodrigues, numa convivência muito amigável e cheia de carinho que me faz me sentir muito em casa. Agradeço à grande professora Néia Barbosa do Grupo de Teatro da Poli e aos amigos que fiz lá: Andrey Luis Barbosa Gomes, Isabela Mosna Esteves, Júlio Barbosa de Moura, Lucas Yohan Salles, Mariana Mendes Lima, Pedro Leite Godinho e muitos outros. Obrigado à professora Bárbara Amaral e aos amigos que fiz em seu grupo de pesquisa, entre eles a Amanda Maria Fonseca, Giulio Camilo e o Gustavo B. Pimentel. E finalmente, os grandes colegas e amigos que fiz no muito simpático e entusiasmante grupo de pesquisa do Gabriel Landi: André Timpanaro, Adalberto Varizi, Alberto Jonatas Bezerra da Silva, Artur Machado Lacerda, Bruno Ortega Goes, Franklin Luis dos Santos Rodrigues, Heitor Peres Casagrande, Lui Zuccherelli de Paula, Marcelo Janovitch B. Pereira, Mariana Afeche Cipolla, Otavio Molitor, Pedro Vinicius Portugal, Rodolfo Reis Soldati e Rodrigo Pereira Silva, pelo apoio que vieram desde a companhia muito amigável e discussões interessantes a assuntos técnicos na pesquisa. Dentre esses amigos do grupo de pesquisa, agradeço também a profunda amizade feita com Gabriel Oliveira Alves, Luis Felipe Santos da Silva e Rolando Ramirez Camasca. Muitos agradecimentos ao professor Manoel Roberto Robilotta pelas profundas e instigantes conversas sobre Física e sobre a vida na carreira acadêmica.

Gostaria de agradecer à Comunidade Bahá'í pela força, guia e apoio. Aos artistas, que me deram mais cor à vida, em específico agradeço à Gal Costa, Jimi Hendrix, Milton Nascimento, Baden Powell, Jorge Ben, Gilberto Gil, Tom Jobim, Cartola, Rita Lee, e muitos outros/as.

Queria também agradecer às funcionárias Rosana Batista Gimenes e Sandra Regina Rodrigues Ribeiro pela constante ajuda no nosso dia-a-dia no DFMT. E à Andrea Wirkus, Cláudia Conde Barioni, Éber de Patto Lima e Marlon Rezende Faria por sempre esclarecer minhas dúvidas na CPG.

O presente trabalho foi realizado com apoio do CNPq, Conselho Nacional de Desenvolvimento Científico e Tecnológico - Brasil.



# *Abstract*

This thesis aims to explore new effects caused by initial correlations in quantum systems, with extensive use of continuous variables methods. Two main projects are highlighted. The first project aims to understand how initial correlations in an environment affect the dynamics of a system interacting with it. We analyze this problem from the point of view of Collisional Models of qubits and bosonic Gaussian states, in which we show how initial correlations between the environmental parts push the system's evolution. As a consequence, the standard Homogenization procedure can be disrupted. In the second project, we use Bayesian Networks to obtain the statistics of general thermodynamic quantities for two initially correlated systems and explore the role of the initial density matrix ambiguity of mixture in these statistics. As an important application, we compute the effects of correlations in the statistics of the heat exchanged. Results for the statistics of the heat are obtained for qubits and, as a novelty, for bosonic Gaussian states.

**Keywords;** Open quantum systems; Quantum Information; Collisional models; Bayesian Networks; Quantum Thermodynamics.

# *Resumo*

Esta tese tem como objetivo explorar novos efeitos causados por correlações iniciais em sistemas quânticos, com grande uso de métodos de variáveis contínuas. Dois projetos principais são destacados. O primeiro projeto visa entender como a presença de correlações iniciais em um ambiente afeta a dinâmica de um sistema que interage com ele. Analisamos este problema do ponto de vista dos Modelos Colisionais de qubits e estados Gaussianos bosônicos, nos quais mostramos como as correlações iniciais entre as partes do ambiente direcionam a evolução do sistema. Como consequência, o procedimento conhecido de homogeneização pode ser corrompido. No segundo projeto, fazemos uso de Redes Bayesianas para obter as estatísticas de grandezas termodinâmicas gerais para dois sistemas inicialmente correlacionados e exploramos o papel da ambigüidade de mistura da matriz densidade inicial nestas estatísticas. Adicionalmente, fizemos uma aplicação importante, a de calcular efeitos das correlações nas estatísticas do calor trocado entre dois sistemas. Os resultados para as estatísticas do calor são obtidos para qubits e, como novidade, para estados Gaussianos bosônicos.

**Palavras-chave:** Sistemas quânticos abertos; Informação Quântica; Modelos colisionais; Redes Bayesianas; Termodinâmica Quântica.

# Contents

<b>1</b>	<b>Introduction</b>	<b>1</b>
1.1	Collisional model with initially correlated ancillae . . . . .	2
1.2	Statistics of thermodynamic quantities using Bayesian Networks . . . . .	3
1.3	Structure of the thesis . . . . .	5
<b>I</b>	<b>Background</b>	<b>7</b>
<b>2</b>	<b>Open Quantum Systems and Collisional Models</b>	<b>8</b>
2.1	The density matrix . . . . .	9
2.2	Dynamics . . . . .	11
2.2.1	Closed systems - Unitary operators . . . . .	11
2.2.2	Open systems - Kraus matrices . . . . .	12
2.3	Collisional Models . . . . .	14
2.3.1	General case (correlated ancillae) . . . . .	14
2.3.2	Markovian case . . . . .	17
2.3.3	Qubit example, thermalizing machines . . . . .	18
2.3.4	steady states . . . . .	21
2.3.5	SWAP and Partial SWAP . . . . .	22
2.3.6	Homogenization . . . . .	23
2.3.7	Physical implementations of CMs . . . . .	26
<b>3</b>	<b>Quantum Information and Bayesian Networks</b>	<b>30</b>
3.1	Generalized measurements . . . . .	30
3.2	Entropy . . . . .	31
3.2.1	The Shannon Entropy . . . . .	31
3.2.2	The von Neumann Entropy . . . . .	33
3.3	Mutual Information and Correlations . . . . .	35
3.3.1	Relative Entropy . . . . .	35
3.3.2	Mutual Information . . . . .	35
3.3.3	Entanglement . . . . .	37
3.3.4	Quantum discord . . . . .	38
3.4	Bayesian Networks . . . . .	41
3.4.1	Definition and examples . . . . .	42
3.4.2	Dynamical BNs for quantum systems (QBNs) . . . . .	45

<b>4</b>	<b>Continuous Variables Framework</b>	<b>47</b>
4.1	Bosonic modes . . . . .	47
4.1.1	Canonical vectors . . . . .	48
4.1.2	CCRs and the symplectic form . . . . .	49
4.2	Second quantization and the Fock space . . . . .	49
4.3	Displacement operator and coherent states . . . . .	51
4.4	Characteristic function . . . . .	55
4.5	Quasi-probability distributions . . . . .	56
4.5.1	Wigner function . . . . .	57
4.5.2	The s-ordered quasi-probability distribution . . . . .	57
4.5.3	Glauber-Sudarshan P-function . . . . .	58
4.5.4	Husimi Q-function . . . . .	58
4.6	Gaussian states . . . . .	59
4.6.1	Definitions . . . . .	59
4.6.2	Bona-fide conditions for covariance matrices . . . . .	61
4.6.3	Dynamics of canonical operators and statistical moments . . . . .	61
4.6.4	Symplectic operators . . . . .	64
4.6.5	Covariance matrix parametrization . . . . .	66
4.6.6	Characteristic function of Gaussian states . . . . .	67
4.7	Gaussian operations . . . . .	67
4.7.1	Tensor product . . . . .	68
4.7.2	Unitary operations . . . . .	69
4.7.3	Partial trace . . . . .	70
4.7.4	Gaussian CPTP-maps . . . . .	72
4.7.5	Applying a channel in only one partition . . . . .	74
4.7.6	One-mode Gaussian channels . . . . .	75
4.8	Entropic quantities for Gaussian states . . . . .	76
4.8.1	Diagonalization of Gaussian states to thermal states of free modes . . . . .	76
4.8.2	Entropy of a Gaussian state . . . . .	77
4.8.3	Quantum discord between two Gaussian bosonic modes . . . . .	78
<b>II</b>	<b>Main projects</b>	<b>87</b>
<b>5</b>	<b>Initially Correlated Ancillae - Minimal Qubit Model CM</b>	<b>88</b>
5.1	Preparing the correlated ancillae environment . . . . .	89
5.1.1	Hamiltonian graph states . . . . .	89
5.1.2	Properties of the initial ancillae and their correlations . . . . .	92
5.2	Breaking Homogenization by initial correlations . . . . .	96
<b>6</b>	<b>Initially Correlated Ancillae - Gaussian States CM</b>	<b>102</b>
6.1	Preliminaries . . . . .	103
6.1.1	The bosonic CM evolution . . . . .	103
6.1.2	The Beam Splitter interaction . . . . .	105
6.1.3	Correlations block-matrices . . . . .	106
6.2	Main results . . . . .	107

6.2.1	Correlated nearest-neighbors . . . . .	107
6.2.2	General case . . . . .	112
6.2.3	Distance dependent correlations . . . . .	114
6.2.4	Ancillae evolution . . . . .	116
6.3	Constructing initially correlated ancillae from H-Graphs . . . . .	118
6.3.1	Constructing covariance matrix elements . . . . .	119
6.3.2	Constructing desired correlations from choosing the cyclic graph . . . . .	122
6.3.3	Application to the case of the Algebraically decaying correlation . . . . .	124
6.3.4	Analysing $\xi_d^{(p)}$ . . . . .	126
<b>7</b>	<b>Obtaining Observable Variations Using QBNs</b>	<b>130</b>
7.1	General results . . . . .	131
7.1.1	Statement of the problem . . . . .	131
7.1.2	Characteristic function of the change probability distribution . . . . .	134
7.1.3	Statistical moments of the change probability distribution . . . . .	135
7.1.4	Comparison with TPM . . . . .	136
7.2	Application to qubits . . . . .	137
7.2.1	Setup and statistical moments . . . . .	138
7.2.2	Obtaining the probability distribution . . . . .	140
7.3	Dependence on the ambiguity of mixtures . . . . .	142
7.3.1	The variance for the qubits case . . . . .	143
7.4	Heat exchanged between bosonic modes . . . . .	145
7.4.1	Statement of the problem . . . . .	145
7.4.2	Initial states in the Simon form . . . . .	147
7.4.3	The heat average and correlations evolution . . . . .	149
7.4.4	The evolution of the heat variance and correlations . . . . .	151
7.4.5	Profile of correlations in the initial state . . . . .	152
7.4.6	Attempts to use coherent states ensembles . . . . .	154
<b>8</b>	<b>Conclusions and further perspectives</b>	<b>157</b>
<b>A</b>	<b>Some proofs and definitions in Open Quantum Systems and Collisional Models</b>	<b>163</b>
A.1	Some properties of purity . . . . .	163
A.2	The partial trace . . . . .	164
A.3	Interaction Picture . . . . .	165
A.4	Thermal states . . . . .	167
A.5	Proof of $\rho_{S,\text{rest}}^n \rightarrow 0$ and $\rho_{A,\text{rest}}^n \rightarrow 0$ . . . . .	168
<b>B</b>	<b>Some proofs and definitions in Quantum Information</b>	<b>172</b>
B.1	Some useful equations . . . . .	172
B.2	Proof of Eq. (3.10) . . . . .	173
<b>C</b>	<b>Some proofs and definitions in Continuous Variables</b>	<b>174</b>
C.1	Notation for vectors and matrices of operators . . . . .	174
C.2	The direct sum . . . . .	175
C.3	General Gaussian integral . . . . .	175

C.4	Proof of Eq. (4.18)	175
C.5	Proof of Eq. (4.26)	176
C.6	Proof of the formula of the coherent state expanded in the Fock basis (Eq. (4.27))	177
C.7	Completeness relation for coherent states	178
C.8	Proof of the Fourier-Weyl relation	178
C.9	Proof of Eq. (4.42)	180
C.10	Proof of Eq. (4.47)	180
C.11	Proof of Eq. (4.49)	181
C.12	Proof of the Robertson-Schrödinger relation (Eq. (4.58))	182
C.13	Density matrix and covariance matrix of free Gaussian bosonic modes	183
C.14	Obtaining symplectic eigenvalues	185
C.15	Justifying the existence of a Hamiltonian matrix corresponding to any symplectic matrix	187
C.16	Proof for the parametrization of Eq. (4.77)	188
C.17	Proof that the commutator between any second order operators is a second order operator	190
C.18	Proof of Eq. (4.114)	191
C.19	Proof of Simon normal form statement	192
C.20	Proof that $S(\mathcal{E}( \alpha\rangle\langle\alpha )) = S(\mathcal{E}( 0\rangle\langle 0 ))$ for any Gaussian channel $\mathcal{E}$	192
C.21	Computations to obtain Eq. (4.129)	193
C.22	Two-mode squeezed thermal state, EPR state, and friends	193
	C.22.1 Two-mode squeezed thermal state	194
	C.22.2 EPR state	195
<b>D</b>	<b>Some proofs and definitions in Obtaining Observables Variations Using QBNs</b>	<b>196</b>
D.1	Proof of Eq. (7.20)	196
D.2	Matrices for generating ensembles in Subsection 7.3.1	198
D.3	The QBN generated by post-measurements	198

# List of Figures

2.1	Schematic of collisions, where the system $S$ is interacting individually with the $k$ -th ancilla during a time $\tau$ going to interact with the next ancilla also during a time $\tau$ . . . . .	15
2.2	Schematic of homogenization. From left to right, the system $S$ interacts with the ancillae at time $0 < t < \tau$ , $\tau < t < 2\tau$ , $2\tau < t < 3\tau$ and $(n - 1)\tau < t < n\tau$ , respectively. The color changes on the system represent the different states it passes through until it gets very similar to the ancillae and the whole system becomes homogeneous. . . . .	24
2.3	Micromaser setup: An atomic beam oven emits Rydberg atoms which pass through a velocity selector tuning the flux of atoms so that each atom passes one at a time through the cavity containing electromagnetic fields. (This figure was taken from Ref. [21].) . . . . .	27
3.1	Three random variables $A$ , $B$ and $C$ disposed in a causal order. . . . .	42
3.2	Example of a directed graph representing relations of causality between random variables. . . . .	44
3.3	A directed graph within an internal cycle, provoking a causal loop between the random variables $A$ , $B$ , $C$ , and $D$ . . . . .	44
3.4	BN for the dynamical evolution of a quantum system. The upper line describes the global state evolution (which we often call <i>hidden layer</i> ) and the dashed arrows indicate the causal dependence of the reduced states on the global states at each instant $t_k$ . . . . .	46
4.1	<i>State decomposition</i> : Depicted in black lines, the state $\hat{\rho}_{AB}$ can be decomposed as an initial state $\hat{\rho}_{aB}$ in which the first mode (in part $A$ ) passes trough a quantum channel $\mathcal{E}$ . <i>Remote preparation</i> : Depicted in red symbols, the effect of the generalized measurement $\mathcal{M}_B$ in $\hat{\rho}_{aB}$ creates the ensemble $\mathcal{P} = \{p_k, \hat{\rho}_{a k}\}_k$ of states in $A$ which, passing through the quantum channel, becomes the ensemble $\mathcal{A} = \{p_k, \hat{\rho}_{a' k}\}_k$ . The ensemble $\mathcal{A}$ is also generated by the backaction, in $A$ , of the generalized measurement $\mathcal{M}_B$ in $\hat{\rho}_{AB}$ . (This figure was taken from Ref. [131] with modifications.) . . . . .	81

4.2	<p><i>State decomposition:</i> Depicted in black lines, the state <math>\hat{\rho}_{AB}</math> can be decomposed as an initial state <math>\hat{\rho}_{aB}</math> in which the first mode (in part <math>A</math>) passes through an inverse squeezing operator <math>\hat{S}^{-1}(r)</math>, a quantum channel <math>\mathcal{E}</math> and a squeezing operator <math>\hat{S}(\xi)</math>. <i>Remote preparation:</i> Depicted in red symbols, the effect of the generalized measurement <math>\mathcal{M}_B</math> in <math>\hat{\rho}_{aB}</math> creates the ensemble <math>\mathcal{P} = \{p_k, \hat{\rho}_{a k}\}_k</math> of states in <math>A</math> which, passing through the quantum channel and squeezing operators, becomes the ensemble <math>\mathcal{A} = \{p_k, \hat{\rho}_{a' k}\}_k</math>. The ensemble <math>\mathcal{A}</math> is also generated by the backaction, in <math>A</math>, of the generalized measurement <math>\mathcal{M}_B</math> in <math>\hat{\rho}_{AB}</math>. (This figure was taken from Ref. [131] with modifications.) . . . . .</p>	83
4.3	<p>Plot of <math>c_+</math> and <math>c_-</math> points, for different fixed <math>a</math> and <math>b</math> of states in the Simon normal form generated <math>2 \times 10^5</math> times by random choices of <math>r</math> and <math>\tau</math>, according to the parametrization of Eqs. (4.131), (4.132), (4.133) and (4.134). The pink curves delimit the bona-fide region of states. . . . .</p>	86
5.1	<p>Cyclic graph with 9 ancillae (at the vertices), each interacting only with the first and second neighbors (interactions represented by the edges). . . . .</p>	91
5.2	<p>Population of the excited state of <math>\rho_A</math> versus total number of ancillae <math>N_A</math>, for different values of <math>k</math>. . . . .</p>	94
5.3	<p>Population of <math>\rho_A</math> versus values of <math>k</math>, for <math>N_A = 11</math>. . . . .</p>	94
5.4	<p>Mutual information between neighbors versus distance between neighbors, for <math>N_A = 7</math> and different values of <math>k</math>. . . . .</p>	95
5.5	<p>Mutual information between first neighbors versus <math>k</math>, for different values of <math>N_A</math>. For larger values of <math>N_A</math>, the plots lose resolution since they are computationally more demanding. . . . .</p>	96
5.6	<p>Plots of population of <math>\rho_S</math> versus number of steps for ancillae prepared with the NN1 cyclic graph with <math>N_A = 17</math>, for different values of <math>k</math>. Each line corresponds to a different value of <math>g</math> strength of the partial SWAP interaction, from top to bottom <math>g = 0.5</math>, <math>g = 1.0</math>, and <math>g = 1.5</math>. The red dashed lines indicate the value of the population of the respective <math>\rho_A</math>, which is the value in which the system's population converges if homogenization happens. . . . .</p>	99
5.7	<p>Plots of population of <math>\rho_S</math> versus number of steps for ancillae prepared with the NN2 cyclic graph with <math>N_A = 17</math>, for different values of <math>k</math>. Each line corresponds to a different value of <math>g</math> strength of the partial SWAP interaction, from top to bottom <math>g = 0.5</math>, <math>g = 1.0</math>, and <math>g = 1.5</math>. The red dashed lines indicate the value of the respective <math>\rho_A</math> population, which is the value in which the system's population converges if homogenization happens. . . . .</p>	100



5.8	Plots of population of $\rho_S$ versus number of steps for ancillae prepared with the NN3 cyclic graph with $N_A = 17$ , for different values of $k$ . Each line corresponds to a different value of $g$ strength of the partial SWAP interaction, from top to bottom $g = 0.5$ , $g = 1.0$ , and $g = 1.5$ . The red dashed lines indicate the value of the respective $\rho_A$ population, which is the value in which the system's population converges if homogenization happens. . . . .	101
6.1	Values of $\frac{\cos(g\tau)K}{K-\cos(g\tau)}$ versus $g\tau$ for different values of $K$ in the interval $g\tau \in [0, 2\pi]$ . . . . .	115
6.2	$\Gamma_n(K, gt)$ versus $n$ for different values of $K$ , for $g = 0.8$ and $t = 1$ fixed.	119
6.3	$\Gamma_n(K, gt)$ versus $n$ for different values of $g$ , for $K = 2$ and $t = 1$ fixed.	120
6.4	Example of a graph with ancillae in the vertices and the thickness of the edges between them represent the strength of the correlations (in this case the correlations are weaker for more distant ancillae), given by the adjacency matrix. . . . .	120
6.5	Correlations ( $\xi_d^{(q)}$ ) versus $d$ : distance of the neighbor ancilla from the first ancilla. The blue line is the correlation given by Eq. (6.66) mirrored from $n/2$ , while the red line is the correlation of the graph state generated by our method. The parameters are $k = 1.0$ , $\xi_0^{(q)} = 1.0$ and $K = 1.05$ , with $n$ indicated above the plots. . . . .	126
6.6	Correlations ( $\xi_d^{(q)}$ ) versus $d$ : distance of the neighbor ancilla from the first ancilla. The blue line is the correlation given by Eq. (6.66) mirrored from $n/2$ , while the red line is the correlation of the graph state generated by our method. The parameters are $k = 1.0$ , $\xi_0^{(q)} = 1.0$ and $K = 2.0$ , with $n$ indicated above the plots. . . . .	127
6.7	Correlations ( $\xi_d^{(q)}$ ) versus $d$ : distance of the neighbor ancilla from the first ancilla. The blue line is the correlation given by Eq. (6.66) mirrored from $n/2$ , while the red line is the correlation of the graph state generated by our method. The parameters are $k = 1.0$ , $\xi_0^{(q)} = 1.0$ and $K = 5.0$ , with $n$ indicated above the plots. . . . .	127
6.8	Correlations ( $\xi_d^{(q)}$ ) versus $d$ : distance of the neighbor ancilla from the first ancilla. The blue line is the correlation given by Eq. (6.66) mirrored from $n/2$ , while the red line is the correlation of the graph state generated by our method. The parameters are $k = 1.0$ , $\xi_0^{(q)} = 1.0$ and $n = 100$ , with $K$ indicated above the plots. . . . .	128
7.1	Heat (in unites of $\omega_0$ )/ Variance of the heat (in unites of $\omega_0^2$ ) versus $t$ . The blue lines represent the heat received by $A$ and the blue dashed lines represent the variance of the heat when the qubits are initially correlated. The red lines represent the heat received by $A$ and the red dashed lines represent the variance of the heat when the qubits are initially uncorrelated. The parameters are $g = 1$ , $\beta_A = 2/\omega_0$ and $\beta_B = 1/\omega_0$ . Each plot has a different value of $\alpha$ . In the first line we have, from left to right, $\text{Im}(\alpha) = -\aleph$ and $\text{Im}(\alpha) = +\aleph$ , and in the second line $\text{Im}(\alpha) = -1/20$ and $\text{Im}(\alpha) = +1/20$ . . . . .	141

7.2	$P(\mathcal{Q}_A)$ versus $t$ , for different values of $\mathcal{Q}_A$ , computed numerically with the inverse Fourier transform of the characteristic function of Eq. (7.28) (green full line) and for different values of $\mathcal{Q}_A$ , using Eqs. (7.29), (7.30), and (7.31) from Ref. [48] (dashed black line). The initial joint state is prepared at $\rho_{AB}(0)$ of Eq. (7.22) with $\beta_A = 2/\omega_0$ , $\beta_B = 1/\omega_0$ , $\alpha = -i \frac{e^{-\omega_0(\beta_A + \beta_B)/2}}{(1 + e^{-\omega_0\beta_A})(1 + e^{-\omega_0\beta_B})}$ and we have $g = 1$ . . . . .	142
7.3	Variance of $\mathcal{Q}_A$ (in units of $\omega_0^2$ ) versus $t$ . The green curves represent the variance computed with the ensembles generated by the respective matrix $M$ (see Appendix D) with the use of Eq. (7.34) while the gray curves represent the variance computed in an eigen-ensemble. The initial state $\rho_{AB}(0)$ is given by Eq. (7.22) with $\beta_A = 2/\omega_0$ , $\beta_B = 1/\omega_0$ and $\alpha = -i \exp[-\omega_0(\beta_A + \beta_B)] / ((1 + e^{-\omega\beta_A})(1 + e^{-\omega\beta_B}))$ . For the unitary $U(g, t)$ we have $g = 1$ . . . . .	146
7.4	Heat average in units of $\omega$ (red), mutual information (black), quantum discord (blue), and classical correlations (yellow) versus time of interaction. Each plot represents a different initial state with different values of $c_+$ and $c_-$ described above each plot, all the initial states are in the Simon form with $a = 1.3$ , $b = 2.0$ . . . . .	151
7.5	Heat variance in units of $\omega^2$ (purple), mutual information (black), quantum discord (blue), and classical correlations (yellow) versus time of interaction. Each plot represents a different initial state, all the initial states are in the Simon form with $a = 1.3$ , $b = 2.0$ , and the correlation terms are described above each plot. (For the case of $c_+ = c_- = 0$ , we amplified the correlation values five times for a visible comparison in the plot.) . . . . .	153
7.6	From left to right: mutual information, quantum discord, and classical information content as a function of $c_+$ (horizontal axis) and $c_-$ (vertical axis), for Simon states prepared with $a = 2$ and $b = 10$ . . . . .	154

# Chapter 1

## Introduction

By the end of the 20th century, the merging of two important fields of knowledge, namely, Information Theory and Quantum Theory, set the formulation of the Quantum Information Theory [1–4]. This formulation was the result of the effort of enlightening questionings concerning the foundations of Quantum Theory as well to the use of these clarifications for the flowering of ideas to new technologies. This movement is often called the *Second Quantum Revolution* [5, 6], and the technologies developed include Quantum Computing [1, 7], Quantum Cryptography [1], Quantum Simulation, Quantum Sensing and Quantum Metrology [8] which caused enormous attention to technology companies and hence even more research interest.

At the heart of such revolution is the concept of *quantum correlations* whose primordial research can be traced to 1935 with the work of Einstein, Podolsky, and Rosen (EPR) [9], Erwin Schrödinger [10] and debates with Niels Bohr [11]. The controversy was mainly about if the predictions of correlations pointed by EPR in Quantum Theory could cause it to be an incomplete theory, in the sense to be a theory with the necessity of additional *hidden variables* locally generated in a common past and without further non-local “spooky” interactions to explain such correlations. Probably the first step to solve this controversy was taken by John Bell in 1964 [12] by proving that, *only if* a certain average of observable respect a set of inequalities (now called Bell inequalities), then the correlations described by EPR could be caused by local hidden variables. It happens that Quantum Theory predicts such violation and this gave rise to the concept of a new kind of fully quantum (in the

sense of without classical analog) correlations, now called *entanglement*, which could not be explained by local hidden variables. These events marked the beginning of what more recently caused the Second Quantum Revolution. Due to the importance of these discoveries nowadays, the most recent Nobel Prize in Physics was awarded to Alain Aspect, John F. Clauser, and Anton Zeilinger due to their pioneering work on violating experimentally Bell's inequalities [13]. Therefore, quantum correlations are recently between the most prominent subjects in pure and applied physics, and exploring new effects concerning them can blossom into new ideas and applications.

Inside this broader context, this thesis has the objective of searching for new effects caused by quantum correlations in cases where systems start their interactions already correlated. We use mainly the tools of quantum continuous variables [14–16] to investigate the effects of initial correlations between quantum systems in their dynamical evolution and thermodynamic quantities. Our work can be stated in two main projects, the first one is concerned with a system evolution interacting with an initially correlated environment, being more concerned with the dynamics of the system. The second project has the main goal of obtaining the statistics of thermodynamic quantities of two initially correlated systems, especially their heat distribution, using the framework of Bayesian Networks. The two projects can be described as follows.

## 1.1 Collisional model with initially correlated ancillae

This first project aims to explore an almost uncharted question of relaxation towards equilibrium: how do initial correlations between the environmental parts affect the system equilibration? The analysis towards the answer in general can easily become intractable as the size of the environment becomes large, also general and standard bath models can present additional features that can obscure the effects caused by the initial correlations. For these reasons, we chose to focus on the so-called collisional models [17–21], in which we assume total control over environment features since here we suppose that the bath is composed of large number of smaller sub-

units (the ancillae) that interact individually with the system one at a time, each of these interactions is called a *collision*. This way, we are able to obtain manageable answers to the problem by extending methods already explored.

The effect of initial correlations between parts of the environment on the system evolution is, as already said, the main inquiry of this project, and it can be understood as the following analogy suggests. Suppose a group of workers (ancillae) want to convince a boss (system) that he/she must buy them new tools, but each of them enters and argues with the boss alone at his office (interact individually and one at a time). If the workers talked to each other before going to the boss' office and have some plan or information shared (correlations), then the result of the boss' mind (final state of the system) will be different than if they had not talked to each other.

Our results reveal an unfamiliar phenomenon of pushing caused by the initial correlations between the environmental parts. We obtain these results numerically for the case where the system and ancillae are qubits and analytically, which is a more complete description, for the case where the system and ancillae are bosonic modes. These last more detailed results were possible due to the use of continuous variables methods. As a comparison to well-known results, we make a contrast with the results of [19], where for a certain kind of interaction and initially identical ancillae, the whole system, and ancillae become a set of identical parts, this is the so-called *homogenization*. We show that homogenization can become impossible if the ancillae are initially correlated.

## 1.2 Statistics of thermodynamic quantities using Bayesian Networks

With the Second Quantum Revolution, increasing attention has been brought to the growing field of Quantum Thermodynamics [22–25] from reasons that range from extending the Thermodynamic laws to the quantum domain, understanding fundamental relations between thermodynamics and information [26–28] to studies of the enhancement of the efficiency of quantum thermal machines using quantum features [29–32]. However, the description of the statistics of thermodynamic quantities,

such as heat and work is often made with the use of the Two-Point Measurement (TPM) procedure [33–35] which spoils the coherence of the initial state and consequently the effect of quantum correlations due to the supposition of measurements. Alternatives without this undesired feature involve work operator definitions [36, 37], which cannot hold fluctuation relations [34, 35, 38–40], and quasi-probabilities [41, 42] which cannot be described by a quantum measurement. The objective of this second project is to fulfill this gap of constructing statistics of thermodynamic quantities that fully accounts for initial quantum correlations and coherence, focusing primarily on the specific case of obtaining the probability distribution for the heat exchange between two initially correlated systems interacting as a closed system.

By making use of the concept of Bayesian Networks (BNs) [43–47] in the context of quantum theory, Ref. [48] successfully described fluctuation relations fully considering the effect of initial correlations and coherence. Additionally, this framework can be described by quantum measurements protocols [49]. Therefore, we chose the BN framework to obtain our statistics for thermodynamic quantities. The BN concept has wide applications in statistics, engineering, and mainly in artificial intelligence. It consists in a method that infers the probabilities of the evolution of the system from conditional distributions of the previous state of the system, supposing a causal relation from this past.

We follow the construction initiated in Ref. [48], focusing on deepening our understanding of the statistics of thermodynamic quantities. We obtain general formulae for the characteristic function (and consequently, the statistical moments) for the probability distribution of the *change* (or variation) of an observable during the evolution of the system, such changes of observable can represent thermodynamic quantities, such as heat and work. Our results reveal a dependence of the probability distribution on the initial density matrix choice of an ensemble to represent it. The consequence of the different choices of ensembles turns out to be one of our main attentions due to the different interpretations it can result.

As our main goal and application, we apply this framework to understand deeply the statistics of heat exchanged between two systems and the consequences of initial

correlations in this exchange. As a well-known effect caused by initial correlations, we recover the heat flow inversion [50–53], which was obtained experimentally for the interaction of two qubits [54]. And we propose conditions for such inversion to happen in the case of two bosonic modes interacting. Due to the unexplored character of the subject, we study the variance of the heat probability distribution and how it behaves with the presence of correlations. This is done numerically for the case of two qubits, and analytically for the case of two bosonic modes. Interesting features are raised due to the different choices of ensembles to be made in continuous variables for bosonic modes, such as the use of quasi-probabilities.

### 1.3 Structure of the thesis

This thesis will be organized as follows. It is divided into two parts, Part I (chapters 2 to 4) resumes the background used to obtain our results, there is no original result among the chapters of this part. In Part II (chapters 5 to 7) we have our main projects and the results contained in these chapters are original. Chapters 5 and 6 refer to the first project of the thesis while chapter 7 refers to the second project.

Chapter 2 contains a brief resume of the Open Quantum Systems paradigm with the essential parts needed to construct our work and we introduce and define the concept of collisional models as well as the notion of homogenization. In Chapter 3 we present a resume of the parts concerning Quantum Information that we shall use. We also define in this chapter precisely what we denominate as correlations and quantum correlations, introducing the concept of *Quantum Discord*, for further use, being a broader concept of quantum correlations than the aforementioned entanglement. The last section of this chapter will make a brief presentation of BNs and how it is applied to describe the evolution of quantum systems.

In Chapter 4 we present the framework of continuous variables. This is an extensive chapter since it permits us to obtain analytical results especially when dealing with Gaussian states, so a considerable part of the text will be restrained to a careful construction and explanation of such methods. This makes a large part of our results to be possibly applicable in the realm of bosonic states and Quantum

Optics [55, 56].

In Chapter 5 we present the structure and results for the simulations of our qubit minimal collisional model with initially correlated ancillae. Chapter 6 is devoted to the structure and analytical results of our collisional model with initially correlated ancillae, where the state and ancillae are bosonic modes. The last section of this chapter will expose our construction of correlated environments made of bosonic Gaussian states with the use of graph states.

Chapter 7 will develop briefly the concept of BN, then apply it to find the statistics for the changes observable for bipartite initially correlated systems in very general terms. Here we expose general results about the statistics of such changes as well as applications to the case of two qubits initially correlated. Finally, we again use the general results to obtain conclusions for the heat probability distribution between two bosonic modes, focusing on the relations between the first moments of such distribution and the quantum correlations between the modes.

Finally, Chapter 8 is devoted to the final remarks and possible future works concerning the thesis results.



# Part I

## Background

## Chapter 2

# Open Quantum Systems and Collisional Models

In the first two sections of this chapter we shall give a short introduction to the paradigm of Open Quantum Systems [57–59] which deals successfully with quantum phenomena, maintaining untouched all Quantum Mechanics postulates, but adding the concept of open evolution in a similar way to the Stochastic Physics [60–62]. This framework had its foundations constructed by von Neumann, Kraus, Lindblad, and many others, generally obtaining the system’s evolution by considering finite time steps, given by Kraus operations, or solving Lindblad Master Equations (analogously as the classical Master Equations case) to obtain continuum time evolution. We shall focus here on the first approach which is the methods used in the present work.

In this paradigm, commonly a bath is decomposed in a continuum of quantum harmonic modes, these modes interact with the system via a coupling that is appropriate to the physical phenomenon in description. Finding the dynamics of the system under this interaction with these baths is normally a daunting problem and most solutions involve Markovian (past independent) approximations. As a less orthodox approach, Collisional Models (CMs) [20, 21, 63] (also dubbed as “Collision Models” and “repeated interaction schemes”) suppose that the bath is composed of a large number of smaller subunits (the ancillae) that interact individually with the system one at a time. In the present quantum formulation, these models were first proposed by Jayaseetha Rau in 1963 [17], which was inspired by Boltzmann’s

*Stosszahlansatz* molecular chaos hypothesis [62, 64].

Since then, CMs have become very attractive for a vast range of applications, ranging from weak measurements to a very satisfactory description of the micromaser [65–70]. At the beginning of the 21st century, the interest in quantum computation brought attention to the implementation of collisional models with interactions involving two qubits, which resulted in the concept of *homogenization* [18, 19], a well-explored concept in this thesis, as well as studies of using CMs to describe the decoherence of qubits [71]. In the past decade, CMs have a major role in studies of non-Markovian dynamics and Quantum Thermodynamics [63, 72–88]. In the last section of this chapter, we shall introduce the framework of CMs, a few examples of models and physical implementations in order to prepare for the description of the first project of this thesis.

## 2.1 The density matrix

Open quantum systems, as the name suggests, deal with systems that interact with an environment capable to exchange energy and information. Although the closed quantum systems formalism could encompass systems that exchange energy (with a time-dependent Hamiltonian), it would never be capable of describing systems that dissipate information. The reason is that all the closed quantum system formalism only deals with the hypothesis that we know in which quantum state the system is and its evolution will be deterministic according to Schrödinger’s Equation. We must have a formalism that takes into account the lack of information about which quantum state the system is and obtain an equation where the evolution is not necessarily deterministic.

In classical stochastic processes or statistical mechanics, when we don’t know the state of the system, we can associate each classical state (for instance a point  $(x, p)$  on the phase space) with a probability  $P(x, p)$  that the system is in this state. In the quantum case, the same can be done for a set of quantum states  $\{|\psi_k\rangle\}$  in a Hilbert space  $\mathcal{H}$ , assigning a probability  $P_k$  for each  $|\psi_k\rangle$ . The difference exists when we compute the average of an observable  $A$ . To accomplish this we must take

into consideration the quantum and classical uncertainties (“classical uncertainties” here refers to the use of probabilities of preparing each quantum state) and we have to make a classical average over quantum averages

$$\langle A \rangle = \sum_k P_k \langle \psi_k | A | \psi_k \rangle. \quad (2.1)$$

In order to compress quantum and classical information into a single object describing the state, von Neumann introduced [89] the **density matrix**

$$\rho = \sum_k P_k |\psi_k\rangle \langle \psi_k|, \quad (2.2)$$

and with this definition, we may write averages like Eq. (2.1) as

$$\langle A \rangle = \sum_k P_k \langle \psi_k | A | \psi_k \rangle = \text{Tr}(A\rho). \quad (2.3)$$

There are some requirements that a generic operator must satisfy to be capable of representing a physical system. First, we must notice that, due to the normalization of the kets  $|\psi_k\rangle$  and probabilities  $\sum_k P_k = 1$ , we must have a density matrix normalization  $\text{Tr}(\rho) = 1$ . And second, for any generic ket  $|\phi\rangle$ , we must have  $\langle \phi | \rho | \phi \rangle = \sum_k P_k |\langle \phi | \psi_k \rangle|^2 \geq 0$ , which states that  $\rho$  must be a *positive semi-definite* matrix (in symbols  $\rho \geq 0$ ). So, for an operator to be able to describe a physical density matrix, it *must* satisfy

$$\text{Positive semi-definite: } \boxed{\rho \geq 0}, \text{ and} \quad (2.4)$$

$$\text{Normalization: } \boxed{\text{Tr}(\rho) = 1}. \quad (2.5)$$

Also, it is important to remember that  $\rho$  *must be a hermitian operator*, and this is covered by the positive semi-definite condition (all positive semi-definite operators are hermitian).

We shall often refer to the density matrix  $\rho$  as “the state” of a given system since it serves as a “distribution” of quantum states. The non-diagonal terms of the density matrix are often called *coherence* terms. These terms are dependent on

the basis we choose to represent the density matrix and represent the superposition terms in the respective basis.

When one has certainty about the state of the system, then we say that the state is *pure*. This happens if for some  $j$ ,  $P_j = 1$  and  $P_k = 0$ ,  $\forall k \neq j$  in Eq. (2.2), which implies that  $\rho = |\psi\rangle\langle\psi|$ , for some state  $|\psi\rangle$  (we omit the  $j$  here just for convenience). In this case, the density matrix is equivalent to the ket  $|\psi\rangle$ , and there is no lack of information about the system. But it is vital to remember that, in general terms, Eq. (2.2) cannot be factorized as a pure state, i.e., we really have a lack of information about which quantum state the system was prepared, and for this case we say that the state is *mixed*.

To show if a density matrix can be parametrized as a pure state or not is, in general not an easy task. To this end, one may define the *purity* of the state  $\rho$  as

$$\mathcal{P}(\rho) = \text{Tr}(\rho^2). \quad (2.6)$$

It can be shown (see appendix A) that the purity of a state  $\rho$  is 1 *if and only if*  $\rho$  is a pure state and also that  $1/d \leq \mathcal{P}(\rho) \leq 1$  for any  $\rho$ , where  $d$  is the dimension of the Hilbert space of the state and  $0 \leq \mathcal{P}(\rho) \leq 1$  for infinite dimensional Hilbert spaces. Consequently, purity is the decisive witness which points out if a state is pure or not.

## 2.2 Dynamics

### 2.2.1 Closed systems - Unitary operators

As we are used to, the dynamics for a closed pure system  $|\psi(t)\rangle$  with a Hamiltonian  $H$  in Quantum Mechanics is given by the Schrödinger Equation (setting  $\hbar \rightarrow 1$  throughout)

$$\boxed{i \frac{\partial |\psi(t)\rangle}{\partial t} = H |\psi(t)\rangle}, \quad (2.7)$$

which has the following solution

$$|\psi(t)\rangle = U(t - t_0) |\psi(t_0)\rangle, \quad (2.8)$$

where, for time-independent Hamiltonians, we have the unitary operator

$$U(t - t_0) = e^{-iH(t-t_0)}, \quad (2.9)$$

and  $|\psi(t_0)\rangle$  is the initial system state.

We may notice that the evolution of any system initially in  $|\psi_k(t_0)\rangle$  also evolves as  $|\psi_k(t)\rangle = U(t-t_0) |\psi_k(t_0)\rangle$ . So for a density matrix like in Eq. (2.2), the evolution is

$$\rho(t) = U(t - t_0)\rho(t_0)U^\dagger(t - t_0), \quad (2.10)$$

for an initial density matrix  $\rho(t_0) = \sum_k P_k |\psi_k(t_0)\rangle \langle \psi_k(t_0)|$  in a closed system.

Eq. (2.10) sets the evolution for any time step  $t - t_0$  of a density matrix and is the solution of the equation that plays the same role as Schrödinger's Equation, but for density matrices, the so-called *von Neumann Equation*

$$\boxed{\frac{d\rho(t)}{dt} = -i[H, \rho(t)]}. \quad (2.11)$$

## 2.2.2 Open systems - Kraus matrices

One of the standard approaches to deal with open quantum systems is to consider the system state  $\rho_S(t_0)$  (acting on a Hilbert space  $\mathcal{H}_S$ ) and environment state  $\rho_E(t_0)$  (acting on a Hilbert space  $\mathcal{H}_E$ ) together as an initially uncorrelated joint system  $\rho_{SE}(t_0) = \rho_S(t_0) \otimes \rho_E(t_0)$  and make a unitary evolution of this joint system  $\rho_{SE}(t) = U(t - t_0)\rho_{SE}(t_0)U^\dagger(t - t_0)$ . The system resulted from tracing out the environment (see Appendix A for the definition of the partial trace) will be our evolved system  $\rho_S(t) = \text{Tr}_E[\rho_{SE}(t)]$  and the map from  $\rho_S(t_0)$  to  $\rho_S(t)$ , in general, will not be unitary. The procedure of evolving unitarily the joint system and tracing out the environment will be frequently used in this thesis and can be made to describe any open quantum system, as the following discussion shows.

Writing the above procedure explicitly, we obtain

$$\boxed{\rho_S(t) = \text{Tr}_E\{U\rho_S(t_0) \otimes \rho_E(t_0)U^\dagger\}}, \quad (2.12)$$

where we are omitting the  $(t - t_0)$  in  $U$  just for practicality. Now if we make a spectral decomposition of the initial environment density matrix

$$\rho_E(t_0) = \sum_m q_m |m\rangle_E \langle m|_E,$$

(where the sub-index  $E$  in  $|m\rangle_E$  just makes it explicit that  $|m\rangle$  belongs to the basis of  $\mathcal{H}_E$  that diagonalizes  $\rho_E$ ) and apply it in Eq. (2.12), we obtain

$$\rho_S(t) = \text{Tr}_E \left\{ \sum_m q_m U |m\rangle_E \rho_S(t_0) \langle m|_E U^\dagger \right\} = \sum_{m,k} q_m \langle k|_E U |m\rangle_E \rho_S(t_0) \langle m|_E U^\dagger |k\rangle_E, \quad (2.13)$$

where in the last equality we computed the partial trace in the same basis as  $|m\rangle_E$ . Finally, if we define (putting  $(t - t_0)$  back to  $U$ )

$$M_{k,m}(t - t_0) = \sqrt{q_m} \langle k|_E U(t - t_0) |m\rangle_E, \quad (2.14)$$

and rename the collective index  $(k, m)$  to  $\alpha$ , we obtain

$$\rho_S(t) = \sum_\alpha M_\alpha(t - t_0) \rho_S(t_0) M_\alpha^\dagger(t - t_0). \quad (2.15)$$

This equation has the form of the *Kraus representation* [90]

$$\boxed{\mathcal{E}(\rho) = \sum_\alpha M_\alpha \rho M_\alpha^\dagger}. \quad (2.16)$$

of a *quantum channel*  $\mathcal{E}$ , where  $M_\alpha$  are called *Kraus matrices* and must satisfy

$$\boxed{\sum_\alpha M_\alpha^\dagger M_\alpha = 1}. \quad (2.17)$$

Quantum channels are the linear operations that transform density matrices

onto density matrices, maintaining all their properties (Eq. (2.4) and Eq. (2.5)) and hence are appropriate operations for the general description of open quantum systems dynamics (such as unitary operators are for closed systems). They are called linear completely positive trace preserving (CPTP) maps<sup>1</sup>. It can be shown (see, for instance, [1, 57, 91]) that every linear CPTP map can be described in the form of a Kraus representation (Eq. (2.16)) and vice-versa for a set of Kraus matrices, thus it sets a necessary and sufficient condition to describe an open system dynamics. We shall follow this scheme in our work, considering interactions that last finite time between part of the environment (the ancillae) and making the partial trace in order to obtain the desired dynamics of our collisional model.

## 2.3 Collisional Models

### 2.3.1 General case (correlated ancillae)

Suppose we have a system  $S$  that starts interacting, at a time  $t = 0$ , with an environment  $E$ , which is separated in  $n$  sub systems  $A_j$  ( $1 \leq j \leq n$ ) named *ancillae*. We say that we have a Collisional Model (CM) whenever the system interacts individually, one at a time, and only once with each ancilla and we call each of these interactions a *collision* (see Fig. 2.1). There are studies on CMs in which the ancillae interact with themselves after the instant  $t = 0$  (see, for instance, [88]), but in our case, we assume that this is not the case.<sup>2</sup>

Given those demands, the depiction of the system's interaction with the  $j$ -th ancilla, during a time  $\tau$  (we suppose all ancilla-system interactions last the same time), is given by a unitary operator

$$U_j = e^{-i\tau H_j}, \quad (2.18)$$

---

<sup>1</sup>Actually, the term *completely positive* means a stronger assumption: that given a density matrix  $\rho$ , then the matrix  $(\mathcal{I} \otimes \mathcal{E})(\rho)$  must also be positive, where  $\mathcal{I}$  is the identity operator acting on an extra system  $R$  of arbitrary dimensionality.

<sup>2</sup>We do consider that the ancillae may interact with themselves before starting the dynamics with the system, in order for them to be initially correlated. In fact, the study of the effects of such initial correlations in the system is one of the main themes of this thesis.



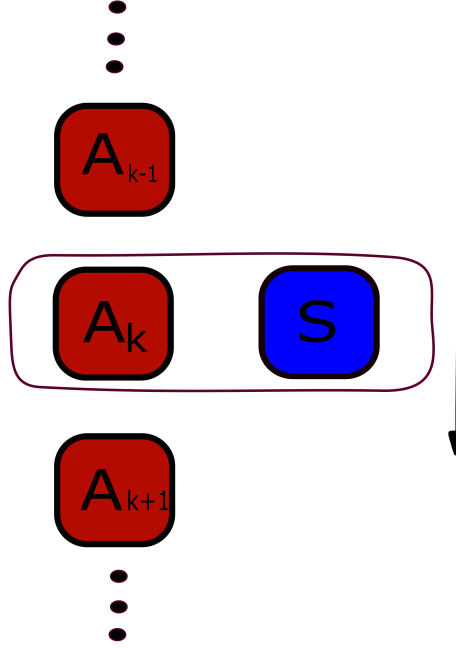


Figure 2.1: Schematic of collisions, where the system  $S$  is interacting individually with the  $k$ -th ancilla during a time  $\tau$  going to interact with the next ancilla also during a time  $\tau$ .

in which

$$H_j = H_S + H_{A_j} + V_j, \quad (2.19)$$

where  $H_S$  is the system's internal Hamiltonian,  $H_{A_j}$  is the internal Hamiltonian of the  $j$ -th ancilla and  $V_j$  describes the interaction between the system and the  $j$ -th ancilla. Then the joint state of the system plus all ancillae after the  $n$ -th collision is given by

$$\rho_{SE}^n = U_n U_{n-1} \cdots U_2 U_1 \rho_S^0 \otimes \rho_E^0 U_1^\dagger U_2^\dagger \cdots U_{n-1}^\dagger U_n^\dagger, \quad (2.20)$$

where we supposed that the initial joint state  $\rho_{SE}^0$  is the tensor product between the initial system  $\rho_S^0$  and the environment  $\rho_E^0$  (remembering, inside this environment are all possibly correlated ancillae) since their interaction only starts at  $t = 0$ . Furthermore, we trace out all the environment in order to obtain the system's *stroboscopic*<sup>3</sup>

<sup>3</sup>“Stroboscopic” means that our interest is only in the evolution steps multiples of  $\tau$ , no attention is given for the intermediate time evolution.

evolution after the  $n$ -th collision

$$\begin{aligned}\rho_S^n &= \text{Tr}_E \{ \rho_{SE}^n \} \\ &= \text{Tr}_E \left\{ U_n U_{n-1} \cdots U_2 U_1 \rho_S^0 \otimes \rho_E^0 U_1^\dagger U_2^\dagger \cdots U_{n-1}^\dagger U_n^\dagger \right\}.\end{aligned}\quad (2.21)$$

Suppose we wish to analyze the evolution of the system after the second collision ( $n = 2$ ), Eq. (2.21) will result in

$$\begin{aligned}\rho_S^2 &= \text{Tr}_E \left\{ U_2 U_1 \rho_S^0 \otimes \rho_E^0 U_1^\dagger U_2^\dagger \right\} \\ &= \text{Tr}_{A_2} \left\{ U_2 \text{Tr}_{A_1} \left\{ U_1 \rho_S^0 \otimes \rho_E^0 U_1^\dagger \right\} U_2^\dagger \right\} \\ &= \text{Tr}_{A_2} \left\{ U_2 \rho_{SA_2} U_2^\dagger \right\} \\ &\neq \text{Tr}_{A_2} \left\{ U_2 \rho_S^1 \otimes \rho_{A_2} U_2^\dagger \right\},\end{aligned}\quad (2.22)$$

where we defined  $\rho_{SA_2} = \text{Tr}_{A_1} \left\{ U_1 \rho_S^0 \otimes \rho_E^0 U_1^\dagger \right\}$  as a density matrix that acts on  $\mathcal{H}_S \otimes \mathcal{H}_{A_2}$ , where  $\mathcal{H}_{S(A_2)}$  is the Hilbert space of  $S(A_2)$ . The last line of Eq.(2.22) above happens because  $\rho_{SA_2}$  cannot, in general, be a tensor product  $\rho_S^1 \otimes \rho_{A_2}$  (where  $\rho_S^1$  is the density matrix of the evolved system after the first collision) due to the initial correlation between the ancillae. This way the  $\rho_S^2$  in Eq. (2.22) cannot result in a map between  $\rho_S^1$  and  $\rho_S^2$ , and the evolution of the system from the first collision into the second will not be a CPTP map. The reason for this is that the initial correlations cause the system evolution to be non-Markovian,<sup>4</sup> since after the first collision the second ancilla already obtains information about the system. The information about the initial system affects the system itself at the second collision, clearly, this narrative also happens for all further collisions.

As the case above suggests, non-Markovianity precludes intermediate maps to be CPTP, i.e., if we have a CPTP map  $\mathcal{E}_{t_2-t_0}$  that evolves a state from  $t_0$  to  $t_2$ , we cannot break it in two CPTP maps  $\mathcal{E}_{t_2-t_1}$  and  $\mathcal{E}_{t_1-t_0}$  such that  $\mathcal{E}_{t_2-t_0} = \mathcal{E}_{t_2-t_1} \mathcal{E}_{t_1-t_0}$  for some intermediate time  $t_1$ . This aspect of Non-Markovianity is studied in CMs

---

<sup>4</sup>In this thesis, it will be sufficient to define a *non-Markovian* evolution of a system as an evolution which depends on the whole past history of the system. Otherwise, if the evolution only depends on the latest state, it is said to be *Markovian*. More refined definitions and characterizations of quantum non-Markovianity can be found in Refs. [92–94].

(see, for instance, Refs. [72–78, 81–88]) and is a caveat for obtaining the evolution of the system, since it makes impossible to gradually describe the system’s evolution by a cumulative sequence of simpler steps. Chapters 5 and 6, which are intended for the results of the first project of the thesis, focus on obtaining non-Markovian dynamics caused by the initial correlations between the ancillae. In the rest of this chapter, we shall present the standard Markovian CMs framework, as well as special cases, such as homogenization, that will contrast with the results of the following chapters.

### 2.3.2 Markovian case

For standard CMs we suppose, in addition to the assumptions above, that initially, all ancillae are uncorrelated so that the environment is

$$\rho_E^0 = \rho_{A_1} \otimes \rho_{A_2} \otimes \cdots \otimes \rho_{A_n}, \quad (2.23)$$

where each  $\rho_{A_j}$  acts on its respective ancilla Hilbert space  $\mathcal{H}_j$ . Using this at Eq. (2.21) we obtain a major simplification in our stroboscopic evolution

$$\rho_S^n = \text{Tr}_{A_n} \left\{ U_n \cdots \text{Tr}_{A_2} \left\{ U_2 \text{Tr}_{A_1} \left\{ U_1 \rho_S^0 \otimes \rho_{A_1} U_1^\dagger \right\} \otimes \rho_{A_2} U_2^\dagger \right\} \cdots \otimes \rho_{A_n} U_n^\dagger \right\}, \quad (2.24)$$

where we just used that the partial trace over  $A_m$  does not affect operators that don’t act on  $\mathcal{H}_{A_m}$ . Now, if we define a map  $\mathcal{E}^{(n)}$ , called *collision map* or *stroboscopic map*, acting on a state  $\rho_S$  as

$$\boxed{\mathcal{E}^{(n)}(\rho_S) = \text{Tr}_{A_n} \left\{ U_n \rho_S \otimes \rho_{A_n} U_n^\dagger \right\}}, \quad (2.25)$$

then Eq. (2.24) can be rewritten as

$$\rho_S^n = \mathcal{E}^{(n)}(\mathcal{E}^{(n-1)}(\cdots \mathcal{E}^{(1)}(\rho_S^0))), \quad (2.26)$$

which represents the successive application of CPTP maps, since the map in Eq. (2.25) is CPTP as a consequence of having a unitary evolution and a partial trace

(see Eq. (2.12)). This successive application of CPTP maps forming a CPTP map indicates that all the stroboscopic dynamics are Markovian. This is a direct consequence of the absence of initial correlations between the ancillae.

As done in most studies in CMs and will be often done in this work, we consider that all the ancillae are identical, thus  $\rho_{A_j} = \rho_A$  for every  $j$ . The internal Hamiltonian of the system and ancillae will be set to 0 (unless specified),<sup>5</sup> and the interaction between the ancillae and the system are equal, i.e.,  $V_j = V$ <sup>6</sup> for all  $j$  in Eq. (2.19) and consequently all unitary operators are the same ( $U_j = U$  for all  $j$ ). In this case, all applications will be identical,  $\mathcal{E}^{(n)} = \mathcal{E}$ ,  $\forall n$ , and hence

$$\rho_S^n = \mathcal{E}^n(\rho_S^0), \quad (2.27)$$

which means that it will be sufficient to find the map  $\mathcal{E}$  and apply it  $n$  times in the initial state in order to obtain the full evolution. Similarly, we can obtain the state of the  $n$ -th ancilla after its collision with the system, it will be the result of tracing out the system from the evolution of  $\rho_S^n \otimes \rho_A$ , explicitly

$$\rho_A^n = \text{Tr}_S \left\{ U \rho_S^n \otimes \rho_A U^\dagger \right\} = \text{Tr}_S \left\{ U (\mathcal{E}^n(\rho_S^0) \otimes \rho_A) U^\dagger \right\}. \quad (2.28)$$

### 2.3.3 Qubit example, thermalizing machines

Proceeding with the restrictions above, we assume that the system and ancillae are qubits (all-qubit model) and that all the ancillae are initially in a *thermal state* (see Appendix A, in particular, Eq. A.22)

$$\rho_{\text{th}} = (1 - p_{\text{th}})P_0 + p_{\text{th}}P_1, \quad (2.29)$$

when  $0 \leq p_{\text{th}} \leq 1/2$ ,  $P_0 = |0\rangle\langle 0|$ ,  $P_1 = |1\rangle\langle 1|$ , are the projectors of the eigenstates of  $\sigma_z$  ( $|0\rangle$  and  $|1\rangle$ ) with eigenvalues  $-1$  and  $1$  respectively. If we set the Hamiltonian of each ancilla qubit to  $H_0 = E\sigma_z$  (with  $E > 0$ ), then  $|0\rangle$  is the ground state qubit

---

<sup>5</sup>Actually, this condition of setting  $H_S$  and  $H_{A_j}$  to 0 is equivalent of demanding that  $H_S = H_{A_j}$ ,  $[H_S, V_j] = 0$ , and going to the interaction picture (see Appendix A).

<sup>6</sup>Of course, the operators  $V_n$  are identical but each act only on the system and their respective ancillae  $A_n$ .

and  $|1\rangle$  is the excited state and hence  $p_{\text{th}}$  is the probability that the qubit is in the ground state. If we now ask which are the unitaries  $U$  that could construct a collision map  $\mathcal{E}$  such that

$$U(\rho_{\text{th}} \otimes \rho_{\text{th}})U^\dagger = \rho_{\text{th}} \otimes \rho_{\text{th}} \quad \text{and} \quad (2.30)$$

$$\rho_S^n = \mathcal{E}^n(\rho_S^0) \xrightarrow{n \rightarrow \infty} \rho_{\text{th}}, \quad \forall \rho_S^0. \quad (2.31)$$

The most general answer is that the unitaries must have the form of Eq. (2.18) (remembering that in this case, they are all identical, independent of  $j$ ) with the Hamiltonian

$$H(g, g_z) = g(\sigma_+ \otimes \sigma_- + \sigma_- \otimes \sigma_+) + g_z \sigma_z \otimes \sigma_z, \quad (2.32)$$

where  $g$  and  $g_z$  are real numbers and

$$\sigma_- = \sigma_+^\dagger = \frac{1}{2}(\sigma_x - i\sigma_y) = |0\rangle\langle 1|. \quad (2.33)$$

This result was obtained in Ref. [18], which also brands any setup responsible for the quantum operation respecting Eqs. (2.30) and (2.31) is called a *thermalizing machine* and the process of the system relaxing towards  $\rho_{\text{th}}$  is called *thermalization*. These terms are easily justified since Eq. (2.30) affirms that if the system is in the same state as the thermal ancillae, then the evolution stagnates, while Eq. (2.31) means that the quantum operation is such that system's state will converge to the thermal ancillae independent of the system's initial state, i.e., this CM setup will make the system thermalize.

As an example of thermalization made with simple computations, we suppose that all the ancillae start with the state  $\rho_A = |0\rangle\langle 0|$  (this is the ground state, which is the thermal state at the limit  $T \rightarrow 0$ , so we are supposing a very cold environment) and the initial system state is an arbitrary qubit which can be always parametrized as

$$\rho_S^0 = \begin{pmatrix} \langle 0 | \rho_S^0 | 0 \rangle & \langle 0 | \rho_S^0 | 1 \rangle \\ \langle 1 | \rho_S^0 | 0 \rangle & \langle 1 | \rho_S^0 | 1 \rangle \end{pmatrix} = \begin{pmatrix} 1-p & C \\ C^* & p \end{pmatrix}, \quad (2.34)$$

where  $0 \leq p \leq 1$  and  $(1 - 2p)^2 + 4|C|^2 \leq 1$  which are conditions that come from positivity and unit trace. Here  $p$  is the *population* of the excited state  $|1\rangle$  and  $C$  is the *coherence*. Now if we explicitly compute the unitary with the Hamiltonian given by Eq. (2.32), we obtain

$$\begin{aligned} U(g, g_z) &= e^{-iH(g, g_z)\tau} \\ &= e^{-i2g_z\tau}(|00\rangle\langle 00| + |11\rangle\langle 11|) + \cos(g\tau)(|10\rangle\langle 10| + |01\rangle\langle 01|) - i\sin(g\tau)(\sigma_+\sigma_- + \sigma_-\sigma_+), \end{aligned} \quad (2.35)$$

where we just used that  $|00\rangle, |11\rangle$  and  $\frac{1}{\sqrt{2}}(|10\rangle \pm |01\rangle)$  are the eigenvectors of  $H(g, g_z)$  with eigenvalues  $g_z, g_z$  and  $\pm g - g_z$ , respectively and use it to expand the exponential operator in the eigenvector basis (also we omitted the tensor product sign  $|a\rangle \otimes |b\rangle = |ab\rangle$  for convenience). We can now use the unitary above to obtain the collision map, according to Eq. (2.25)

$$\begin{aligned} \mathcal{E}(\rho_S^0) &= \text{Tr}_A \left\{ U(g, g_z) \rho_S^0 \otimes |0\rangle\langle 0| U^\dagger(g, g_z) \right\} \\ &= \begin{pmatrix} (1-p) + \sin^2(g\tau)p & e^{2ig_z\tau} \cos(g\tau)C \\ e^{-2ig_z\tau} \cos(g\tau)C^* & \cos^2(g\tau)p \end{pmatrix}. \end{aligned} \quad (2.36)$$

By iterating this map<sup>7</sup>  $n$  times in order to obtain the system's evolution after the  $n$ -th collision (according to Eq. (2.27)), we obtain

$$\rho_S^n = \begin{pmatrix} 1 - p_n & C_n \\ C_n^* & p_n \end{pmatrix}, \quad (2.37)$$

where  $C_n = e^{2ig_z n\tau} \cos^n(g\tau)C$  and  $p_n = \cos^{2n}(g\tau)p$ . As we can see,  $C_n$  and  $p_n$  go to 0 as  $n$  gets large (of course, if  $g\tau$  isn't an integer multiplied by  $\pi$ ). This highlights two effects of dissipation due to the bath: the *decoherence* (the vanishing of the off-diagonal terms), as usually happens when a quantum system is interacting with a thermal bath (in this case, even with the bath at a very low temperature), and the decay of the population of the excited state  $|1\rangle$ , pushing the system to the steady

---

<sup>7</sup>For the case of  $g_z = 0$  this map is the same as the well-known *amplitude damping* [1, 91].

state  $|0\rangle\langle 0|$ . This steady state is nothing but the thermalization of the system towards the initial 0 temperature ancillae state.

### 2.3.4 steady states

We already tacitly used the concept of *steady state* as the state in which the system converges after a long time interacting with the environment. For making this definition more concrete, we say that a state  $\rho^*$  is a steady state of a map  $\mathcal{E}$ , if and only if

$$\boxed{\mathcal{E}(\rho^*) = \rho^*}. \quad (2.38)$$

$\rho^*$  is also called a fixed point of the map.

Notice that the steady state need not be unique. A map that has a unique steady state is called *ergotic*, and if

$$\mathcal{E}^n(\rho) \rightarrow \rho^*, \quad (2.39)$$

for large  $n$  and any density matrix  $\rho$ , then this map is said to be *mixing*. Consequently, any mixing map is ergotic, and thus if one proves the mixing of a map which leads the initial state to  $\rho^*$ , it will be the unique steady state (this will be our procedure in bosonic CMs in Chapter 5).

The process of thermalization in Eqs. (2.30) and (2.31) is a mixing map which has  $\rho_{th}$  as fixed point. A slightly more general concept is that of *thermal operations*, in which the ancillae and system need not have identical Hilbert spaces but the system thermalizes at the same temperature as the ancillae. This is an important concept in the context of *Resource Theories* and it can be proved that any energy-conserving unitary generating a CM map like in Eq. (2.25) (with ancillae in thermal states) is a thermal operation [95]. This kind of unitary will describe the main interactions studied in this thesis, including the *Partial SWAP*.

### 2.3.5 SWAP and Partial SWAP

An important specific case of a thermalizing machine is generated from the interaction given by  $g_z = g/2$  in Eq. (2.32). Here the Hamiltonian will have the form

$$H(g, g/2) = \frac{g}{2} \vec{\sigma} \cdot \vec{\sigma}, \quad (2.40)$$

where  $\vec{\sigma} \cdot \vec{\sigma} = \sigma_x^1 \otimes \sigma_x^2 + \sigma_y^1 \otimes \sigma_y^2 + \sigma_z^1 \otimes \sigma_z^2$ , we used that  $\sigma_+^1 \sigma_-^2 + \sigma_-^1 \sigma_+^2 = \frac{1}{2}(\sigma_x^1 \sigma_x^2 + \sigma_y^1 \sigma_y^2)$  and here  $\sigma_i^{1(2)}$  means the  $i$  Pauli matrix acting in the first(second) qubit. This Hamiltonian is, except for a constant term, equivalent to the *SWAP Operation*

$$S = \frac{1}{2} (\mathbf{I} + \vec{\sigma} \cdot \vec{\sigma}), \quad (2.41)$$

where  $\mathbf{I}$  is the identity operator. The SWAP operation is a very important quantum channel having applications from Open Quantum Systems to Quantum Computation. Its main property is that, given two states  $|\psi\rangle$  and  $|\phi\rangle$ , then

$$\boxed{S(|\psi\rangle \otimes |\phi\rangle) = |\phi\rangle \otimes |\psi\rangle.} \quad (2.42)$$

Actually, Eq. (2.42) is a more general definition of the SWAP, being valid for any Hilbert space. Conversely, Eq. (2.41) is equivalent to Eq. (2.42) only for the case of two qubits.

A direct consequence of Eq. (2.42) is

$$SS = S^2 = \mathbf{I}, \quad (2.43)$$

which can be used to directly show that the SWAP generates the *Partial SWAP Operation*

$$\boxed{U_P(g\tau) = e^{-ig\tau S} = \cos(g\tau)\mathbf{I} + i \sin(g\tau)S.} \quad (2.44)$$

It can be shown (see Ref. [19]) that the Partial SWAP of Eq. (2.44) is, except for an



irrelevant phase term, the only unitary  $U$  that satisfies the following two properties

$$\mathrm{Tr}_1\{U\rho \otimes \rho U^\dagger\} = \rho \quad \text{and} \quad (2.45)$$

$$\mathrm{Tr}_2\{U\rho \otimes \rho U^\dagger\} = \rho, \quad (2.46)$$

for qubits (the subscripts 1 and 2 indicate that the partial trace is realized in the subspace of the first and second two-level Hilbert space, respectively). In Chapter 6, in the continuous variables context, we shall present the *Beam Splitter* as the Partial SWAP, with the same properties, for the bosonic modes case.

### 2.3.6 Homogenization

We shall focus on the procedure proposed in [19], where the so-called *homogenization* was defined for qubits systems. This procedure consists of a CM where all ancillae have the same structure as the system (like qubits, in the case of [19]), are initially identical and *uncorrelated* and the unitary responsible for the interactions between system and ancillae acts in such a way that, after the system collides with all the ancillae, the system and ancillae will be all approximately identical.

The homogenization procedure is very similar to the procedure of thermalization, but in this case, as we shall see, we are free to involve any kind of ancillae state in the process, not only thermal states. The process is outlined as follows. Suppose we have a CM with identical ancillae initially in a *generic* state  $\rho_A^0$  and a system initially at state  $\rho_S^0$  and they interact in each collision via the same unitary  $U$  (the condition here are just like in the thermalizing machine, but notice that the ancillae state  $\rho_A$  don't need to be at a thermal state). Hence the system after the  $n$ -th collision will evolve according to the stroboscopic map in Eq. (2.27) and the  $n$ -th ancilla after its collision with the system will be given by (2.28). We say that *homogenization happens when for all  $\delta > 0$  there is a finite number of collisions  $N_\delta$  such that*

$$D(\rho_S^N, \rho_A) \leq \delta, \quad \forall N \geq N_\delta, \quad (2.47)$$

$$D(\rho_A^n, \rho_A) \leq \delta, \quad \forall n, \quad 1 \leq n \leq N, \quad (2.48)$$

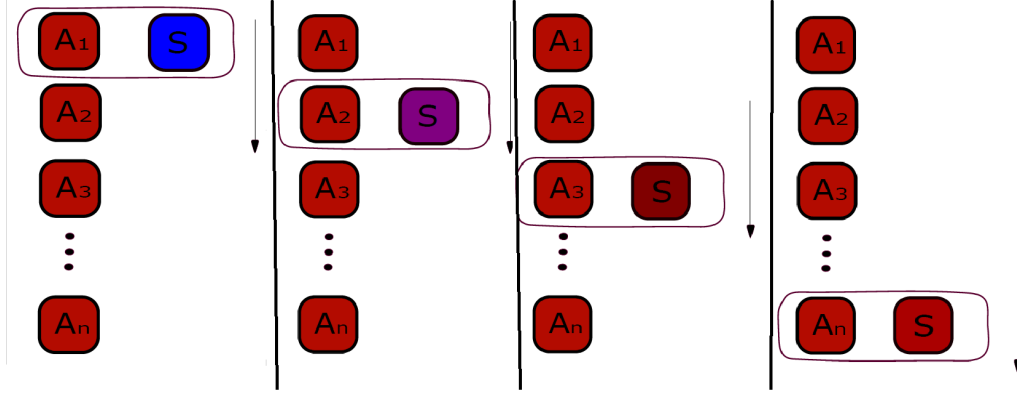


Figure 2.2: Schematic of homogenization. From left to right, the system  $S$  interacts with the ancillae at time  $0 < t < \tau$ ,  $\tau < t < 2\tau$ ,  $2\tau < t < 3\tau$  and  $(n-1)\tau < t < n\tau$ , respectively. The color changes on the system represent the different states it passes through until it gets very similar to the ancillae and the whole system becomes homogeneous.

where  $D(\bullet, \bullet)$  means any distance between operators, and in this work we shall use the trace distance.<sup>8</sup>

These two conditions mean that not only the system must get as close as we want to the initial ancillae state  $\rho_A$ , independent of the initial system state  $\rho_S^0$ , but also the ancillae must never get too distant from its initial state after their collision with the system. The result is that the final states must all be similar, and the ancillae turn the system to look like one of them, transforming the system and environment into a homogeneous set of very similar parts (see Fig. 2.2).

It can be shown, for the all-qubit case, that homogenization is achieved if the unitary  $U$  that rules the interaction in the collisions is the Partial SWAP given in Eq. (2.44). This can be seen by the direct application of the Markovian form of CMs using this particular unitary. Starting with Eq. (2.25), we obtain

$$\rho_S^1 = c^2 \rho_S^0 + s^2 \rho_A + ics(\rho_A \rho_S^0 - \rho_S^0 \rho_A), \quad (2.50)$$

when  $c$  and  $s$  are  $\cos(g\tau)$  and  $\sin(g\tau)$ , respectively. Following the interaction of the same channel  $n$  times, as Eq. (2.27) suggests, we obtain the system's state after the

<sup>8</sup>Suppose we have two density matrices  $\rho$  and  $\sigma$ , then the **trace distance** between them will be

$$D(\rho, \sigma) = \frac{1}{2} \text{Tr} |\rho - \sigma|, \quad (2.49)$$

where  $|A| = \sqrt{A^\dagger A}$  is the positive square root of  $A^\dagger A$ .

$n$ -th collision

$$\begin{aligned}
 \rho_S^n &= c^2 \rho_S^{n-1} + s^2 \rho_A + ics(\rho_A \rho_S^{n-1} - \rho_S^{n-1} \rho_A) \\
 &= s^2 \sum_{j=0}^{n-1} c^{2j} \rho_A + \rho_{\text{rest}}^n \\
 &= (1 - c^{2n}) \rho_A + \rho_{S,\text{rest}}^n
 \end{aligned} \tag{2.51}$$

where  $\rho_{S,\text{rest}}^n$  is a  $\rho_S^0$  dependent part that will go to 0 as  $n \rightarrow \infty$  (see Appendix A). Similarly, we can use Eq. (2.28) and the equation above to obtain the state of the  $n$ -th ancilla after its collision

$$\begin{aligned}
 \rho_A^n &= s^2 \rho_S^{n-1} + c^2 \rho_A + ics(\rho_S^{n-1} \rho_A - \rho_A \rho_S^{n-1}) \\
 &= s^2(1 - c^{2(n-1)}) \rho_A + \rho_{A,\text{rest}}^n,
 \end{aligned} \tag{2.52}$$

where  $\rho_{A,\text{rest}}^n$  is also a  $\rho_S^0$  dependent part that goes to 0 as  $n \rightarrow \infty$  (see Appendix A), meaning that  $\rho_S^n \rightarrow \rho_A$  and  $\rho_A^n \rightarrow \rho_A$  for large  $n$ . Therefore, both system and ancillae converge to  $\rho_A$  for sufficiently large  $n$ .

There is one more restriction needed so that homogenization can be correctly achieved. Notice that in the first line of Eq. (2.52) the term  $(\rho_S^{n-1} \rho_A - \rho_A \rho_S^{n-1})$  is the one responsible for  $\rho_{A,\text{rest}}^n$  and it gets smaller at each collision since  $\rho_S^{n-1}$  gets closer to  $\rho_A$  (this is a consequence of the proof from Appendix A, Section A.5), hence we conclude that  $\rho_A^n$  gets closer to  $\rho_A$  at each collision. From this observation, we conclude that

$$D(\rho_A^n, \rho_A) \leq D(\rho_A^{n-1}, \rho_A), \tag{2.53}$$

which means that the first collision pushes the ancilla further away while the next collision pushes lesser and lesser (which makes sense since the system gets closer and closer to  $\rho_A$ ). Thus the condition from Eq. (2.48) actually bounds  $D(\rho_A^1, \rho_A)$  for each  $\delta$ , putting a bound in the Partial SWAP parameter  $g\tau$ . This restriction turns out to be (see Appendix A for the proof)

$$\sin(g\tau) \leq \sqrt{\delta/2}. \tag{2.54}$$

Finally, this sets the sufficient conditions for homogenization, which can be used for quantum cloning protocols and quantum-safe cryptography with a classical communication [19]. We can also prove, as will be done in Chapter 6, that homogenization can also happen when the system and ancillae are bosonic states. This proof will be done analytically obtaining the stroboscopic evolution for all time steps. Importantly, in both cases, homogenization demands that the steady state of the system for this kind of CM must be the initial state of the ancillae itself. The main original result of the first project of this thesis is to show that the presence of initial correlations between the ancillae in CMs tends to push the steady states far from their original steady states and, in the special case of homogenization, push the steady state away from the ancillae state [96].

### 2.3.7 Physical implementations of CMs

In this subsection we present a few examples about how CMs can describe important open quantum systems dynamics, going beyond a set of theoretical insightful models.

A very intuitive dynamic that can be associated with CMs is the one concerning a dilute gas of particles, following Boltzman's *Stosszahlansatz* molecular chaos hypothesis [64]. However, these models need to consider the time interval  $\tau$  during the interaction between the system and each ancilla to be a random variable in order to obtain a reliable description of gases [62]. This set of CMs, which are frequently called *stochastic CMs*, do have not the same structure and dynamics as the models described in this chapter, which are sometimes called *periodic CMs*. Recently, an insightful manner to mimic any stochastic CM using periodic CMs was proposed [97].

Perhaps the most natural physical setup that can fit a CM description is the *micromaser* [69, 70]. In general terms, a *maser* is a device similar to a laser, producing coherent photons around the microwave spectrum by stimulated emission, as opposed to a laser, which produces coherent photons around the visible light spectrum. The micromaser is a specific case where a filtered stream of Rydberg atoms (heavy atoms with valence electrons behaving approximately as electrons of a hydrogen atom, see Ref. [98]) are sent through a cavity so that each atom flies

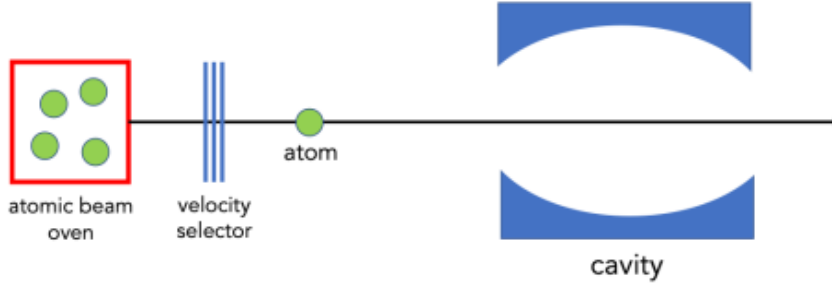


Figure 2.3: Micromaser setup: An atomic beam oven emits Rydberg atoms which pass through a velocity selector tuning the flux of atoms so that each atom passes one at a time through the cavity containing electromagnetic fields. (This figure was taken from Ref. [21].)

alone inside the cavity and interacts *individually* with the electromagnetic fields inside the cavity (see Fig. 2.3). This way, the CM described above for the Markovian case is almost perfectly suitable since we can treat each atom as an individual ancilla (uncorrelated with the other atoms) that interacts one at a time with the electromagnetic field of the cavity, which plays the role of the system.

The micromaser setup is also the most adequate apparatus for the application of the *Janyes-Cummings* (JC) model,<sup>9</sup> since both consider the presence of only one atom at a time interacting with the cavity field, being different from most lasers and masers where the cavity field actually interacts collectively with many atoms. Therefore, the CM describing the micromaser has the JC interaction Hamiltonian

$$V = g(a\sigma_+ + a^\dagger\sigma_-), \quad (2.55)$$

where  $g$  is the interaction strength,  $a$  ( $a^\dagger$ ) are the annihilation (creation) operators of the field mode<sup>10</sup> and  $\sigma_-$  ( $\sigma_+$ ) are the qubits operators given by Eq. (2.33).

The setup can then be modeled by the Markovian CM with identical ancillae and interactions, as described in Subsec. 2.3.2, with the interaction Hamiltonian of Eq. (2.19) given by Eq. (2.55) in the interaction picture (see Appendix A). Such CM is an approximation of the real micromaser setup but can reproduce the main important features of the real phenomena [98, 99]. A more complete description of

<sup>9</sup>The JC model is a largely applicable model of *light-matter* interaction [55, 57, 91], where the matter is described by a qubit (in this case, the atom) and the light is an electromagnetic mode.

<sup>10</sup>Importantly, the atom qubit interacts only with *one mode* of the electromagnetic spectrum in the cavity. This is justified by the *rotating wave approximation* (RWA) [55, 91].

the micromaser can be found in Refs. [98, 100].

Beyond the micromaser example, which is a direct application of CMs in a physical setup, CMs are extremely useful to create effective models of realistic open quantum systems situations. Important examples include the full simulation of Markovian dynamics from single qubits [73, 101] and the reproduction of any Markovian dynamics with the *multipartite collision model* (a generalization of the CM described in this chapter with multipartite system) [102].

Finally, another major example is the fact that a CM description can also emerge very naturally from one of the most common microscopic system-bath models, namely the interaction with the one-dimensional waveguide. In this model, the system is described by a generic system with frequency  $\omega_0$  and annihilation (creation) operator  $A(A^\dagger)$ , and the environment is represented by a continuum of bosonic modes, with annihilation (creation) operators  $b_\omega(b_\omega^\dagger)$  and frequencies that range from  $-\infty$  to  $\infty$ . The Hamiltonian of the full joint system is given by

$$H = H_S + H_E + V, \quad (2.56)$$

where

$$H_S = \omega_0 A^\dagger A, \quad H_E = \int_{-\infty}^{\infty} d\omega (\omega_0 + \omega) b_\omega^\dagger b_\omega \quad \text{and} \quad V = \sqrt{\frac{\gamma}{2\pi}} \int_{-\infty}^{\infty} d\omega (A^\dagger b_\omega + A b_\omega^\dagger), \quad (2.57)$$

where  $\gamma$  is a constant coupling strength. This is the so-called *white noise* coupling [55]. The above Hamiltonian is justified by the RWA (which explains the presence of non-physical negative frequencies) together with the *weak coupling approximation*, which is very often used in quantum optics [55, 57, 103].

By making a Fourier transform we can define *time modes*, for any real  $t$ ,

$$b_t = \frac{1}{\sqrt{2\pi}} \int_{-\infty}^{\infty} d\omega b_\omega e^{-i\omega t}. \quad (2.58)$$

These time modes can represent quantum harmonic modes since they satisfy  $[b_t, b_{t'}^\dagger] = \delta(t - t')$  and  $[b_t, b_{t'}] = [b_t^\dagger, b_{t'}^\dagger] = 0$ . In order to make a discrete time step evolution, we can discretize the real line in intervals with equal lengths so that  $t_n - t_{n-1} = \Delta t$

for finite  $\Delta t$  and any integer  $n$ . This way, we may redefine the time modes for discrete steps

$$b_n = \frac{1}{\sqrt{\Delta t}} \int_{t_{n-1}}^{t_n} dt b_t, \quad (2.59)$$

which also satisfies the commutation relations for any  $n$ . Going to the interaction picture (see Appendix A), the Hamiltonian of Eqs. (2.56) and (2.57) reduces to

$$V_n = \sqrt{\frac{\gamma}{\Delta t}} (A^\dagger b_n + A b_n^\dagger), \quad (2.60)$$

which is time-dependent, since the interaction will affect only each mode  $n$  when  $t \in [t_n, t_{n-1}]$ . Consequently, this model is exactly a CM where the ancillae are described by the time discrete modes represented by the operators  $b_n(b_n^\dagger)$ . This CM picture of open systems under white noise is explained and applied in the context of waveguide-QED in Refs. [103, 104]. In this thesis, such CM in which all the ancillae are bosonic modes will be explored in detail, since its formalism makes it possible to obtain analytical solutions to the effects of initial correlations between the ancillae in the system's dynamics.

# Chapter 3

## Quantum Information and Bayesian Networks

*Quantum Information* (QI) is a largely growing field in the past decades, especially with the advent of promising new quantum technologies [105]. The rich history of the creation and development of this field is well narrated in Ref. [1] and excellent introductory and detailed texts approaching general themes about QI are found in Refs. [1, 2, 15]. In this Chapter, we mainly focus on the aspects of quantum information used to quantify correlations between quantum states and how to identify which correlations have intrinsic quantum aspects. These subjects are going to be essential for the analysis and interpretation of the main projects of this thesis.

As a second subject of this Chapter, we present the concept of *Bayesian Networks*. The exposition will be brief and primarily focused on the application needed for our second project (Chapter 7).

### 3.1 Generalized measurements

Quantum measurements are among the most controversial subjects of quantum mechanics, hence the discussion of its postulates can render extensive texts. Here we only expose the postulates which are useful to the present thesis. More complete discussions explaining and motivating the postulates are given in Refs. [1, 2, 15, 57, 106] and examples for the exposition of interpretations are given in Refs. [106, 107].



The postulates are the following:

- Any measurement can be described in terms of a set of Kraus matrices  $\{M_k\}_k$ , satisfying Eq. (2.17), given the measurement setup. Each of these choices defines a *Positive Operator Value Measure* (POVM).<sup>1</sup> The result of each measurement is labeled by a index  $k$  of the the corresponding Kraus matrix  $M_k$ ;
- The probability of obtaining the outcome  $k$  is

$$p_k = \text{Tr}(M_k \rho M_k^\dagger); \quad (3.1)$$

- After the measurement is done, if the result of  $k$  is recorded, the effect of the measurement in the state  $\rho$ , called *backaction*, will be to evolve

$$\rho \rightarrow \frac{M_k \rho M_k^\dagger}{p_k}. \quad (3.2)$$

The items above are sufficient to describe any generalized quantum measurement. An important class of quantum measurements is the *projective measurements*, where the Kraus matrices  $M_k$  are simply the projectors  $|k\rangle \langle k|$  in some basis  $\{|k\rangle\}_k$ . This results in the familiar “wave function collapse” rule  $p_k = |\langle \psi | k \rangle|^2$  and  $|\psi\rangle \rightarrow |k\rangle$  for measuring a pure state  $|\psi\rangle$ .

## 3.2 Entropy

### 3.2.1 The Shannon Entropy

Entropy is a central concept not only in QI but also in Classical Information Theory [108]. Since Shannon’s revolutionary paper in 1948 [109], the quantity now known as *Shannon entropy* can be undoubtedly interpreted as a measure of the average information carried by a random variable *after* we learn its value. At the same time, as is often done in physics, we interpret it as the lack of information we have about a random variable *before* we learn its value.

---

<sup>1</sup>The POVM is a set of operators  $\{E_k\}_k$  such that  $E_k = M_k^\dagger M_k$ .

If we have a random variable  $X$  with a probability distribution  $p(X)$ , then the Shannon entropy associated with this distribution is<sup>2</sup>

$$H(p(X)) = - \sum_x p(x) \log p(x), \quad (3.3)$$

where we consider the limit  $\lim_{y \rightarrow 0} y \log y = 0$ , for the case where  $p(x) = 0$ . As already mentioned, this quantity measures the average information carried by a random variable, given its probability distribution. A heuristic justification for this statement can be given as follows.

Let  $X$  be a random variable with the corresponding probability distribution  $p(X)$  and suppose that we want to construct a “surprise” function (say  $\mathcal{S}$ ) which measures the amount of unexpected learning that would be obtained if it is revealed to us the value of this random variable. For instance, if we learn that  $x$  is the value of the random variable and  $p(x)$  is close to 1, it means that the learning was not unexpected resulting in  $\mathcal{S}(x)$  small. Conversely, if  $p(x) \ll 1$ , then  $\mathcal{S}(x)$  should be a large number. Hence, intuitively we expect  $\mathcal{S}(x)$  to be inversely proportional to  $p(x)$ , but it is also desirable that it respects the additive property, i.e. having the surprise of learning  $x$  and of learning  $y$  (in symbols  $\mathcal{S}(x, y)$ ) should give  $\mathcal{S}(x) + \mathcal{S}(y)$ . The only function of  $p(X)$  that satisfies both properties (except by a multiplicative constant) is

$$\mathcal{S}(x) = \log \left( \frac{1}{p(x)} \right). \quad (3.4)$$

Intuitively, this unexpected learning can be identified as information since unexpected results tend to be more relevant and give us more information. Hence, the average of this value can be interpreted as the average of information obtained if we learn a random variable

$$\langle \mathcal{S} \rangle = \sum_x p(x) \mathcal{S}(x) = - \sum_x p(x) \log(p(x)), \quad (3.5)$$

which is exactly the Shannon entropy.

This intuitive, although not formal, argument was taken from Ref. [27]. More

---

<sup>2</sup>Here the log is taken as the natural logarithm. This differs from many QI and information theory books which define the log with base 2.

formal arguments for the Shannon entropy interpretation can be found in Refs. [1, 2, 108] and in Shannon's original paper [109].

### 3.2.2 The von Neumann Entropy

We also need a quantity that encompasses the information content of a quantum state. For defining this quantity, we assume it depends on the density matrix  $\rho$  of a quantum state since it has the informational content of the probability distribution of each possible pure quantum state (see Sec. 2.1). But naively one could guess that, given a density matrix

$$\rho = \sum_i p_i |\psi_i\rangle \langle \psi_i|, \quad (3.6)$$

the appropriate entropy that represents the quantum state should be just the Shannon entropy of the probability distribution of the states  $\{|\psi_i\rangle\}_i$

$$H(p_i) = - \sum_i p_i \log(p_i). \quad (3.7)$$

It turns out that this is not a good choice since the probability distribution  $\{p_i\}_i$  is dependent on the ensemble  $\{|\psi_i\rangle\}_i$  and in general, the states  $\{|\psi_i\rangle\}_i$  are not necessarily orthogonal, hence indistinguishable. The interpretation of Shannon entropy as being the average measure of information only makes sense if we can distinguish the outcomes of the random variables.

A more accurate attempt would be to make the spectral decomposition

$$\rho = \sum_i \lambda_i |\lambda_i\rangle \langle \lambda_i|, \quad (3.8)$$

where  $\{\lambda_i\}_i$  and  $\{|\lambda_i\rangle\}_i$  are the eigenvalues and eigenvectors of  $\rho$ , respectively, and compute the Shannon entropy of the eigenvalues<sup>3</sup>

$$H(\lambda_i) = - \sum_i \lambda_i \log(\lambda_i). \quad (3.9)$$

---

<sup>3</sup>The eigenvalues of  $\rho$  are also a valid probability distribution (see Appendix A).

This equation can be rewritten as

$$-\sum_i \lambda_i \log(\lambda_i) = -\text{Tr}(\rho \log \rho), \quad (3.10)$$

its proof is simple and can be found in Appendix B. The quantity above is invariant under a change of basis since the eigenvalues are basis independent. Importantly, the eigenstates  $\{|\lambda_i\rangle\}_i$  are orthogonal and thus are distinguishable, hence it represents a more suitable entropy for quantum states. This quantity is the *von Neumann entropy*

$$\boxed{S(\rho) = -\text{Tr}(\rho \log \rho)}, \quad (3.11)$$

and is the correct candidate to represent the information contained in a quantum state [1, 2, 15].

From Eq. (3.10) it is immediate to see that the von Neumann entropy is always a positive quantity. Another important aspect is that the von Neumann entropy vanishes for pure states and assumes its maximal value at the maximally mixed state  $\rho = \mathbf{I}/d$ , for finite-dimensional Hilbert states with dimension  $d$ . Thus

$$0 \leq S(\rho) \leq \log d. \quad (3.12)$$

Indeed, the von Neumann entropy has a similar interpretation as the purity (see Eq. (2.6)). If we have a pure state, then we have no ignorance about the system since we know in which state the system was prepared, and if we have a maximally mixed state, then we have the most ignorant case since we have an equal probability that the system was prepared in any state.

The von Neumann entropy has an enormous set of properties [1, 2, 15]. But in this thesis, it will be sufficient to use the fact that it is a quantity invariant under a unitary transformation<sup>4</sup> and to work with its conceptual role of representing the amount of ignorance we have about a quantum system. We shall use this concept in the construction of quantities representing *correlations*. From now on, we refer

---

<sup>4</sup>Suppose that  $U$  is a unitary transformation and that  $\rho' = U\rho U^\dagger$ . Then  $S(\rho') = \text{Tr}(U\rho U^\dagger \log(U\rho U^\dagger)) = \text{Tr}(U\rho U^\dagger U \log(\rho) U^\dagger) = \text{Tr}(\rho \log \rho) = S(\rho)$ , wherein the second equality we used that a unitary  $U$  infiltrates in any well-defined function of operators.

to the von Neumann entropy of a quantum state simply as the *entropy*.

## 3.3 Mutual Information and Correlations

### 3.3.1 Relative Entropy

As an entropic-like distance, we shall define the *Relative Entropy*<sup>5</sup> or *Kullback-Leibler divergence*

$$S(\rho||\sigma) = \text{Tr}(\rho \log \rho) - \text{Tr}(\rho \log \sigma), \quad (3.13)$$

where  $\rho$  and  $\sigma$  are density matrices. This quantity is always non-negative

$$S(\rho||\sigma) \geq 0, \quad (3.14)$$

and vanishes for the case where  $\rho = \sigma$ . The proof of such inequality is non-trivial and can be found in Refs. [1, 15].

From the non-negativity of relative entropy, we can have an intuitive idea of entropic distance. Although it is important to underline that this is not an actual distance, since it is not symmetric, i.e., in general,  $S(\rho||\sigma) \neq S(\sigma||\rho)$ , and does not satisfy the triangle inequality.

### 3.3.2 Mutual Information

We are interpreting entropy as the measure of ignorance over a quantum system. A useful quantity would be the *information* of a quantum system described by a quantum state  $\rho$ . It is intuitively defined as the entropic distance between the state  $\rho$  and the state in which the ignorance is maximum. In other words, it is the relative entropy between the state  $\rho$  and the maximally mixed state  $\pi = \mathbf{I}/d$  (assuming a

---

<sup>5</sup>This Relative Entropy is often called *Quantum Relative Entropy* since it is the quantum counterpart of the classical Relative Entropy defined as  $H(p(x)||q(x)) = \sum_x p(x) \log \left( \frac{p(x)}{q(x)} \right)$ , given two probability distributions  $p(x)$  and  $q(x)$ .

$d$ -dimensional Hilbert space)

$$\begin{aligned}\mathcal{I}(\rho) &= S(\rho||\pi) \\ &= \log(d) - S(\rho).\end{aligned}\tag{3.15}$$

From Eq. (3.12) we obtain that

$$0 \leq \mathcal{I}(\rho) \leq \log(d),\tag{3.16}$$

with its minimum at  $\rho = \pi$  and maximum where  $\rho$  is a pure state.

With this concept in hand, it is straightforward to have an intuitive idea of the quantity called *mutual information*. Given a system divided in two parties  $A$  and  $B$ , in which the global state is  $\rho_{AB}$ , the mutual information between the two parties is defined as

$$\boxed{\mathcal{I}_{\rho_{AB}}(A : B) = S(\rho_{AB}||\rho_A \otimes \rho_B)},\tag{3.17}$$

where  $\rho_A = \text{Tr}_B(\rho_{AB})$  and  $\rho_B = \text{Tr}_A(\rho_{AB})$ .

The mutual information embraces all the content of the *correlations* between the parties  $A$  and  $B$ . In general,  $\rho_A \otimes \rho_B \neq \rho_{AB}$  since the partial trace which generates the local state  $\rho_A$  vanishes with all the  $B$  dependence, i.e., their correlations. Thus the product  $\rho_A \otimes \rho_B$  represents completely uncorrelated states and consequently its distance to the global state  $\rho_{AB}$  measures their correlations.

A more explicit representation of the aforementioned ideas can be seen in the following formulas. From the definition of relative entropy (Eq. (3.13)), we have

$$S(\rho_{AB}||\rho_A \otimes \rho_B) = -S(\rho_{AB}) - \text{Tr}(\rho_{AB} \ln \rho_A) - \text{Tr}(\rho_{AB} \ln \rho_B).\tag{3.18}$$

Now, notice that

$$\begin{aligned}-\text{Tr}(\rho_{AB} \log \rho_A) &= -\text{Tr}_A(\text{Tr}_B(\rho_{AB}) \log \rho_A) \\ &= -\text{Tr}_A(\rho_A \log \rho_A) \\ &= S(\rho_A),\end{aligned}\tag{3.19}$$

with a similar result for  $-\text{Tr}(\rho_{AB} \log \rho_B)$  and applying it in Eq. (3.18), we obtain

$$\boxed{\mathcal{I}_{\rho_{AB}}(A : B) = S(\rho_A) + S(\rho_B) - S(\rho_{AB})}, \quad (3.20)$$

which is a simpler way to compute mutual information in various applications.

Finally, using the definition of information (Eq. (3.15)) in Eq. (3.20) and the fact that  $\log(d_A d_B) = \log d_A + \log d_B$ , we conclude that

$$\boxed{\mathcal{I}_{\rho_{AB}}(A : B) = \mathcal{I}(\rho_{AB}) - \mathcal{I}(\rho_A) - \mathcal{I}(\rho_B)}, \quad (3.21)$$

where  $d_A(d_B)$  is the dimension of the Hilbert space of  $A(B)$ . The equation above simply states that “the mutual information between  $A$  and  $B$  is the information contained in  $\rho_{AB}$  minus the information contained locally in  $\rho_A$  and  $\rho_B$ ”, that is, the mutual information represent the correlations between the parties.

### 3.3.3 Entanglement

We gave justifications for the fact that the mutual information represents the total correlations between two parties. However, to conclude which of these correlations have quantum origins without classical counterparts is a hard task and still a very fruitful research field nowadays [110]. Here, we briefly introduce the concept of *entanglement*, which is the most known type of quantum correlation, due to its applications as an important resource in quantum technologies and conceptual problems [111].

Suppose a system is divided into two parties  $A$  and  $B$ . A pure state  $|\psi\rangle$  representing this system is called a *product state* if it can be parametrized as a tensor product

$$|\psi\rangle = |\psi_A\rangle \otimes |\psi_B\rangle, \quad (3.22)$$

where  $|\psi_A\rangle$  ( $|\psi_B\rangle$ ) belong to the Hilbert space of  $A(B)$ . Any pure state which is not a product state is called an *entangled state*.

Notice that in the case of pure states, it is not hard to have a decisive witness of entanglement. If a state  $|\psi\rangle$  is a product state just like in Eq. (3.22), then clearly

the partial trace of its density matrix over  $A$  or  $B$  will result in a pure state, i.e.

$$\mathrm{Tr}_A(|\psi\rangle\langle\psi|) = |\psi_B\rangle\langle\psi_B|. \quad (3.23)$$

Otherwise, if a state  $|\psi\rangle$  is an entangled state, then the partial trace of its density matrix over  $A$  or  $B$  will result in a mixed state. Consequently, the entropy of the reduced state will be non-zero. So, if

$$S(\mathrm{Tr}_{A(B)}(|\psi\rangle\langle\psi|)) > 0, \quad (3.24)$$

the state will be entangled. Otherwise, it will be a product state.

With the use of the *Schmidt decomposition* [1, 2, 91], it can be shown that for any pure state  $S(\mathrm{Tr}_A(|\psi\rangle\langle\psi|)) = S(\mathrm{Tr}_B(|\psi\rangle\langle\psi|))$  and this quantity can also represent a quantifier of entanglement.

Unfortunately, in the case of mixed states, the problem of quantifying entanglement is much more challenging. For a system divided in parties  $A$  and  $B$ , a state  $\rho$  is said to be *separable* when

$$\rho = \sum_i p_i \rho_A^i \otimes \rho_B^i, \quad (3.25)$$

where  $\{p_i\}_i$  is a probability distribution,  $\rho_A^i$  are density matrices in  $A$  and  $\rho_B^i$  are density matrices in  $B$ . A mixed state is said to be entangled when it is not a separable state.

The meaning of Eq. (3.25) is that a separable state is a classical mixture of quantum states  $\rho_A^i$  and  $\rho_B^i$  which are only locally quantum. It can be shown that such states can always be prepared by the so-called *Local Operations and Classical Communications* (LOCCs) [111]. To distinguish if a mixed state is separable or not is, in general, a very arduous task.

### 3.3.4 Quantum discord

Due to the difficulty mentioned above in characterizing entanglement for mixed states, we focus on another quantifier of quantum correlations, the so-called *quantum discord*.



The concept of quantum discord was first proposed in Refs. [112–114]. It is a discrepancy between the mutual information among two parties and the maximum amount of information we can get from one party by measuring the other party. Intuitively, one may think that the maximum information we can get by one party looking at the other party is equal to their total correlations, but we shall see that this statement is true only for classical systems. For quantum systems, we get a mismatch due to quantum backactions.

This can be seen in the following discussion. Given a system divided into two parties  $A$  and  $B$ , suppose that their states can be represented by classical probability distributions  $p(X)^A$  and  $p(Y)^B$ , respectively. We can define the *conditional entropy*

$$H(A|B) = - \sum_y p(y)^B \sum_x p(x|y)^A \log(p(x|y)^A), \quad (3.26)$$

which is the average of the Shannon entropy of the conditional probability of  $A$  given we obtain an outcome from  $B$ , this conditional probability distribution is given by *Bayes' Theorem* [108]

$$\boxed{p(x|y)^A = \frac{p(x, y)^{AB}}{p(y)^B}}, \quad (3.27)$$

where  $p(x, y)^{AB}$  is the joint probability of measuring  $X$  and  $Y$  and obtaining  $x$  and  $y$  as results.

The conditional entropy in Eq. (3.26) is interpreted as the lack of information we have about  $A$  given we know the outcomes of  $B$ . It can be shown (see Appendix B) that the mutual information between  $A$  and  $B$  is given by<sup>6</sup>

$$\boxed{\mathcal{I}(A : B) = H(A) - H(A|B)}, \quad (3.28)$$

where  $H(A)$  is the Shannon entropy of  $A$  given its probability distribution  $p(X)^A$ . The equation above simply states that the mutual information between  $A$  and  $B$  is the ignorance of  $A$  less the ignorance of  $A$  given that we know the outcomes of  $B$ .

We can try to define a similar conditional entropy for the quantum case. In this

---

<sup>6</sup>This mutual information, defined for classical systems, has exactly the form of Eq. (3.20), but switching von Neumann entropies for Shannon entropies and density matrices for probability distributions.

case, obtaining the outcome of the subsystem  $B$  cannot be done without taking into consideration the effects of the measurement on it. Hence we suppose that if choose a generalized measurement described by the Kraus matrices  $\{M_k^B\}_k$  in  $B$ , the joint system  $\rho_{AB}$  will suffer a backaction

$$\rho_{AB|k} = \frac{(\mathbf{I}_A \otimes M_k^B)\rho_{AB}(\mathbf{I}_A \otimes M_k^B)^\dagger}{p_k}, \quad (3.29)$$

if the outcome is  $k$ , with probability

$$p_k^B = \text{Tr} \left( (\mathbf{I}_A \otimes M_k^B)\rho_{AB}(\mathbf{I}_A \otimes M_k^B)^\dagger \right). \quad (3.30)$$

With the reduced state  $\rho_{A|k} = \text{Tr}_B(\rho_{AB|k})$  we can define the *quantum-classical conditional entropy*

$$S_M(A|B) = \sum_k p_k^B S(\rho_{A|k}), \quad (3.31)$$

which follows exactly the same idea of the conditional entropy of Eq. (3.26), but with the influence of the backaction in the quantum state and the dependence on the choice of measurement  $\{M_k^B\}_k$ . Its interpretation is also similar, it represents the ignorance of the system  $A$  given we know the outcomes of the generalized measurements  $\{M_k^B\}_k$ .

It is useful to define the quantity

$$\mathcal{J}_M(A|B) = S(\rho_A) - S_M(A|B), \quad (3.32)$$

which means the information obtained by  $A$  with the outcomes of the quantum measurement  $\{M_k^B\}_k$  of  $B$ , very similar to the mutual information in Eq. (3.28). For the classical case, the quantity equivalent to Eq. (3.32) must be the mutual information, but for the quantum case, this is not always true. For this reason, one defines the *quantum discord*

$$\boxed{\mathcal{D}_M(A|B) = \mathcal{I}(A : B) - \mathcal{J}_M(A|B)}, \quad (3.33)$$

meaning the mismatch between the total correlations and the information obtained

by  $A$  after the outcomes of  $\{M_k^B\}_k$  in  $B$ .

A more compelling quantity is the *measurement independent discord*

$$\boxed{\mathcal{D}(A|B) = \min_{\{M_k^B\}_k} \mathcal{D}_M(A|B)}, \quad (3.34)$$

which is the minimum discord obtained over all possible measurements. It is the case where we obtain the maximum information about  $A$  with measurements in  $B$ , i.e., maximizing  $\mathcal{J}_M(A|B)$ . A non-zero value of this quantity means that there is no measurement that can give us full information about the correlations, as is possible in classical systems. From now on we shall refer to the measurement independent discord simply as the *quantum discord* (and to the quantum discord of Eq. (3.33) as the *measurement dependent discord*).

This correlation quantifier, without classical counterparts, has several applications in quantum information, quantum thermodynamics, open quantum systems, and many-body physics [110]. In this thesis, it will be useful to indicate genuine quantum correlations between Gaussian systems in Chapter ??.

## 3.4 Bayesian Networks

*Bayesian Networks* (BNs) was first introduced in its modern terms by Judea Pearl in 1985 [47]. In Judea's words, his study was "motivated by attempts to devise a computational model for humans' inferential reasoning", from which he obtained a graph-type model for inferring probabilities from conditional distributions disposed in a causal order. This concept is used in a large range of applications, mainly in Artificial Intelligence, which was its initial proposal application.

This concise presentation will focus only on the necessary concepts for the second project of the thesis, which took a large inspiration from [48] in introducing the BN concept to quantum systems. For a complete introduction to the subject of BNs, see Refs. [43–46].

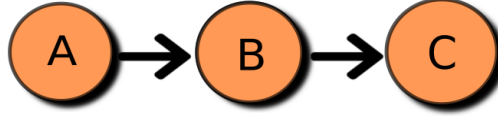


Figure 3.1: Three random variables  $A$ ,  $B$  and  $C$  disposed in a causal order.

### 3.4.1 Definition and examples

Suppose we have three random variables  $A$ ,  $B$ , and  $C$  disposed in a causal order where  $A$  causes  $B$  and  $B$  causes  $C$  (see Fig. 3.1). The approach to relating these quantities is to assign to each arrow a conditional probability according to the causal order. For instance, for the case of Fig. 3.1, the joint probability distribution  $P(A, B, C)$  is

$$\begin{aligned}
 P(A, B, C) &= P(C|B, A)P(B, A) \\
 &= P(C|B, A)P(B|A)P(A) \\
 &= P(C|B)P(B|A)P(A), \tag{3.35}
 \end{aligned}$$

where the last equation holds since the random variable  $C$  depends only on  $B$ .<sup>7</sup>

For more complex relations of causality, instead of an ordered string (as in Fig. 3.1) the causal orders can be described by directed graphs where the directed edges mean causal relations and each vertex represents a random variable. Fig. 3.2 gives an example of a directed graph describing more complex relations of causality. For this case, the joint probability  $P(A, B, C, D, E, F)$  is

$$\begin{aligned}
 P(A, B, C, D, E, F) &= P(F|A, B, C, D, E)P(A, B, C, D, E) \\
 &= P(F|C)P(A, B, C)P(F|D)P(D)P(F|E)P(E), \tag{3.36}
 \end{aligned}$$

where in the last equality we used that the random variable  $F$  only depends on  $C$ ,  $D$ , and  $E$  and these three variables are independent of each other. The joint probability

<sup>7</sup>Of course, the random variable  $C$  has a causal relation with  $A$ . But, once the random variable  $B$  is known ( $B = b$ ), the random variable  $C$  will be fully specified by  $P(C|B = b)$ , thus  $A$  and  $C$  become independent. This property is known as a *d-separation* between  $A$  and  $C$  [44, 45].

$P(A, B, C)$  can be computed separately

$$\begin{aligned}
 P(A, B, C) &= P(C|A, B)P(A, B) \\
 &= P(C|A)P(C|B)P(B|A)P(A) \\
 &= P(C|A)P(C|B)P(B|A)P(A).
 \end{aligned} \tag{3.37}$$

Combining the two equations above, we obtain

$$P(A, B, C, D, E, F) = P(C|A)P(F|C)P(C|B)P(B|A)P(A)P(F|D)P(D)P(F|E)P(E). \tag{3.38}$$

If in a directed graph there is a link from  $A$  to  $B$ , we say that  $A$  is a *parent* of  $B$ . In the directed graph of Fig. 3.2  $F$  has parents  $C, D$  and  $E$ ;  $C$  has parents  $A$  and  $B$ , and  $B$  has only the parent  $A$ . Notice that in Eq. (3.38), the joint probability distribution is just the chain product of the conditional probabilities between the random variables and their parents times the probability distributions of the random variables without parents. This is a general property of *Bayesian Networks*, the BNs are sets of random variables with their causal relations described in acyclic directed graphs<sup>8</sup>. For similar reasons as the examples above, we have the following theorem [44, 45].

**Theorem (Chain rule for Bayesian Networks):** For the set  $\{A_1, \dots, A_n\}$  of all random variables in a BN, the joint probability distribution will be

$$\boxed{P(A_1, \dots, A_n) = \prod_{i=1}^n P(A_i|\text{pa}(A_i))}, \tag{3.39}$$

where  $\text{pa}(A_i)$  is the set of all parents of  $A_i$ .

For these reasons, BNs yield a compact representation for joint probability distributions of sets of random variables with causal relations.

---

<sup>8</sup>Acyclic directed graphs are directed graphs which have no cycles in their inner structure, or directed loops. This avoids causal loops causing feedback cycles (see Fig. 3.3), which makes the modeling too difficult.[44]

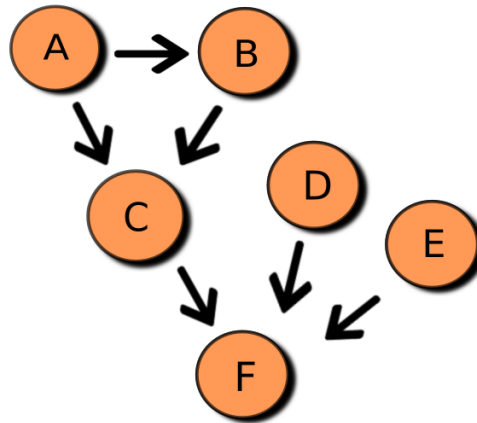


Figure 3.2: Example of a directed graph representing relations of causality between random variables.

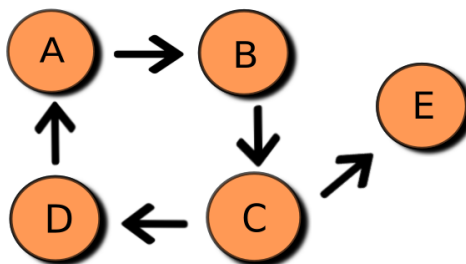


Figure 3.3: A directed graph within an internal cycle, provoking a causal loop between the random variables  $A$ ,  $B$ ,  $C$ , and  $D$ .

### 3.4.2 Dynamical BNs for quantum systems (QBNs)

In this Subsection we make an application of BNs for estimating the probability of reduced quantum systems to be in a particular conditional trajectory as the system evolves, these are called *Quantum Bayesian Networks (QBNs)*. This structure will be the basis of the second main project of this thesis and has great influence from [48, 115, 116].

The setup is the following. Consider a state divided into two parties  $A$  and  $B$  and with the initial joint state

$$\rho_{AB}(0) = \sum_s P_s |\psi_s(0)\rangle \langle \psi_s(0)|, \quad (3.40)$$

where  $\{P_s, |\psi_s(0)\rangle\}_s$  is an ensemble of quantum states which are not necessarily orthogonal. If we have a global unitary evolution  $U(t)$  of the joint system, then each state of the ensemble  $\{|\psi_s(0)\rangle\}_s$  will evolve deterministically as

$$|\psi_s(t)\rangle = U(t) |\psi_s(0)\rangle. \quad (3.41)$$

Looking now at the reduced local systems, suppose we have observable  $\mathcal{O}_A$  in  $A$  and  $\mathcal{O}_B$  in  $B$  with eigenvectors  $\{|a_i\rangle\}_i$  and  $\{|b_j\rangle\}_j$ , respectively. We know that if the global state is  $|\psi_s(t)\rangle$ , then the conditional probability of the reduced states being in the eigenkets  $|a_k\rangle$  in  $A$  and  $|b_k\rangle$  in  $B$  is<sup>9</sup>

$$\boxed{P(a_k, b_k | \psi_s(t)) = |\langle a_k, b_k | \psi_s(t)\rangle|^2.} \quad (3.42)$$

With this conditional probability in hand, we can create a BN (see Fig 3.4) for estimating the probability of the joint system to be successively observed in the states  $|a_0, b_0\rangle, |a_1, b_1\rangle, \dots, |a_n, b_n\rangle$  for time instants  $(0, t_1, \dots, t_n)$ , respectively. From the Theorem given in Eq. (3.39), the probability of realizing such states is

$$\boxed{\mathcal{P}(\psi_s(0), a_0, b_0, a_1, b_1, \dots, a_n, b_n) = P_s P(a_0, b_0 | \psi_s(0)) P(a_1, b_1 | \psi_s(t_1)) \cdots P(a_n, b_n | \psi_s(t_n)),} \quad (3.43)$$

---

<sup>9</sup>We will denote  $|a_k, b_k\rangle$  as the tensor product of vectors in  $A$  and  $B$ ,  $|a_k, b_k\rangle = |a_k\rangle_A \otimes |b_k\rangle_B$ .

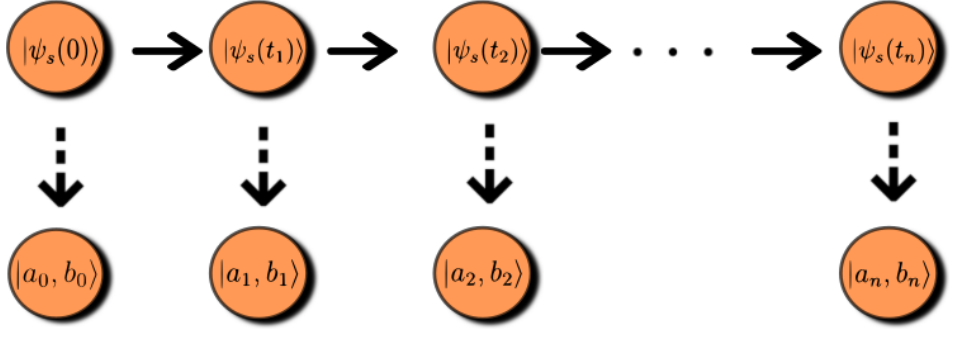


Figure 3.4: BN for the dynamical evolution of a quantum system. The upper line describes the global state evolution (which we often call *hidden layer*) and the dashed arrows indicate the causal dependence of the reduced states on the global states at each instant  $t_k$ .

where we omitted the conditional probabilities from  $\psi_s(t_k)$  to  $\psi_s(t_{k+1})$  since these transitions are deterministic and thus the conditional probabilities are 1 and, remembering,  $P_s$  is the ensemble probability distribution of the initial state of Eq. (3.40). Consequently, the only global probability on which this joint distribution depends is on the initial ensemble  $\{\psi_s(0)\}_s$ .

Finally, for obtaining a conditional trajectory  $(a_0, b_0, a_1, b_1, \dots, a_n, b_n)$  of the reduced states, we must only marginalize over all  $s$  from the initial density matrix ensemble

$$\mathcal{P}(a_0, b_0, a_1, b_1, \dots, a_n, b_n) = \sum_s P_s P(a_0, b_0 | \psi_s(0)) P(a_1, b_1 | \psi_s(t_1)) \cdots P(a_n, b_n | \psi_s(t_n)). \quad (3.44)$$

These results will be essential for obtaining the average shifts observable in the second project of the thesis, shown in Chapter 7.



# Chapter 4

## Continuous Variables Framework

### 4.1 Bosonic modes

In this chapter, we shall describe the framework of quantum continuous variables. This exposition is based mostly on Serafini's pedagogical compendium [14], also well-marked references can be founded in [15, 16]. The subject consists of the set of tools needed to describe the degrees of freedom that satisfy canonical commutation relations (CCR)

$$\boxed{[\hat{q}_j, \hat{p}_j] = i}, \quad (4.1)$$

where  $\hat{q}_j$  and  $\hat{p}_j$  are, respectively, the position and momentum operators<sup>1</sup> of the degree of freedom  $j$ . The degrees of freedom that satisfy Eq. (4.1) are called *bosonic modes* (in contrast to *fermionic modes* that satisfy anti-commutation relations).

This structure is widely used in quantum optics [55, 56], quantum information and quantum computation [1, 2, 15, 117], for instance in continuous variables clusters [118], many-body and condensed matter physics [119, 120]. In our case, we shall use it in our first project to describe a CM in which the system and ancillae are bosonic modes as a realization of the bosonic case described in the subsection 2.3.7 and in the second project as an application of the heat distribution obtained with QBNs.

We will focus on using *Gaussian states* and *Gaussian operations*. This enables

---

<sup>1</sup>In this chapter, as well as in the chapters involving continuum variables, we identify all operators acting on some Hilbert space with a hat. The reason for such terminology will make itself clear in the following sections.

us to describe the effects of the environment in the system with the same idea of tracing out the environment as in Eq. (2.12) but with a much smaller number of variables. This will simplify dramatically the complexity of our computations.

### 4.1.1 Canonical vectors

We now define some objects concerning bosonic modes that will simplify our treatment and notation. We start with the vector of operators

$$\hat{\mathbf{r}} = (\hat{q}_1, \hat{p}_1, \hat{q}_2, \hat{p}_2, \dots, \hat{q}_n, \hat{p}_n)^\top, \quad (4.2)$$

where  $n$  is the total number of modes of the system in question. As we can see,  $\hat{\mathbf{r}}$  is nothing but the vector of all canonical operators (or quadratures) of a system.

Moreover, we have the creation and annihilation operators  $\hat{a}_j^\dagger$  and  $\hat{a}_j$ , related to the quadrature variables by

$$\hat{a}_j = \frac{\hat{q}_j + i\hat{p}_j}{\sqrt{2}}, \quad (4.3)$$

the main importance of these last operators becomes clear in the *second quantization* context, as will be detailed later in this Chapter, in Section 4.2. For arranging these operators we define the vector

$$\hat{\mathbf{a}} = (\hat{a}_1, \hat{a}_1^\dagger, \hat{a}_2, \hat{a}_2^\dagger, \dots, \hat{a}_n, \hat{a}_n^\dagger)^\top. \quad (4.4)$$

The elements of  $\hat{\mathbf{a}}$  can be related to the elements of  $\hat{\mathbf{r}}$  by means of Eq. (4.3), resulting in

$$\hat{\mathbf{a}} = \bar{U}\hat{\mathbf{r}}, \quad (4.5)$$

where<sup>2</sup>

$$\bar{U} = \bigoplus_{j=1}^n \bar{u}, \quad \text{with } \bar{u} = \frac{1}{\sqrt{2}} \begin{pmatrix} 1 & i \\ 1 & -i \end{pmatrix}. \quad (4.6)$$

---

<sup>2</sup>The symbol  $\oplus$  means the *direct sum* operation, see Appendix C, Section C.2, for the definition.

### 4.1.2 CCRs and the symplectic form

Given a system of  $n$  bosonic modes ordered according to Eq. (4.2), we define a  $2n \times 2n$  matrix  $\Omega$  as

$$\begin{aligned}\Omega &= \bigoplus_{j=1}^n \Omega_1 \\ &= \mathbb{I}_n \otimes \Omega_1, \\ \text{where } \Omega_1 &= \begin{pmatrix} 0 & 1 \\ -1 & 0 \end{pmatrix},\end{aligned}\tag{4.7}$$

called *symplectic form*. It has the following properties that shall be useful to us

$$\Omega = -\Omega^\top \quad (\text{anti-symmetric}),\tag{4.8}$$

$$\Omega = -\Omega^{-1} \Leftrightarrow \Omega^2 = -\mathbb{I}_{2n},\tag{4.9}$$

$$\Omega\Omega^\top = \Omega^\top\Omega = -\Omega^2 = \mathbb{I}_{2n},\tag{4.10}$$

where  $\mathbb{I}_k$  is the  $k \times k$  identity matrix.

The importance of the symplectic form makes itself clear when we write the CCR (Eq. (4.1)) in terms of  $\hat{\mathbf{r}}$ , resulting in

$$\boxed{[\hat{\mathbf{r}}, \hat{\mathbf{r}}^\top] = i\Omega},\tag{4.11}$$

where we used the notation given in Appendix C, specially Eqs. (C.3) and (C.6). This will be the cornerstone to define the symplectic group during this chapter.

## 4.2 Second quantization and the Fock space

The second quantization formalism is based on the idea of counting how many particles or “field excitations” each bosonic mode has. It is based on the structure existent from the creation and annihilation operators (Eq. (4.3)). If a mode  $j$  has its local Hamiltonian  $\hat{H}_j = \omega_j \left( \hat{a}_j^\dagger \hat{a}_j + \frac{1}{2} \right)$ , then the eigenvectors of such Hamiltonian are discretized as  $|m\rangle_j$ , where  $m$  is a natural number. This way, the spectrum will

be

$$H_j |m\rangle_j = \omega_j \left(m + \frac{1}{2}\right) |m\rangle_j, \quad (4.12)$$

having a lower bound when  $m = 0$  such that  $\hat{a}_j |0\rangle_j = 0$ . The eigenvectors  $|m\rangle_j$  relate to themselves and with the operators as

$$\hat{a}_j |m\rangle_j = \sqrt{m} |m-1\rangle_j, \quad (4.13)$$

$$\hat{a}_j^\dagger |m\rangle_j = \sqrt{m+1} |m+1\rangle_j. \quad (4.14)$$

The results above are just the standard Simple Quantum Harmonic Oscillator solution that can be found in any Quantum Mechanics textbook. But now this structure is used to interpret the excitations as the number of particles in a mode. For instance  $|3\rangle_j$  represents a state with 3 particles in the mode  $j$ ,  $|8\rangle_k$  a state with 8 particles in the mode  $k$  and so on. The space to accommodate this scheme is called *Fock space*, which is the tensor product of the Hilbert spaces corresponding to each number of particles.<sup>3</sup> For a mode  $j$ , the corresponding Fock space is

$$\mathcal{F}_j = \mathcal{H}_0^j \otimes \mathcal{H}_1^j \otimes \mathcal{H}_2^j \otimes \mathcal{H}_3^j \otimes \dots = \bigotimes_{m=0}^{\infty} \mathcal{H}_m^j, \quad (4.15)$$

where  $\mathcal{H}_m^j$  is the Hilbert space with  $m$  particles of the mode  $j$ . A tensor product of all the eigenvectors of the free mode Hamiltonian (like in Eq. (4.12)) is called a *Fock basis*, and is a basis of the Fock space. Finally, if we are working with a system of  $n$  modes, the full Hilbert space will be

$$\mathcal{H} = \bigotimes_{j=1}^n \mathcal{F}_j. \quad (4.16)$$

In this work, we shall always be acting in a Hilbert space like in Eq. (4.16) whenever we have a system of  $n$  bosonic modes.

---

<sup>3</sup>It is important to remember that the tensor product of Hilbert spaces is also a Hilbert space, thus Fock spaces are Hilbert spaces.

### 4.3 Displacement operator and coherent states

Of major importance in continuous variable quantum mechanics is the unitary *displacement operator* (or *Weyl operator*) defined as

$$\hat{D}_{\mathbf{r}} = e^{i\mathbf{r}^\top \Omega \hat{\mathbf{r}}}, \quad (4.17)$$

where  $\mathbf{r}$  is an arbitrary  $2n$  vector with real components, and notice that  $\hat{D}_{\mathbf{r}}^\dagger = \hat{D}_{-\mathbf{r}}$ . The name “displacement” turns out to be intuitive if we look at the following property

$$\boxed{\hat{D}_{\mathbf{r}}^\dagger \hat{\mathbf{r}} \hat{D}_{\mathbf{r}} = \hat{\mathbf{r}} - \mathbf{r}}, \quad (4.18)$$

i.e., the action of this unitary on the vector of canonical operators is just its displacement (this equation is proved in Appendix C, Section C.4).

Another relation frequently used is the *composition* property

$$\boxed{\hat{D}_{\mathbf{r}_1 + \mathbf{r}_2} = \hat{D}_{\mathbf{r}_1} \hat{D}_{\mathbf{r}_2} e^{i\mathbf{r}_1^\top \Omega \mathbf{r}_2 / 2}}, \quad (4.19)$$

where  $\mathbf{r}_1$  and  $\mathbf{r}_2$  are generic  $2n$  vectors with real components. The composition property can be proved by direct application of the *Baker-Campbell-Hausdorff* (BCH) or *Zassenhaus* formula,<sup>4</sup> and it can be an alternative way of defining the non-commutative properties of the canonical quantum operators.

Displacement operators are also used to define *coherent states*, which may be seen as a cornerstone to phase space methods in continuum variables. First, define  $\alpha$  as a vector of length  $n$  with complex components

$$\alpha_j = (q_j + ip_j) / \sqrt{2}, \quad (4.21)$$

with  $q_j$  and  $p_j$  being real numbers. And define the  $2n$  real vector  $\mathbf{r}$  related to  $q_j$  and

---

<sup>4</sup>This formula can be formulated as follows, let  $\hat{A}$  and  $\hat{B}$  be operators, then

$$e^{\hat{A} + \hat{B}} = e^{\hat{A}} e^{\hat{B}} e^{-\frac{1}{2i} [\hat{A}, \hat{B}]} e^{\frac{1}{3i} (2[\hat{B}, [\hat{A}, \hat{B}]] + [\hat{A}, [\hat{A}, \hat{B}]])} \dots \quad (4.20)$$

$p_j$  as

$$\mathbf{r} = (q_1, p_1, q_2, p_2, \dots, q_n, p_n)^\top. \quad (4.22)$$

Then we can rewrite Eq. (4.17) as

$$\hat{D}_\alpha = \hat{D}_{-\mathbf{r}} = e^{\sum_{j=1}^n (\alpha_j \hat{a}_j^\dagger - \alpha_j^* \hat{a}_j)}. \quad (4.23)$$

It can be shown, using the BCH formula, that

$$\boxed{\hat{D}_\alpha^\dagger \hat{a}_j \hat{D}_\alpha = \hat{a}_j + \alpha_j.} \quad (4.24)$$

We are now in the position to define the coherent state  $|\alpha\rangle$  as

$$\boxed{|\alpha\rangle = \hat{D}_\alpha |0\rangle,} \quad (4.25)$$

where  $|0\rangle = \bigotimes_{j=1}^n |0\rangle_j$  is the vacuum of the whole Hilbert space of Eq. (4.16). Consequently,  $|\alpha\rangle$  is the eigenvector of the  $\hat{a}_j$  operators (see the proof of the following equation in Appendix C, Section C.5)

$$\hat{a}_j |\alpha\rangle = \alpha_j |\alpha\rangle. \quad (4.26)$$

It is often useful to describe a coherent state  $|\alpha\rangle$ <sup>5</sup> in the Fock basis. This is given by the following equation (see Appendix C, Section C.6, for the proof)

$$\boxed{|\alpha\rangle = \sum_{m=0}^{\infty} e^{-|\alpha|^2/2} \frac{\alpha^m}{\sqrt{m!}} |m\rangle.} \quad (4.27)$$

Other important properties for further use are

$$\boxed{\hat{D}_\alpha \hat{D}_\beta = e^{\frac{1}{2}(\alpha\beta^* - \alpha^*\beta)} \hat{D}_{\alpha+\beta},} \quad (4.28)$$

this is equivalent to the composition property of Eq. (4.19), and the overlap between

---

<sup>5</sup>In this case, as in all the following results and demonstrations, we will assume all coherent states as being of only one mode (say, mode  $k$ ), i.e.,  $|\alpha_k\rangle = \hat{D}_{\alpha_k} |0\rangle$ , where  $\hat{D}_{\alpha_k} = e^{\alpha_k \hat{a}_k^\dagger - \alpha_k^* \hat{a}_k}$  but we shall omit the  $k$  for simplicity of notation. The generalization to a number  $n$  of modes is straightforward since  $|\alpha\rangle = \bigotimes_{j=1}^n |\alpha_j\rangle$  and  $\hat{D}_\alpha = \prod_{j=1}^n \hat{D}_{\alpha_j}$ .

two coherent states  $|\alpha\rangle$  and  $|\beta\rangle$

$$\begin{aligned}
 \langle\beta|\alpha\rangle &= \langle 0|\hat{D}_{-\beta}\hat{D}_\alpha|0\rangle \\
 &= \langle 0|\hat{D}_{\alpha-\beta}|0\rangle e^{\frac{1}{2}(\alpha\beta^*-\alpha^*\beta)} \\
 &= \langle 0|\alpha-\beta\rangle e^{\frac{1}{2}(\alpha\beta^*-\alpha^*\beta)} \\
 &= e^{-\frac{1}{2}|\alpha-\beta|^2} e^{\frac{1}{2}(\alpha\beta^*-\alpha^*\beta)}, \tag{4.29}
 \end{aligned}$$

where in the second equality we used Eq. (4.28) and in the last equality we applied  $\langle 0|$  in Eq. (4.27) to obtain the overlap between  $|0\rangle$  and a coherent state. This overlap results in

$$\begin{aligned}
 \langle 0|\alpha\rangle &= \sum_{m=0}^{\infty} e^{-|\alpha|^2/2} \frac{\alpha^m}{\sqrt{m!}} \langle 0|m\rangle \\
 &= \sum_{m=0}^{\infty} e^{-|\alpha|^2/2} \frac{\alpha^m}{\sqrt{m!}} \delta_{0,m} \\
 &= e^{-|\alpha|^2/2}.
 \end{aligned}$$

Moreover, the set of all the coherent states  $\{|\alpha\rangle, \alpha \in \mathbb{C}\}$  form an “overcomplete” basis for the Hilbert space of the corresponding mode. This means that, although it is not an orthogonal set, as we can see in Eq. (4.29), the set can span all the Hilbert space. Indeed, a completeness relation can be shown (see Appendix C, Section C.7) involving the coherent basis

$$\boxed{\frac{1}{\pi} \int_{\mathbb{C}} d^2\alpha |\alpha\rangle \langle\alpha| = \hat{\mathbb{I}}}, \tag{4.30}$$

where  $\hat{\mathbb{I}}$  is the identity operator of the Hilbert space and  $\int_{\mathbb{C}} d^2\alpha$  means an integration over the entire complex plane. This provides an alternative way of computing the

trace of an operator by using continuous variables

$$\begin{aligned}
 \text{Tr}\{\hat{A}\} &= \sum_{m=0}^{\infty} \langle m | \hat{A} | m \rangle \\
 &= \frac{1}{\pi} \int_{\mathbb{C}} d^2\alpha \sum_{m=0}^{\infty} \langle m | \alpha \rangle \langle \alpha | \hat{A} | m \rangle \\
 &= \frac{1}{\pi} \int_{\mathbb{C}} d^2\alpha \langle \alpha | \hat{A} \sum_{m=0}^{\infty} | m \rangle \langle m | \alpha \rangle \\
 &= \frac{1}{\pi} \int_{\mathbb{C}} d^2\alpha \langle \alpha | \hat{A} | \alpha \rangle.
 \end{aligned} \tag{4.31}$$

To end our presentation about coherent states and displacement operators, we shall present the *Fourier-Weyl relation*. This is the statement that any bounded operator  $\hat{A}$  acting on the Hilbert space of a mode can be constructed by an integral of displacement operators weighted by  $\text{Tr}\{\hat{D}_\alpha \hat{A}\}$  (see the proof in Appendix C, Section C.8). More precisely

$$\boxed{\hat{A} = \frac{1}{\pi} \int_{\mathbb{C}} d^2\alpha \text{Tr}\{\hat{D}_\alpha \hat{A}\} \hat{D}_{-\alpha}.} \tag{4.32}$$

This relation follows an idea similar to a Fourier expansion. When we have a function of a real variable  $x$  expanded as  $f(x) = \frac{1}{2\pi} \int dp \mathcal{F}(p) e^{-ixp}$ , the weight here is the Fourier transform  $\mathcal{F}(p)$  and the function  $e^{-ixp}$  has the same role as the displacement operator in Eq. (4.32). This parallel will be useful to gain some intuition on the concept of *characteristic function* of a density matrix, which will be discussed below in Sec. 4.4.

A direct consequence of the Fourier-Weyl relation is the orthogonality relation<sup>6</sup> for displacement operators. If we put the displacement operator itself as  $\hat{A}$  in Eq. (4.32), we obtain

$$\hat{D}_\beta = \frac{1}{\pi} \int_{\mathbb{C}} d^2\alpha \text{Tr}\{\hat{D}_\alpha \hat{D}_\beta\} \hat{D}_{-\alpha},$$

---

<sup>6</sup>This orthogonality is defined in terms of the *Hilbert-Schmidt inner product* between two operators. Given two operators  $\hat{A}$  and  $\hat{B}$  in a Hilbert space, their Hilbert-Schmidt inner product will be  $\text{Tr}\{\hat{A}^\dagger \hat{B}\}$ .



which means that we can treat the trace term as a Dirac delta function

$$\boxed{\text{Tr}\{\hat{D}_{-\alpha}\hat{D}_{\beta}\} = \pi\delta^2(\beta - \alpha),} \quad (4.33)$$

which is the desired orthogonality relation. Moreover, the orthogonality relation can be rewritten for  $n$  modes in the real plane as

$$\boxed{\text{Tr}\{\hat{D}_{\mathbf{r}}\hat{D}_{-\mathbf{s}}\} = (2\pi)^n\delta^{2n}(\mathbf{r} - \mathbf{s}).} \quad (4.34)$$

## 4.4 Characteristic function

The *characteristic function* of a density matrix  $\hat{\rho}$  is the weight function of the Fourier-Weil relation (Eq. (4.32)) if we expand the density matrix itself. More precisely, if

$$\hat{\rho} = \frac{1}{\pi} \int_{\mathbb{C}} d^2\alpha \chi(\alpha) \hat{D}_{-\alpha}, \quad (4.35)$$

then, from the Fourier-Weyl relation (Eq. (4.32))

$$\chi(\alpha) = \text{Tr}\{\hat{D}_{\alpha}\hat{\rho}\} \quad (4.36)$$

is the characteristic function. The existence of this function for every  $\hat{\rho}$  is guaranteed by the validity of the Fourier-Weyl relation.

From making the straightforward generalization to  $n$  modes and the change of variables from  $\alpha$  to  $\mathbf{r}$  (given by Eq. (4.21)), Eq. (4.35) results in

$$\hat{\rho} = \frac{1}{(2\pi)^n} \int_{\mathbb{R}^{2n}} d\mathbf{r} \chi(\mathbf{r}) \hat{D}_{\mathbf{r}}, \quad (4.37)$$

where  $d\mathbf{r} = dq_1 dp_1 dq_2 dp_2 \cdots dq_n dp_n$  similar to a phase space integral, and

$$\chi(\mathbf{r}) = \text{Tr}\{\hat{D}_{-\mathbf{r}}\hat{\rho}\}. \quad (4.38)$$

Again, this follows the same reasoning as the characteristic function  $\varphi(y)$  of a probability density function  $p(x)$ , which are related by  $p(x) = \frac{1}{2\pi} \int dy \varphi(y) e^{-ixy}$ .

Here the characteristic function is the Fourier transform of the probability density and has the role of a weight function in the integral, similarly  $\chi(\mathbf{r})$  has the role of the weight and  $\hat{D}_{\mathbf{r}}$  has the role of  $e^{-ixy}$  in Eq. (4.37).

Since a physical density matrix  $\hat{\rho}$  must satisfy a set of properties, there is also a set of properties that  $\chi(\mathbf{r})$  must satisfy in order to describe a physical state. First of all, from the definition we can conclude that the characteristic function must be a continuous function. Now, from the normalization condition of Eq. (2.5), we must have

$$\begin{aligned}\chi(0) &= \text{Tr}\{\hat{D}_0\hat{\rho}\} \\ &= \text{Tr}\{\hat{\rho}\} \\ &= 1,\end{aligned}\tag{4.39}$$

where 0 here means the  $2n$  vector of entries 0 and we used that  $\hat{D}_0 = \mathbb{I}$ , where  $\mathbb{I}$  is the  $2n$  identity matrix. Furthermore, the positive semi-definite condition ( $\hat{\rho} \geq 0$ ) is equivalent to following condition over the characteristic function  $\chi(\mathbf{r})$ :

$$\Upsilon \geq 0,\tag{4.40}$$

where  $\Upsilon$  is a  $2n \times 2n$  complex matrix, completely defined given a characteristic function  $\chi(\mathbf{r})$ , such that  $\Upsilon_{jk} = \chi(\mathbf{r}_j - \mathbf{r}_k)e^{i\mathbf{r}_k^\top \Omega \mathbf{r}_j}/2$ . The justification for this condition can be found in Ref. [14].

Also, from the fact that  $\hat{\rho}$  is hermitian, we must have  $\chi(\mathbf{r})^* = \chi(-\mathbf{r})$  and it can be shown that this is also a consequence of  $\Upsilon \geq 0$  (as it should be since  $\hat{\rho} \geq 0$  implies  $\hat{\rho}$  hermitian).

## 4.5 Quasi-probability distributions

If we construct a phase space of a system with the eigenvalues of canonical operators, it is possible to define weight functions in this phase space which are used to compute the average of observables. These weight functions are called *quasi-probability distributions* since they don't satisfy necessary probability distribution properties

but can have similar interpretations.

### 4.5.1 Wigner function

We can define the *Wigner function* (or *W-function*) as the Fourier transform of the characteristic function

$$W(\alpha) = \frac{1}{\pi^2} \int_{\mathbb{C}} d\beta^2 \chi(\alpha) e^{(\alpha\beta^* - \alpha^*\beta)}. \quad (4.41)$$

Going to a phase space constructed with the eigenvalues of the quadrature operators, via Eq. (4.21), we obtain (see Appendix C, Section C.9)

$$W(q, p) = \frac{2}{\pi} \int_{\mathbb{R}} dq' e^{i2pq'} \langle q - q' | \hat{\rho} | q + q' \rangle. \quad (4.42)$$

Now, if we integrate  $W(q, p)$  over all  $p$ , we have

$$\boxed{\frac{1}{2} \int_{-\infty}^{\infty} dp W(q, p) = \langle q | \hat{\rho} | q \rangle}, \quad (4.43)$$

so the integral of the Wigner function over the quadrature eigenvalues of  $p$  is twice the probability distribution of the projective measuring of the conjugate quadrature  $q$ . Analogous results are easily obtained for any pair of quadrature operators.

### 4.5.2 The s-ordered quasi-probability distribution

For  $s \in [-1, 1]$ , we can define the *s-ordered characteristic function* as

$$\chi_s(\alpha) = \text{Tr}(\hat{D}_\alpha \hat{\rho}) e^{\frac{s}{2}|\alpha|^2}, \quad (4.44)$$

reducing to the characteristic function  $\chi_s(\alpha)$  when  $s = 0$ , that is  $\chi_0(\alpha) = \chi(\alpha)$ .

Further, we can define the *s-ordered quasi-probability distribution*  $W_s(\alpha)$  as the Fourier transform of the s-ordered characteristic function

$$W_s(\alpha) = \frac{1}{\pi^2} \int_{\mathbb{C}} d^2\beta e^{(\alpha\beta^* - \alpha^*\beta)} \chi_s(\beta), \quad (4.45)$$

which reduces to the Wigner function for the case of  $s = 0$ .

This is a normalized function, since

$$\begin{aligned} \int_{\mathbb{C}} d^2\alpha W_s(\alpha) &= \int_{\mathbb{C}} d^2\beta \delta^2(\beta) \chi_s(\beta) \\ &= \chi(0) \\ &= 1. \end{aligned} \tag{4.46}$$

We shall expose in the following that other important quasi-probabilities result from the  $s$ -ordered quasi-probabilities for  $s = 1$  and  $s = -1$ .

### 4.5.3 Glauber-Sudarshan P-function

For the case of  $s = 1$ , the  $s$ -ordered quasi-probability satisfies an exceptional property. It will be the function responsible for the diagonal decomposition of the density matrix described by the modes of  $\alpha$ , i.e., if we define  $P(\alpha) = W_1(\alpha)$ , then

$$\hat{\rho} = \int_{\mathbb{C}} d^2\alpha P(\alpha) |\alpha\rangle \langle\alpha|. \tag{4.47}$$

The equation above is proved in Appendix C, Section C.10, and  $P(\alpha)$  is called the *Glauber-Sudarshan P-representation* (or *P-function*).

### 4.5.4 Husimi Q-function

One can define the *Husimi Q-function* as

$$Q(\alpha) = W_{-1}(\alpha). \tag{4.48}$$

The function  $Q(\alpha)$  receives the interpretation of being the probability of a *heterodyne measurement* to yield the outcome  $\alpha$ . A heterodyne measurement is a generalized measurement with Kraus matrices  $M_\alpha = \frac{1}{\sqrt{\pi}} |\alpha\rangle \langle\alpha|$ , where  $|\alpha\rangle$  is a coherent state. These measurements are of major importance in Quantum Optics [55,

121, 122]. One can prove (see Appendix C, Section C.11, for the proof) that

$$Q(\alpha) = \frac{1}{\pi} \langle \alpha | \hat{\rho} | \alpha \rangle, \quad (4.49)$$

and hence the Husimi Q-function is a valid probability distribution.

Finally, it is worth mentioning that the quasi-probability distributions are extremely useful to computations of averages of creation and annihilation operators in normal, anti-normal, and symmetric ordering [14, 55, 123]. In this thesis, we shall not use such properties directly.

## 4.6 Gaussian states

### 4.6.1 Definitions

We start by defining the *second-order Hamiltonian* as a Hamiltonian that is constructed as a degree two polynomial of canonical operators, we chose to study the case where

$$\hat{H} = \frac{1}{2} \hat{\mathbf{r}}^\top H \hat{\mathbf{r}} + \hat{\mathbf{r}}^\top \mu, \quad (4.50)$$

where  $H$  is a  $2n \times 2n$  real matrix and a positive definite matrix ( $H > 0$ )<sup>7</sup> called the *Hamiltonian matrix*<sup>8</sup> (notice that this is not the Hamiltonian *operator*) and  $\mu$  is a real vector with dimension  $2n$ . A more suitable way of representing general second-order Hamiltonians is given as follows. If we assign

$$\tilde{\mathbf{r}} = -H^{-1}\mu, \quad (4.51)$$

---

<sup>7</sup> $H$  must be symmetric (since  $\hat{H}$  must be hermitian). But, additionally, the positive definite restriction is there to ensure the thermodynamic stability of the thermal state (i.e., their eigenvalues must be positive and bounded from below).

<sup>8</sup>The term *Hamiltonian matrix* is often given to the matrix  $\Omega H$  by many authors. We follow a different nomenclature in order to agree with Ref. [14].

then, except for a constant term, we can write

$$\begin{aligned}\hat{H} &= \frac{1}{2} \hat{D}_{-\tilde{\mathbf{r}}} \hat{\mathbf{r}}^\top H \hat{D}_{\tilde{\mathbf{r}}} \\ &= \frac{1}{2} (\hat{\mathbf{r}} - \tilde{\mathbf{r}})^\top H (\hat{\mathbf{r}} - \tilde{\mathbf{r}}).\end{aligned}\tag{4.52}$$

Equipped with these definitions, we define Gaussian states as *thermal states with a second-order Hamiltonian  $\hat{H}$  in which its Hamiltonian matrix is positive definite  $H > 0$*

$$\boxed{\hat{\rho}_G = \frac{e^{-\beta \hat{H}}}{Z}},\tag{4.53}$$

where  $Z = \text{Tr}\{e^{-\beta \hat{H}}\}$  is the partition function and  $\beta > 0$  is the inverse of the temperature (here we also always set the Boltzmann constant to 1). This definition includes pure states, which can be taken as the limit of the above equation with  $\beta \rightarrow \infty$

$$\hat{\rho}_{\text{pure}} = \lim_{\beta \rightarrow \infty} \frac{e^{-\beta \hat{H}}}{Z}.\tag{4.54}$$

Another important concept in the context of Gaussian states is the statistical moments, i.e., the averages of different orders of canonical operators. The *first moments* are the average of the canonical operators

$$\boxed{\langle \hat{\mathbf{r}} \rangle = \text{Tr}\{\hat{\rho}_G \hat{\mathbf{r}}\}}.\tag{4.55}$$

As for the second moment, it is convenient to combine them in terms of the *covariance matrix*

$$\boxed{\begin{aligned}\sigma &= \frac{1}{2} \text{Tr} \left[ \hat{\rho}_G \{(\hat{\mathbf{r}} - \bar{\mathbf{r}}), (\hat{\mathbf{r}} - \bar{\mathbf{r}})^\top\} \right] \\ &= \frac{1}{2} \left\langle \{(\hat{\mathbf{r}} - \bar{\mathbf{r}}), (\hat{\mathbf{r}} - \bar{\mathbf{r}})^\top\} \right\rangle,\end{aligned}}\tag{4.56}$$

where the anti-commutator inside the trace is defined just like in Appendix C, Section C.1 and we defined  $\bar{\mathbf{r}} = \langle \hat{\mathbf{r}} \rangle$  (see Eq. (4.55)). If we execute the anti-commutator, use the distributive property of averages, and use Eq. (4.11) in the

equation above, we obtain

$$\sigma = \langle \hat{\mathbf{r}} \hat{\mathbf{r}}^\top \rangle - \langle \hat{\mathbf{r}} \rangle \langle \hat{\mathbf{r}} \rangle^\top - \frac{i}{2} \Omega, \quad (4.57)$$

which can be a much more suitable way of computing the covariance matrix.

### 4.6.2 Bona-fide conditions for covariance matrices

Given that covariance matrices represent the second moments of canonical operators, they must have restrictions on their components due to uncertainty relations. The restriction is given by the following inequality (see Appendix C, Section C.12, for the proof of this condition)

$$\sigma + \frac{i\Omega}{2} \geq 0. \quad (4.58)$$

This is the restriction that a covariance matrix must obey to represent a valid quantum state and is called *Roberson-Schrödinger relation*, or also referred to as *bona-fide* condition.

### 4.6.3 Dynamics of canonical operators and statistical moments

We start our development for the dynamics of Gaussian states by analyzing the evolution of the vector of canonical operators  $\hat{\mathbf{r}}$  in the Heisenberg picture for closed systems under the action of a second-order Hamiltonian from Eqs. (4.50) and (4.52). Additionally, we analyze the evolution of the statistical moments for closed systems under the same Hamiltonian.

For the vector of canonical operators, the Heisenberg Equation implies

$$\frac{d\hat{\mathbf{r}}_j}{dt} = (\Omega H \hat{\mathbf{r}})_j + (\Omega \mu)_j. \quad (4.59)$$

The equation above is equivalent to stating that, remembering that  $H > 0$ ,

$$\begin{aligned}\frac{d\hat{\mathbf{r}}}{dt} &= \Omega(H\hat{\mathbf{r}} + \mu) \\ &= \Omega H(\hat{\mathbf{r}} + H^{-1}\mu).\end{aligned}\tag{4.60}$$

So, if we define  $\hat{\mathbf{r}}'$  such that

$$\hat{\mathbf{r}} = \hat{\mathbf{r}}' - H^{-1}\mu,\tag{4.61}$$

then

$$\frac{d\hat{\mathbf{r}}'}{dt} = \Omega H\hat{\mathbf{r}}',\tag{4.62}$$

which has the solution

$$\hat{\mathbf{r}}'(t) = e^{\Omega H(t-t_0)}\hat{\mathbf{r}}'(t_0).$$

Now using that  $\hat{\mathbf{r}}'(t_0) = \hat{\mathbf{r}}(t_0) + H^{-1}\mu$  and  $\hat{\mathbf{r}}'(t) = \hat{\mathbf{r}}(t) + H^{-1}\mu$  in the equation above, we obtain

$$\hat{\mathbf{r}}(t) = e^{\Omega H(t-t_0)}\hat{\mathbf{r}}(t_0) + \left(e^{\Omega H(t-t_0)} - \mathbb{I}\right) H^{-1}\mu,\tag{4.63}$$

where  $\mathbb{I}$  is the  $2n \times 2n$  identity operator. This is the general solution for the Heisenberg vector of canonical operators that we intended to find. The solution above can be rewritten in terms of  $\tilde{\mathbf{r}}$  from Eq. (4.51) as

$$\boxed{\hat{\mathbf{r}}(t) = \hat{D}_{\tilde{\mathbf{r}}} \left( e^{\Omega H(t-t_0)} \hat{D}_{-\tilde{\mathbf{r}}} \hat{\mathbf{r}}(t_0) \hat{D}_{\tilde{\mathbf{r}}} \right) \hat{D}_{-\tilde{\mathbf{r}}}.\tag{4.64}}$$

Notice that the general solution above reduces to the simple form

$$\boxed{\hat{\mathbf{r}}(t) = e^{\Omega H(t-t_0)}\hat{\mathbf{r}}(t_0),\tag{4.65}}$$

if  $\mu = 0$ . The general solution of Eq. (4.64) can be understood as translating  $\hat{\mathbf{r}}(t_0)$  so that the Hamiltonian has purely quadratic terms in this new frame (see Eq. (4.52)); making the quadratic Hamiltonian evolution and then translating back the vector to its initial frame.

Focusing now on the dynamics of statistical moments, we start by studying the first moment's evolution. The time derivative for the vector of the first moments



given in Eq. (4.55) can be obtained by applying the density matrix  $\hat{\rho}$  in both sides of Eq. (4.60) and taking the trace, arriving at

$$\frac{d\langle\hat{\mathbf{r}}\rangle}{dt} = \Omega(H\langle\hat{\mathbf{r}}\rangle + \mu). \quad (4.66)$$

The equation above has the exact same structure as Eq. (4.60), thus its solution is analogous

$$\boxed{\langle\hat{\mathbf{r}}(t)\rangle = \langle\hat{D}_{\hat{\mathbf{r}}}\left(e^{\Omega H(t-t_0)}\hat{D}_{-\hat{\mathbf{r}}}\hat{\mathbf{r}}(t_0)\hat{D}_{\hat{\mathbf{r}}}\right)\hat{D}_{-\hat{\mathbf{r}}}\rangle}. \quad (4.67)$$

Again, if the Hamiltonian has no linear term ( $\mu = 0$ ), we have

$$\boxed{\langle\hat{\mathbf{r}}(t)\rangle = e^{\Omega H(t-t_0)}\langle\hat{\mathbf{r}}(t_0)\rangle}. \quad (4.68)$$

For the second moment, we study the evolution of the covariance matrix. From taking the derivative of Eq. (4.57) with respect to time, we obtain

$$\frac{d\sigma}{dt} = \frac{d}{dt}\langle\hat{\mathbf{r}}\hat{\mathbf{r}}^\top\rangle - \frac{d\langle\hat{\mathbf{r}}\rangle}{dt}\langle\hat{\mathbf{r}}\rangle^\top - \langle\hat{\mathbf{r}}\rangle\frac{d\langle\hat{\mathbf{r}}\rangle^\top}{dt}, \quad (4.69)$$

for computing the term with  $\frac{d}{dt}\langle\hat{\mathbf{r}}\hat{\mathbf{r}}^\top\rangle$  we observe that, in the Heisenberg picture,

$$\begin{aligned} \frac{d}{dt}(\hat{\mathbf{r}}\hat{\mathbf{r}}^\top) &= \frac{d\hat{\mathbf{r}}}{dt}\hat{\mathbf{r}}^\top + \hat{\mathbf{r}}\frac{d\hat{\mathbf{r}}^\top}{dt} \\ &= \Omega H\hat{\mathbf{r}}\hat{\mathbf{r}}^\top + \Omega\mu\hat{\mathbf{r}}^\top + \hat{\mathbf{r}}\hat{\mathbf{r}}^\top(\Omega H)^\top + \hat{\mathbf{r}}(\Omega\mu)^\top, \end{aligned}$$

where in the second equality we used Eq. (4.60) and the transpose of it. We can now apply the density matrix in the equation above and take the trace of it, obtaining

$$\frac{d}{dt}\langle\hat{\mathbf{r}}\hat{\mathbf{r}}^\top\rangle = \Omega H\langle\hat{\mathbf{r}}\hat{\mathbf{r}}^\top\rangle + \Omega\mu\langle\hat{\mathbf{r}}^\top\rangle + \langle\hat{\mathbf{r}}\hat{\mathbf{r}}^\top\rangle(\Omega H)^\top + \langle\hat{\mathbf{r}}\rangle(\Omega\mu)^\top. \quad (4.70)$$

Lastly, using Eq. (4.70), the transpose of it, Eq. (4.60) and the transpose of it in Eq. (4.69), we obtain

$$\boxed{\frac{d\sigma}{dt} = \Omega H\sigma + \sigma(\Omega H)^\top}, \quad (4.71)$$

which is our differential equation for a general second-order Hamiltonian evolution

of the covariance matrix. Its solution is simple and is given by

$$\boxed{\sigma(t) = e^{\Omega H(t-t_0)} \sigma(t_0) \left( e^{\Omega H(t-t_0)} \right)^\top}. \quad (4.72)$$

There are three things that must be observed in the solution above. First, the evolution of  $\sigma(t)$  does not depend on the first moment  $\langle \hat{\mathbf{r}}(t) \rangle$ , both of them evolve in a *decoupled* way. Second, the solution of  $\sigma(t)$  does not depend at all on the linear terms of the Hamiltonian, it only depends on the Hamiltonian matrix  $H$  of the quadratic part. Third, the matrix  $e^{\Omega H(t-t_0)}$  clearly plays a major role in both  $\sigma(t)$  and  $\langle \hat{\mathbf{r}}(t) \rangle$  solutions; for this reason, and further simplifications in the following of the thesis, we shall refer to it as  $S_H = e^{\Omega H t}$  (from now on we set  $t_0 = 0$  just for convenience).

#### 4.6.4 Symplectic operators

As already anticipated above, the matrix  $S_H$  has a major role in the evolution of statistical moments. We shall point out the condition that these operators must satisfy in order to describe valid a physical evolution for vectors of operators. These conditions are analogous to the condition of unitarity for evolution operators acting on Hilbert space states.

Since in our applications, we shall deal only with quadratic Hamiltonians without linear terms, and the extension to Hamiltonians with linear terms can be simply accounted with applications of displacement operators in Eqs. (4.52), (4.64) and (4.67), we shall from now on only consider quadratic Hamiltonians. Hence the evolution will be fully described by the Hamiltonian matrix  $H$ .

In this context (where  $\tilde{\mathbf{r}} = 0$ ) we obtain, by Eq. (4.65),

$$\hat{\mathbf{r}}(t) = \hat{S}_H^\dagger \hat{\mathbf{r}}(0) \hat{S}_H = S_H \hat{\mathbf{r}}(0), \quad (4.73)$$

where  $\hat{S}_H = e^{-i\hat{H}t}$  is the time evolution unitary operator. This implies, for any

vector of canonical operators  $\hat{\mathbf{r}}$ , that

$$\hat{S}_H^\dagger \hat{\mathbf{r}} \hat{S}_H = S_H \hat{\mathbf{r}}, \quad (4.74)$$

this equation makes explicit part of the enormous simplification that the continuous variables framework can offer to us. The left-hand side sets the evolution to the canonical operators given by the unitary operators acting at each one of the vector elements, remembering that these unitaries act on an infinite-dimensional Hilbert space. This evolution is equally obtained, on the right-hand side, by the action of a much simpler  $2n \times 2n$  matrix (with real components) on the canonical vector, simplifying manifestly our computations.

Notice that the evolution operator  $\hat{S}_H$  is unitary and thus represents a physical transformation between states. Therefore, it must maintain the CCR for the vectors of canonical operators  $\hat{\mathbf{r}}$ , i.e., if we call  $\hat{\mathbf{r}}' = \hat{S}_H^\dagger \hat{\mathbf{r}} \hat{S}_H$ , then we must also have  $[\hat{\mathbf{r}}', \hat{\mathbf{r}}'^\top] = i\Omega$ . This must imply, from Eq. (4.74) that

$$\begin{aligned} [\hat{\mathbf{r}}', \hat{\mathbf{r}}'^\top] &= [S_H \hat{\mathbf{r}}, (S_H \hat{\mathbf{r}})^\top] \\ &= S_H [\hat{\mathbf{r}}, \hat{\mathbf{r}}] S_H^\top \\ &= i S_H \Omega S_H^\top \\ &= i\Omega. \end{aligned} \quad (4.75)$$

The equation above implies that

$$S_H \Omega S_H^\top = \Omega,$$

is the necessary and sufficient condition for a real  $2n \times 2n$  matrix to be considered a transformation capable of substituting the unitary evolution as in Eq. (4.74). Stating properly, any  $2n \times 2n$  real matrix  $S$  that satisfies

$$\boxed{S \Omega S^\top = \Omega}, \quad (4.76)$$

is called a *symplectic transformation* and forms a *symplectic group* with the others

transformations satisfying this property,<sup>9</sup> in symbols  $S \in Sp_{2n, \mathbb{R}}$ . This is the group in which all the elements can possibly describe a physical unitary transformation acting in  $2n$  vectors of operators.

### 4.6.5 Covariance matrix parametrization

It can be shown that for Gaussian states we have a one-to-one parametrization of the density matrix in terms of the first moments and the covariance matrix of the state. More precisely, if we know the covariance matrix  $\sigma$  (Eq. (4.56)) and the first moments  $\bar{\mathbf{r}} = \langle \hat{\mathbf{r}} \rangle$  (Eq. (4.55)) of a Gaussian state than we can obtain its density matrix by the relation

$$\hat{\rho}_G = \frac{e^{-\frac{1}{2}(\hat{\mathbf{r}}-\bar{\mathbf{r}})^\top M(\hat{\mathbf{r}}-\bar{\mathbf{r}})}}{Z},$$

where  $M = 2\text{arccoth}(2i\Omega\sigma)i\Omega,$

(4.77)

and  $Z = \text{Tr} \left( e^{-\frac{1}{2}(\hat{\mathbf{r}}-\bar{\mathbf{r}})^\top M(\hat{\mathbf{r}}-\bar{\mathbf{r}})} \right)$  is just a normalization constant.

The proof for the parametrization of Eq. (4.77) can be found in Appendix C, Section C.16, and is made with the use of the *Normal Mode Decomposition* or *Williamson's theorem*. This theorem can be stated as follows. Suppose  $M$  is a  $2n \times 2n$  positive definite real matrix, then there is a symplectic transformation  $S \in Sp_{2n, \mathbb{R}}$ , such that

$$M = SDS^\top,$$
(4.78)

where

$$D = \text{diag}(d_1, d_1, \dots, d_n, d_n),$$
(4.79)

with  $d_j > 0, \forall j \in [1, \dots, n]$  called *symplectic eigenvalues*.<sup>10</sup> In Appendix C, Section C.14, we present a method of obtaining the symplectic eigenvalues given a positive definite matrix  $M$ .

Conversely, if we have the density matrix of a Gaussian operator  $\hat{\rho}_G$ , we can

---

<sup>9</sup>We call an application of a transformation  $A$  on a transformation  $\mathcal{O}$  as *application by congruence* when we have  $A\mathcal{O}A^\top$ . For instance, in Eq. (4.76) at the left hand side  $S$  acts by congruence in  $\Omega$ .

<sup>10</sup>The proof of this theorem can be found in Refs. [14, 124–128].

obtain its first moments and covariance matrix by Eqs. (4.55) and (4.56), thus completing the one to one correspondence.

This correspondence is another critical advantage of dealing with Gaussian states. A density matrix description of a bosonic Gaussian state requires infinite elements, while the description of a  $2n$  vector of averages and a  $2n \times 2n$  covariance matrix requires a finite number of parameters. This parametrization of quantum states in first and second moments is analogous to the intuitive parametrization of Gaussian probability distributions in terms of their first and second moments.

### 4.6.6 Characteristic function of Gaussian states

Another important aspect of Gaussian states is that their characteristic function has a particularly simple form. Using Eq. (4.77) in the definition of Eq. (4.38), one can show<sup>11</sup> that the characteristic function of a Gaussian state with first moments vector  $\bar{\mathbf{r}} = \langle \hat{\mathbf{r}} \rangle$  and covariance matrix  $\sigma$  is

$$\chi_G(\mathbf{r}) = e^{-\frac{1}{2}\mathbf{r}^\top \Omega^\top \sigma \Omega \mathbf{r}} e^{i\mathbf{r}^\top \Omega^\top \bar{\mathbf{r}}}. \quad (4.80)$$

Since a state is Gaussian if and only if its characteristic function has the form described above, this equation will be very useful to distinguish the Gaussianity of a state.

## 4.7 Gaussian operations

Given the very useful properties of Gaussian states pointed out above, it is of our interest to find quantum operations (in the sense of quantum channels, defined in Section 2.2) that preserve this Gaussian status of the states. These operations are called *Gaussian operations* or *Gaussian channels*.

In this thesis, we shall follow the protocol described in Section 2.2 for obtaining an open system evolution. This means that we will construct an initially uncorrelated joint system by making a tensor product between the system and the

---

<sup>11</sup>This is done in detail in Chapter 4 of Ref. [14].

environment state, then we shall make the unitary evolution of the joint state and finally trace out the environment in order to obtain the open system description. In the following, we will prove that all of such operations: the tensor product, the unitary evolution (generated by second-order Hamiltonians), and the partial trace, are Gaussian operations. This enables us to use only first moments and covariance matrices to completely describe our system during the evolution of our system and environment starting at Gaussian states.

### 4.7.1 Tensor product

Suppose two Gaussian states  $\hat{\rho}_A$  with  $m$  modes and  $\hat{\rho}_B$  with  $n$  modes, first moments  $\bar{\mathbf{r}}_A = \langle \hat{\mathbf{r}}_A \rangle$  and  $\bar{\mathbf{r}}_B = \langle \hat{\mathbf{r}}_B \rangle$  and covariance matrices  $\sigma_A$  and  $\sigma_B$  respectively. Using the Gaussian characteristic function (Eq. (4.80)) and Eq. (4.37), we obtain

$$\begin{aligned}
 \hat{\rho}_A \otimes \hat{\rho}_B &= \frac{1}{(2\pi)^{2(m+n)}} \int_{\mathbb{R}(2m)} d\mathbf{r}_A e^{-\frac{1}{4}\mathbf{r}_A^\top \Omega^\top \sigma_A \Omega \mathbf{r}_A} e^{i\mathbf{r}_A^\top \Omega^\top \bar{\mathbf{r}}_A} \hat{D}_{\mathbf{r}_A} \otimes \int_{\mathbb{R}(2n)} d\mathbf{r}_B e^{-\frac{1}{4}\mathbf{r}_B^\top \Omega^\top \sigma_B \Omega \mathbf{r}_B} e^{i\mathbf{r}_B^\top \Omega^\top \bar{\mathbf{r}}_B} \hat{D}_{\mathbf{r}_B} \\
 &= \frac{1}{(2\pi)^{2(m+n)}} \int_{\mathbb{R}(2m+2n)} d\mathbf{r}_A d\mathbf{r}_B e^{-\frac{1}{4}\mathbf{r}_A^\top \Omega^\top \sigma_A \Omega \mathbf{r}_A - \frac{1}{4}\mathbf{r}_B^\top \Omega^\top \sigma_B \Omega \mathbf{r}_B + i\mathbf{r}_A^\top \Omega^\top \bar{\mathbf{r}}_A + i\mathbf{r}_B^\top \Omega^\top \bar{\mathbf{r}}_B} \hat{D}_{\mathbf{r}_A} \otimes \hat{D}_{\mathbf{r}_B} \\
 &= \frac{1}{(2\pi)^{2(m+n)}} \int_{\mathbb{R}(2m+2n)} d\mathbf{r} e^{-\frac{1}{4}\mathbf{r}^\top \Omega^\top \sigma \Omega \mathbf{r} + i\mathbf{r}^\top \Omega^\top \bar{\mathbf{r}}} \hat{D}_{\mathbf{r}}, \tag{4.81}
 \end{aligned}$$

where  $\mathbf{r} = \begin{pmatrix} \mathbf{r}_A \\ \mathbf{r}_B \end{pmatrix}$  and  $\sigma = \sigma_A \oplus \sigma_B$ . In the third equality, we regrouped the terms in the exponential and used that  $\mathbf{r}_A^\top \Omega^\top \sigma_A \Omega \mathbf{r}_A + \mathbf{r}_B^\top \Omega^\top \sigma_B \Omega \mathbf{r}_B = \mathbf{r}^\top \Omega^\top \sigma \Omega \mathbf{r}$  and that  $\mathbf{r}_A^\top \Omega^\top \bar{\mathbf{r}}_A + \mathbf{r}_B^\top \Omega^\top \bar{\mathbf{r}}_B = \mathbf{r}^\top \Omega^\top \bar{\mathbf{r}}$ , which is a direct consequence of the definition of direct sum.<sup>12</sup> Finally, also in the third equality of the equation above, we used that  $\hat{D}_{\mathbf{r}} = \hat{D}_{\mathbf{r}_A} \otimes \hat{D}_{\mathbf{r}_B}$  which is a direct consequence from the definition of the Weyl operator (Eq. (4.17)).

Eq. (4.81) shows explicitly that the tensor product of two Gaussian states  $\hat{\rho}_A$  and  $\hat{\rho}_B$  is a Gaussian state since it has a characteristic function on the same form as Eq. (4.80). Moreover, it shows that we can construct a tensor product of two Gaussian states  $\hat{\rho}_A$  and  $\hat{\rho}_B$  by making the following operations in their first moments

---

<sup>12</sup>We are implicitly assuming that  $\Omega$  has the dimensions according to the vectors in which it is acting, i.e., switching the  $n$  in Eq. (4.7) in each case for convenience.

and covariance matrices

$$\langle \hat{\mathbf{r}} \rangle = \begin{pmatrix} \langle \hat{\mathbf{r}}_A \rangle \\ \langle \hat{\mathbf{r}}_B \rangle \end{pmatrix} \quad \text{and} \quad (4.82)$$

$$\sigma = \sigma_A \oplus \sigma_B. \quad (4.83)$$

## 4.7.2 Unitary operations

To show that unitary operators, generated by second-order Hamiltonians, are Gaussian operations it is sufficient to show that if an initial state is of the form of Eq. (4.53), then its unitary evolution  $\hat{\rho}'_G = \hat{U}\hat{\rho}_G\hat{U}^\dagger$  (where  $\hat{U}$  is a unitary operator) will also be of the form of Eq. (4.53). Therefore, suppose that our initial state is given by Eq. (4.53), then if we have a unitary evolution given by  $\hat{U} = e^{-i\hat{H}'}$ , where  $\hat{H}'$  is a generic second-order Hamiltonian, the evolution of the state will have the form

$$\begin{aligned} \hat{\rho}'_G &= \hat{U} \frac{e^{-\beta\hat{H}}}{Z} \hat{U}^\dagger \\ &= \frac{e^{-\beta\hat{U}\hat{H}\hat{U}^\dagger}}{Z}, \end{aligned}$$

now if we call  $\hat{H}'' = \hat{U}\hat{H}\hat{U}^\dagger$ , then we need only to show that  $\hat{H}''$  is a second-order Hamiltonian in order to complete our proof. In fact

$$\begin{aligned} \hat{H}'' &= \hat{U}\hat{H}\hat{U}^\dagger \\ &= e^{-i\hat{H}'}\hat{H}e^{i\hat{H}'} \\ &= \hat{H} - i[\hat{H}', \hat{H}] - \frac{1}{2!}[\hat{H}', [\hat{H}', \hat{H}]] + \frac{i}{3!}[\hat{H}', [\hat{H}', [\hat{H}', \hat{H}]]] + \dots, \end{aligned} \quad (4.84)$$

this is obtained with the use of another BCH formula.<sup>13</sup> This proof is completed by the fact that any commutator between second-order operators is a second-order operator (see Appendix C, Section C.17, for a proof of this statement), hence  $H''$  is a second-order Hamiltonian.

---

<sup>13</sup>Given two operators  $\hat{A}$  and  $\hat{B}$ , then

$$e^{\hat{A}}\hat{B}e^{-\hat{A}} = \hat{B} + [\hat{A}, \hat{B}] + \frac{1}{2!}[\hat{A}, [\hat{A}, \hat{B}]] + \frac{1}{3!}[\hat{A}, [\hat{A}, [\hat{A}, \hat{B}]]] + \frac{1}{4!}[\hat{A}, [\hat{A}, [\hat{A}, [\hat{A}, \hat{B}]]]] + \dots, \quad (4.85)$$

The unitary evolution for Gaussian states will be described by the symplectic transformations  $S_H$  as in Eq. (4.74). And it is sufficient to know the evolution of the first moments and covariance matrix from the following equations already obtained in Subsection 4.6.3

$$\langle \mathbf{r}(t) \rangle = S_H \langle \mathbf{r}(0) \rangle \quad \text{and} \quad (4.86)$$

$$\sigma(t) = S_H \sigma(0) S_H^\top, \quad (4.87)$$

since the Gaussianity of the states is preserved.

### 4.7.3 Partial trace

Suppose we have a global system  $AB$  composed of two subsystems  $A$  and  $B$  of  $m$  and  $n$  bosonic modes, respectively, and we prescribe the canonical operators of  $AB$  as  $\hat{\mathbf{r}} = \begin{pmatrix} \hat{\mathbf{r}}_A \\ \hat{\mathbf{r}}_B \end{pmatrix}$ , where  $\hat{\mathbf{r}}_A$  and  $\hat{\mathbf{r}}_B$  are the canonical operators of the subspace  $A$  and  $B$ , respectively. Then if the global state  $\hat{\rho}_{AB}$  is Gaussian, it can be fully described by its first moments  $\bar{\mathbf{r}} = \langle \hat{\mathbf{r}} \rangle$  and covariance matrix  $\sigma$ , which can be parametrized as

$$\bar{\mathbf{r}} = \begin{pmatrix} \bar{\mathbf{r}}_A \\ \bar{\mathbf{r}}_B \end{pmatrix} \quad \text{and} \quad (4.88)$$

$$\sigma = \begin{pmatrix} \sigma_A & \xi_{AB} \\ \xi_{AB}^\top & \sigma_B \end{pmatrix}, \quad (4.89)$$

where  $\bar{\mathbf{r}}_A$  and  $\bar{\mathbf{r}}_B$  are vectors of  $2m$  and  $2n$  real numbers, respectively and  $\sigma_A$ ,  $\sigma_B$  and  $\xi_{AB}$  are matrices of  $2m \times 2m$ ,  $2n \times 2n$  and  $2m \times 2n$  real numbers, respectively. Moreover, the reduced state  $\hat{\rho}_A = \text{Tr}_B(\hat{\rho}_{AB})$  will also be a Gaussian state with its first moments given by  $\bar{\mathbf{r}}_A$  and covariance matrix  $\sigma_A$ , completely describing the subsystem  $A$ . Analogously, the reduced state  $\hat{\rho}_B = \text{Tr}_A(\hat{\rho}_{AB})$  will also be a Gaussian state with first moments  $\bar{\mathbf{r}}_B$  and covariance matrix  $\sigma_B$ .

The above affirmation can be proved as follows. Suppose we know the statistical moments of  $AB$  ( $\bar{\mathbf{r}}$  and  $\sigma$ ). Then, from the characteristic function of a Gaussian



state (Eq. (4.80)), we have

$$\hat{\rho}_{AB} = \frac{1}{(2\pi)^{m+n}} \int_{\mathbb{R}^{2(m+n)}} d\mathbf{r} e^{-\frac{1}{4}\mathbf{r}^\top \Omega^\top \sigma \Omega \mathbf{r} + i\mathbf{r}^\top \Omega \bar{\mathbf{r}}} \hat{D}_{\mathbf{r}}.$$

If we parametrize  $\mathbf{r} = (\mathbf{r}_A \ \mathbf{r}_B)^\top$  where  $\mathbf{r}_A$  and  $\mathbf{r}_B$  are  $2m$  and  $2n$  real vectors, respectively, then

$$\hat{\rho}_{AB} = \frac{1}{(2\pi)^{m+n}} \int_{\mathbb{R}^{2m}} d\mathbf{r}_A \int_{\mathbb{R}^{2n}} d\mathbf{r}_B e^{-\frac{1}{4}(\mathbf{r}_A \ \mathbf{r}_B) \Omega^\top \sigma \Omega (\mathbf{r}_A \ \mathbf{r}_B)^\top + i(\mathbf{r}_A \ \mathbf{r}_B) \Omega (\bar{\mathbf{r}}_A \ \bar{\mathbf{r}}_B)^\top} \hat{D}_{\mathbf{r}_A} \otimes \hat{D}_{\mathbf{r}_B},$$

where we used Eq. (4.88) and that  $\hat{D}_{\mathbf{r}} = \hat{D}_{\mathbf{r}_A \oplus \mathbf{r}_B} = \hat{D}_{\mathbf{r}_A} \otimes \hat{D}_{\mathbf{r}_B}$ , from the definition of the Weyl operator (Eq. (4.17)). Computing the reduced state  $\hat{\rho}_A = \text{Tr}_B (\hat{\rho}_{AB})$  and remembering that the partial trace  $\text{Tr}_B$  acts only on the operators that belong to the Hilbert space of  $B$  (thus all the exponential term and  $\hat{D}_{\mathbf{r}_A}$  of the equation above remain unaffected by the trace) we obtain

$$\begin{aligned} \text{Tr}_B (\hat{\rho}_{AB}) &= \\ \frac{1}{(2\pi)^{m+n}} \int_{\mathbb{R}^{2m}} d\mathbf{r}_A \int_{\mathbb{R}^{2n}} d\mathbf{r}_B e^{-\frac{1}{4}(\mathbf{r}_A \ \mathbf{r}_B) \Omega^\top \sigma \Omega (\mathbf{r}_A \ \mathbf{r}_B)^\top + i(\mathbf{r}_A \ \mathbf{r}_B) \Omega (\bar{\mathbf{r}}_A \ \bar{\mathbf{r}}_B)^\top} \hat{D}_{\mathbf{r}_A} \otimes \text{Tr}_B (\hat{D}_{\mathbf{r}_B}). \end{aligned} \quad (4.90)$$

From the orthogonality relation of Eq. (4.34), if we choose  $\mathbf{s} = 0$  and use that  $\hat{D}_0 = 1$ , we obtain

$$\text{Tr}(\hat{D}_{\mathbf{r}}) = (2\pi)^n \delta^{2n}(\mathbf{r}).$$

Applying the above equation in Eq. (4.90) results in

$$\text{Tr}_B (\hat{\rho}_{AB}) = \frac{1}{(2\pi)^m} \int_{\mathbb{R}^{2m}} d\mathbf{r}_A e^{-\frac{1}{4}(\mathbf{r}_A \ \mathbf{r}_B) \Omega^\top \sigma \Omega (\mathbf{r}_A \ \mathbf{r}_B)^\top + i(\mathbf{r}_A \ \mathbf{r}_B) \Omega (\bar{\mathbf{r}}_A \ \bar{\mathbf{r}}_B)^\top} \Big|_{\mathbf{r}_B=0} \hat{D}_{\mathbf{r}_A}. \quad (4.91)$$

Computing explicitly the exponential components

$$\begin{aligned} (\mathbf{r}_A \ \mathbf{r}_B) \Omega^\top \sigma \Omega (\mathbf{r}_A \ \mathbf{r}_B)^\top &= \begin{pmatrix} \mathbf{r}_A^\top & \mathbf{r}_B^\top \end{pmatrix} \begin{pmatrix} \Omega_{m \times m}^\top & 0 \\ 0 & \Omega_{n \times n} \end{pmatrix} \begin{pmatrix} \sigma_A & \sigma_{AB} \\ \sigma_{AB}^\top & \sigma_B \end{pmatrix} \begin{pmatrix} \Omega_{m \times m} & 0 \\ 0 & \Omega_{n \times n} \end{pmatrix} \begin{pmatrix} \mathbf{r}_A \\ \mathbf{r}_B \end{pmatrix} \\ &= \mathbf{r}_A^\top \Omega^\top \sigma_A \Omega \mathbf{r}_A + \mathbf{r}_B^\top \Omega^\top \sigma_{AB} \Omega \mathbf{r}_A + \mathbf{r}_A^\top \Omega^\top \sigma_{AB} \Omega \mathbf{r}_B + \mathbf{r}_B^\top \Omega^\top \sigma_B \Omega \mathbf{r}_B, \end{aligned}$$

where again we stated that  $\Omega$  has dimensions according to the vector in which it acts. Similarly, we have

$$\mathbf{r}^\top \Omega^\top \bar{\mathbf{r}} = \mathbf{r}_A^\top \Omega^\top \bar{\mathbf{r}}_A + \mathbf{r}_B^\top \Omega^\top \bar{\mathbf{r}}_B.$$

Consequently, the equations above imply

$$e^{-\frac{1}{4}(\mathbf{r}_A \ \mathbf{r}_B)\Omega^\top \sigma \Omega(\mathbf{r}_A \ \mathbf{r}_B)^\top + i(\mathbf{r}_A \ \mathbf{r}_B)\Omega(\bar{\mathbf{r}}_A \ \bar{\mathbf{r}}_B)^\top} \Big|_{\mathbf{r}_B=0} = e^{-\frac{1}{4}\mathbf{r}_A^\top \Omega^\top \sigma_A \Omega \mathbf{r}_A + i\mathbf{r}_A^\top \Omega \bar{\mathbf{r}}_A},$$

and using this equation in Eq. (4.91), we finally obtain

$$\text{Tr}_B(\hat{\rho}_{AB}) = \frac{1}{(2\pi)^m} \int_{\mathbb{R}^{2m}} d\mathbf{r}_A e^{-\frac{1}{4}\mathbf{r}_A^\top \Omega^\top \sigma_A \Omega \mathbf{r}_A + i\mathbf{r}_A^\top \Omega \bar{\mathbf{r}}_A} \hat{D}_{\mathbf{r}_A}. \quad (4.92)$$

This proves that the reduced state  $\hat{\rho}_A$  is a Gaussian state completely described by the first moments  $\bar{\mathbf{r}}_A$  and covariance matrix  $\sigma_A$ , since its characteristic function has the form of a Gaussian one (Eq. (4.80)) with the desired parameters. The proof is analogous for the reduced system  $\hat{\rho}_B$ .

#### 4.7.4 Gaussian CPTP-maps

We have completed the proof that all operations we shall use in our open system evolution are Gaussian operators. Now we present the form of Gaussian CPTP-maps that this description creates.

Suppose we have a Gaussian system of  $n$  bosonic modes initially at a state with first moments vector  $\bar{\mathbf{r}}_S$  and covariance matrix  $\sigma_S$ . Similarly, initially, we have a Gaussian environment of  $m$  bosonic modes with first moments  $\bar{\mathbf{r}}_E$  and covariance matrix  $\sigma_E$ . If the initial system-environment joint state is uncorrelated they are described by a tensor product. Hence, from Eqs. (4.82) and (4.83), we have

$$\bar{\mathbf{r}}_{SE} = \begin{pmatrix} \bar{\mathbf{r}}_S \\ \bar{\mathbf{r}}_E \end{pmatrix} \quad \text{and} \quad \sigma_{SE} = \sigma_S \oplus \sigma_E, \quad (4.93)$$

where  $\bar{\mathbf{r}}_{SE}$  is the first-moment vector of the initial joint state and  $\sigma_{SE}$  is the covari-

ance matrix of the initial joint state.

Let the unitary evolution of the joint system be given by the symplectic matrix

$$S = \begin{pmatrix} A & B \\ C & D \end{pmatrix}, \quad (4.94)$$

where  $A$  is a  $2n \times 2n$  real matrix,  $B$  is a  $2n \times 2m$  real matrix,  $C$  is a  $2m \times 2n$  real matrix and  $D$  is a  $2m \times 2m$  real matrix. Then, from Eqs. (4.86) and (4.87), we have

$$\bar{\mathbf{r}}'_{SE} = \begin{pmatrix} A\bar{\mathbf{r}}_S + B\bar{\mathbf{r}}_E \\ C\bar{\mathbf{r}}_S + D\bar{\mathbf{r}}_E \end{pmatrix}, \quad (4.95)$$

for the evolved first moments  $\bar{\mathbf{r}}'_{SE}$ . And

$$\sigma'_{SE} = \begin{pmatrix} A\sigma_S A^\top + B\sigma_E B^\top & A\sigma_S C^\top + B\sigma_E D^\top \\ C\sigma_S A^\top + D\sigma_E B^\top & C\sigma_S C^\top + D\sigma_E D^\top \end{pmatrix}, \quad (4.96)$$

for the evolved covariance matrix  $\sigma'_{SE}$ .

Finally, by taking the partial trace of the environment (see Subsection 4.7.3), we obtain

$$\bar{\mathbf{r}}'_S = A\bar{\mathbf{r}}_S + B\bar{\mathbf{r}}_E, \quad (4.97)$$

for the evolved first moments. And

$$\sigma'_S = A\sigma_S A^\top + B\sigma_E B^\top, \quad (4.98)$$

for the evolved covariance matrix.

If we define the  $2n \times 2n$  real matrices  $X = A$  and  $Y = \sigma_E B^\top$  and the  $2n$  vector  $\mathbf{d} = B\bar{\mathbf{r}}_E$ , we conclude that the following evolution

$$\bar{\mathbf{r}}_S \mapsto X\bar{\mathbf{r}}_S + \mathbf{d} \quad \text{and} \quad (4.99)$$

$$\sigma_S \mapsto X\sigma_S X^\top + Y, \quad \text{with} \quad (4.100)$$

$$Y + i\Omega \geq iX\Omega X^\top, \quad (4.101)$$

can represent any Gaussian CPTP-maps of a system  $n$  bosonic modes. The condition of Eq. (4.101) assures that the covariance matrices still satisfy the bona-fide condition. The necessity of this condition can be shown by demanding the Eq. (4.58) condition to the evolved covariance matrix of Eq. (4.100) and using the constraints on  $X$  and  $Y$  due to the fact that the matrix  $S$  (of Eq. (4.94)) is symplectic.

Conversely to the result above, one can show (see, for instance, Chapter 5 of Ref. [14]) that any matrices  $X$  and  $Y$  satisfying Eq. (4.101) can represent a Gaussian map which acts on the system via the transformations of Eqs. (4.99) and (4.100). Furthermore, one can always consider the environment as a  $2n$ -modes state initially at the vacuum ( $\sigma_E = \mathbb{I}/2$ ) to construct such a Gaussian channel (for this case, the quantum channel will have  $\mathbf{d} = 0$ ).

This construction for the evolution in bosonic modes will be the approach used in Chapter 6 to obtain the analytical results for the collisional model with initially correlated ancillae.

### 4.7.5 Applying a channel in only one partition

A useful result for further use is the following. Suppose that we have a Gaussian system with two parties  $A$ , with  $n$  modes, vector of first moments  $\bar{\mathbf{r}}_A$  and covariance matrix  $\sigma_A$ , and  $B$ , with  $m$  modes, vector of first moments  $\bar{\mathbf{r}}_B$  and covariance matrix  $\sigma_B$ . Now, suppose we have a quantum channel acting only in  $A$  given by Eqs. (4.99), (4.100) and (4.101) with the respective vector  $\mathbf{d}$  and matrices  $X$  and  $Y$  (simultaneously, the identity operation acts in  $B$ ). Then the global resulting map will be

$$\begin{pmatrix} \bar{\mathbf{r}}_A \\ \bar{\mathbf{r}}_B \end{pmatrix} \mapsto \begin{pmatrix} X\bar{\mathbf{r}}_A + \mathbf{d} \\ \bar{\mathbf{r}}_B \end{pmatrix} \quad \text{and} \quad (4.102)$$

$$\begin{pmatrix} \sigma_A & \xi \\ \xi^\top & \sigma_B \end{pmatrix} \mapsto \begin{pmatrix} X\sigma_A X^\top + Y & X\xi \\ \xi^\top X^\top & \sigma_B \end{pmatrix}. \quad (4.103)$$

The proof of this result can be found in Chapter 5 of Ref. [14].

### 4.7.6 One-mode Gaussian channels

As an important example of Gaussian channels, we present the classes of all possible Gaussian quantum channels acting in one-mode states. Any Gaussian quantum channel for one-mode bosonic systems can be described by a vector  $\bar{\mathbf{d}} \in \mathbb{R}^2$  and  $2 \times 2$  real matrices  $\mathbf{T}$  (called *transmission matrix*) and  $\mathbf{N}$  (called *noise matrix*) playing the role of  $X$  and  $Y$ , respectively, in Eqs. (4.99) and (4.100). Accordingly, the condition of Eq. (4.101) will result in the conditions

$$\mathbf{N} = \mathbf{N}^\top \geq 0 \quad \text{and} \quad \det \mathbf{N} \geq (\det \mathbf{T} - 1)^2. \quad (4.104)$$

In Ref. [129], it was shown that the general structure of such transformations can be reduced to a simple set of classes of matrices  $\mathbf{T}$  and  $\mathbf{N}$  together with displacement operations to generate  $\mathbf{d}$ . The classes are the following

- Class  $A_1$ :  $\mathbf{T} = 0$  and  $\mathbf{N} = (\bar{n} + 1/2)\mathbb{I}_2$ , for  $\bar{n} \geq 0$ . This means that the state is turned completely into a thermal state, thus the channel is called *completely depolarizing channel*;
- Class  $A_2$ :  $\mathbf{T} = \text{diag}(1, 0)$  and  $\mathbf{N} = (\bar{n} + 1/2)\mathbb{I}_2$ . This channel is *phase-sensitive*, i.e., the state's amplification of the second moments depends on the quadrature;
- Class  $B_1$ :  $\mathbf{T} = \mathbb{I}_2$  and  $\mathbf{N} = \text{diag}(0, 1)/2$ , for  $\bar{n} \geq 0$ . This channel is also phase-sensitive;
- Class  $B_2$ :  $\mathbf{T} = \mathbb{I}_2$  and  $\mathbf{N} = \frac{\bar{n}}{2}\mathbb{I}_2$ , for  $\bar{n} \geq 0$ . This channel just adds classical noise to the system, thus called *additive-noise channel*, it encompasses the case of the identity transformation for  $\bar{n} = 0$ ;
- Class  $C$ :  $\mathbf{T} = \sqrt{\tau} \mathbb{I}_2$  where  $\tau > 0$  and  $\tau \neq 1$ . For the case of  $0 \leq \tau \leq 1$ ,  $\mathbf{N} = (1 - \tau)(\bar{n} + 1/2)$ , for  $\bar{n} \geq 0$ , this case is called the *lossy channel* (this contemplates the *Beam-Splitter* case to be seen in Chapter 6). For the case of  $\tau > 1$ ,  $\mathbf{N} = (\tau - 1)(\bar{n} + 1/2)$ , for  $\bar{n} \geq 0$ , this case is called the *amplifier*

channel (this contemplates the *Two-Mode Squeezing* case.<sup>14</sup>)

- Class *D*:  $\mathbf{T} = \sqrt{|\tau|}\sigma_z$  for  $\tau < 0$  and  $\mathbf{N} = (1 + |\tau|)(\bar{n} + 1/2)\mathbb{I}_2$ . This channel is also phase-sensitive and it can be seen as the environmental outcome of a two-mode squeezing operation.

This classification will be helpful to the construction of a method for computing the quantum discord in two-mode bosonic states exposed in Subsection 4.8.3.

## 4.8 Entropic quantities for Gaussian states

Obtaining the entropy and related quantities, such as Mutual Information and Quantum Discord, of Gaussian states will be necessary to quantify correlations between bosonic modes in our second project of the thesis, especially in Chapter 7. Here we present how to compute these quantities. For obtaining the entropy of a Gaussian state, it will be useful to present the following diagonalization.

### 4.8.1 Diagonalization of Gaussian states to thermal states of free modes

Given a Gaussian state (Eq. (4.53)) with  $n$  bosonic modes and a general second-order Hamiltonian in the form of Eq. (4.52), we can write the density matrix of the state as

$$\hat{\rho}_G = \frac{e^{-(\hat{\mathbf{r}}-\bar{\mathbf{r}})^\top M(\hat{\mathbf{r}}-\bar{\mathbf{r}})}}{Z}, \quad (4.105)$$

where  $Z = \text{Tr} \left( e^{-(\hat{\mathbf{r}}-\bar{\mathbf{r}})^\top M(\hat{\mathbf{r}}-\bar{\mathbf{r}})} \right)$  and  $M$  is a positive definite  $2n \times 2n$  matrix. We have, from Williamson's theorem (Eq. (4.78)), that

$$(\hat{\mathbf{r}} - \bar{\mathbf{r}})^\top M(\hat{\mathbf{r}} - \bar{\mathbf{r}}) = (\hat{\mathbf{r}} - \bar{\mathbf{r}})^\top \mathbf{S} \mathbf{D} \mathbf{S}^\top (\hat{\mathbf{r}} - \bar{\mathbf{r}}), \quad (4.106)$$

where  $\mathbf{S} \in Sp_{2n, \mathbb{R}}$  and  $\mathbf{D} = \text{diag}(d_1, d_1, \dots, d_n, d_n)$  is the diagonal matrix of symplectic eigenvalues. From the fact that the transpose of a symplectic transformation

---

<sup>14</sup>See Refs. [55, 121, 122] for the definition of the two-mode squeezing operation.

is also symplectic,<sup>15</sup> we have that  $\tilde{S} = S^\top$  is symplectic and hence

$$\begin{aligned}
 (\hat{\mathbf{r}} - \bar{\mathbf{r}})^\top M (\hat{\mathbf{r}} - \bar{\mathbf{r}}) &= (\hat{\mathbf{r}} - \bar{\mathbf{r}})^\top \tilde{S}^\top \mathbf{D} \tilde{S} (\hat{\mathbf{r}} - \bar{\mathbf{r}}) \\
 &= \hat{S}^\dagger (\hat{\mathbf{r}} - \bar{\mathbf{r}})^\top \hat{S} \mathbf{D} \hat{S}^\dagger (\hat{\mathbf{r}} - \bar{\mathbf{r}}) \hat{S} \\
 &= \hat{S}^\dagger \hat{D}_{\hat{\mathbf{r}}}^\dagger \hat{\mathbf{r}}^\top \mathbf{D} \hat{\mathbf{r}} \hat{D}_{\hat{\mathbf{r}}} \hat{S},
 \end{aligned} \tag{4.107}$$

where  $\hat{D}_{\hat{\mathbf{r}}}$  is a displacement operator (and we used Eq. (4.18)) and  $\hat{S}$  is a unitary such that  $\hat{S}^\dagger \hat{\mathbf{r}} \hat{S} = \tilde{S} \hat{\mathbf{r}}$ .<sup>16</sup> Finally, using the relation above in Eq. (4.105), we obtain

$$\boxed{\hat{\rho}_G = \hat{S}^\dagger \hat{D}_{\hat{\mathbf{r}}}^\dagger \hat{\rho}_{\text{free}} \hat{D}_{\hat{\mathbf{r}}} \hat{S}}, \tag{4.108}$$

where

$$\hat{\rho}_{\text{free}} = \frac{e^{-\hat{\mathbf{r}}^\top \mathbf{D} \hat{\mathbf{r}}}}{Z} \tag{4.109}$$

is a thermal state of  $n$  non-interacting modes with energies given by the symplectic eigenvalues of  $M$ . The density matrix of thermal  $n$  free bosonic modes is obtained in Appendix C (Eq. (C.33)). Explicitly, we have

$$\boxed{\hat{\rho}_{\text{free}} = \bigotimes_{j=1}^n \hat{\rho}_{\text{free}_j}, \quad \text{with} \tag{4.110}$$

$$\boxed{\hat{\rho}_{\text{free}_j} = \frac{1}{\nu_j + 1/2} \sum_{n_j=0}^{\infty} \left( \frac{\nu_j - 1/2}{\nu_j + 1/2} \right)^{n_j} |n_j\rangle \langle n_j|, \tag{4.111}$$

where  $\nu_j$  are the symplectic eigenvalues for the covariance matrix of the state  $\hat{\rho}_G$ .<sup>17</sup>

## 4.8.2 Entropy of a Gaussian state

From Eq. (4.108) we observe that any Gaussian state can be described as a unitary transformation of a thermal state of free modes. Since the von Neumann Entropy is

<sup>15</sup>This can be proved by taking the transpose of Eq. (4.76) and using that  $\Omega^\top = -\Omega$ .

<sup>16</sup>This relation is possible since for any  $S \in Sp_{2n, \mathbb{R}}$ , there is a real and symmetric  $2n \times 2n$  matrix  $H$  such that  $H = \Omega^\top \log S$  and  $\hat{S}^\dagger \hat{\mathbf{r}} \hat{S} = \hat{S} \hat{\mathbf{r}}$ , where  $\hat{S} = e^{-i \frac{1}{2} \hat{\mathbf{r}}^\top H \hat{\mathbf{r}}}$  (see Appendix C, Section C.15, for the proof).

<sup>17</sup>A consequence of the parametrization of Eq. (4.77) is that the elements of the covariance matrix of the state  $\hat{\rho}_{\text{free}}$  are the symplectic eigenvalues of the covariance matrix of  $\hat{\rho}_G$ .

invariant under unitary transformations, we conclude (in this Chapter, we denote the von Neumann entropy by  $\mathbf{S}(\bullet)$  in order to differentiate it from symplectic matrices)

$$\mathbf{S}(\hat{\rho}_G) = \mathbf{S}(\hat{\rho}_{\text{free}}). \quad (4.112)$$

Using Eq. (4.110) we obtain<sup>18</sup>

$$\mathbf{S}(\hat{\rho}_G) = \sum_{j=1}^n \mathbf{S}(\hat{\rho}_{\text{free}_j}). \quad (4.113)$$

Finally, using Eq. (4.111), we have (see Appendix C, Section C.18, for a proof)

$$\boxed{\mathbf{S}(\hat{\rho}_G) = \sum_{j=1}^n g(\nu_j)}, \quad (4.114)$$

where  $\nu_j$  are the symplectic eigenvalues of the covariance matrix of  $\hat{\rho}_G$  and

$$\boxed{g(x) = (x + 1/2) \log(x + 1/2) - (x - 1/2) \log(x - 1/2)}. \quad (4.115)$$

### 4.8.3 Quantum discord between two Gaussian bosonic modes

With the formulae of Eqs. (4.114) and (4.115), it is possible to compute the entropy of any Gaussian state given its covariance matrix. Consequently, we can use this formula also to compute any entropy-dependent quantity. Among these quantities is the Mutual Information, which is a quantifier of *total* correlations and can be computed with the use of Eq. (3.20). However, to compute a quantifier of *quantum* correlations for Gaussian states is a hard task [110, 130]. Therefore, in this section, we only focus on the computation of Quantum Discord between two Gaussian bosonic modes, which will be used in Chapter 7, for the second project of this thesis.

There is no closed formula to compute the Quantum Discord between two Gaussian bosonic modes. Notwithstanding, in Ref. [131] it was obtained a closed formula for computing this quantity for a very rich and useful set of states. Here we present

---

<sup>18</sup>Here we used that  $\mathbf{S}(\otimes_n \hat{\rho}_n) = \sum_n \mathbf{S}(\hat{\rho}_n)$ . This is a consequence of the fact that  $\mathbf{S}(\hat{\rho}_A \otimes \hat{\rho}_B) = \mathbf{S}(\hat{\rho}_A) + \mathbf{S}(\hat{\rho}_B)$ . Indeed  $\mathbf{S}(\hat{\rho}_A \otimes \hat{\rho}_B) = -\text{Tr}((\hat{\rho}_A \otimes \hat{\rho}_B) \log(\hat{\rho}_A \otimes \hat{\rho}_B)) = -\text{Tr}((\hat{\rho}_A \otimes \hat{\rho}_B) \log(\hat{\rho}_A)) - \text{Tr}((\hat{\rho}_A \otimes \hat{\rho}_B) \log(\hat{\rho}_B)) = -\text{Tr}_A(\hat{\rho}_A \log(\hat{\rho}_A)) - \text{Tr}_B(\hat{\rho}_B \log(\hat{\rho}_B)) = \mathbf{S}(\hat{\rho}_A) + \mathbf{S}(\hat{\rho}_B)$ .



the main results of this paper. The main proofs of this Section are contained in the Supplemental Material of Ref. [131], which is a highly self-contained and pedagogical text, so we make reference to this text when needed and to our proofs in Appendix C when we deem necessary.

First, we make a useful definition. It can be shown (see Appendix C, Section C.19) that any covariance matrix for a Gaussian state of two modes can be transformed into the following form by means of single-mode symplectic transformations

$$\sigma_S = \begin{pmatrix} a & 0 & c_+ & 0 \\ 0 & a & 0 & c_- \\ c_+ & 0 & b & 0 \\ 0 & c_- & 0 & b \end{pmatrix}, \quad (4.116)$$

for  $a$  and  $b$  positive real numbers and  $c_+$  and  $c_-$  are real numbers constrained so that the covariance matrix is bona-fide. This form is named *Simon normal form*. The normal form facilitates our treatment since each covariance matrix in a normal form represents a class of states which have the same amount of quantum correlations between the two parties (because each of these states can be transformed into another by successive local symplectic transformations, which represents local unitary transformations).

In order to make a clearer explanation for the method of Ref. [131] for obtaining the quantum discord between two bosonic modes, we start by showing how to compute the quantum discord for the *Two-mode squeezed thermal state (TMST)*. This state is represented by the following covariance matrix

$$\sigma_{\text{tmst}} = \begin{pmatrix} a & 0 & c & 0 \\ 0 & a & 0 & -c \\ c & 0 & b & 0 \\ 0 & -c & 0 & b \end{pmatrix}, \quad (4.117)$$

for positive  $a, b$  and  $c$  and null first moment (see Appendix C, Section C.22, for a more detailed definition). Notice that the TMST's covariance matrix is simply the

Simon normal form with opposite correlation terms  $c_+$  and  $c_-$ .

The method can be described in two steps. First step: **state decomposition**. We construct our target Gaussian state  $\hat{\rho}_{AB}$  (in this case, the TMST), made of two parties  $A$  and  $B$  (each being single modes), as an application of a local quantum channel  $\mathcal{E}$  in  $A$  of an initial Gaussian state  $\hat{\rho}_{aB}$ , i.e.,

$$\hat{\rho}_{AB} = (\mathcal{E}_A \otimes \mathcal{I}_B)(\hat{\rho}_{aB}), \quad (4.118)$$

where  $\mathcal{I}$  represents the identity channel.

We chose the quantum channel  $\mathcal{E}$  to be a *phase-insensitive Gaussian channel*, these are the classes  $A_1$ ,  $B_2$  and  $C$  described in Subsection 4.7.6. Given an input covariance matrix  $\sigma_{\text{in}}$  of the state, it will transform as

$$\sigma_{\text{in}} \rightarrow (\mathbf{T} \oplus \mathbb{I}_2)\sigma_{\text{in}}(\mathbf{T}^\top \oplus \mathbb{I}_2) + (\mathbf{N} \oplus \mathbf{0}), \quad (4.119)$$

where  $\mathbf{T} = \sqrt{\tau} \mathbb{I}_2$ , with  $\tau \geq 0$  and  $\mathbf{N} = \eta \mathbb{I}_2$ , with  $\eta \geq |1 - \tau|$ .

We also chose  $\hat{\rho}_{aB}$  to be the *Einstein-Podolsky-Rosen* (EPR) state, which has a null first moment and has the following covariance matrix

$$\sigma_{aB} = \begin{pmatrix} \beta \mathbb{I}_2 & \sqrt{\beta^2 - 1} \mathbf{C} \\ \sqrt{\beta^2 - 1} \mathbf{C} & \beta \mathbb{I}_2 \end{pmatrix}, \quad (4.120)$$

where  $\mathbf{C} = \text{sign}(c_+) \sigma_z$  and  $\beta > 0$  ( $\beta$  here is not playing the role of the inverse of temperature). These choices ensure that the state decomposition of Eq. (4.118) correctly results in a TMST state parametrized as (see Supplemental Material of Ref. [131] for the proof)

$$\sigma_{AB} = \begin{pmatrix} (\tau\beta + \eta) \mathbb{I}_2 & \sqrt{\tau(\beta^2 - 1)} \mathbf{C} \\ \sqrt{\tau(\beta^2 - 1)} \mathbf{C} & \beta \mathbb{I}_2 \end{pmatrix}, \quad (4.121)$$

where  $\tau \geq 0$  and  $\eta \geq |1 - \tau|$  are parameters of the phase-insensitive Gaussian channel.

Second: **remote preparation**. We make a local generalized measurement

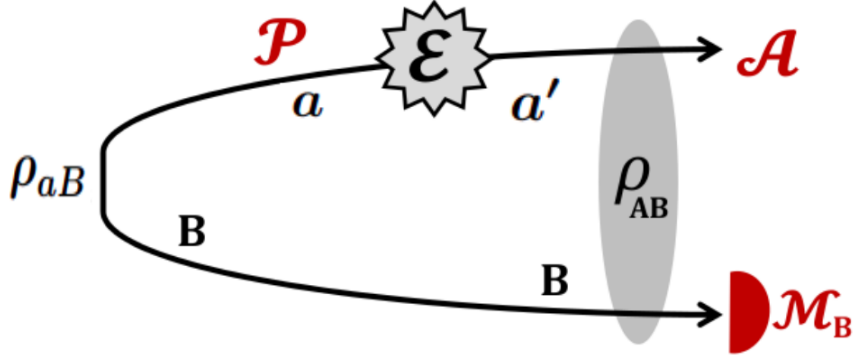


Figure 4.1: *State decomposition*: Depicted in black lines, the state  $\hat{\rho}_{AB}$  can be decomposed as an initial state  $\hat{\rho}_{aB}$  in which the first mode (in part  $A$ ) passes through a quantum channel  $\mathcal{E}$ . *Remote preparation*: Depicted in red symbols, the effect of the generalized measurement  $\mathcal{M}_B$  in  $\hat{\rho}_{aB}$  creates the ensemble  $\mathcal{P} = \{p_k, \hat{\rho}_{a|k}\}_k$  of states in  $A$  which, passing through the quantum channel, becomes the ensemble  $\mathcal{A} = \{p_k, \hat{\rho}_{a'|k}\}_k$ . The ensemble  $\mathcal{A}$  is also generated by the backaction, in  $A$ , of the generalized measurement  $\mathcal{M}_B$  in  $\hat{\rho}_{AB}$ . (This figure was taken from Ref. [131] with modifications.)

$\mathcal{M}_B = \{M_k\}_k$  in  $B$ . The application of such measurement in  $\hat{\rho}_{aB}$  causes an ensemble  $\mathcal{P} = \{p_k, \hat{\rho}_{a|k}\}_k$  as its backaction in  $A$ . The resulting ensemble of applying the local generalized measurement  $\mathcal{M}_B$  in  $\hat{\rho}_{AB}$  is  $\mathcal{A} = \{p_k, \hat{\rho}_{a'|k}\}_k$ , with

$$\hat{\rho}_{a'|k} = \mathcal{E}(\hat{\rho}_{a|k}), \quad (4.122)$$

as a consequence of Eq. (4.118) (see Fig. 4.1).

If we chose  $\mathcal{M}_B = \text{het}_B$  to be a heterodyne measurement (see the last paragraph of page 57), the backaction of the state  $\hat{\rho}_{aB}$  in  $A$  will result in an ensemble of coherent states  $\mathcal{P} = \{Q(\alpha), \hat{\rho}_{a|\alpha} = |\alpha\rangle\langle\alpha|\}_\alpha$ , where  $|\alpha\rangle$  are coherent states and  $Q(\alpha)$  is the Husimi Q-function (see Supplemental Material of Ref. [131] for the proof of this statement). These coherent states are the inputs of the phase-insensitive Gaussian channel  $\mathcal{E}$ . Consequently, from Eq. (4.118) and from the definition of the quantum-classical conditional entropy (Eq. (3.31)), we obtain

$$\begin{aligned} \mathbf{S}_{\text{het}_B}(A|B) &= \int_{\mathbb{C}} d^2\alpha Q(\alpha) \mathbf{S}(\mathcal{E}(|\alpha\rangle\langle\alpha|)) \\ &= \mathbf{S}(\mathcal{E}(|0\rangle\langle 0|)). \end{aligned} \quad (4.123)$$

The second equality of the equation above comes from the normalization of the Husimi Q-function and from the fact that  $\mathbf{S}(\mathcal{E}(|\alpha\rangle\langle\alpha|)) = \mathbf{S}(\mathcal{E}(|0\rangle\langle 0|))$  for any coherent state  $|\alpha\rangle$  (this statement is proved in Appendix C, Sec. C.20).

For computing the quantum discord, we must find the generalized measurement which minimizes the quantum-classical conditional entropy (Eq. (3.31)). In order to find this minimum, we use the seminal result of Refs. [132, 133], which states that the vacuum (or any translation of it, i.e., coherent states) minimizes the output entropy of a phase-insensitive Gaussian channel  $\mathcal{E}$  among all possible states, i.e.,

$$\mathbf{S}[\mathcal{E}(|0\rangle\langle 0|)] = \inf_{\hat{\rho}} \mathbf{S}[\mathcal{E}(\hat{\rho})]. \quad (4.124)$$

From this result, we conclude that the heterodyne measurement is a strong candidate to minimize the quantum-classical conditional entropy. Indeed, Eqs. (4.123) and (4.124) imply

$$\mathbf{S}_{\text{het}_B}(A|B) = \inf_{\hat{\rho}} \mathbf{S}[\mathcal{E}(\hat{\rho})]. \quad (4.125)$$

To complete the proof that  $\mathbf{S}_{\text{het}_B}(A|B)$  is the smaller quantum-classical conditional entropy, notice that, for any set  $\{M_k\}_k$  of generalized measurements

$$\begin{aligned} \mathbf{S}_M(A|B) &= \sum_k p_k \mathbf{S}(\hat{\rho}_{a'|k}) \\ &\geq \inf_{\mathcal{A}} \mathbf{S}(\hat{\rho}_{a'|k}) \\ &= \inf_{\mathcal{P}} \mathbf{S}[\mathcal{E}(\hat{\rho}_{a|k})] \\ &\geq \inf_{\hat{\rho}} \mathbf{S}(\mathcal{E}(\hat{\rho})), \end{aligned} \quad (4.126)$$

where the first equality above comes from the definition of Eq. (3.31), the first inequality says that the average is greater or equal to the infimum of  $\mathcal{A}$ , the second equality comes from Eq. (4.122) and the last inequality comes from the fact that  $\mathcal{P}$  is contained in the set of all possible one-mode density matrices.

From the equation above and Eq. (4.125), we conclude that

$$\mathbf{S}_M(A|B) \geq \mathbf{S}_{\text{het}_B}(A|B), \quad (4.127)$$

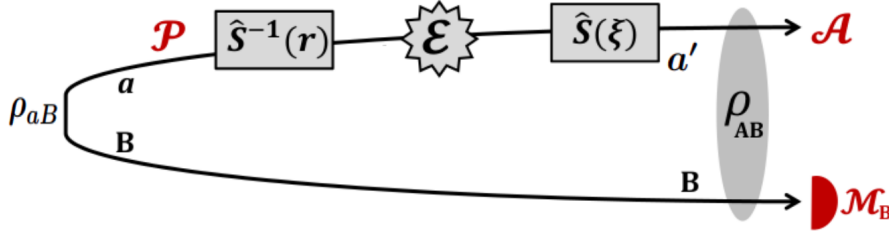


Figure 4.2: *State decomposition*: Depicted in black lines, the state  $\hat{\rho}_{AB}$  can be decomposed as an initial state  $\hat{\rho}_{aB}$  in which the first mode (in part  $A$ ) passes through an inverse squeezing operator  $\hat{S}^{-1}(r)$ , a quantum channel  $\mathcal{E}$  and a squeezing operator  $\hat{S}(\xi)$ . *Remote preparation*: Depicted in red symbols, the effect of the generalized measurement  $\mathcal{M}_B$  in  $\hat{\rho}_{aB}$  creates the ensemble  $\mathcal{P} = \{p_k, \hat{\rho}_{a|k}\}_k$  of states in  $A$  which, passing through the quantum channel and squeezing operators, becomes the ensemble  $\mathcal{A} = \{p_k, \hat{\rho}_{a'|k}\}_k$ . The ensemble  $\mathcal{A}$  is also generated by the backaction, in  $A$ , of the generalized measurement  $\mathcal{M}_B$  in  $\hat{\rho}_{AB}$ . (This figure was taken from Ref. [131] with modifications.)

for every generalized measurement  $\{M_k\}_k$ , implying that  $\mathbf{S}_{\text{het}_B}(A|B)$  is the minimum of the possible quantum-classical conditional entropy. Therefore, we have a closed formula for the quantum discord. From Eqs. (3.20) (3.32), (3.33) and (3.34), we have

$$\begin{aligned} \mathcal{D}(A|B) &= \mathbf{S}(\hat{\rho}_{AB}) + \min_{\{M_k^B\}_k} \mathbf{S}_M(A|B) - \mathbf{S}(\hat{\rho}_B) \\ &= \mathbf{S}(\hat{\rho}_{AB}) + \mathbf{S}(\mathcal{E}(|0\rangle\langle 0|)) - \mathbf{S}(\hat{\rho}_B), \end{aligned} \quad (4.128)$$

where in the second equality we used Eqs. (4.123) and (4.127). Computing explicitly the entropies (see Appendix C, Section C.21), we have finally obtain

$$\boxed{\mathcal{D}(A|B) = g(\beta) - g(\nu_-) - g(\nu_+) + g\left(\frac{\tau + \eta}{2}\right)}, \quad (4.129)$$

where  $\nu_-$  and  $\nu_+$  are the symplectic eigenvalues of the TMST covariance matrix  $\sigma_{AB}$  (Eq. (4.121)) and  $g(\bullet)$  is defined according to Eq. (4.115).

At this point, we can generalize the method described for computing the quantum discord of a TMST state in order to extend it to a larger set of correlated two-mode states. The two steps in the previous case will be modified as follows.

First step: **state decomposition**. In this case, we intend to construct a tar-

get Gaussian state  $\hat{\rho}_{AB}$  in the Simon normal form (Eq. (4.116)). We first extend our phase-insensitive Gaussian channel  $\mathcal{E}$  to include phase-sensitive channels with negative transmissivities, i.e., we can also have  $\tau \leq 0$ , this is the case  $D$  described in Subsection 4.7.6. Then, supposing again the initial state  $\hat{\rho}_{aB}$  as being the EPR state, with covariance matrix given by Eq. (4.120), we generate our state  $\hat{\rho}_{AB}$  by the following operation

$$\hat{\rho}_{AB} = ((\mathcal{S}_\xi \mathcal{E} \mathcal{S}_r^{-1})_A \otimes \mathcal{I}_B)(\hat{\rho}_{aB}), \quad (4.130)$$

where  $\mathcal{S}_x(\hat{\rho}) = \hat{S}(x)\hat{\rho}\hat{S}^\dagger(x)$  is the unitary one-mode *squeezing operation* and  $\hat{S}(x)$  is the *squeezing operator* with  $r \in [\beta^{-1}, \beta]$  and  $\xi = r \frac{\sqrt{\eta r^{-1} + |\tau|\beta}}{\sqrt{\eta r + |\tau|\beta}}$ .<sup>19</sup> The necessity of the additional squeezing operations in the decomposition made above and the choices of  $r$  and  $\xi$  will be explained in the next step. As consequence of Eq. (4.130), the state  $\hat{\rho}_{AB}$  will have a covariance matrix  $\sigma_{AB}$  given in the Simon normal form (Eq. (4.116)), with the following parametrization

$$a = \theta(r)\theta(r^{-1}), \quad \theta(r) = \sqrt{\eta r + |\tau|\beta}, \quad (4.131)$$

$$b = \beta, \quad (4.132)$$

$$c_+ = \pm \sqrt{|\tau|(\beta^2 - 1)\theta(r^{-1})/\theta(r)}, \quad (4.133)$$

$$c_- = \mp \text{sign}[\tau] \sqrt{|\tau|(\beta^2 - 1)\theta(r)/\theta(r^{-1})}, \quad (4.134)$$

where  $\tau \in \mathbb{R}$ ,  $\eta \geq |1 - \tau|$ ,  $r \in [\beta^{-1}, \beta]$  and the ambiguity in the sign of Eqs. (4.133) and (4.134) comes from the ambiguity of  $\mathbf{C} = \text{sign}(\sigma_+) \sigma_z$ .<sup>20</sup>

Second step: **remote preparation**. In this case, we chose to make the local generalized measurement  $\mathcal{M}_B$  in  $B$  such that  $\{M_\alpha(u) = |\alpha, u\rangle \langle \alpha, u|\}_\alpha$ , where  $|\alpha, u\rangle = \hat{S}(u)|\alpha\rangle$  being  $|\alpha\rangle$  a coherent state and  $\hat{S}(u)$  the squeezing operator for  $u > 0$ . The backaction of this measurement in  $B$  will result in an ensemble  $\mathcal{P} = \{p_\alpha, \hat{\rho}_{a|\alpha}\}_\alpha$  in  $A$  such that the covariance matrix of the states  $\hat{\rho}_{a|\alpha}$  will be

<sup>19</sup>The action of the squeezing operation in Gaussian states is described by the symplectic matrix  $S(x) = \begin{pmatrix} x^{1/2} & 0 \\ 0 & x^{-1/2} \end{pmatrix}$ , for  $x > 0$ .

<sup>20</sup>The proof of the parametrization above can be found in details in the Supplemental Material of Ref. [131].

$\sigma_{a|\alpha} = \text{diag}(r^{-1}, r)$ , where  $r = (1 + u\beta)(u + \beta)^{-1}$  (the proof of this affirmation can be found in the Supplemental Material of Ref. [131]). Moreover, we wish to turn these states into coherent states, so we apply the inverse squeezing unitary channel  $\mathcal{S}_r^{-1}$ . This enables us to use again the result of Refs. [132, 133] (Eq. (4.124)),<sup>21</sup> from which we conclude that

$$\begin{aligned} \inf_{\hat{\rho}} \mathbf{S}(\mathcal{E}(\hat{\rho})) &= \mathbf{S}(\mathcal{E}(\mathcal{S}_r^{-1}(\hat{\rho}_{a|\alpha}))) \\ &= \mathbf{S}(\mathcal{E}(|0\rangle\langle 0|)), \end{aligned} \quad (4.135)$$

for every  $\hat{\rho}_{a|\alpha} \in \mathcal{P}$ , since all  $\mathcal{S}_r^{-1}(\hat{\rho}_{a|\alpha})$  are coherent states.

Proceeding in analogy with the argument of the TMST state, we conclude that the quantum discord of the state  $((\mathcal{E}\mathcal{S}_r^{-1})_A \otimes \mathcal{I}_B)(\hat{\rho}_{aB})$  is also given by Eq. (4.129). Finally, to turn the state into the Simon normal form, we apply the squeezing operation  $\mathcal{S}_\xi$  in  $A$ , with  $\xi = \frac{\sqrt{\eta r^{-1} + |\tau|\beta}}{\sqrt{\eta r + |\tau|\beta}}$ , and we obtain the parametrization of Eqs. (4.131), (4.132), (4.133) and (4.134). The operation  $\mathcal{S}_\xi$  is unitary and local in  $A$ , hence it does not interfere with any entropic quantity.

This method (see Fig. 4.2) gives the exact quantum discord between two modes for a large set of states in the Simon normal form. Such a set generated by the parametrization of Eqs. (4.131), (4.132), (4.133) and (4.134) cannot range all possible bona-fide states in the Simon normal form but encompasses a considerable amount of them. This can be seen in the plots of Fig. 4.3, where we randomly picked  $2 \times 10^5$  values of  $\tau$  and  $r$  having fixed different values of  $a$  and  $b$ .<sup>22</sup> The plots expose visually the range that can be accessible by the parametrization inside the region of possibles  $c_+$  and  $c_-$  delimited by the bona-fide conditions. It also indicates the inability of such parametrization to achieve states with  $c_+$  and  $c_-$  near 0. For larger values of  $a$  and  $b$ , it can be seen that the parametrization is more capable to

<sup>21</sup>Which is also valid for our extended phase-insensitive Gaussian channel  $\mathcal{E}$  (for all  $\eta \in \mathbb{R}$ ).

<sup>22</sup>With  $a$  and  $b$  fixed, we choose randomly  $r \in [b^{-1}, b]$ . As a consequence of Eqs. (4.131), (4.132), (4.133) and (4.134), we will have  $\eta = \frac{\sqrt{4a^2 r^2 + (r^2 - 1)\tau^2 b^2 - (1 + r^2)|\tau|b}}{2r}$  defined in terms of  $a$ ,  $b$  and  $r$  and  $\tau$  will be restricted to  $\tau \in [\tau_{\min}, \tau_{\max}]$ , where  $\tau_{\min} = \frac{b + (br + 2)r - \sqrt{(r^2 - 1)^2 b^2 + 4a^2 r(r + b)(rb + 1)}}{2(r + b)(rb + 1)}$  and  $\tau_{\max} = \frac{b + (br - 2)r - \sqrt{(r^2 - 1)^2 b^2 - 4a^2 r(r - b)(rb - 1)}}{2(r - b)(rb - 1)}$  for  $b \geq a$ , which is also randomly chosen within this range.

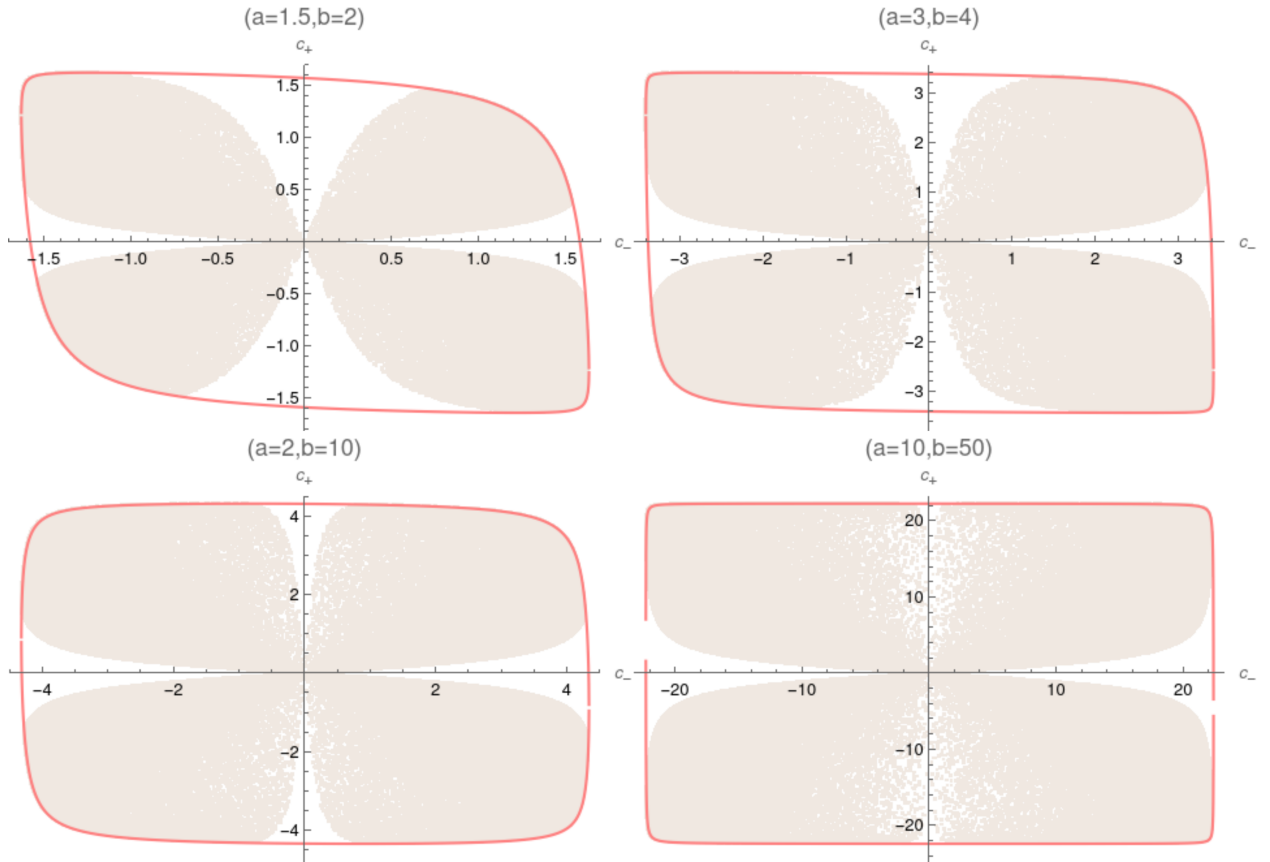


Figure 4.3: Plot of  $c_+$  and  $c_-$  points, for different fixed  $a$  and  $b$  of states in the Simon normal form generated  $2 \times 10^5$  times by random choices of  $r$  and  $\tau$ , according to the parametrization of Eqs. (4.131), (4.132), (4.133) and (4.134). The pink curves delimit the bona-fide region of states.

fill the region inside the bona-fide allowed states and can generate more points near  $c_+ = 0$  and  $c_- = 0$ . Although the regions exactly at  $c_+ = 0$  and  $c_- = 0$  are never accessible, this will not compromise our use of this method in Chapter 7.



## **Part II**

### **Main projects**

# Chapter 5

## Initially Correlated Ancillae - Minimal Qubit Model CM

As already anticipated in the Introduction and Sec. 2.3.1, our first project of this thesis focuses on dealing with Collisional Models (CMs) with initially correlated ancillae. This is the first Chapter concerning to the first project, and we will explore and obtain results for the evolution of a system interacting with correlated ancillae for the case where all the parties are made of qubits. The results of this Chapter will support the main results of Chapter 6 where we obtain a more complete description of the evolution of the system and ancillae in the case where all the parties are made of bosonic modes.

Initially correlated ancillae in a CM cause the system's evolution (given by Eq. (2.21)) to be described by a non-Markovian map, as already stressed in Subsection 2.3.1. We cannot treat it as a set of successive steps of separated maps, since in the very first interaction of the system with the first ancilla, all the other ancillae may start to be correlated with the system. Clearly, the problem will be much more intractable than the uncorrelated case, and maybe it would be impossible for one to find analytically the system's steady state, just like it was done for some cases in Chapter 2, for qubits. For this reason, we computed Eq. (2.21) numerically for a (not very large, but sufficient) finite number of collisions in order to observe the effects of the initial ancillae correlations using the Partial SWAP (Eq. (2.44)) as the unitary dynamics of each collision. These results are contrasted with the

case where the local ancillae states are the same but are not correlated between themselves, and definitely show that the presence of correlations pushes the system to a different steady state.

As it was presented in Sec. 2.3.6, a direct consequence of the fact that all ancillae are locally identical and from the Partial SWAP unitary in each collision is that we have the following steady state of the system

$$\rho_S^* = \lim_{n \rightarrow \infty} \rho_S^n = \rho_A, \quad (5.1)$$

where  $\rho_A$  is the local state of each ancilla. This phenomenon is called Homogenization [18, 19], described in Section 2.3.6, and in this Chapter we prove, for qubits, that the presence of initial correlations between the ancillae can prevent it to happen. Thus we conclude that the pushing caused by the correlations can break Homogenization. The interesting point of it is that, as far as a local observer knows, the system is only interacting via a partial SWAP with locally identical parts, but the system is being driven to a different state than the local state of the ancillae. Therefore, the main goal of this Chapter and of Chapter 6 is to prove the presence of such pushing.

In order to be able to simulate a setup physically feasible to implement such CM with initially correlated ancillae, we make use of *Hamiltonian graph states* [118, 134–138]. By putting the ancillae to interact with each other via such Hamiltonian, *before* the interaction with the system starts, we prepare an environment of correlated ancillae. This structure will be described as follows.

## 5.1 Preparing the correlated ancillae environment

### 5.1.1 Hamiltonian graph states

We want to have a structure that is capable of encompassing as many ancillae as we want since Homogenization tends to happen for a large number of collisions. Also, we assume that our set of ancillae is translationally invariant. This means that, if

$\rho_E = \rho_{A_1 A_2 \dots A_n}$  is the environment global state made of all the  $N_A$  ancillae, then

$$\rho_{A_k A_{k+1} \dots A_{k+l-1}} = \text{Tr}_{E/\{k, \dots, k+l-1\}} \rho_E = \rho_{A_1 A_2 \dots A_l}, \text{ with } 1 \leq k \leq N_A, \quad (5.2)$$

where the subscript  $E/\{k, \dots, k+l-1\}$  means that all the ancillae but the ones at the set  $\{k, \dots, k+l-1\}$  are traced out.<sup>1</sup> The equation above means that the reduced state of any set of  $l$  neighbors' ancillae is the same, no matter their position. Clearly, this condition implies that the local state of each ancilla must be the same (which corresponds to  $l = 1$  in Eq. (5.2)).

The condition above can be accomplished if we start with a state of uncorrelated ancillae  $|\Phi\rangle = \bigotimes_{k=1}^{N_A} |\phi\rangle$ , where the state  $|\phi\rangle$  is arbitrary, and then evolve it according to the Hamiltonian

$$H_G = k \sum_{i,j} G_{ij} H_{ij}, \quad (5.3)$$

where  $k$  is an interaction strength,  $G_{ij}$  are the matrix elements of the adjacency matrix of a graph (to be explained in a moment), and  $H_{ij}$  represents a certain Hamiltonian interaction between ancillae  $i$  and  $j$ . For concreteness, we choose

$$H_{ij} = \sigma_x^i \otimes \sigma_x^j, \quad (5.4)$$

where  $\sigma_x$  stands for the  $x$  Pauli matrix.

The adjacency matrix elements of a graph specify the strength between the connection of each vertex of the graph. For instance, if  $G_{ij}$  is the element  $ij$  of an adjacency matrix  $G$ , its number is a measure of the strength of the connection between the vertex  $i$  and  $j$  of the graph. In our setup, we suppose that each vertex of the graph represents an ancilla, and their edges, as well as the adjacency matrix elements, represent the interaction strength between them.

In general, we don't need to have  $G_{ij} = G_{ji}$  which means that the connection between two vertices of a graph does not need to be symmetric. For instance, if the graph represents the traffic flow between two locations, the traffic can be stronger in one way than in the other. But, in our case, we only use symmetric graphs

---

<sup>1</sup>If  $k+l$  surpass  $N_A$ , the sequence continues considering the first  $k+l-N_A$  ancillae.

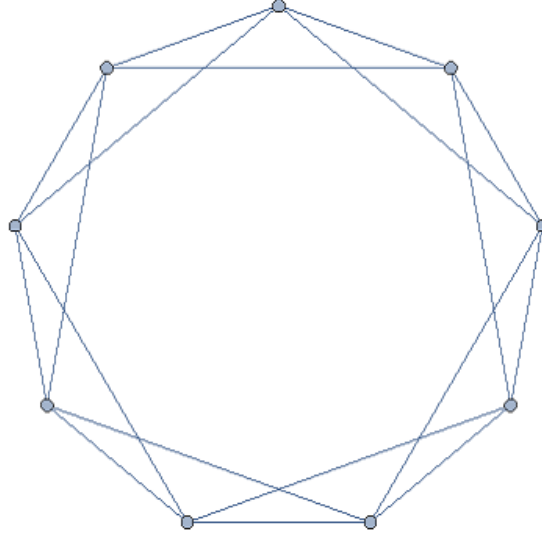


Figure 5.1: Cyclic graph with 9 ancillae (at the vertices), each interacting only with the first and second neighbors (interactions represented by the edges).

( $G_{ij} = G_{ji}$ ), this is due to the fact that, since  $H_{ij} = H_{ji}$ , then the sum of Eq. (5.3) will only affect the symmetric part of  $G$ . We also assume that our graph is *cyclic*, i.e., the connection strength between the vertices only depend on their distances, to ensure the translationally invariant character of the ancillae (Eq. (5.2)). This last restriction induces the adjacency matrix to be a *circulant matrix* [139], which means that the  $G_{ij}$  elements must depend only on the distance between  $i$  and  $j$  and we set the diagonal elements to 0. For instance, for  $N_A = 5$  we have

$$G = \begin{pmatrix} 0 & c_1 & c_2 & c_3 & c_2 & c_1 \\ c_1 & 0 & c_1 & c_2 & c_3 & c_2 \\ c_2 & c_1 & 0 & c_1 & c_2 & c_3 \\ c_3 & c_2 & c_1 & 0 & c_1 & c_2 \\ c_2 & c_3 & c_2 & c_1 & 0 & c_1 \\ c_1 & c_2 & c_3 & c_2 & c_1 & 0 \end{pmatrix}, \quad (5.5)$$

where  $c_1, c_2$  and  $c_3$  are arbitrary real coefficients. As an example, if we want only first and second neighbors interactions in our graph (see Fig. 5.1), we put  $c_j = 0, \forall j > 2$ .

### 5.1.2 Properties of the initial ancillae and their correlations

In the previous section, we outlined how to prepare the ancillae before the dynamics of the CM start. Now, we show explicit examples of preparations and the correlations that this process causes between the ancillae.

As already indicated, the whole environment will be described by

$$\rho_E = |\psi_E\rangle \langle \psi_E|, \quad (5.6)$$

where

$$|\psi_E\rangle = e^{-iH_G t} |\phi\rangle, \quad (5.7)$$

and  $H_G$  is given by Eq. (5.3), generated by a specific cyclic graph that we choose in each case.

Next, we obtain the values for the density matrices of the reduced state of each individual ancilla, by tracing out the rest of the environment

$$\rho_A = \rho_{A_j} = \text{Tr}_{\{A_2, A_3, \dots, A_{N_A}\}} (\rho_E), \quad \forall j. \quad (5.8)$$

Additionally, we also compute the values for the joint density matrices for each pair of ancillae 1 and  $j$

$$\rho_{A_1, A_j} = \text{Tr}_{E/\{1, j\}} (\rho_E). \quad (5.9)$$

Finally, we compute the mutual information between the first ancilla and its neighbors,<sup>2</sup> from Eq. (3.20) and the density matrices from the equations above, in order to measure their total correlations.

These computations are done numerically. We set the interaction time of Eq. (5.7) as  $t = 1$ , together with the interaction given by Eq. (5.4). This interaction turns the reduced qubits states  $\rho_A$  to be diagonal in the  $\sigma_z$  basis, i.e., a qubit thermal state. And thus it is sufficient for us only to study the population  $p = \langle 1 | \rho_A | 1 \rangle$  of the excited state, in order to describe the state  $\rho_A$  (see Appendix A, Section A.4).

---

<sup>2</sup>The mutual information doesn't depend on which pair of ancillae we choose to compute it, but only on the distance between them, as a consequence of our translational invariant condition.

In other words, the ancilla local state will always be in the form

$$\rho_A = \begin{pmatrix} 1-p & 0 \\ 0 & p \end{pmatrix}, \quad (5.10)$$

with  $0 \leq p \leq 1/2$ . Finally, we choose  $|\phi\rangle = |0\rangle$  and obtained the following results.

- We studied the population of the individual ancilla  $\rho_A$  (Eq. (5.8)) for cyclic graphs where each ancilla interacts only with their first nearest-neighbors (NN1) with equal intensities ( $c_1 = 1$ ), only with their first and second nearest-neighbors (NN2) with equal intensities ( $c_1 = c_2 = 1$ ) and only with their first, second and third nearest-neighbors (NN3) with equal intensities ( $c_1 = c_2 = c_3 = 1$ ). We investigated how the population of  $\rho_A$  depends on the total number of ancillae  $N_A$ . The answer is that, for a number of  $N_A \gtrsim 6$ , the population tends to stabilize independent of  $N_A$ . This happens because the interactions occur between a small number of nearest-neighbors, and, as  $N_A$  gets larger, the total number of neighbors each ancilla will interact with saturates. For instance, for NN2, each ancilla will interact with a maximum of 4 neighbors, so when  $N_A = 5$  each ancilla of NN2 already interacts with its maximum of neighbors. These observations are exemplified in the plots of Fig. 5.2.
- We studied the population dependence on the values of the interaction strength  $k$  in Eq. (5.3), obtaining a peak of the populations at  $k = \pi/8$  when  $p = 0.5$  (i.e. maximally mixed state and infinite temperature limit) and a minimum at  $k = \pi/4$  when  $p = 0$  (i.e. ground state and zero temperature limit) and then the population oscillates with a period of  $\pi/4$  in  $k$  for NN1, NN2, and NN3. A plot of the populations versus  $k$  for different values of  $N_A$  is given in Fig. 5.3. The exact same pattern is seen for the plots with different  $N_A$ 's;
- In Fig. 5.4, we compute the mutual information as a function of the distance between neighbors for NN1, NN2, and NN3. This shows that, in general, the ancillae get correlated with distant neighbors, even in the NN1 case. Intuitively, the mutual information between closest neighbors tends to be greater than with the more distant neighbors. An exception happens in the NN3 case

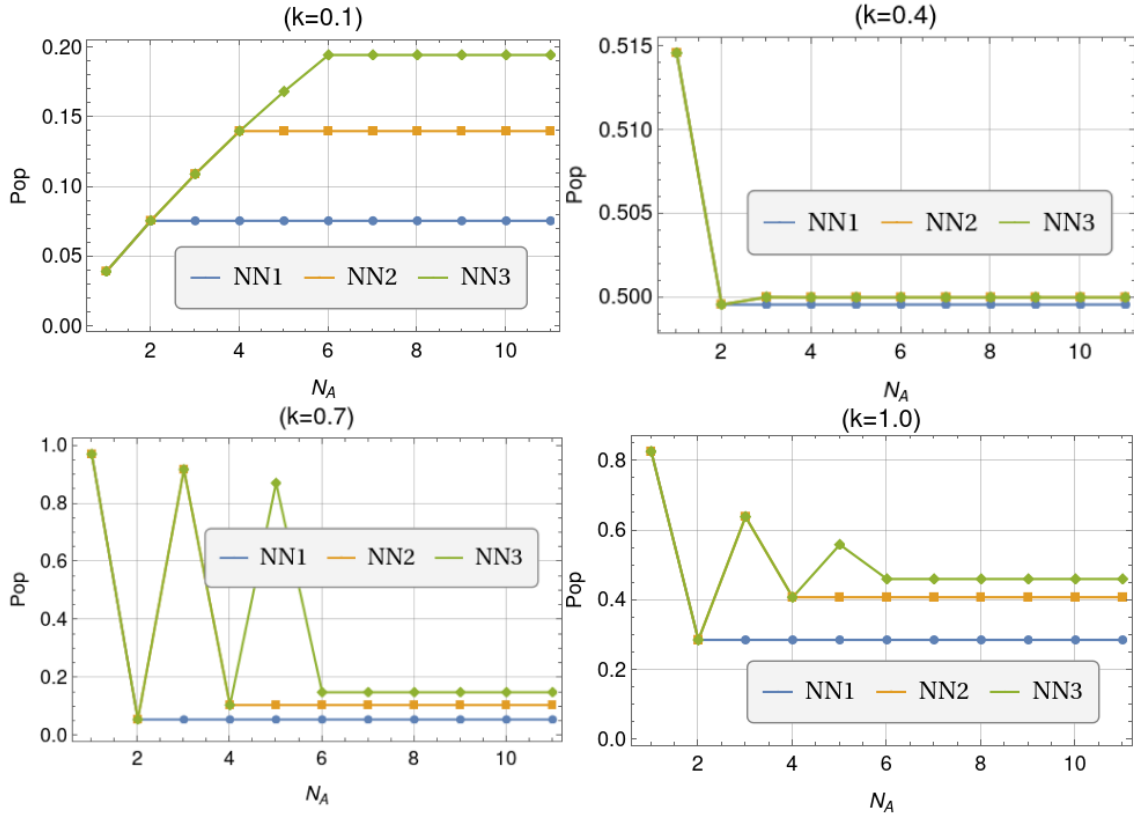


Figure 5.2: Population of the excited state of  $\rho_A$  versus total number of ancillae  $N_A$ , for different values of  $k$ .

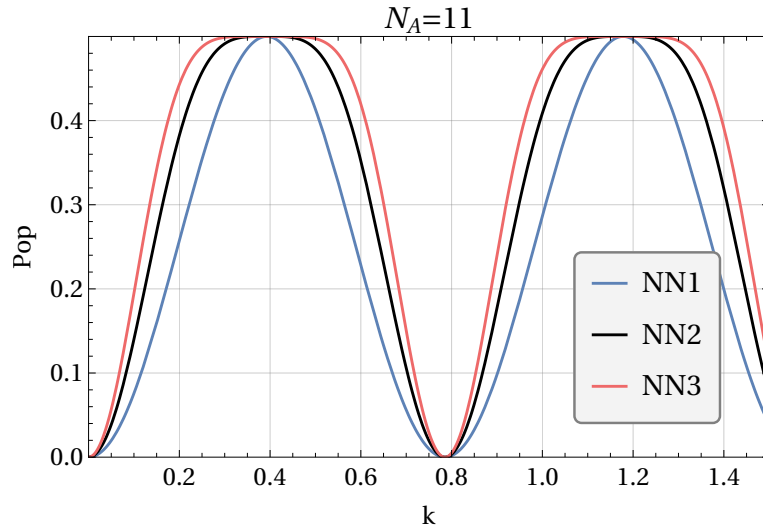


Figure 5.3: Population of  $\rho_A$  versus values of  $k$ , for  $N_A = 11$ .



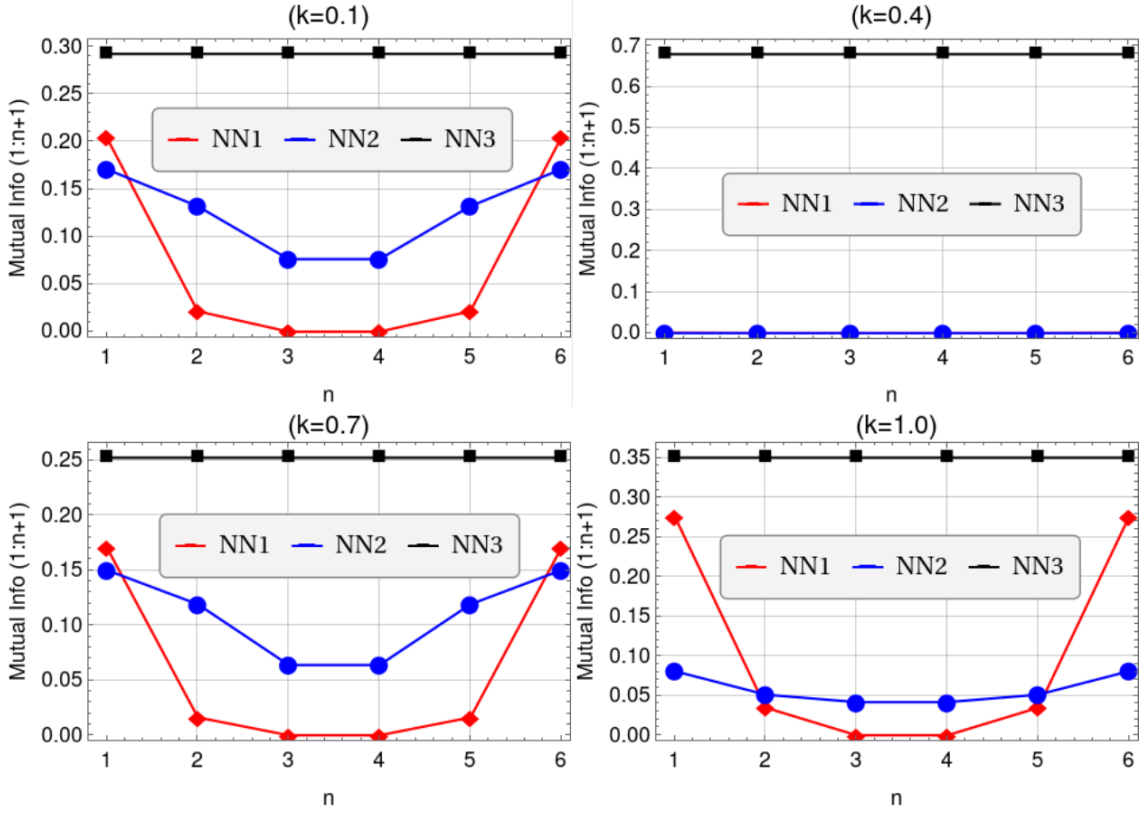


Figure 5.4: Mutual information between neighbors *versus* distance between neighbors, for  $N_A = 7$  and different values of  $k$ .

with  $N_A = 7$ , where the mutual information tends to be very similar for any neighbor distance, this is a consequence of the fact that in this case, each ancilla interacts equally with every other six ancillae. Additionally, we can see that we have no mutual information between the neighbors in NN1 and NN2 for the case of  $k = 0.4$ , while in this case we have higher mutual information in NN3 than for any other values of  $k$ ;

- We analyzed the mutual information between nearest neighbors as a function of  $k$  for different values of  $N_A$  in Fig. 5.5. This exposes a periodic behavior of the mutual information as a function of  $k$  (with a period of  $\pi/4$ ), and peaks of maxima for the mutual information in regions close to  $k = 0.1$  and  $k = 0.7$  for NN1, and around  $k = 0.15$  and  $k = 0.65$  for NN2 and NN3. For  $N_A \leq 7$ , we observe a higher maximum peak of the mutual information at  $k \approx 0.4$  in NN3, while this region corresponds to a minimum for NN1 and NN2, which justifies the behavior of the mutual information in Fig. 5.4 for  $k = 0.4$ . Interestingly,

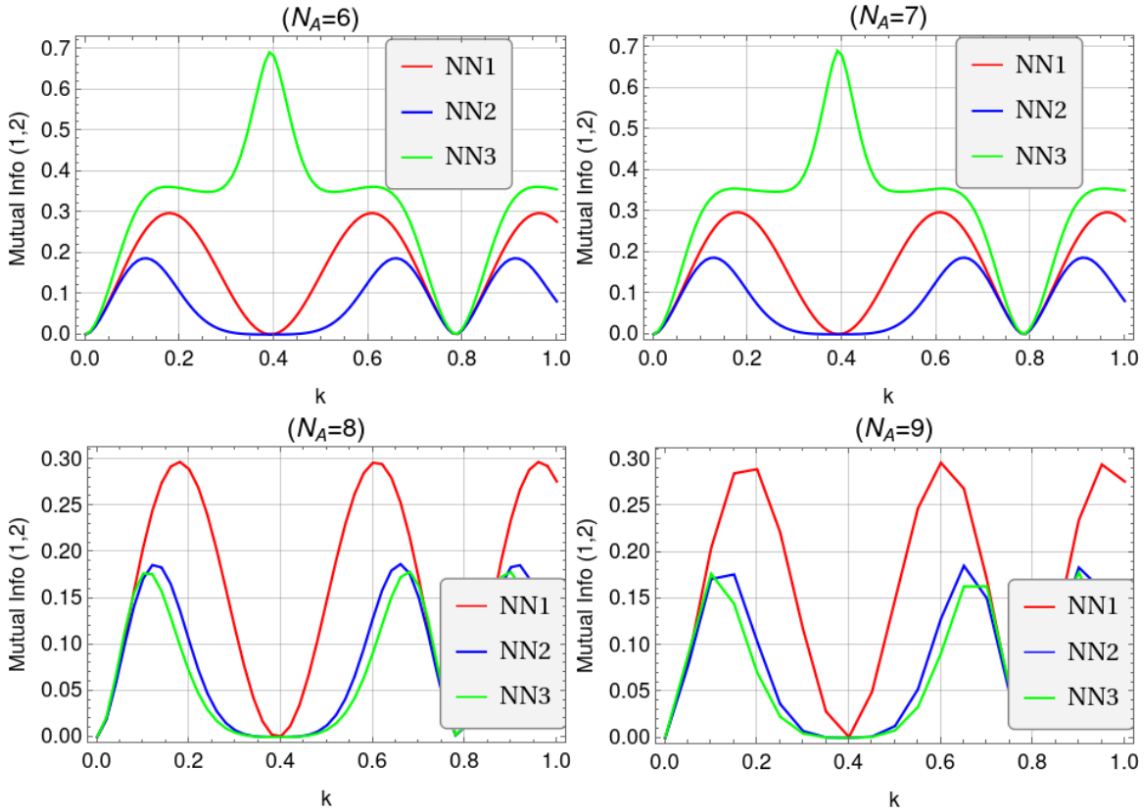


Figure 5.5: Mutual information between first neighbors *versus*  $k$ , for different values of  $N_A$ . For larger values of  $N_A$ , the plots lose resolution since they are computationally more demanding.

this maximum peak of the mutual information for NN3 seems to vanish for  $N_A > 7$  and, as in NN1 and NN2, this region around  $k \approx 0.4$  have a minimum for NN3. These observations about the correlations' dependence on  $k$  will be useful to our choice of parameters in order to investigate the dynamics of the CM and the effects of the correlations in the evolution of the system, in the next Section.

## 5.2 Breaking Homogenization by initial correlations

Finally, we present the results for the CM evolution with a Partial SWAP unitary (Eq. (2.44)) describing the interaction between each locally identical ancilla and the system, just like the Homogenization process described in Sec. 2.3.6. But now, we

suppose the presence of initial correlations between the ancillae, which oblige us to compute directly Eq. (2.21) to obtain the system's evolution after each collision. In this case, we don't have the option of decomposing the evolution as a successive operation of simpler channels. Consequently, these computations using Eq. (2.21) needed to be done numerically.

We set the correlated ancillae forming the initial environment  $\rho_E^0$  as being the Hamiltonian graph states presented in the former Section, choosing the same set of cyclic graphs NN1, NN2, and NN3, we now chose  $N = 17$  in order to have enough collisions so that the system reaches its steady state. We also constructed another environment by removing the correlations between the ancillae in these Hamiltonian graph states, but keeping the same local ancilla-reduced state  $\rho_A$  (such that  $\rho_E = \rho_A^{\otimes NA}$ ). This way, we prepare two environments, one causing a Non-Markovian evolution with correlated ancillae and the other with a Markovian evolution (exactly as the standard homogenization of Sec. 2.3.6), both having the ancillae in the same local state  $\rho_A$ .

As in standard CMs outlined in Sec. 2.3, we start at  $t = 0$  and the stroboscopic evolution is given in steps of  $\tau$  (for these computations we choose  $\tau = 1$ ), which is the duration of each collision. We initialized the system's qubit at the ground state  $\rho_S^0 = |0\rangle\langle 0|$  and we can again describe the system's state by its population of the excited state. We analyzed the dynamics for the Hamiltonian graph states with different values of  $k$  (in the Hamiltonian of Eq. (5.3)). From the analysis of Figs. (5.4) and (5.5) we searched for the graph states that would maximize the initial correlations between the ancillae and, consequently, maximize the deviation of the system steady state with respect to the case of independent ancillae, therefore breaking Homogenization. We also analyzed how different values of  $g$  for the strength of the Partial SWAP in Eq. (2.44) affected the desired pushing. We present the following results:

- As can be seen in Figs. 5.6, 5.7 and 5.8, the parameter  $k$  has a central role in the pushing effect of the correlations over the system's evolution, since it significantly affects the correlations between the ancillae, as was observed in Fig. 5.5. From this same Figure, we also deduced that the region around

$k \approx 0.4$  may have a minimum for the mutual information of NN1, NN2, and NN3 for the case of NN3 we suppose that  $k \approx 0.4$  corresponds to a minimum in the mutual information for  $N_A \geq 8$  due to Fig. 5.5), and hence there would be fewer correlations to cause the pushing. This fact can be seen in the plots of NN2 and NN3 (Figs. 5.7 and 5.8), where there is no breaking of homogenization for  $k = 0.4$ . Adversely, for NN1 (Fig. 5.6) we see that the pushing is still present in  $k = 0.4$ , which can be caused by the non-vanishing mutual information between the ancillae since the behavior of the mutual information can be different than in Fig. 5.5 for larger  $N_A$ . Also from Fig. 5.5, we suppose large correlation effects in the regions around  $k = 0.15$  and  $k = 0.65$  for NN1,  $k = 0.15$  and  $k = 0.7$  for NN2, and  $k = 0.1$  and  $k = 0.7$  for NN3. This is confirmed by the plots of Figs. 5.6, 5.7 and 5.8 since, for the initially correlated ancillae case with these values of  $k$ , clearly the system's steady state deviates from the homogenization in the uncorrelated case;

- Finally, we also study different values of  $g$  (the strength of the Partial SWAP interaction, given in Eq. (2.44)) in the plots of Figs. 5.6, 5.7 and 5.8. They show the pattern that, for lower values of  $g$ , exemplified by  $g = 0.5$ , the homogenization takes more steps to happen, but the effect of the correlations is stronger than for larger  $g$ 's. This seems to suggest that a greater thermalization (or homogenization) time allows the correlations to act more in the system's evolution, for greater values of  $g$ , e.g.  $g = 1.5$ , the system homogenizes too rapidly, so the correlation effects are unseen. Lastly, the Partial SWAP depends trigonometrically on  $g$  (see Eq. (2.44)), therefore, the effects of  $g$  in the system's evolution will oscillate, as  $g$  grows, repeating the results in cycles of  $\pi$ .

The analysis above clearly confirms the pushing effect on the system's evolution and the breaking of Homogenization caused by the presence of initial correlations between the ancillae, for the case where the system and ancillae are qubits. These results are also published in [96].

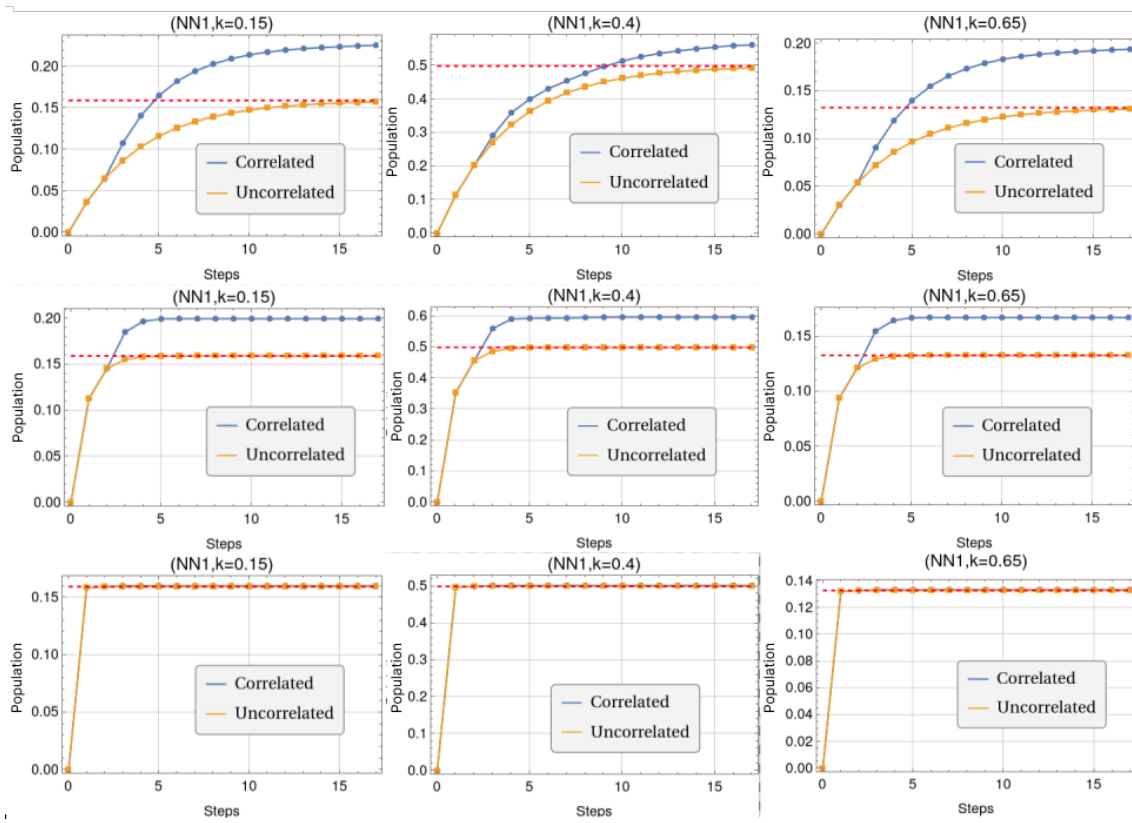


Figure 5.6: Plots of population of  $\rho_S$  versus number of steps for ancillae prepared with the NN1 cyclic graph with  $N_A = 17$ , for different values of  $k$ . Each line corresponds to a different value of  $g$  strength of the partial SWAP interaction, from top to bottom  $g = 0.5$ ,  $g = 1.0$ , and  $g = 1.5$ . The red dashed lines indicate the value of the population of the respective  $\rho_A$ , which is the value in which the system's population converges if homogenization happens.

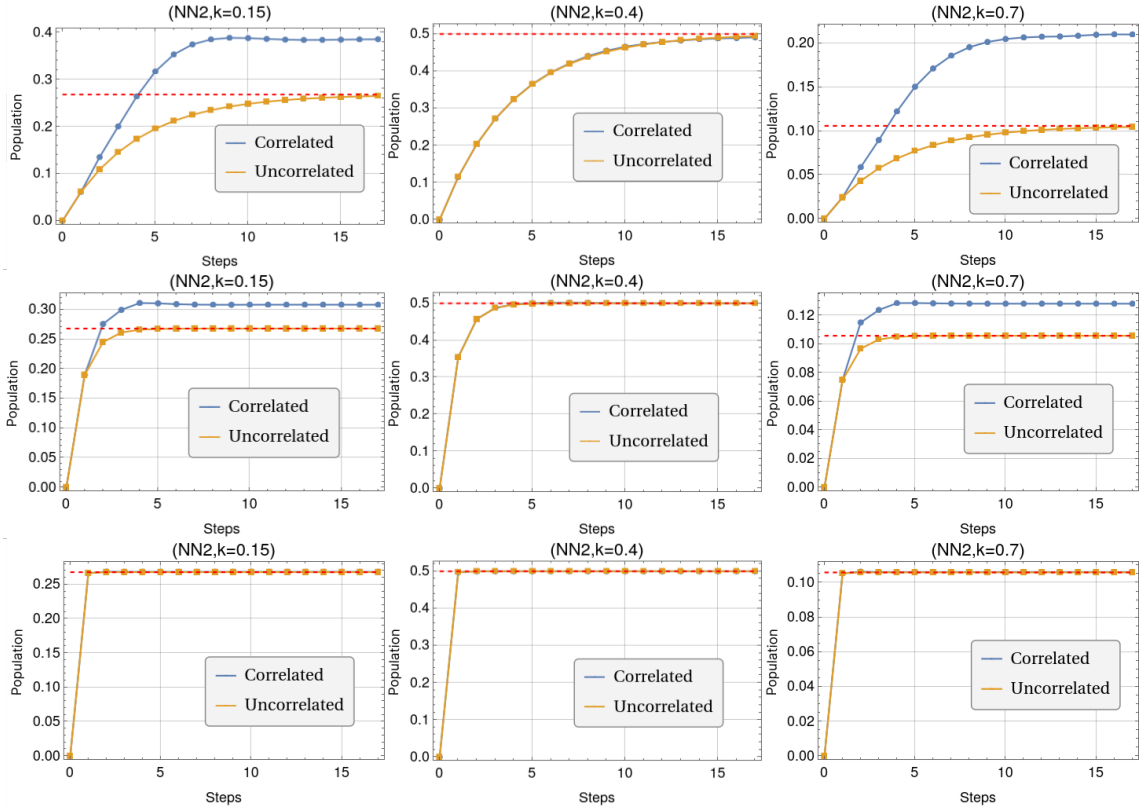


Figure 5.7: Plots of population of  $\rho_S$  versus number of steps for ancillae prepared with the NN2 cyclic graph with  $N_A = 17$ , for different values of  $k$ . Each line corresponds to a different value of  $g$  strength of the partial SWAP interaction, from top to bottom  $g = 0.5$ ,  $g = 1.0$ , and  $g = 1.5$ . The red dashed lines indicate the value of the respective  $\rho_A$  population, which is the value in which the system's population converges if homogenization happens.

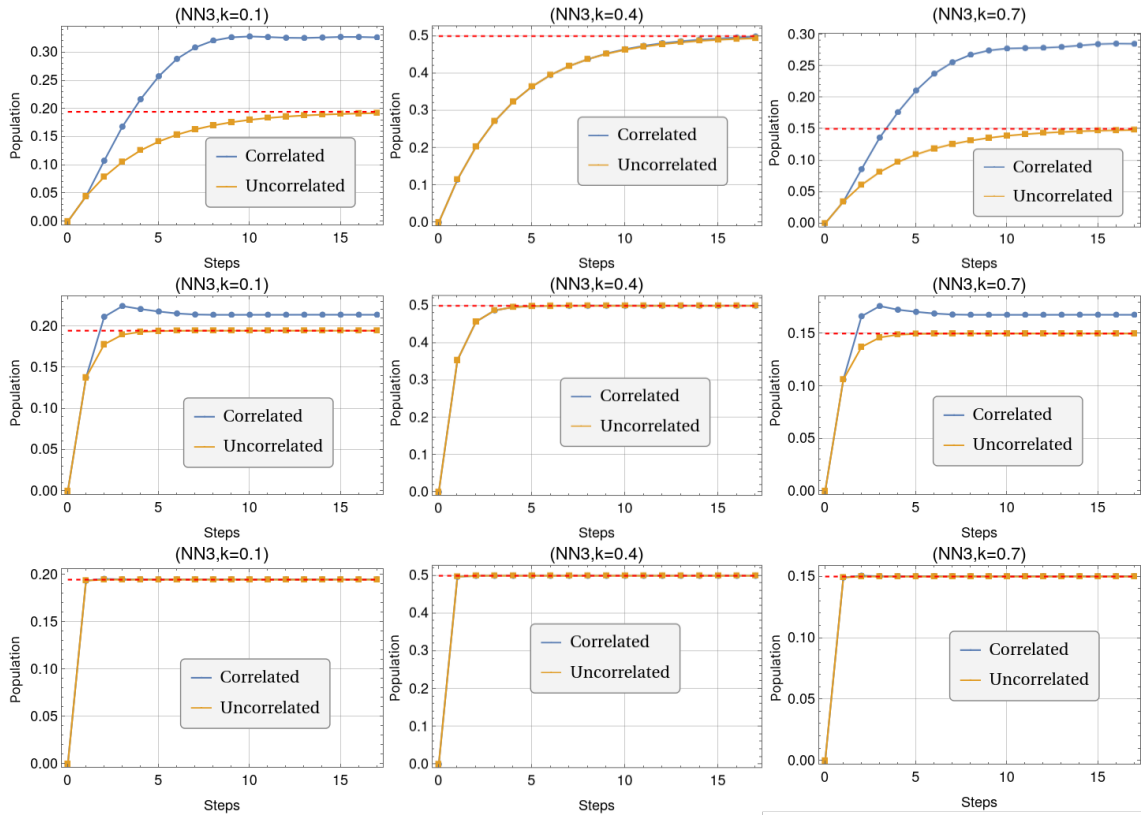


Figure 5.8: Plots of population of  $\rho_S$  versus number of steps for ancillae prepared with the NN3 cyclic graph with  $N_A = 17$ , for different values of  $k$ . Each line corresponds to a different value of  $g$  strength of the partial SWAP interaction, from top to bottom  $g = 0.5$ ,  $g = 1.0$ , and  $g = 1.5$ . The red dashed lines indicate the value of the respective  $\rho_A$  population, which is the value in which the system's population converges if homogenization happens.

# Chapter 6

## Initially Correlated Ancillae - Gaussian States CM

In this Chapter, we present the main results of the second project of this thesis. We obtain simple analytical formulae for the evolution of the system for *any* number of initially correlated ancillae in the CM, as described in Sec. 2.3, with a Partial SWAP unitary in bosonic modes states. Here we observe a direct influence of the initial correlations between the ancillae in the system's evolution, which cause a linear (and independent of the initial system state) term on the system's steady state. This presents a clear image of the pushing caused by the correlations and the breaking of Homogenization. These results are also described in [96].

The results were possible since we consider the system and ancillae bosonic modes starting in Gaussian states. This simplifies remarkably the computations, as explained in Sec. 4.6. Now we only study the covariance matrices which will completely describe our system and environment.<sup>1</sup> Also, the continuous variables formalism made possible a much more simple description of the dynamics, because now the evolution is given by the  $2(N_A + 1) \times 2(N_A + 1)$  (where  $N_A$  is the total number of ancillae) symplectic matrices, instead of unitaries that act directly in the infinite-dimensional Hilbert space. These characteristics of our object of study al-

---

<sup>1</sup>For instance, in Chapter 5 we were able to compute numerically a maximum of only 17 collisions in our CM since this would involve the preparation of 17 ancillae in the environment. In order to fully describe the environment density matrix the computations involved  $2^{17} \times 2^{17}$  matrices. While for Gaussian states, an environment made of 100 ancillae can be fully described by a  $200 \times 200$  covariance matrix.



low us to manipulate simple matrices analytically, for a low number of ancillae and collisions, and then induce the results for arbitrary numbers. The procedure will be detailed in the following.

## 6.1 Preliminaries

### 6.1.1 The bosonic CM evolution

As we already pointed out above, the system and environment are composed of bosonic modes. We have one mode for our system and  $N_A$  modes for the environment (each mode represents one ancilla). All of them start the evolution in Gaussian states, thus their initial states  $\rho_S^0$  and  $\rho_E^0$  will be fully described by their covariance matrices  $\sigma_S^0$  and  $\sigma_E^0$  and their first moments  $\langle \hat{\mathbf{r}}_S^0 \rangle$  and  $\langle \hat{\mathbf{r}}_E^0 \rangle$ . Now we assume, without loss of generality, that  $\langle \hat{\mathbf{r}}_S^0 \rangle = 0$  and  $\langle \hat{\mathbf{r}}_E^0 \rangle = 0$  (where 0 here means a respective vector of 0 in all entries), which will ensure that the first moments will remain 0 during the evolution, remaining for us only the analysis of the covariance matrices.<sup>2</sup>

We will follow the procedure explained in Subsec. 2.3.1 to represent the dynamics of the CM. Since we are dealing with Gaussian states and quadratic-Hamiltonian unitaries (the Beam Splitter, to be presented in the next Subsection), all the following steps will maintain the Gaussian character of the states, as proved in Section 4.7. Further results from Section 4.7 will also be used.

We start by supposing that the system and environment start uncorrelated at time  $t = 0$ , so their joint state will be given by  $\rho_{SE}^0 = \rho_S^0 \otimes \rho_E^0$ . The tensor product is a Gaussian operation and the resulting covariance matrix will be

$$\sigma_{SE}^0 = \sigma_S^0 \oplus \sigma_E^0, \quad (6.1)$$

from Eq. (4.83).

Then we make a unitary evolution, which is described by a symplectic matrix

---

<sup>2</sup>This last restriction can contemplate the general analysis since, as we shall study the evolution under the Partial SWAP unitary, the evolution of the first moments is given by Eq. (4.68). So, if the system starts with some arbitrary first moment  $\bar{\mathbf{r}}$ , then we can always translate such first moment to 0 (which will not affect the covariance matrix since its evolution equation, Eq. (4.71), is decoupled from the first moments) and Eq. (4.68) guarantee that its evolution will be trivial.

$S_H^1$  (which will be related to the unitary used, in our case, the Partial SWAP), using Eq. (4.72)

$$\sigma_{SE}^1 = S_H^1 \sigma_{SE}^0 (S_H^1)^\top, \quad (6.2)$$

where  $\sigma_{SE}^1$  is the covariance matrix of the joint system plus environment state after the *first* collision.

Next, in order to obtain the system's evolution, we separate the joint covariance matrix as

$$\sigma_{SE}^1 = \begin{pmatrix} \sigma_S^1 & \xi_{SE}^1 \\ (\xi_{SE}^1)^\top & \sigma_E^1 \end{pmatrix}, \quad (6.3)$$

where  $\sigma_S^1$  is a  $2 \times 2$  block matrix,  $\sigma_E^1$  is a  $2N_A \times 2N_A$  block matrix and  $\xi_{SE}^1$  is a  $2 \times 2N_A$  block matrix. As it is demonstrated in Sec. 4.7,  $\sigma_S^1$  will be the covariance matrix of the reduced state of the system, i.e., the system obtained after tracing out the environment. For obtaining the following steps of the system's evolution, we just proceed to evolve the joint system  $SE$  with the respective unitaries

$$\sigma_{SE}^n = S_H^n S_H^{n-1} \dots S_H^1 \sigma_{SE}^0 (S_H^1)^\top \dots (S_H^{n-1})^\top (S_H^n)^\top \quad (6.4)$$

and again separate the evolved joint system as

$$\sigma_{SE}^n = \begin{pmatrix} \sigma_S^n & \xi_{SE}^n \\ (\xi_{SE}^n)^\top & \sigma_E^n \end{pmatrix}, \quad (6.5)$$

taking  $\sigma_S^n$  as the covariance matrix of our evolved reduced state. Furthermore,  $\sigma_E^n$  is the covariance matrix of the environment's reduced state.

The reason that we must evolve the *whole* joint system in Eq. (6.4) is that we cannot have a map from intermediate covariance matrices of the system to the final one since we must consider the non-Markovian effects caused by the initial correlations between the ancillae. This has the same reasoning of why we cannot break the map of Eq. (2.21) into a succession of intermediate maps. In fact, notice the resemblance between Eqs. (6.4) and (2.20) and note that Eq. (6.5) has the same role as Eq. (2.21).

### 6.1.2 The Beam Splitter interaction

Here, we present the unitary that we shall use in our CM for each collision. It is an interaction of immense importance in Quantum Optics, the so-called *Beam-Splitter* (*BS*) [14, 15, 55, 98, 121]. The BS can be defined by the following interaction Hamiltonian between two bosonic modes  $A$  and  $B$

$$\hat{H}_{BS} = \frac{g}{2}(\hat{p}_A \hat{q}_B - \hat{q}_A \hat{p}_B), \quad (6.6)$$

where  $g > 0$ .

In the following, we will show that the unitary generated by this Hamiltonian satisfies the Partial SWAP conditions (Eqs. (2.45) and (2.46)) for the Gaussian bosonic modes case.

The interaction Hamiltonian above is quadratic in terms of canonical operators, hence it can be decomposed in terms of Eq. (4.50) with  $\mu = 0$  and the Hamiltonian matrix

$$H_{BS} = \begin{pmatrix} 0 & -ig\sigma_y \\ ig\sigma_y & 0 \end{pmatrix}, \quad (6.7)$$

where each entry of the matrix above is a  $2 \times 2$  matrix and  $\sigma_y$  is the  $y$  Pauli matrix. Therefore, the corresponding symplectic transformation will be

$$\begin{aligned} S_{BS} &= e^{\Omega H_{BS} \tau} \\ &= \begin{pmatrix} c & s \\ -s & c \end{pmatrix}, \end{aligned} \quad (6.8)$$

where  $c = \cos(g\tau)$ ,  $s = \sin(g\tau)$ ,  $\tau$  is the duration of the interaction and each entry is multiplied by  $\mathbb{I}_2$ .

If the modes  $A$  and  $B$  are Gaussian, they can be described by covariance matrices  $\sigma_A$  and  $\sigma_B$ . And if they are uncorrelated and happen to be in the same local state ( $\sigma_A = \sigma_B = \sigma$ ), their joint covariance matrix will be

$$\sigma_{AB} = \begin{pmatrix} \sigma & 0 \\ 0 & \sigma \end{pmatrix}. \quad (6.9)$$

Hence, the unitary Beam Splitter operation in this state will be given by

$$\begin{aligned} S_{BS}\sigma_{AB}S_{BS}^\top &= \begin{pmatrix} c & -s \\ s & c \end{pmatrix} \begin{pmatrix} \sigma & 0 \\ 0 & \sigma \end{pmatrix} \begin{pmatrix} c & s \\ -s & c \end{pmatrix} \\ &= \begin{pmatrix} \sigma & 0 \\ 0 & \sigma \end{pmatrix}. \end{aligned} \quad (6.10)$$

Consequently, the partial traces in  $A$  and  $B$  will result in the same state as the initial, satisfying Eqs. (2.45) and (2.46). These Equations are necessary and sufficient conditions for a unitary operator to be a Partial SWAP [19].

### 6.1.3 Correlations block-matrices

Before presenting our results, we will expose important properties of the block matrices that will describe completely the correlations between our ancillae. Suppose two ancillae of our environment, representing the modes  $j$  and  $k$ , respectively. We can take a block matrix made of the covariance matrix terms

$$\begin{aligned} \xi_{j,k} &= \begin{pmatrix} \sigma_{2j-1,2k-1} & \sigma_{2j-1,2k} \\ \sigma_{2j,2k-1} & \sigma_{2j,2k} \end{pmatrix} \\ &= \begin{pmatrix} \langle q_j q_k \rangle - \langle q_j \rangle \langle q_k \rangle & \langle q_j p_k \rangle - \langle q_j \rangle \langle p_k \rangle \\ \langle p_j q_k \rangle - \langle p_j \rangle \langle q_k \rangle & \langle p_j p_k \rangle - \langle p_j \rangle \langle p_k \rangle \end{pmatrix}, \end{aligned} \quad (6.11)$$

where we used canonical operators of different modes commute and Eq. (4.57). Now, given the reduced state  $\rho_{j,k}$  of the modes  $j$  and  $k$ , its covariance matrix will be

$$\sigma_{j,k} = \begin{pmatrix} \sigma_j & \xi_{j,k} \\ \xi_{j,k}^\top & \sigma_k \end{pmatrix}, \quad (6.12)$$

where  $\sigma_{j(k)}$  is the local covariance matrix of  $j(k)$ . Furthermore, from the deduction of Eq. (4.83), we have  $\xi_{j,k} = 0^3$  if and only if  $\rho_{j,k} = \rho_j \otimes \rho_k$  is the tensor product of the local density matrices. From Eq. (3.17), the mutual information between  $j$

---

<sup>3</sup>In this context,  $0$  means *null matrix*.

and  $k$  is  $\mathcal{I}(j : k) = 0$  when  $\rho_{j,k} = \rho_j \otimes \rho_k$ , consequently  $\xi_{j,k} = 0$  is *necessary and sufficient* to  $\mathcal{I}(j : k) = 0$ .

For this reason, we often name these components as *correlations* between bosonic modes of Gaussian states. For instance, for an environment made of 5 ancillae, we have

$$\sigma_E = \begin{pmatrix} \sigma_{A_1} & \xi_{1,2} & \xi_{1,3} & \xi_{1,4} & \xi_{1,5} \\ \xi_{1,2}^\top & \sigma_{A_2} & \xi_{2,3} & \xi_{2,4} & \xi_{2,5} \\ \xi_{1,3}^\top & \xi_{2,3}^\top & \sigma_{A_3} & \xi_{3,4} & \xi_{3,5} \\ \xi_{1,4}^\top & \xi_{2,4}^\top & \xi_{3,4}^\top & \sigma_{A_4} & \xi_{4,5} \\ \xi_{1,5}^\top & \xi_{2,5}^\top & \xi_{3,5}^\top & \xi_{4,5}^\top & \sigma_{A_5} \end{pmatrix}, \quad (6.13)$$

where all the terms inside the above matrix are actually  $2 \times 2$  block matrices,  $\sigma_{A_n}$  are the covariance matrices of the  $n$ -th ancilla reduced state and  $\xi_{j,k}$  represents the correlations between the ancillae  $j$  and  $k$ .

## 6.2 Main results

### 6.2.1 Correlated nearest-neighbors

We start with a simple, yet insightful result. We apply the system evolution procedure presented in Subsection 6.1.1 for the case where we have  $N_A$  ancillae that are correlated only with their nearest neighbors. Additionally, we start supposing that the ancillae are not necessarily identical for obtaining a more general result and then restricting it to identical ancillae and comparing it to Homogenization. This means that the correlation terms of the environment will be in the form  $\xi_{j,k} = \xi_{j,k} \delta_{k,j+1}$ . Therefore, the environment of correlated ancillae will initialize in a state with the

following  $2N_A \times 2N_A$  covariance matrix<sup>4</sup>

$$\sigma_E^0 = \begin{pmatrix} \sigma_{A_1} & \xi_{1,2} & 0 & \cdots & 0 \\ \xi_{1,2}^\top & \sigma_{A_2} & \xi_{2,3} & \cdots & 0 \\ 0 & \xi_{3,4}^\top & \sigma_{A_3} & \ddots & \vdots \\ \vdots & \ddots & \ddots & \ddots & \xi_{N_A-1,N_A} \\ 0 & 0 & \cdots & \xi_{N_A-1,N_A}^\top & \sigma_{A_{N_A}} \end{pmatrix}. \quad (6.14)$$

The joint system will start as

$$\begin{aligned} \sigma_{SE}^0 &= \sigma_S^0 \oplus \sigma_E^0 \\ &= \begin{pmatrix} \sigma_S^0 & 0 & 0 & \cdots & 0 \\ 0 & \sigma_{A_1} & \xi_{1,2} & \cdots & 0 \\ 0 & \xi_{1,2}^\top & \sigma_{A_2} & \ddots & \ddots \\ \vdots & \ddots & \ddots & \ddots & \xi_{N_A-1,N_A} \\ 0 & 0 & \cdots & \xi_{N_A-1,N_A}^\top & \sigma_{A_{N_A}} \end{pmatrix}. \end{aligned} \quad (6.15)$$

This joint state evolves as the system evolves unitarily (collides) with each ancilla  $j$ . They interact via the Hamiltonian

$$\hat{H}_j = \hat{H}_S + \hat{H}_{A_j} + \hat{H}_{BS_j}, \quad (6.16)$$

where  $\hat{H}_S = \frac{\omega}{2}(\hat{q}_S^2 + \hat{p}_S^2)$ ,  $\hat{H}_{A_j} = \frac{\omega}{2}(\hat{q}_{A_j}^2 + \hat{p}_{A_j}^2)$ , for  $\omega > 0$ ,  $\hat{q}_{S(A_j)}$  and  $\hat{p}_{S(A_j)}$  are the quadrature operators of the system (ancilla  $j$ ) and

$$\hat{H}_{BS_j} = \frac{g}{2}(\hat{p}_S \hat{q}_{A_j} - \hat{q}_S \hat{p}_{A_j}), \quad (6.17)$$

for  $g > 0$ , is the Beam Splitter interaction of the system with each ancilla  $j$ . We have that  $\hat{H}_S$  and  $\hat{H}_{A_j}$  are local Hamiltonians, so we can set them to 0 by going to the interaction picture (see Appendix A).

Proceeding, we compute the symplectic transformation corresponding to the

---

<sup>4</sup>In this Section, every matrix element is a  $2 \times 2$  block matrix, or a number multiplied by  $\mathbb{I}_2$ .

unitary generated by the Hamiltonian  $\hat{H}_j$  in the interaction picture

$$S_H^j = e^{\Omega H_{BS_j} \tau}, \quad (6.18)$$

where  $H_{BS_j}$  is the  $(2N_A + 1) \times (2N_A + 1)$  Hamiltonian matrix corresponding to  $\hat{H}_{BS_j}$  from Eq. (6.17) and  $\tau$  is the duration of the collision. For  $j = 1$  (first collision), we have the following matrix Hamiltonian matrix

$$H_{BS}^1 = \begin{pmatrix} 0 & -ig\sigma_y & 0 & \cdots & 0 \\ ig\sigma_y & 0 & 0 & \cdots & 0 \\ 0 & 0 & 0 & \cdots & 0 \\ \vdots & \vdots & \vdots & \ddots & \vdots \\ 0 & 0 & 0 & \cdots & 0 \end{pmatrix}, \quad (6.19)$$

where  $\sigma_y$  is the  $y$  Pauli matrix. Consequently, we have the following  $(2N_A + 1) \times (2N_A + 1)$  symplectic matrix

$$S_H^1 = \begin{pmatrix} c & s & 0 & \cdots & 0 \\ -s & c & 0 & \cdots & 0 \\ 0 & 0 & 1 & \cdots & 0 \\ \vdots & \vdots & \vdots & \ddots & \vdots \\ 0 & 0 & 0 & \cdots & 1 \end{pmatrix}, \quad (6.20)$$

where  $c = \cos(g\tau)$  and  $s = \sin(g\tau)$ .

In a completely analogous way, we have the Hamiltonian matrices corresponding

to the next collisions

$$\begin{aligned}
 H_{BS}^2 &= \begin{pmatrix} 0 & 0 & -ig\sigma_y & \cdots & 0 \\ 0 & 0 & 0 & \cdots & 0 \\ ig\sigma_y & 0 & 0 & \cdots & 0 \\ \vdots & \vdots & \vdots & \ddots & \vdots \\ 0 & 0 & 0 & \cdots & 0 \end{pmatrix}, \\
 &\quad \vdots \\
 H_{BS}^{N_A-1} &= \begin{pmatrix} 0 & 0 & \cdots & 0 & -ig\sigma_y \\ 0 & 0 & \cdots & 0 & 0 \\ \vdots & \vdots & \ddots & \vdots & \vdots \\ 0 & 0 & \cdots & 0 & 0 \\ ig\sigma_y & 0 & \cdots & 0 & 0 \end{pmatrix}, \tag{6.21}
 \end{aligned}$$

and obtain the respective symplectic matrices

$$\begin{aligned}
 S_H^2 &= \begin{pmatrix} c & 0 & s & \cdots & 0 \\ 0 & 1 & 0 & \cdots & 0 \\ -s & 0 & c & \cdots & 0 \\ \vdots & \vdots & \vdots & \ddots & \vdots \\ 0 & 0 & 0 & \cdots & 1 \end{pmatrix}, \\
 &\quad \vdots \\
 S_H^{N_A-1} &= \begin{pmatrix} c & 0 & \cdots & 0 & s \\ 0 & 1 & \cdots & 0 & 0 \\ \vdots & \vdots & \ddots & \vdots & \vdots \\ 0 & 0 & \cdots & 1 & 0 \\ -s & 0 & \cdots & 0 & c \end{pmatrix}. \tag{6.22}
 \end{aligned}$$

Next, we continue to follow the procedure described in Subsection 6.1.1 using the symplectic transformations above. Now we obtain the joint system's first collisional step evolution by computing  $\sigma_{SE}^1 = S_H^1 \sigma_{SE}^0 (S_H^1)^\top$  and taking the system's covariance



matrix as in Eq. (6.5), obtaining<sup>5</sup>

$$\sigma_S^1 = c^2 \sigma_S^0 + s^2 \sigma_{A_1}. \quad (6.23)$$

Doing the next step evolution  $\sigma_{SE}^2 = S_H^2 \sigma_{SE}^1 (S_H^2)^\top$ , we obtain

$$\sigma_S^2 = c^4 \sigma_S^0 + c^2 s^2 \sigma_{A_1} + s^2 \sigma_{A_2} + cs^2 (\xi_{1,2} + \xi_{1,2}^\top).$$

And again,  $\sigma_{SE}^3 = S_H^3 \sigma_{SE}^2 (S_H^3)^\top$  for the third step, obtaining

$$\sigma_S^3 = c^6 \sigma_S^0 + c^4 s^2 \sigma_{A_1} + c^2 s^2 \sigma_{A_2} + s^2 \sigma_{A_3} + c^3 s^2 (\xi_{1,2} + \xi_{1,2}^\top) + cs^2 (\xi_{2,3} + \xi_{2,3}^\top).$$

From this, we can begin to see a pattern, from which we can induce

$$\boxed{\sigma_S^n = c^{2n} \sigma_S^0 + \sum_{k=1}^n c^{2(n-k)} s^2 \sigma_{A_k} + \sum_{k=1}^{n-1} c^{2k-1} s^2 (\xi_{k-1,k} + \xi_{k-1,k}^\top)}, \quad (6.24)$$

for the system's covariance matrix after the  $n^{\text{th}}$  collision.

Now, if we suppose that the ancillae are identical  $\sigma_{A_k} = \sigma_A$ , as in the Homogenization case, we obtain, after the use of the geometric sum and some simplifications

$$\sigma_S^n = c^{2n} \sigma_S^0 + (1 - c^{2n}) \sigma_A + \sum_{k=1}^{n-1} c^{2k-1} s^2 (\xi_{k-1,k} + \xi_{k-1,k}^\top).$$

The equation above indicates that, if the correlation terms are 0, Homogenization will happen. Indeed, for null correlation terms, if  $g\tau$  are such that  $|c| < 1$ , then we will have the steady state  $\sigma_S^\infty = \sigma_A$ .

Also supposing that the nearest-neighbor correlations have the same intensity  $\xi_{k-1,k} = \xi$ , for a  $2 \times 2$  block-matrix  $\xi$ , we have

$$\boxed{\sigma_S^n = c^{2n} \sigma_S^0 + (1 - c^{2n}) \sigma_A + c(1 - c^{2(n-1)}) (\xi + \xi^\top)}. \quad (6.25)$$

Finally, we obtain, for the case of identical ancillae and same-intensity nearest-

---

<sup>5</sup>It is important to remember here that  $\sigma_{A_1}$  is a covariance matrix constructed by averages rather than an operator acting on the Hilbert space of  $A_1$ . Hence, its elements can contribute to the elements of  $\sigma_S^1$ .

neighbor correlations, the steady state, which is computed by taking the limit  $n \rightarrow \infty$  (considering that  $|c| < 1$ )

$$\boxed{\sigma_S^\infty = \sigma_A + c(\xi + \xi^\top)}. \quad (6.26)$$

The equation above is our first result of obtaining an analytical equation that describes the CM with the presence of initially correlated ancillae, computing the effects of such correlations. Also, by changing the entries of  $\xi$  we can have control over the pushing of the entries of the steady state, driving it away from the ancilla's covariance matrix  $\sigma_A$ . This shows a simple and clear visualization of how the correlations break Homogenization, and how we can obtain an additional term in the steady state of the system which is completely dependent on global correlations, although the system interacts only locally with ancillae that are locally identical.

Another intriguing observation about the result above can be done. If we consider the initial state of the system and of the local ancillae as thermal states, the additional correlation term  $\cos(g\tau)(\xi + \xi^\top)$  can heat or cool down the system's steady state, depending only on the sign of  $\cos(g\tau)$ . For instance, if the system and local ancillae initial states are thermal states at the same temperature, the term  $\cos(g\tau)(\xi + \xi^\top)$  can dictate the action of the CM as a thermal machine or a refrigerator depending only on the values of  $g\tau$ .

## 6.2.2 General case

Proceeding analogously as in the case of the nearest-neighbor correlation presented above, we can obtain the general evolution of a system interacting with  $N_A$  ancillae, all correlated with themselves, via BS interactions. Since the interactions are the same, the symplectic matrices used in the case of the nearest-neighbor correlation (Eqs. (6.20) and (6.22)) still describe the unitary dynamics. The only difference is in the initial environment state, its covariance matrix  $\sigma_E^0$  will have the most general form, given, for instance, in Eq. (6.13) (for the case of  $N_A = 5$ ). We initialize with the joint system's covariance matrix  $\sigma_S^0 \otimes \sigma_E^0$  and, using Eq. (6.4), we proceed analogously as in the case of the nearest-neighbor correlation for obtaining

the evolution of the system-environment joint state covariance matrix. This way, obtaining the local system's covariance matrices from Eq. (6.5), we achieve the following chain of equations

$$\begin{aligned}
 \sigma_S^1 &= s^2 \sigma_{A_1} + c^2 \sigma_S^0, \\
 \sigma_S^2 &= c^4 \sigma_S^0 + c^2 s^2 \sigma_{A_1} + s^2 \sigma_{A_2} + cs^2 (\xi_{1,2} + \xi_{1,2}^\top), \\
 \sigma_S^3 &= c^6 \sigma_S^0 + c^4 s^2 \sigma_{A_1} + c^2 s^2 \sigma_{A_2} + s^2 \sigma_{A_3} + c^3 s^2 (\xi_{1,2} + \xi_{1,2}^\top) + c^2 s^2 (\xi_{1,3} + \xi_{1,3}^\top) + cs^2 (\xi_{2,3} + \xi_{2,3}^\top), \\
 \sigma_S^4 &= c^8 \sigma_S^0 + c^6 s^2 \sigma_{A_1} + c^4 s^2 \sigma_{A_2} + c^2 s^2 \sigma_{A_3} + s^2 \sigma_{A_4} + c^5 s^2 (\xi_{1,2} + \xi_{1,2}^\top) + c^4 s^2 (\xi_{1,3} + \xi_{1,3}^\top) \\
 &\quad + c^3 s^2 (\xi_{1,4} + \xi_{1,4}^\top) + c^3 s^2 (\xi_{2,3} + \xi_{2,3}^\top) + c^2 s^2 (\xi_{2,4} + \xi_{2,4}^\top) + cs^2 (\xi_{3,4} + \xi_{3,4}^\top), \\
 &\quad \vdots
 \end{aligned} \tag{6.27}$$

from which, after some observation, we can induce the pattern for the system's covariance matrix after the  $n^{\text{th}}$  collision

$$\boxed{\sigma_S^n = c^{2n} \sigma_S^0 + \sum_{j=1}^n c^{2(n-j)} s^2 \sigma_{A_j} + s^2 \sum_{j=1}^{n-1} \sum_{\ell>j}^n c^{2n-j-\ell} (\xi_{j,\ell} + \xi_{j,\ell}^\top).} \tag{6.28}$$

Although the very general status of the solution above, it will give us more interesting results if we analyze more particular cases. First of all, if we suppose that again all ancillae are equal  $\sigma_{A_j} = \sigma_A$  and using the geometric sum, we obtain

$$\sigma_S^n = c^{2n} \sigma_S^0 + (1 - c^{2n}) \sigma_A + s^2 \sum_{j=1}^{n-1} \sum_{\ell>j}^n c^{2n-j-\ell} (\xi_{j,\ell} + \xi_{j,\ell}^\top). \tag{6.29}$$

The equation above shows that Homogenization is achieved again if we have no correlations, since in this case, we have the steady state  $\sigma_S^\infty = \sigma$  if  $|c| < 1$ . Also, it is worth noting that the third term of the right-hand side will be fully responsible for the pushing caused by the correlations and the breaking of Homogenization. This term is entirely independent of the system's initial state and from the ancillae local conditions.

### 6.2.3 Distance dependent correlations

We can proceed with a very intuitive restriction from the case above. That is, if the correlations terms between the ancillae of the initial global state depend only on the distance between the ancillae, i.e., they only depend on  $\ell - j = d$

$$\xi_{j,\ell} = \xi_{|j-\ell|} = \xi_d. \quad (6.30)$$

This simplifies Eq. (6.29) to

$$\sigma_S^n = c^{2n} \sigma_S^0 + (1 - c^{2n}) \sigma_A + s^2 \sum_{m=1}^{n-1} c^{2m} \sum_{d=1}^m c^{-d} (\xi_d + \xi_d^\top). \quad (6.31)$$

Here, we can have another way of computing the evolution of the system in the case of the nearest-neighbors correlation, by restricting  $\xi_d = \delta_{1,d} \xi$  in the equation above, arriving at the same results. But another interesting application is for the *Algebraically decaying correlations* case, where we consider that the correlations decay exponentially with the distance

$$\xi_d = K^{1-d} \xi, \quad d = 1, 2, \dots, \quad (6.32)$$

for some  $2 \times 2$  matrix  $\xi$  and  $K > 1$ . Using this choice in Eq. (6.31), we obtain

$$\sigma_S^n = c^{2n} \sigma_S^0 + (1 - c^{2n}) \sigma_A + \frac{K s^2}{cK - 1} \left( \frac{c^2 - c^{2n}}{s^2} - \frac{c^{n-1} K^{1-n} - 1}{1 - c^{-1} K} \right) (\xi + \xi^\top), \quad (6.33)$$

where we used the geometric sum twice and made a few algebraic manipulations. From the solution above, we obtain the system's steady state (for  $|c| < 1$ )

$$\sigma_S^\infty = \sigma_A + \frac{cK}{K - c} (\xi + \xi^\top). \quad (6.34)$$

Now, notice that the case  $K \gtrsim 1$  means long-range correlations, while  $K \gg 1$  are related to short-range correlations. This short-range correlation result is in total agreement with the nearest-neighbors correlation result. Indeed, if we take the limit of  $K \rightarrow \infty$ , the steady state in Eq. (6.34) reduces to the nearest-neighbors

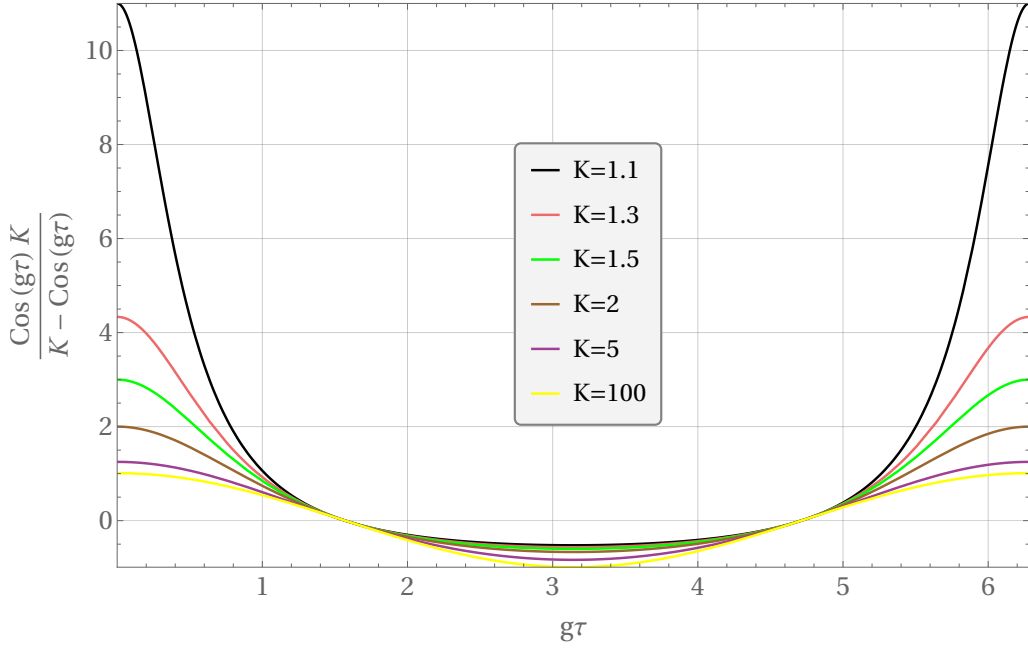


Figure 6.1: Values of  $\frac{\cos(g\tau)K}{K - \cos(g\tau)}$  versus  $g\tau$  for different values of  $K$  in the interval  $g\tau \in [0, 2\pi]$ .

correlations steady state of Eq. (6.26), i.e.

$$\sigma_A + \frac{cK}{K - c}(\xi + \xi^\top) \xrightarrow{K \rightarrow \infty} \sigma_A + c(\xi + \xi^\top).$$

On the other hand, for the long-range correlations case, we have large values of the correlation effects for small  $K$ . See, for instance, Fig. 6.1, which shows the behaviour of  $\frac{cK}{K - c}$  in function of  $g\tau$ , for different values of  $K$ . For small values of  $K$ , the function  $\frac{cK}{K - c}$  increases dramatically for  $g\tau$  close to 0 or  $2\pi$ , amplifying the effects of the correlation matrix  $\xi$ . As in the nearest-neighbor correlations case, the sign of the function multiplying  $(\xi + \xi^\top)$  can be positive or negative. Although in this case, for small values of  $K$ , we see a much larger potential for the positive sign case and the negative sign case. Recalling, positive or negative values of  $\frac{cK}{K - c}(\xi + \xi^\top)$  can sign that the effect of correlations heats or cool down the system, respectively. This happens in the case where the system and ancillae start at thermal states and when the matrix  $\xi$  is diagonal with positive identical elements. Again, this indicates that this CM can serve as a thermal machine or a refrigerator depending on the value of  $g\tau$  and  $K$ .

## 6.2.4 Ancillae evolution

Here we will obtain each ancilla's local covariance matrix after its collision with the state, for the general case of initially correlated ancillae. Importantly, the local density matrices of each ancilla can change only *during* the collision with the system, after each collision, the respective local state of the ancilla doesn't change. This can be seen as a consequence of the *no-signaling principle*,<sup>6</sup> which states that *local* operations in a *local* state cannot affect any properties of another *local* state. Of course, every collision can affect the *correlations* between any ancillae, this happens because the *global* state of the environment is affected at each collision.

We use the exact same procedure used in Subsection 6.2.2. Analogously, we start with the most general environment  $\sigma_E^0$  and evolve the joint system  $\sigma_S^0 \otimes \sigma_E^0$  by using Eq. (6.4) with the symplectic matrices of Eqs. (6.20) and (6.22). In the final step, we separate the covariance matrix of the joint state as in Eq. (6.5), but we now take the local covariance matrix of the evolved ancilla (inside the covariance matrix of the evolved environment  $\sigma_E^n$ ), instead of taking the system's covariance matrix. The result for the first four evolved ancillae after their collisions are given in the following chain of equations

$$\begin{aligned}
 \sigma'_{A_1} &= s^2 \sigma_S + c^2 \sigma_{A_1}, \\
 \sigma'_{A_2} &= c^2 s^2 \sigma_S + c^2 \sigma_{A_2} + s^4 \sigma_{A_1} - cs^2 (\xi_{1,2} + \xi_{1,2}^\top), \\
 \sigma'_{A_3} &= c^4 s^2 \sigma_S + c^2 \sigma_{A_3} + s^4 \sigma_{A_2} + c^2 s^4 \sigma_{A_1} + cs^4 (\xi_{1,2} + \xi_{1,2}^\top) - c^2 s^2 (\xi_{1,3} + \xi_{1,3}^\top) - cs^2 (\xi_{2,3} + \xi_{2,3}^\top), \\
 \sigma'_{A_4} &= c^6 s^2 \sigma_S + c^2 \sigma_{A_4} + s^4 \sigma_{A_3} + c^2 s^4 \sigma_{A_2} + c^4 s^4 \sigma_{A_1} + c^3 s^4 (\xi_{1,2} + \xi_{1,2}^\top) + c^2 s^4 (\xi_{1,3} + \xi_{1,3}^\top) \\
 &\quad - c^3 s^2 (\xi_{1,4} + \xi_{1,4}^\top) + cs^4 (\xi_{2,3} + \xi_{2,3}^\top) - c^2 s^2 (\xi_{2,4} + \xi_{2,4}^\top) - cs^2 (\xi_{3,4} + \xi_{3,4}^\top), \quad (6.35)
 \end{aligned}$$

where  $\sigma'_{A_j}$  is the covariance matrix of the ancilla  $j$  after its collision with the system. Analyzing the equations above, we induce that the covariance matrix an ancilla

---

<sup>6</sup>An exposition to the no-signaling principle can be seen in [91].

$n \geq 2$  after its collision with the system is given by

$$\begin{aligned} \sigma'_{A_n} &= c^{2n-1} s^2 \sigma_S + s^4 \sum_{k=1}^{n-1} c^{2(n-k-1)} \sigma_{A_k} + c^2 \sigma_{A_n} + \sum_{m=1}^{n-1} \sum_{n'>m}^{n-1} c^{2n-2-n'-m} s^4 (\xi_{m,n'} + \xi_{m,n'}^\top) \\ &\quad - \sum_{m=1}^{n-1} c^{n-m} s^2 (\xi_{m,n} + \xi_{m,n}^\top). \end{aligned} \quad (6.36)$$

The equation above is quite general, but we can obtain a more conclusive analysis by making some restrictions. For studying the Homogenization case, we suppose that all ancillae are initially identical  $\sigma_{A_j} = \sigma_A$  for every  $j$ . After supposing it in the equation above, using the geometric sum, and making algebraic simplifications, we obtain

$$\begin{aligned} \sigma'_{A_n} &= c^{2(n-1)} s^2 (\sigma_S - \sigma_A) + \sigma_A + \sum_{m=1}^{n-1} \sum_{n'>m}^{n-1} c^{2n-n'-m-2} s^4 (\xi_{m,n'} + \xi_{m,n'}^\top) \\ &\quad - \sum_{m=1}^{n-1} c^{n-m} s^2 (\xi_{m,n} + \xi_{m,n}^\top). \end{aligned} \quad (6.37)$$

Clearly, for this case of initially identical ancillae, if we have null correlations terms and  $|c| < 1$ , then  $\sigma_S^\infty = \sigma$ . This means that, after a large number of collisions, the ancilla will practically not modify its state after interacting with the system. This agrees with the last Homogenization condition (Eq. (2.48)) and it is the final step in order to show that, in the absence of initial correlations between the ancillae, our CM of the system and initially identical ancillae of bosonic modes, interacting via the BS, indeed corresponds to the Homogenization in the bosonic case.

Again, if we make a restriction over the correlations matrix, making it only distance dependent (Eq. (6.30)), we obtain

$$\begin{aligned} \sigma'_{A_n} &= c^{2(n-1)} s^2 (\sigma_S - \sigma_A) + \sigma_A + \sum_{m=1}^{n-1} \sum_{d=1}^{n-m-1} c^{2n-d-2m-2} s^4 (\xi_d + \xi_d^\top) \\ &\quad - \sum_{m=1}^{n-1} c^d s^2 (\xi_d + \xi_d^\top). \end{aligned} \quad (6.38)$$

In order to consider the cases studied in the previous Subsection for the system's evolution, we suppose Algebraically decaying correlations, given by Eq. (6.32). Using this type of correlation in the Equation above, we have, after using the geometric

sum twice and making algebraic manipulations

$$\sigma'_{A_n} = c^{2(n-1)}s^2(\sigma_S - \sigma_A) + \sigma_A + \Gamma_n(K, gt)(\xi + \xi^\top), \quad (6.39)$$

where

$$\begin{aligned} \Gamma_n(K, \tau) &= -s^2K \frac{cK^{-1} - (cK^{-1})^n}{1 - cK^{-1}} + \frac{s^4K}{c^2} \left( \frac{1}{cK - 1} \frac{c^2 - c^{2n}}{s^2} - \frac{cK(c^{-1}K)^{1-n} - cK}{(cK - 1)(1 - c^{-1}K)} \right), \\ c &= \cos(\tau), \\ \text{and } s &= \sin(\tau). \end{aligned} \quad (6.40)$$

The function  $\Gamma_n(K, \tau)$  will dictate the correlations effects on the  $n^{\text{th}}$  ancilla state after its collision with the system. This function vanishes at the limit of large  $n$ , verily

$$\begin{aligned} \Gamma_\infty(K, \tau) &= -s^2K \frac{cK^{-1}}{1 - cK^{-1}} + s^4K \left( \frac{1}{(cK - 1)s^2} + \frac{c^{-1}K}{(cK - 1)(1 - c^{-1}K)} \right) \\ &= -s^2K \frac{cK^{-1}}{1 - cK^{-1}} + s^2K \left( \frac{cK^{-1}}{1 - cK^{-1}} \right) \\ &= 0. \end{aligned} \quad (6.41)$$

Additionally, we see, from the plots of Figs. 6.2 and 6.3, that after oscillating in the first collision, the function  $\Gamma_n(K, \tau)$  converges monotonically to 0 for large  $n$ . Therefore, the effects of correlations in each ancilla decrease as the ancillae collide with the system until they eventually vanish.

### 6.3 Constructing initially correlated ancillae from H-Graphs

In this Section, we describe a method for constructing an environment of bosonic ancillae whose correlations depend only on the distance between the ancillae. This justifies the form of the environment correlations supposed in the last Section (especially in Subsection 6.2.3) by means of construction made with known systems and



operations.

The procedure to create such environments is again by making use of *Hamiltonian graph states* or *H-graphs* [118, 134–138] and is completely analogous to the procedure presented in Section 5.1 for qubits ancillae. However, due to the versatile tools of continuous variables, we create a protocol for constructing environments with the desired form of distance-dependent correlations using H-graphs. Furthermore, graph-states can be produced experimentally by means of optical preparation with squeezing plus interferometry [140, 141] or optical parametric oscillators [142], therefore the construction presented here is a feasible example for the experimental implementation of a correlated environment. The protocol is described as follows.

### 6.3.1 Constructing covariance matrix elements

If we want an environment with  $n$  bosonic modes, suppose initially that the environment state is in the  $n$ -mode vacuum  $|\phi\rangle = |0\rangle^{\otimes n}$ . To create graph states, first, we define the unitary operator

$$\mathcal{V} = e^{-ik \sum_{i,j} G_{ij} H_{ij}}, \quad (6.42)$$

where  $G_{ij}$  are the elements of the adjacency matrix  $G$  representing a graph where the vertices are the ancillae and the edges represent the interactions between them

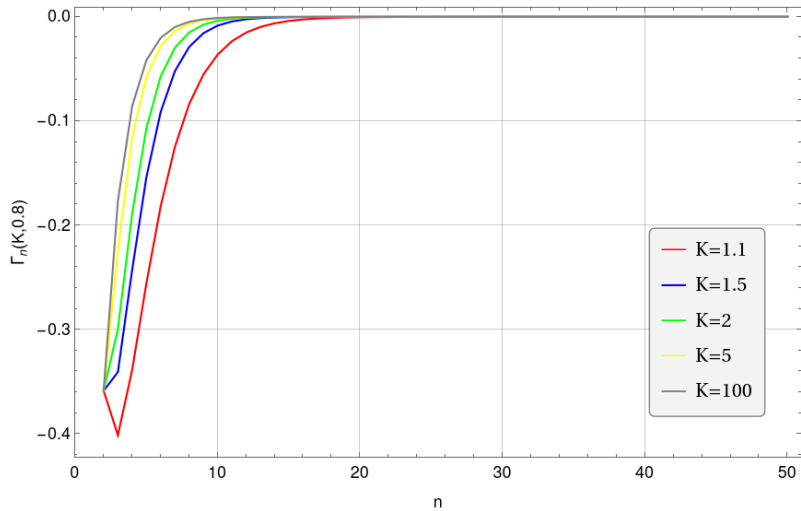


Figure 6.2:  $\Gamma_n(K, gt)$  versus  $n$  for different values of  $K$ , for  $g = 0.8$  and  $t = 1$  fixed.

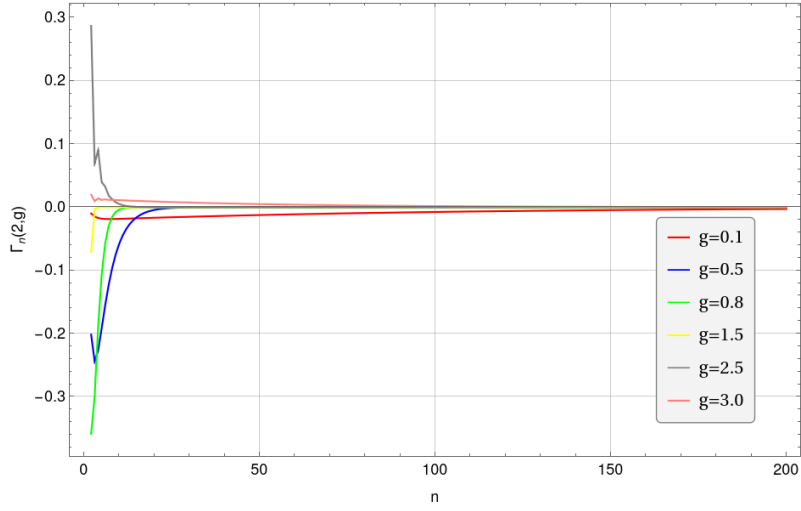


Figure 6.3:  $\Gamma_n(K, gt)$  versus  $n$  for different values of  $g$ , for  $K = 2$  and  $t = 1$  fixed.

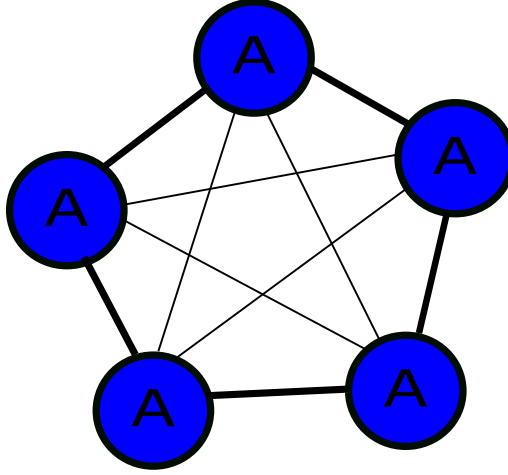


Figure 6.4: Example of a graph with ancillae in the vertices and the thickness of the edges between them represent the strength of the correlations (in this case the correlations are weaker for more distant ancillae), given by the adjacency matrix.

(see Fig. 6.4) and

$$H_{ij} = \frac{i}{2} \sum_{ij} (\hat{a}_i^\dagger \hat{a}_j^\dagger - \hat{a}_i \hat{a}_j), \quad (6.43)$$

is the two-mode squeezing interaction Hamiltonian between the modes  $i$  and  $j$ , the operator  $\hat{a}_i$  ( $\hat{a}_i^\dagger$ ) corresponds to the annihilator (creator) operator of the mode  $i$ . And the graph state is defined as the application of this unitary in the vacuum

$$|\psi_E\rangle = \mathcal{V}|\phi\rangle. \quad (6.44)$$

With the canonical commutation relations, one can show that the evolution of

the canonical operators for each mode  $i$  will be given by

$$\mathcal{V}^\dagger \hat{q}_i \mathcal{V} = \sum_j M_{ij} \hat{q}_j \quad \text{and} \quad (6.45)$$

$$\mathcal{V}^\dagger \hat{p}_i \mathcal{V} = \sum_j M_{ij}^{-1} \hat{p}_j, \quad (6.46)$$

where

$$M = e^{Gk}. \quad (6.47)$$

Consequently, we can compute the average of the anti-commutators of the canonical operators, resulting in

$$\frac{1}{2} \langle \{q_i, q_j\} \rangle = \frac{1}{2} (MM^\top)_{ij}, \quad (6.48)$$

$$\frac{1}{2} \langle \{p_i, p_j\} \rangle = \frac{1}{2} [(M^\top M)^{-1}]_{ij}, \quad \text{and} \quad (6.49)$$

$$\langle q_i p_j \rangle = 0. \quad (6.50)$$

Supposing now that  $G$  is the adjacency matrix of a cyclic graph, then it must be a circulant matrix [139].<sup>7</sup> The diagonalization of such a matrix is given by

$$G = \mathcal{O} \Lambda \mathcal{O}^\dagger, \quad (6.51)$$

where the elements of  $\mathcal{O}$  are discrete Fourier transforms

$$\mathcal{O}_{l,m} = \frac{e^{i2\pi lm/n}}{\sqrt{n}}, \quad l, m = 0, \dots, n-1, \quad (6.52)$$

and  $\Lambda$  is the matrix of eigenvalues  $\Lambda_{l,m} = \delta_{l,m} \lambda_k$ , where

$$\lambda_j = 2 \sum_{l=0}^{(n-1)/2} c_l \cos(2\pi lj/n), \quad (6.53)$$

assuming  $n$  odd for convenience.

---

<sup>7</sup>Remembering, cyclic graphs are graphs in which the connection strength between the vertices only depend on their distances. Hence the coefficients have the same value  $c_j$  for each diagonal and  $c_j = c_{n-j}$ , for every  $0 \leq j \leq n-1$ , since we demand that the adjacency matrix must be symmetric. See, for instance, Eq. (5.5).

From these equations and Eqs. (6.48), (6.49) and (6.50), we obtain, for cyclic graphs, after algebraic manipulations

$$\begin{aligned}\langle q_j q_{j'} \rangle &= \frac{1}{2n} \sum_l \exp \left[ i \frac{2\pi l}{n} (j - j') + 2k\lambda_l \right] \quad \text{and} \\ \langle p_j p_{j'} \rangle &= \frac{1}{2n} \sum_l \exp \left[ i \frac{2\pi l}{n} (j - j') - 2k\lambda_l \right].\end{aligned}$$

This results in equal local covariance matrices for the ancillae

$$\sigma_A = \frac{1}{2n} \begin{pmatrix} \sum_{m=0}^{n-1} e^{2k\lambda_m} & 0 \\ 0 & \sum_{m=0}^{n-1} e^{-2k\lambda_m} \end{pmatrix}. \quad (6.54)$$

And correlations block matrices depending only on the distance between the ancillae

$$\xi_d = \begin{pmatrix} \xi_d^{(q)} & 0 \\ 0 & \xi_d^{(p)} \end{pmatrix}, \quad (6.55)$$

where

$$\xi_d^{(q)} = \langle q_j q_{j+d} \rangle = \frac{1}{2n} \sum_{m=0}^{n-1} e^{i2\pi dm/n + 2k\lambda_m} \quad \text{and} \quad (6.56)$$

$$\xi_d^{(p)} = \langle p_j p_{j+d} \rangle = \frac{1}{2n} \sum_{m=0}^{n-1} e^{i2\pi dm/n - 2k\lambda_m}. \quad (6.57)$$

### 6.3.2 Constructing desired correlations from choosing the cyclic graph

Here we describe a protocol for obtaining a desired form of correlation term  $\xi_d^{(q)}$  by choosing properly the coefficients of the adjacency matrix.

First notice that we can rewrite Eq. (6.56) as

$$\xi_d^{(q)} = \sum_{l=0}^{n-1} a_l e^{i\theta_d l}, \quad (6.58)$$

where  $a_l = \frac{e^{2k\lambda_l}}{2n}$  and  $\theta_d = \frac{2\pi d}{n}$ . Now, since  $\lambda_{n-l} = \lambda_l$ , we have that  $a_{n-l} = a_l$ ,

additionally, from  $\lambda_l = \lambda_{-l}$  we also have  $a_l = a_{-l}$ . Using these facts, we can write<sup>8</sup>

$$\sum_{l=0}^{n-1} a_l e^{i\theta_d l} = \sum_{l=-(n-1)/2}^{(n-1)/2} a_l e^{i\theta_d l}. \quad (6.59)$$

Therefore, for large number of ancillae  $n$ , we can approximate  $\xi_d^{(q)}$  to a Fourier Series

$$\xi_d^{(q)} = \sum_{l=-\infty}^{\infty} a_l e^{i\theta_d l}, \quad (6.60)$$

from which we can obtain the coefficient of the series

$$a_l = \frac{1}{2\pi} \int_0^{2\pi} \xi_d^{(q)} e^{-i\theta_d l} d\theta_d, \quad (6.61)$$

where  $\theta_d = \frac{2\pi d}{n}$  approaches to a continuous variable due to the large  $n$  approximation.

We, therefore, obtained a formula for  $a_l$  given a desired form of distance-dependent correlation  $\xi_d^{(q)}$ . Inverting the definition of  $a_l$ , we obtain the adjacency matrix  $G$  eigenvalues in function of  $\xi_d^{(q)}$

$$\lambda_l = \frac{\log(2na_l)}{2k}. \quad (6.62)$$

Finally, from the eigenvalues of the circulant adjacency matrix  $G$ , we can obtain its coefficients by noticing that, from Eq. (6.53), if we go to the large  $n$  limit, the eigenvalues will also be a Fourier Series

$$\lambda(\theta_l) = \sum_{j=0}^{\infty} 2c_j \cos(j\theta_l), \quad (6.63)$$

where  $\theta_l = \frac{2\pi l}{n}$ . From this Fourier Series, we obtain the coefficients

$$c_0 = \frac{1}{4\pi} \int_{-\pi}^{\pi} \lambda(\theta_l) d\theta_l \quad \text{and} \quad (6.64)$$

$$c_j = \frac{1}{2\pi} \int_{-\pi}^{\pi} \lambda(\theta_l) \cos(j\theta_l) d\theta_l \quad \text{for } j \geq 1, \quad (6.65)$$

where  $\theta_j$  approaches a continuous variable for large  $n$ . Whence, from Eqs. (6.61),

---

<sup>8</sup>One can prove this equation by noticing that  $\sum_{l=0}^{n-1} a_l e^{i\theta_d l} = \sum_{l=0}^{(n-1)/2} a_l e^{i\theta_d l} + \sum_{l=(n+1)/2}^{n-1} a_l e^{i\theta_d l}$  and using  $a_{n-l} = a_l$ ,  $a_l = a_{-l}$  and  $\theta_d = \frac{2\pi d}{n}$  to show that  $\sum_{l=(n+1)/2}^{n-1} a_l e^{i\theta_d l} = \sum_{l=-(n-1)/2}^{-1} a_l e^{i\theta_d l}$ .

(6.62), (6.64) and (6.65) we have a procedure of obtaining the coefficients of the circulant adjacency matrix  $G$  from a desired correlation term  $\xi_d^{(q)}$  depending on the distance between the ancillae.

### 6.3.3 Application to the case of the Algebraically decaying correlation

As an important example, which generates an environment as the one used in Subsection 6.2.3, we apply these results to find the coefficients for the adjacency matrix of the cyclic graph which generates the graph state environment with correlations depending on the distance  $d$  described by

$$\xi_d^{(q)} = K^{1-d} \xi_0^{(q)}, \quad (6.66)$$

where  $\xi_0^{(q)}$  is a real number and  $K > 1$ .

From using Eq. (6.61), we obtain

$$a_l = 2nK \log(K) \frac{1 - (-1)^l K^{-n/2}}{4\pi^2 l^2 + n^2 \log^2(K)} \xi_0^{(q)}, \quad (6.67)$$

and after some manipulations, we can write, for large  $n$

$$a(\theta_l) = \frac{2K \log(K)}{n} \frac{1}{\theta_l^2 + \log^2(K)} \xi_0^{(q)},$$

where  $\theta_l = \frac{2\pi l}{n}$ . Moreover, from Eq. (6.62) we obtain

$$\lambda(\theta_l) = \left[ \frac{1}{2k} \log(4K \log(K)) - \frac{1}{2k} \log(\theta_l^2 + \log^2(K)) \right] \xi_0^{(q)}.$$

Finally, for obtaining the coefficients of  $G$ , we must evaluate the integrals from Eqs.

(6.64) and (6.65)

$$\begin{aligned}
 c_0 &= \frac{1}{4\pi} \int_{-\pi}^{\pi} \left[ \frac{1}{2k} \log(4K \log(K)) - \frac{1}{2k} \log(\theta_l^2 + \log^2(K)) \right] \xi_0^{(q)} d\theta_l \quad \text{and} \quad (6.68) \\
 c_j &= \frac{1}{2\pi} \int_{-\pi}^{\pi} \left[ \frac{1}{2k} \log(4K \log(K)) - \frac{1}{2k} \log(\theta_l^2 + \log^2(K)) \right] \xi_0^{(q)} \cos(j\theta_l) d\theta_l \quad \text{for } j \geq 1. \quad (6.69)
 \end{aligned}$$

To obtain such coefficients, these integrals must be computed numerically.

A cyclic graph has its vertices disposed of in the form of a ring (see, for instance, Figs. 5.1 and 6.4). Therefore, if we want correlations in the form of Eq. (6.66), the correlations of the first ancilla with its neighbors will decay in relation to its nearest neighbors and then raise again, since the last neighbors close the ring. In Figs. 6.5, 6.6, 6.7 and 6.8 we plotted the values of the correlations of the first ancilla with its neighbors. We computed the correlations according to Eq. (6.66) mirrored in  $n/2$ , mimicking the behavior of the correlations between ancillae disposed of in a ring form, and computed the correlations of the graph states generated by using Eqs. (6.68) and (6.69) to prepare the coefficients for the adjacency matrix  $G$  and using Eqs. (6.48), (6.49) and (6.50) to obtain the covariance matrix elements (and correlations) of the graph state. These plots show a good match between the correlations generated by the graph states and the desired form of the mirrored Eq. (6.66).

From choosing the parameters  $k = 1.0$  and  $\xi_0^{(q)} = 1.0$  we see that our method using graph states creates the desired correlations mostly if  $K$  is not too close to 1.0, but for  $K = 1.05$  a number of  $n = 100$  of ancillae causes a match between the correlations which is almost perfect, as can be seen in Fig. 6.5. However, for values of  $K$  too big, we don't have a very satisfactory match, even for a number of  $n = 100$  ancillae, as can be seen in Fig. 6.8.

Therefore, we conclude that for a region of  $1.5 \lesssim K \lesssim 10.0$  and  $n \gtrsim 50$ , our method of creating an environment with correlations in the form of Eq. (6.66) with graph states is satisfactory.

### 6.3.4 Analysing $\xi_d^{(p)}$

If we use the method described above to create the desired correlations  $\xi_d^{(q)}$  in graph states, we automatically constrain the correlations referring to the  $\xi_d^{(p)}$  canonical operators  $\hat{p}$ . In fact, from Eq. (6.57), we can write

$$\xi_d^{(p)} = \sum_{l=-(n-1)/2}^{(n-1)/2} b_l e^{i2\pi dl/n}, \quad (6.70)$$

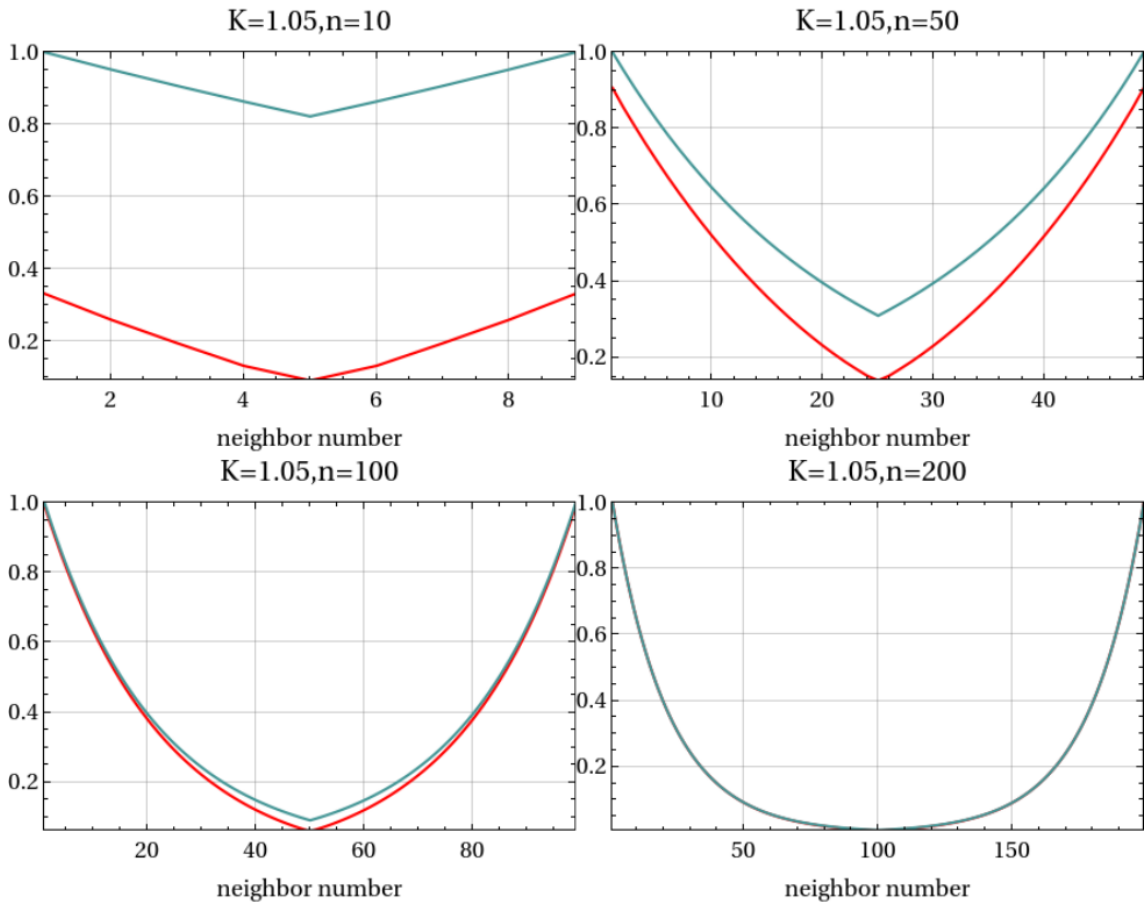


Figure 6.5: Correlations ( $\xi_d^{(q)}$ ) versus  $d$ : distance of the neighbor ancilla from the first ancilla. The blue line is the correlation given by Eq. (6.66) mirrored from  $n/2$ , while the red line is the correlation of the graph state generated by our method. The parameters are  $k = 1.0$ ,  $\xi_0^{(q)} = 1.0$  and  $K = 1.05$ , with  $n$  indicated above the plots.



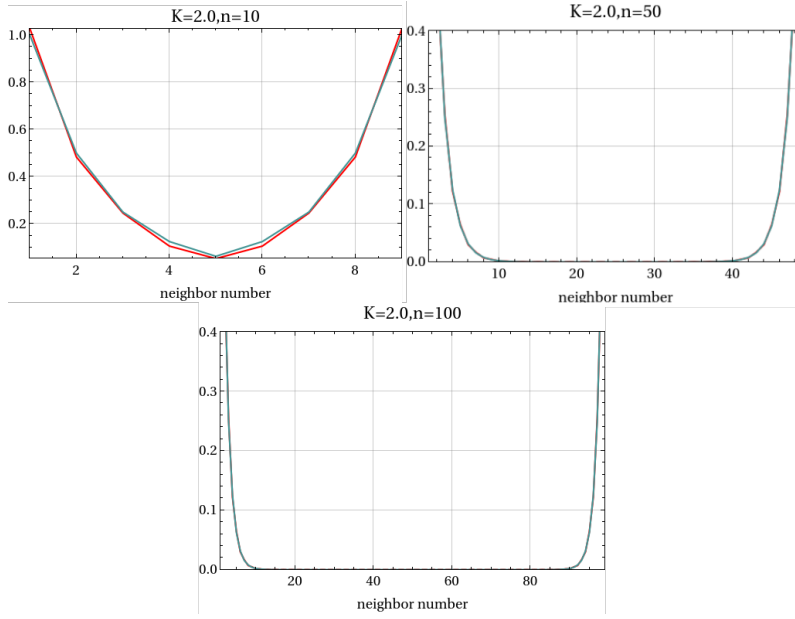


Figure 6.6: Correlations ( $\xi_d^{(q)}$ ) versus  $d$ : distance of the neighbor ancilla from the first ancilla. The blue line is the correlation given by Eq. (6.66) mirrored from  $n/2$ , while the red line is the correlation of the graph state generated by our method. The parameters are  $k = 1.0$ ,  $\xi_0^{(q)} = 1.0$  and  $K = 2.0$ , with  $n$  indicated above the plots.

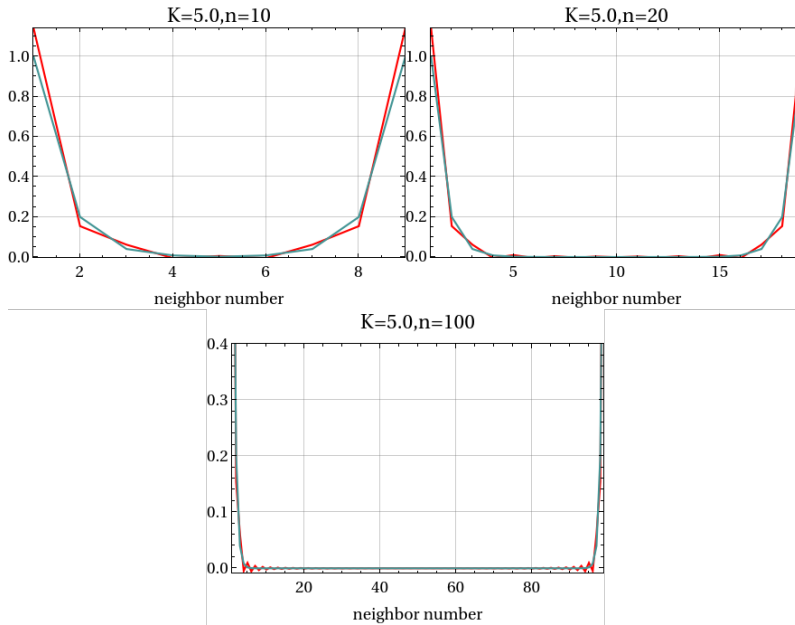


Figure 6.7: Correlations ( $\xi_d^{(q)}$ ) versus  $d$ : distance of the neighbor ancilla from the first ancilla. The blue line is the correlation given by Eq. (6.66) mirrored from  $n/2$ , while the red line is the correlation of the graph state generated by our method. The parameters are  $k = 1.0$ ,  $\xi_0^{(q)} = 1.0$  and  $K = 5.0$ , with  $n$  indicated above the plots.

where  $b_l = \frac{e^{-2k\lambda_k}}{2n}$ . And we also have, by definition, that the coefficient of the correlation  $\xi_d^{(q)}$  is  $a_l = \frac{e^{2k\lambda_k}}{2n}$ . Therefore we can relate them by

$$b_l = \frac{1}{4a_l n^2}, \quad (6.71)$$

from which we conclude that  $\xi_d^{(p)}$  is completely fixed by  $\xi_d^{(q)}$ .

As an example, we take again the case of Algebraic correlations from Eq. (6.66). In this case, we have, from the equation above and Eq. (6.67), for large  $n$

$$b_l = \frac{4\pi^2 l^2 + n^2 \log(K)^2}{2nK \log(K)} \frac{1}{4n^2}. \quad (6.72)$$

Applying this in Eq. (6.70) and making a large  $n$  approximation, we obtain

$$\begin{aligned} \xi_d^{(p)} &= \sum_{l=-(n-1)/2}^{(n-1)/2} \frac{4\pi^2 l^2 + n^2 \log(K)^2}{2nK \log(K)} \frac{1}{4n^2} e^{i2\pi dl/n} \\ &\approx \int_{-\pi}^{\pi} \frac{\theta^2 + \log(K)^2}{16\pi K \log(K)} e^{i\theta d} d\theta \\ &= \frac{(-1)^d}{4\pi K \log(K) d^2}. \end{aligned} \quad (6.73)$$

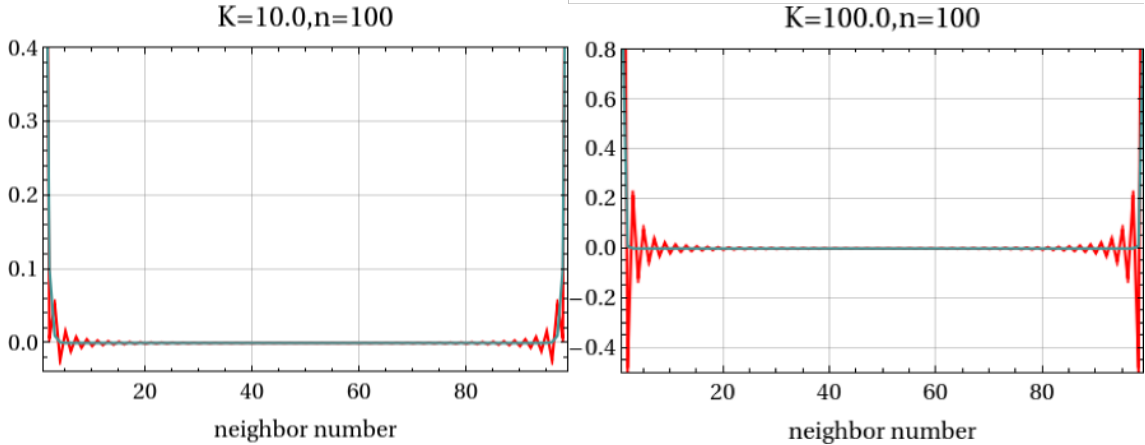


Figure 6.8: Correlations ( $\xi_d^{(q)}$ ) versus  $d$ : distance of the neighbor ancilla from the first ancilla. The blue line is the correlation given by Eq. (6.66) mirrored from  $n/2$ , while the red line is the correlation of the graph state generated by our method. The parameters are  $k = 1.0$ ,  $\xi_0^{(q)} = 1.0$  and  $n = 100$ , with  $K$  indicated above the plots.

Therefore, for creating a correlation of Eq. (6.66) type for  $\xi_d^{(q)}$ , we must obtain an oscillating correlation decaying with  $d^2$  type for  $\xi_d^{(p)}$ . This oscillating  $\xi_d^{(p)}$  is also obtained, for instance, if we create and prepare the correlations from a nearest-neighbor interaction graph state (see Ref. [96]).

Fortunately, despite the fact that we cannot create correlation terms  $\xi_d^{(q)}$  and  $\xi_d^{(p)}$  which decay equally with the distance, their effect in the initially correlated CM always acts linearly in the system's evolution (see Eq. (6.31)). Hence, such correlations affect the system's evolution differently and can be computed separately.

# Chapter 7

## Obtaining Observable Variations

### Using QBNs

This is the Chapter concerning the second main project of this thesis. This project has as its principal goal to compute the statistics of the heat distribution between two initially correlated parties using Quantum Bayesian Networks (QBNs), described in Subsection 3.4.2. The QBN formalism, inspired mostly in Ref. [48], has the advantage of estimating a probability distribution for a *process* to happen during a system's evolution without supposing that a measurement is made. This is opposite to the most commonly used *Two-Point Measurement (TPM)* protocol [33–35]. For the TPM protocol, two measurements are made to obtain the outcome of a desired observable for the party of interest at two points in time, this way the change of the observable is obtained during the process. The unwanted character of this procedure is the fact that after each measurement the backaction completely destroys the coherence of the joint state density matrix, therefore consuming the quantum correlation between the parties. The presence of initial correlations can cause interesting effects on thermodynamic processes, one of our main influences is the inversion of heat flow caused by initial correlations [50–53]. Hence, finding a reliable way of computing the statistics observable in such processes can be a fruitful objective.

In this present Chapter, we construct a more general formalism used to compute the statistics for the change of any local observable during a process in which the party of a joint system evolves. In the second part of the Chapter we apply, as

an example, such general results for the case where the two parties are qubits, recovering part of the results of Refs. [48] and [54] and exploring the consequences of our formalism to the study of the variance of the heat distribution in this case. In the third part of the Chapter, we bring our analysis of the consequences of choosing different ensembles for the initial density matrix of the joint system over the QBN statistics, since we found out that this statistic is dependent on the initial density matrix ambiguity of mixtures. This inquiry creates important interpretative caveats and thus is one of the main questions of this project. In the final part of this Chapter, we expose the formalism to obtain the heat distribution of the heat exchange between two bosonic modes. We obtain the evolution of the distribution of the two first moments as we observe how the correlations are consumed in the process. As an important result, we spot the heat flow inversion caused by correlations for the bosonic case. Finally, we describe the difficulties of using the coherent state ensemble to describe the QBN, which leads us to the use of quasi-probabilities.

## 7.1 General results

### 7.1.1 Statement of the problem

The setup is the same as the one described in Subsection 3.4.2. As already stated, the system is composed of two parties  $A$  and  $B$  and we suppose that they evolve according to a unitary operator  $U(t)$ . The joint system starts its evolution in the state

$$\rho_{AB}(0) = \sum_s P_s |\psi_s(0)\rangle \langle \psi_s(0)|, \quad (7.1)$$

where  $\{P_s, |\psi_s(0)\rangle\}_s$  is an ensemble of quantum states, and we have the observable  $\mathcal{O}_A(t)$  (which can be time-dependent) acting in  $A$  and  $\mathcal{O}_B(t)$  in  $B$  with eigenvalues (eigenvectors)  $\{a_i(t)\}_i$  ( $\{|a_i(t)\rangle\}_i$ ) and  $\{b_j(t)\}_j$  ( $\{|b_j(t)\rangle\}_j$ ), respectively. Then, the QBN infer that the probability of the joint system to be observed in the states  $(|a_0, b_0\rangle, |a_1, b_1\rangle \cdots, |a_n, b_n\rangle)$  in the respective time instants  $(0, t_1, \cdots, t_n)$  is (see the

deduction of Eq. (3.44) and Fig. 3.4 for the Bayesian Network graph)

$$P(a_0, b_0, a_1, b_1, \dots, a_n, b_n) = \sum_s P_s P(a_0, b_0 | \psi_s(0)) P(a_1, b_1 | \psi_s(t_1)) \cdots P(a_n, b_n | \psi_s(t_n)), \quad (7.2)$$

where

$$\begin{aligned} P(a_k, b_k | \psi_s(t)) &= |\langle a_k, b_k | \psi_s(t) \rangle|^2 \\ &= |\langle a_k, b_k | U(t) | \psi_s(0) \rangle|^2 \end{aligned} \quad (7.3)$$

is the conditional probability for the joint state to be observed in  $|a_k, b_k\rangle$  given that the system started at  $|\psi_s(0)\rangle$ .

Here we use the QBN formalism to infer the statistics of a quantity we call the *change of the observable*  $\mathcal{O}_A(t)$ , in symbols  $\Delta\mathcal{O}_A$ . This *change* happens during a process, i.e., as the system evolves between two points in time. Accordingly, we only need the conditional trajectory probability distribution of Eq. (7.2) for two points in time

$$\mathcal{P}(a_0, b_0, a_t, b_t) = \sum_s P_s P(a_0, b_0 | \psi_s(0)) P(a_t, b_t | \psi_s(t)), \quad (7.4)$$

where we rename  $t_1 = t$  and  $a_1(b_1) = a_t(b_t)$ .

Importantly, this conditional trajectory probability distribution satisfies standard probability distribution marginalization properties. Consider, for instance,

$$\begin{aligned} \sum_{b_0, b_t} \mathcal{P}(a_0, b_0, a_t, b_t) &= \sum_{b_0, b_t, s} P_s |\langle a_0, b_0 | \psi_s(0) \rangle|^2 |\langle a_t, b_t | \psi_s(t) \rangle|^2 \\ &= \sum_s P_s \langle \psi_s(0) | a_0 \rangle \left( \sum_{b_0} |b_0\rangle \langle b_0| \right) \langle a_0 | \psi_s(0) \rangle \langle \psi_s(t) | a_t \rangle \left( \sum_{b_t} |b_t\rangle \langle b_t| \right) \langle a_t | \psi_s(t) \rangle \\ &= \sum_s P_s |\langle a_0 | \psi_s(0) \rangle|^2 |\langle a_t | \psi_s(t) \rangle|^2 \\ &= \mathcal{P}(a_0, a_t). \end{aligned} \quad (7.5)$$

And analogously, we have  $\sum_{a_0, a_t} \mathcal{P}(a_0, b_0, a_t, b_t) = \mathcal{P}(b_0, b_t)$ . Furthermore, consider

the sum

$$\begin{aligned}
 \sum_{a_0, b_0} \mathcal{P}(a_0, b_0, a_t, b_t) &= \sum_{s, a_0, b_0} P_s |\langle a_0, b_0 | \psi_s(0) \rangle|^2 |\langle a_t, b_t | \psi_s(t) \rangle|^2 \\
 &= \sum_s P_s \langle \psi_s(0) | \left( \sum_{a_0, b_0} |a_0, b_0\rangle \langle a_0, b_0| \right) | \psi_s(0) \rangle \langle \psi_s(t) | a_t, b_t \rangle \langle a_t, b_t | \psi_s(t) \rangle \\
 &= \langle a_t, b_t | \left( \sum_s P_s | \psi_s(t) \rangle \langle \psi_s(t) | \right) | a_t, b_t \rangle \\
 &= \langle a_t, b_t | \rho_{AB}(t) | a_t, b_t \rangle, \tag{7.6}
 \end{aligned}$$

which is the standard probability distribution  $P(a_t, b_t)$  obtained from the postulates of Quantum Mechanics. Analogously we also obtain  $\sum_{a_t, b_t} \mathcal{P}(a_0, b_0, a_t, b_t) = \langle a_0, b_0 | \rho_{AB}(0) | a_0, b_0 \rangle$ .

With the use of this conditional probability, we can construct the probability of obtaining a change  $\Delta a$  in the observable  $\mathcal{O}_A(t)$  during two points in time

$$\boxed{p(\Delta \mathcal{O}_A = \Delta a) = \sum_{a_t, a_0} \delta(\Delta a - (a_t - a_0)) \mathcal{P}(a_0, a_t).} \tag{7.7}$$

Our main inquiry in this Chapter is to investigate the aspects of this probability distribution, and how the initial correlations between the parts of the global system affect it. Notice that this change can represent thermodynamic quantities. For instance, for the case where  $\mathcal{O}_A$  is the Hamiltonian of the subsystem  $A$ , for a global time-independent Hamiltonian, the quantity  $\Delta \mathcal{O}_A$  will be the *heat*, which is the focus of this project. This definition of heat, as being the difference between the average of the final and initial local energy which changes *only* due to the variation of the local state, means that this quantity represents the variation of energy due to the stochastic evolution of the state as it interacts with its surroundings. The work is devoted to the case where the change of energy is caused by an external driving controlling the Hamiltonian of the system. These definitions of heat and work can be studied in Ref. [25].

### 7.1.2 Characteristic function of the change probability distribution

In order to obtain a useful expression for the probability distribution of Eq. (7.7), we can resort to the characteristic function of it

$$G_{\mathcal{O}_A}(k) = \int_{-\infty}^{\infty} (d\Delta a) e^{ik\Delta a} p(\Delta\mathcal{O}_A = \Delta a). \quad (7.8)$$

Using Eq. (7.7) in the definition above, we obtain

$$G_{\mathcal{O}_A}(k) = \sum_{a_0, a_t} e^{ik(a_t - a_0)} \mathcal{P}(a_0, a_t). \quad (7.9)$$

Proceeding, we expand the distribution  $\mathcal{P}(a_0, a_t)$  in the equation above, then we have<sup>1</sup>

$$\begin{aligned} G_{\mathcal{O}_A}(k) &= \sum_{a_t, a_0, s} e^{ik(a_t - a_0)} P_s |\langle a_0 | \psi_s \rangle|^2 |\langle a_t | U(t) | \psi_s \rangle|^2 \\ &= \sum_{a_t, a_0, s} P_s \langle a_0 | \psi_s \rangle \langle \psi_s | e^{-ik a_0} | a_0 \rangle \langle a_t | U(t) | \psi_s \rangle \langle \psi_s | U^\dagger(t) e^{ik a_t} | a_t \rangle \\ &= \sum_{a_t, a_0, s} P_s \langle a_0 | \psi_s \rangle \langle \psi_s | e^{-ik \mathcal{O}_A(0)} | a_0 \rangle \langle a_t | U(t) | \psi_s \rangle \langle \psi_s | U^\dagger(t) e^{ik \mathcal{O}_A(t)} | a_t \rangle \\ &= \sum_s P_s \langle \psi_s | e^{-ik \mathcal{O}_A(0)} \left( \sum_{a_0} | a_0 \rangle \langle a_0 | \right) | \psi_s \rangle \langle \psi_s | U^\dagger(t) e^{ik \mathcal{O}_A(t)} \left( \sum_{a_t} | a_t \rangle \langle a_t | \right) U(t) | \psi_s \rangle \\ &= \sum_s P_s \langle \psi_s | e^{-ik \mathcal{O}_A(0)} | \psi_s \rangle \langle \psi_s | U^\dagger(t) e^{ik \mathcal{O}_A(t)} U(t) | \psi_s \rangle. \end{aligned} \quad (7.10)$$

From which we obtain the result

$$\boxed{G_{\Delta\mathcal{O}_A}(k) = \sum_s P_s \langle \psi_s | e^{-ik \mathcal{O}_A(0)} | \psi_s \rangle \langle \psi_s | e^{ik \mathcal{O}_{A_H}(t)} | \psi_s \rangle.} \quad (7.11)$$

where

$$\mathcal{O}_{A_H}(t) = U^\dagger(t) \mathcal{O}_A(t) U(t) \quad (7.12)$$

is the operator  $\mathcal{O}_A(t)$  in the Heisenberg picture.

An important comment that can be made here about the characteristic function

---

<sup>1</sup>From now on, we call  $|\psi_s\rangle = |\psi_s(0)\rangle$  for simplicity.



of Eq. (7.11) is that it has a non-trivial dependence on the choice for the ensemble of pure states to represent the initial density matrix of the joint state (Eq. (7.1)). This dependence comes from the fact that the trajectory probability of Eq. (7.2) is explicitly constructed under the ensemble choice. A possible way to interpret this dependence is related to the possibility for the probability of Eq. (7.2) to be associated with different measurement protocols in order to be accessible experimentally. For instance, for the choice of the ensemble of eigenstates of the initial density matrix, there is a proposal for extracting its probability using identical copies of a quantum system and postselection [49]. Proposals for measurement protocols in order to obtain distributions related to other ensemble choices can be a fruitful future research theme.

### 7.1.3 Statistical moments of the change probability distribution

An important utility of the characteristic function is that we can easily obtain formulae for the statistic moments of the random variables from it. This can be done, for the characteristic function of the distribution above, by the equation<sup>2</sup>

$$\langle (\Delta \mathcal{O}_A)^n \rangle = (-i)^n \frac{\partial^n (G_{\mathcal{O}_A}(k))}{\partial k^n} \Big|_{k=0}. \quad (7.13)$$

Using this equation in the result of Eq. (7.11), we obtain the average of  $\mathcal{O}_A(t)$

$$\boxed{\langle \Delta \mathcal{O}_A \rangle = \sum_s P_s \langle \psi_s | (\mathcal{O}_{A_H}(t) - \mathcal{O}_A(0)) | \psi_s \rangle}, \quad (7.14)$$

which can be rewritten as

$$\boxed{\langle \Delta \mathcal{O}_A \rangle = \text{Tr} \{ (\mathcal{O}_{A_H}(t) - \mathcal{O}_A(0)) \rho_{AB}(0) \}}. \quad (7.15)$$

This equation for the first moment makes clear that the average of  $\mathcal{O}_A(t)$  computed using QBNs takes into consideration all coherences of the initial state as well as

---

<sup>2</sup>This relation between statistical moments and the characteristic function can be obtained simply by direct differentiation of Eq. (7.8) and setting  $k = 0$ .

quantum correlations, as opposed to the TPM protocol, as desired. Interestingly, we can see that this quantity is independent of the ensemble choice of the initial density matrix.

The second moment of  $\mathcal{O}_A(t)$  is

$$\langle (\Delta \mathcal{O}_A(t))^2 \rangle = \sum_s P_s \left( \langle \psi_s | \left( (\mathcal{O}_{A_H}(t))^2 + (\mathcal{O}_A(0))^2 \right) | \psi_s \rangle - 2 \langle \psi_s | \mathcal{O}_A(0) | \psi_s \rangle \langle \psi_s | \mathcal{O}_{A_H}(t) | \psi_s \rangle \right). \quad (7.16)$$

In this equation, we already start to observe a dependence on the choice of the ensemble of the initial density matrix in the second moment of the distribution. For higher moments the results will be more complex but with a similar aspect. We restrict the focus to these two moments since they will already expose the desired attributes of the probability distribution for our analysis.

#### 7.1.4 Comparison with TPM

Here we will compare our results for the statistics obtained using QBN with the standard TPM statistics.<sup>3</sup> The TPM supposes that measurements are made for two points in time in order to obtain the variation (or change) of some observable. So, supposing the same bipartite setup presented to the QBN case in Subsection 7.1.1, we additionally suppose that a projective measurement is made initially in the eigenbasis  $\{|a_0\rangle\}_{a_0}$  of the operator  $\mathcal{O}_A(0)$  and finally in the eigenbasis  $\{|a_t\rangle\}_{a_t}$  of the operator  $\mathcal{O}_A(t)$ . The probability of the initial global system  $\rho_{AB}(0)$  to have outcomes  $a_0$  and  $a_t$ , respectively, in these two measurements is

$$\mathcal{P}_{\text{TPM}}(a_0, a_t) = P(a_t|a_0)P(a_0), \quad (7.17)$$

where  $P(a_0) = P_{a_0} = \langle a_0 | \rho_A(0) | a_0 \rangle$ , with  $\rho_A = \text{Tr}_B(\rho_{AB}(0))$ , is the probability of the first measurement to have an outcome  $a_0$ . While  $P(a_t|a_0)$  is the probability of having an outcome  $a_t$  for the second measurement after the backaction of the first

---

<sup>3</sup>In Section II of Ref. [34] the TPM statistics is presented in details.

measurement and the evolution between them

$$P(a_t|a_0) = \text{Tr} \left\{ |a_t\rangle \langle a_t| U(t) \rho'_{AB}(0) U^\dagger(t) |a_t\rangle \langle a_t| \right\}, \quad (7.18)$$

where  $\rho'_{AB}(0) = \frac{|a_0\rangle \langle a_0| \rho_{AB}(0) |a_0\rangle \langle a_0|}{P_{a_0}}$  is the backaction of  $\rho$  after the first measurement and  $U(t)$  is the unitary evolution operator between the two measurements.

If now we desire to obtain the probability of a change  $\Delta a$  in the observable  $\mathcal{O}_A(t)$  with this probability distribution, we define

$$p_{\text{TPM}}(\Delta \mathcal{O}_A = \Delta a) = \sum_{a_t, a_0} \delta(\Delta a - (a_t - a_0)) \mathcal{P}_{\text{TPM}}(a_0, a_t). \quad (7.19)$$

Using Eqs. (7.17) and (7.18), we obtain (see Appendix D for the computation) the following characteristic function for this probability distribution

$$G_{\mathcal{O}_{A\text{TPM}}}(k) = \text{Tr} \left\{ e^{ik\mathcal{O}_A(t)} e^{-ik\mathcal{O}_A(0)} \mathcal{D}_{\mathcal{O}_A(0)}(\rho_{AB}(0)) \right\}, \quad (7.20)$$

where  $\mathcal{D}_{\mathcal{O}_A(0)}(\bullet) = \sum_{a_0} |a_0\rangle \langle a_0| \bullet |a_0\rangle \langle a_0|$  and  $\{|a_0\rangle\}_{a_0}$  are the eigenvectors of  $\mathcal{O}_A(0)$ .

The only dependence of the joint system's initial state in this characteristic function is given by  $\mathcal{D}_{\mathcal{O}_A(0)}(\rho_{AB}(0))$ . Thus all contributions from the initial coherence, in the eigenbasis of  $\mathcal{O}_A(0)$  vanish in contrast with the QBN characteristic function of Eq. (7.11) which takes into account the coherence of the initial state. Importantly, the QBN characteristic function of Eq. (7.11), compute in the ensemble choice of the eigenvectors of  $\rho_{AB}(0)$ , *is equivalent* to the TPM characteristic function in Eq. (7.20) for the case where  $[\rho_{AB}(0), \mathcal{O}_A(0)] = 0$ , which is the case where there is no coherence for the initial state in the eigenbasis of  $\mathcal{O}_A(0)$ .

## 7.2 Application to qubits

Here we apply our general results to the case where the systems  $A$  and  $B$  are qubits. As already said, our main goal is to obtain the heat probability distribution during an interaction taking into account the effects of the initial correlations between the parties. Among other results, this predicts the inversion of the heat flow caused by

initial correlations. The first experimental observation of this fact was obtained for this two-qubit setup in Ref. [54] and we describe these statistics with our results using QBNs. Reference [48], which initially proposed QBNs, also described the heat average of [54] using QBNs and its probability distribution for specific initial states. Thus our analysis with two-qubit systems will serve as a sanity check for our general methods of obtaining the statistical moments of the heat probability distribution and its characteristic function by comparing our results with the ones obtained in Refs. [48, 54] and, additionally, we are now able to compute the unexplored second moment of the heat distribution.

### 7.2.1 Setup and statistical moments

We suppose that the two qubits have local Hamiltonians  $H_{A(B)} = \omega_0(1 - \sigma_z^{A(B)})/2$ , interacting via the unitary

$$U(g, t) = e^{-it\frac{\pi}{2g}(\sigma_+^A \otimes \sigma_-^B + \sigma_-^A \otimes \sigma_+^B)}, \quad (7.21)$$

for  $\sigma_{+(-)}$  defined according to Eq. (2.33). The joint system starts at the state

$$\rho_{AB}(0) = \rho_{\text{th}}^A \otimes \rho_{\text{th}}^B + \chi_{AB}, \quad (7.22)$$

where

$$\rho_{\text{th}}^{A(B)} = \frac{1}{(1 + e^{-\omega_0\beta_{A(B)}})} \begin{pmatrix} 1 & 0 \\ 0 & e^{-\omega_0\beta_{A(B)}} \end{pmatrix},$$

are the locally thermal states of the Hamiltonian  $H_{A(B)}$ <sup>4</sup> and the term

$$\chi_{AB} = \begin{pmatrix} 0 & 0 & 0 & 0 \\ 0 & 0 & \alpha & 0 \\ 0 & \alpha^* & 0 & 0 \\ 0 & 0 & 0 & 0 \end{pmatrix},$$

---

<sup>4</sup>These locally thermal states are different from the one described in Appendix A, Section A.4, only due to their local Hamiltonians. Also, the unitary of Eq. (7.21) is simply the Partial SWAP of Eq. (2.44) multiplied by a phase. The slight differences in these definitions from the previous Chapters are made in order to have a better comparison with the results of Ref. [48].

is responsible for the coherence and correlations between the parties with  $\alpha$  satisfying  $|\alpha| \leq \exp[-\omega_0(\beta_A + \beta_B)] / \left( (1 + e^{-\omega_0\beta_A})(1 + e^{-\omega_0\beta_B}) \right)$  for the positivity of the density matrix. In fact, the mutual information between the parties is 0 when  $\alpha$  is null and reaches its maximum when  $|\alpha| = \aleph$ , where

$$\aleph = \exp[-\omega_0(\beta_A + \beta_B)] / \left( (1 + e^{-\omega_0\beta_A})(1 + e^{-\omega_0\beta_B}) \right), \quad (7.23)$$

which is a result obtained in Ref. [54].

As already said, for the case where the Hamiltonian is time-independent, we define the *heat* received by the subsystem  $A$  as the change of the local Hamiltonian  $H_A$  during the evolution from time 0 to  $t$

$$\mathcal{Q}_A(t) = \Delta H_A. \quad (7.24)$$

Using the result of Eq. (7.14) for the average of the change of an operator, we have

$$\langle \mathcal{Q}_A(t) \rangle = \text{Tr} \left\{ \left( U^\dagger(g, t) H_A U(g, t) - H_A \right) \rho_{AB}(0) \right\}. \quad (7.25)$$

Computing the trace using Eqs. (7.21) and (7.22), we obtain

$$\langle \mathcal{Q}_A(t) \rangle = \omega_0 \left[ \text{Im}(\alpha) \sin\left(\frac{\pi t}{g}\right) + \frac{1}{2} \sin^2\left(\frac{\pi t}{2g}\right) \left( \tanh\left(\frac{\omega_0\beta_A}{2}\right) - \tanh\left(\frac{\omega_0\beta_B}{2}\right) \right) \right]. \quad (7.26)$$

This result describes correctly the heat flow inversion caused by the initial correlations between the two qubits. This can be achieved for negative values of  $\text{Im}(\alpha)$ , as can be seen in Fig. 7.1. In this figure, we can spot the heat average initially going from the colder system  $A$  to the hotter system  $B$  for the cases where  $\text{Im}(\alpha) < 0$  and a stronger manifestation of such effect for the case with maximum correlation, i.e., for  $\text{Im}(\alpha) = -\aleph$ .

Additionally, with the result of Eq. (7.16), we can obtain the second moment of

the heat probability distribution

$$\begin{aligned} \langle \mathcal{Q}_A^2(t) \rangle &= \sum_i \lambda_i \langle \lambda_i | \left( (U^\dagger(g, t) H_A U(g, t))^2 + H_A^2 \right) | \lambda_i \rangle \\ &\quad - 2 \langle \lambda_i | H_A | \lambda_i \rangle \langle \lambda_i | U^\dagger(g, t) H_A U(g, t) | \lambda_i \rangle, \end{aligned} \quad (7.27)$$

where  $\{\lambda_i\}_i$  and  $\{|\lambda_i\rangle\}_i$  are the eigenvalues and eigenvectors of the initial density matrix  $\rho_{AB}(0)$ . We *choose* to compute the second moment in the eigenvector ensemble of the initial density matrix since it is the ensemble that causes the smaller variance (to be seen in the next section). With this, we compute (see Fig. 7.1) numerically the heat variance  $\text{Var}(\mathcal{Q}_A)(t) = \langle \mathcal{Q}_A^2(t) \rangle - \langle \mathcal{Q}_A(t) \rangle^2$  for different choices of  $\alpha$  for  $\beta_A = 2/\omega_0$  and  $\beta_B = 1/\omega_0$ , i.e., initially  $A$  colder than  $B$ . For both negative and positive values of  $\text{Im}(\alpha)$ , the presence of correlations decreases considerably the maximum of the variance. Interestingly, for the cases where the mutual information has its maximum  $\text{Im}(\alpha) = \pm\aleph$  we have a higher diminishing of the variance than in the smaller correlation case of  $\text{Im}(\alpha) = \pm 1/20$ . This seems to indicate that the greater the correlations, the smaller the variance, which is a pattern that will also be seen in the last Section of this Chapter, on the bosonic modes case. Intuitively, we could think of this reduction of the variance as an approximation to the classical thermodynamic case. However, we might interpret this as a case where correlations decrease the entropy of the processes, and hence this could be possibly a cause for the reduction of the variance. This reasoning was influenced by Ref. [143], which affirms that mutual correlations between parties can be analogous to an information reservoir, similar to a Maxwell's demon.

## 7.2.2 Obtaining the probability distribution

We can compute the characteristic function for the heat probability distribution using the result of Eq. (7.11) to the conditions above, obtaining

$$G_{\mathcal{Q}_A}(k) = \sum_s \lambda_s \langle \lambda_s | e^{-ikH_A} | \lambda_s \rangle \langle \lambda_s | e^{ikU^\dagger(g, t) H_A U(g, t)} | \lambda_s \rangle. \quad (7.28)$$

As a sanity check, we numerically computed the probability distribution of the

heat from this characteristic function by applying the inverse Fourier transform on it for a set of parameters. The computation was not possible in analytical form, since the integral of the inverse Fourier transform of the characteristic function from Eq. (7.28) is not analytically tractable. We now compare it to the probability distributions obtained in Ref. [48].

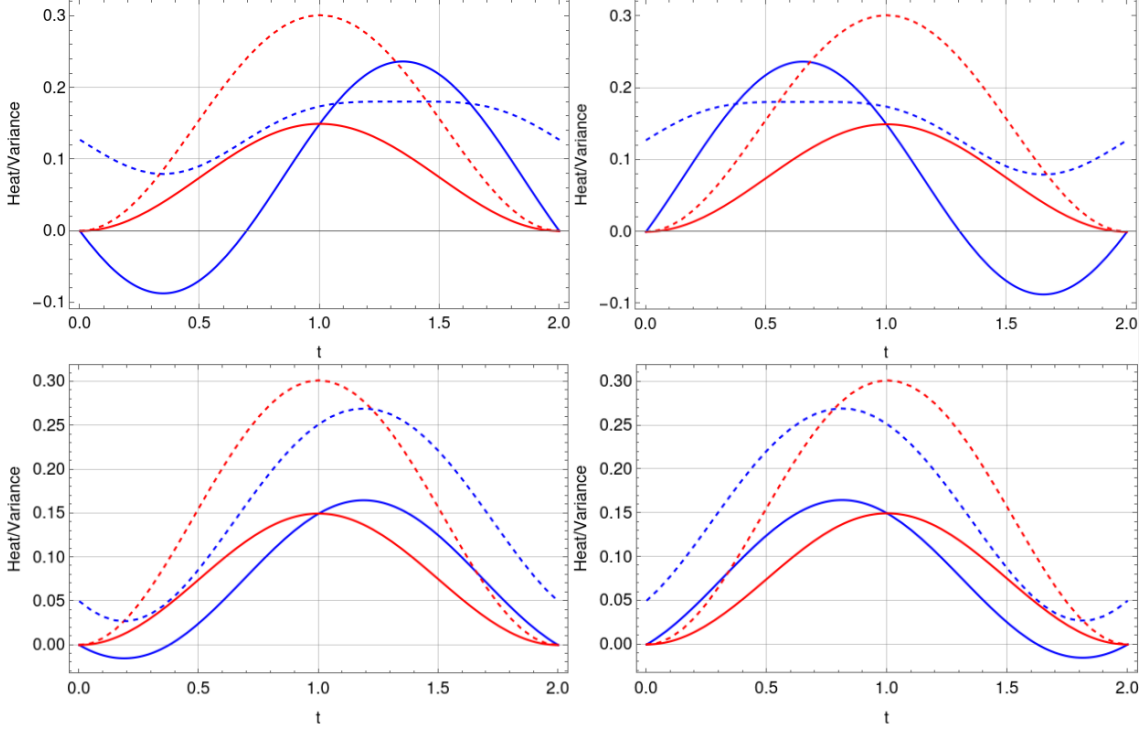


Figure 7.1: Heat (in unites of  $\omega_0$ )/ Variance of the heat (in unites of  $\omega_0^2$ ) versus  $t$ . The blue lines represent the heat received by  $A$  and the blue dashed lines represent the variance of the heat when the qubits are initially correlated. The red lines represent the heat received by  $A$  and the red dashed lines represent the variance of the heat when the qubits are initially uncorrelated. The parameters are  $g = 1$ ,  $\beta_A = 2/\omega_0$  and  $\beta_B = 1/\omega_0$ . Each plot has a different value of  $\alpha$ . In the first line we have, from left to right,  $\text{Im}(\alpha) = -\aleph$  and  $\text{Im}(\alpha) = +\aleph$ , and in the second line  $\text{Im}(\alpha) = -1/20$  and  $\text{Im}(\alpha) = +1/20$ .

The probability distributions of Ref. [48] are

$$P(Q_A = -\omega_0) = \frac{e^{\omega_0\beta_B} \left( e^{\omega_0\beta_A/2} \cos\left(\frac{\pi t}{2g}\right) + e^{\omega_0\beta_B/2} \sin\left(\frac{\pi t}{2g}\right) \right)^2}{(e^{\omega_0\beta_A} + 1)(e^{\omega_0\beta_B} + 1)(e^{\omega_0\beta_A} + e^{\omega_0\beta_B})}, \quad (7.29)$$

$$P(Q_A = 0) = \frac{\left( e^{\omega_0\beta_A} + e^{\omega_0\beta_B} \right) \left( 2 + e^{\omega_0\beta_A} + e^{\omega_0\beta_B} + 2e^{\omega_0(\beta_A+\beta_B)} \right) + \left( e^{\omega_0\beta_A} - e^{\omega_0\beta_B} \right)^2 \cos\left(\frac{\pi t}{g}\right)}{2(e^{\omega_0\beta_A} + 1)(e^{\omega_0\beta_B} + 1)(e^{\omega_0\beta_A} + e^{\omega_0\beta_B})} + \frac{2e^{\omega_0(\beta_A+\beta_B)/2} \left( e^{\omega_0\beta_A} - e^{\omega_0\beta_B} \right) \sin\left(\frac{\pi t}{g}\right)}{2(e^{\omega_0\beta_A} + 1)(e^{\omega_0\beta_B} + 1)(e^{\omega_0\beta_A} + e^{\omega_0\beta_B})}, \quad (7.30)$$

$$P(Q_A = +\omega_0) = \frac{e^{\omega_0\beta_A} \left( e^{\omega_0\beta_B/2} \cos\left(\frac{\pi t}{2g}\right) - e^{\omega_0\beta_A/2} \sin\left(\frac{\pi t}{2g}\right) \right)^2}{(e^{\omega_0\beta_A} + 1)(e^{\omega_0\beta_B} + 1)(e^{\omega_0\beta_A} + e^{\omega_0\beta_B})}. \quad (7.31)$$

As an example, in Fig. 7.2 we plot the probability distributions of  $Q_A = -\omega_0$ ,  $Q_A = 0$  and  $Q_A = +\omega_0$  computed numerically for initial states  $\rho_{AB}(0)$  with  $\beta_A = 2/\omega_0$ ,  $\beta_B = 1/\omega_0$  and  $\alpha = -i \frac{e^{-\omega_0(\beta_A+\beta_B)/2}}{(1+e^{-\omega_0\beta_A})(1+e^{-\omega_0\beta_B})}$  during an evolution in time. These plots match perfectly with the curves of the probabilities above.

### 7.3 Dependence on the ambiguity of mixtures

In the results of Eqs. (7.11) and (7.16) an explicit dependence can be verified of the characteristic function and of the second moment of the change  $\Delta\mathcal{O}_A$  on the choice of the ensemble of states  $\{P_s, |\psi_s\rangle\}_s$  for the mixture of states in the initial density matrix of Eq. (7.1).<sup>5</sup> Therefore, this dependence is present in the

<sup>5</sup>Remember that in further equations after Eq. (7.1) we omitted the (0) in  $|\psi_s(0)\rangle$  for simplicity of notation.

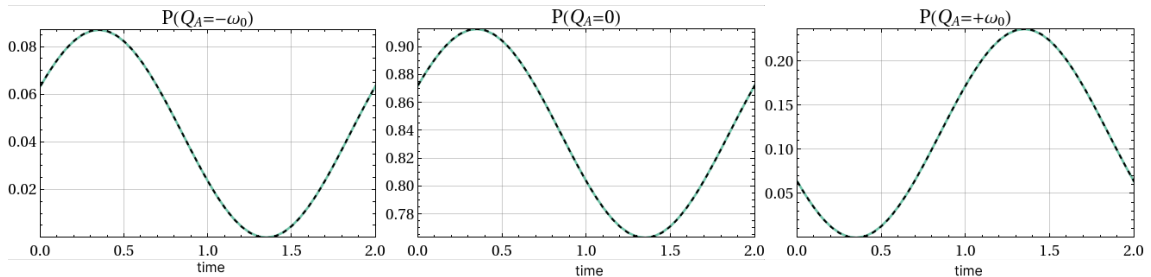


Figure 7.2:  $P(Q_A)$  versus  $t$ , for different values of  $Q_A$ , computed numerically with the inverse Fourier transform of the characteristic function of Eq. (7.28) (green full line) and for different values of  $Q_A$ , using Eqs. (7.29), (7.30), and (7.31) from Ref. [48] (dashed black line). The initial joint state is prepared at  $\rho_{AB}(0)$  of Eq. (7.22) with  $\beta_A = 2/\omega_0$ ,  $\beta_B = 1/\omega_0$ ,  $\alpha = -i \frac{e^{-\omega_0(\beta_A+\beta_B)/2}}{(1+e^{-\omega_0\beta_A})(1+e^{-\omega_0\beta_B})}$  and we have  $g = 1$ .



probability distribution of  $\Delta\mathcal{O}_A$ . The dependence is a consequence of the fact that our construction of the QBN is a causal network stemming from different possible initial states. Although different choices of these initial states result in the same initial density matrix, they don't necessarily cause the same chain of events with the same chances of occurring.

A compelling result is that, although we have a probability distribution dependence on the ambiguity of mixtures, the average of the  $\Delta\mathcal{O}_A$  has not. This can be clearly seen in the result of Eq. (7.15). On the other hand, the second moment does depend on the ensemble choice for the initial density matrix, and thus the variance will also depend on it.

### 7.3.1 The variance for the qubits case

Due to its importance in the statistics of a random variable, we analyze in more detail the variance dependence on the ambiguity of mixtures. We compute its values for different choices of ensembles of the initial density matrix for the case of qubits states described in Sec. 7.2. Here, the random variable under analysis is the heat received by  $A$ :  $\Delta H_A = \mathcal{Q}_A$ . We obtain the variance of the heat

$$\text{Var}(\mathcal{Q}_A)(t) = \langle \mathcal{Q}_A^2(t) \rangle - \langle \mathcal{Q}_A(t) \rangle^2, \quad (7.32)$$

from Eq. (7.25) for computing the average and Eq. (7.16) for computing the second moment, from which we have

$$\begin{aligned} \langle \mathcal{Q}_A^2(t) \rangle &= \text{Tr} \left\{ \left( (U^\dagger(g, t) H_A U(g, t))^2 + H_A^2 \right) \rho_{AB}(0) \right\} \\ &\quad - 2 \sum_s P_s \langle \psi_s | H_A | \psi_s \rangle \langle \psi_s | U^\dagger(g, t) H_A U(g, t) | \psi_s \rangle, \end{aligned} \quad (7.33)$$

depending on the ensemble  $\{P_s, |\psi_s\rangle\}_s$  of the initial density matrix.

For generating a set of different ensembles for the same initial density matrix  $\rho_{AB}(0)$ , we recall a seminal result from Ref. [144]. This reference reveals that, given a density matrix  $\rho$  with an *eigen-ensemble*<sup>6</sup>  $\{\lambda_i, |\lambda_j\rangle\}_j$ , we can generate an ensemble

---

<sup>6</sup>An *eigen-ensemble* of a density matrix  $\rho$  is an ensemble of  $\rho$  in which all elements are orthonormal eigenvectors.

$\{P_i, |\psi_i\rangle\}_i$  of  $\rho$  with the formula

$$\boxed{\sqrt{P_i} |\psi_i\rangle = \sum_{j=1}^k \sqrt{\lambda_j} M_{ij} |\lambda_j\rangle, \quad i = 1, \dots, r,} \quad (7.34)$$

where  $k = \dim(\text{Support}(\rho))$ ,<sup>7</sup>  $r \geq k$  and  $M_{ij}$  are the elements of any  $r \times k$  matrix  $M$  whose columns are orthonormal vectors in  $\mathbb{C}^r$ .<sup>8</sup>

Using this result, we suppose an initial state  $\rho_{AB}(0)$  given by Eq. (7.22) with  $\beta_A = 2/\omega_0$ ,  $\beta_B = 1/\omega_0$  and  $\alpha = -i \exp[-\omega_0(\beta_A + \beta_B)] / ((1 + e^{-\omega\beta_A})(1 + e^{-\omega\beta_B}))$ . For the generation of eight different equivalent ensembles of  $\rho_{AB}(0)$ , we used Eq. (7.34) with eight different choices of matrices  $M$  (see the matrices chosen in Appendix D). In Fig. 7.3, we see the variance as a function of time computed using such ensembles in Eq. (7.33) and compared with the computation of the variance using the eigen-ensemble. We see the pattern that the variance computed in general ensembles is greater than or equal to the variance computed in an eigen-ensemble.

From these results, we have physical reasons to suppose that the eigen-ensemble is the choice of the ensemble that minimizes the variance of the probability distribution for a change of an observable using a QBN. This is a *conjecture* which comes from the results mentioned and from the following ideas. The intuition of this conjecture is in our supposition that the presence of indistinguishability between non-orthogonal states of an ensemble can increase the variance of a distribution generated by such an ensemble. Therefore, the conjecture is a consequence of noticing that the eigen-ensembles are the only ones without such superpositions. Counterexamples or proof for such conjecture can be a future research exploration.

<sup>7</sup>The set  $\text{Support}(\rho)$  is the linear space spanned by the set of eigenvectors of  $\rho$  with non-zero eigenvalues.

<sup>8</sup>This can be proved simply by noticing that, given  $P_i$  and  $|\psi_i\rangle$  defined by Eq. (7.34), we have

$$\begin{aligned} \sum_{i=1}^r P_i |\psi_i\rangle \langle \psi_i| &= \sum_{i=1}^r \sum_{l=1, m=1}^{k, k} M_{il}^* M_{im} \sqrt{\lambda_m \lambda_l} |\lambda_m\rangle \langle \lambda_l| \\ &= \sum_{m=1}^k \lambda_m |\lambda_m\rangle \langle \lambda_m| \\ &= \rho, \end{aligned} \quad (7.35)$$

where in the second equality we used that the columns of  $M$  are orthonormal vectors.

In Fig. 7.3, we see that for the case of the matrices  $M_7$  and  $M_8$  (see Appendix D), the ensembles are also composed by eigenvectors of  $\rho_{AB}(0)$ , but they are non-orthogonal to each other. Consequently, their variances have higher values than the ones generated for an eigen-ensemble.<sup>9</sup> Furthermore, the matrix  $M_8$  generates a more superposed ensemble than the one generated by  $M_7$ . Hence we can see a larger variance in this case.

## 7.4 Heat exchanged between bosonic modes

We continue to pursue the main goal of the second project of this thesis: to obtain the probability distribution of the heat exchanged by two systems using QBNs due to its advantage to describe the statistics of initially correlated quantum systems. In this Section, we obtain results for the probability distribution of the heat exchanged between two initially correlated Gaussian bosonic modes. We expose numerical results concerning the first two moments of the heat probability distribution in this case, and finally, we present the difficulties of our explorations concerning an attempt to use coherent states as an ensemble of the initial density matrix.

### 7.4.1 Statement of the problem

We suppose that the systems  $A$  and  $B$  are bosonic modes with local Hamiltonians

$$\hat{H}_{A(B)} = \omega \left( \hat{a}^\dagger (\hat{b}^\dagger) \hat{a} (\hat{b}) + \frac{1}{2} \right), \quad (7.36)$$

where  $\hat{a}(\hat{a}^\dagger)$  and  $\hat{b}(\hat{b}^\dagger)$  are the annihilator (creator) operators of the modes in  $A$  and  $B$ , respectively. Their interaction is given by the beam splitter unitary

$$U(t) = e^{-it\hat{H}_{BS}}, \quad (7.37)$$

where

$$\hat{H}_{BS} = ig(\hat{a}^\dagger \hat{b} - \hat{b}^\dagger \hat{a}). \quad (7.38)$$

---

<sup>9</sup>Remember that the eigen-ensemble definition demands that the vectors are orthogonal among them, in addition to eigenvectors.

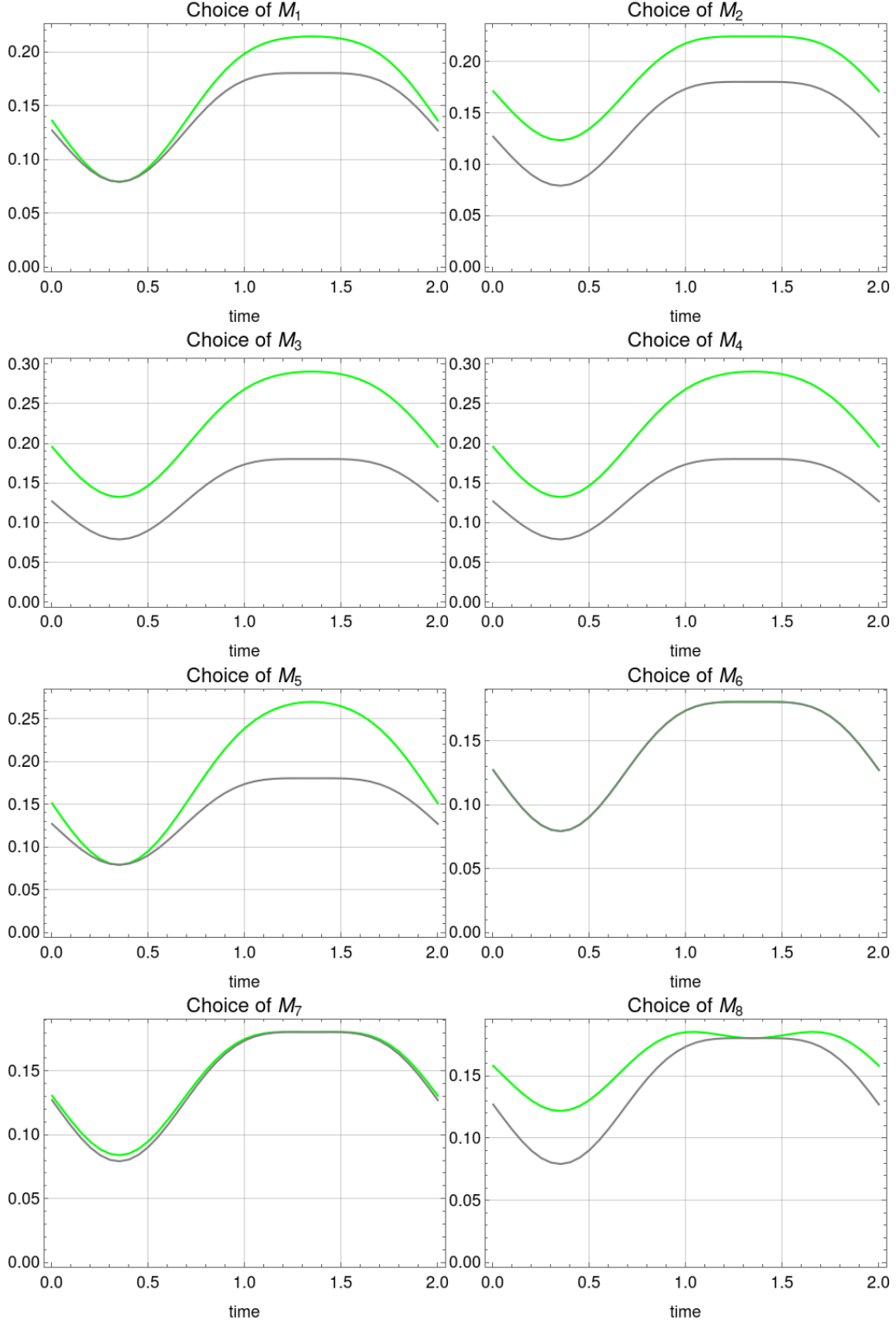


Figure 7.3: Variance of  $Q_A$  (in units of  $\omega_0^2$ ) versus  $t$ . The green curves represent the variance computed with the ensembles generated by the respective matrix  $M$  (see Appendix D) with the use of Eq. (7.34) while the gray curves represent the variance computed in an eigen-ensemble. The initial state  $\rho_{AB}(0)$  is given by Eq. (7.22) with  $\beta_A = 2/\omega_0$ ,  $\beta_B = 1/\omega_0$  and  $\alpha = -i \exp[-\omega_0(\beta_A + \beta_B)] / ((1 + e^{-\omega\beta_A})(1 + e^{-\omega\beta_B}))$ . For the unitary  $U(g, t)$  we have  $g = 1$ .

We now suppose that the initial global state is given by Eq. (7.1), with the restriction that the states are Gaussian and the initial averages of the state canonical moments are 0. Consequently, according to the results of Chapter 4 (see Subsection 4.6.5), the state can be fully described by a covariance matrix. Additionally, the system evolution is a consequence of a unitary global evolution generated by a quadratic Hamiltonian followed by a partial trace, hence all evolved states of the system are Gaussian (see Chapter 4, Section 4.7).

Again, we define the *heat* received by the system  $A$  as the variation of its local Hamiltonian  $\hat{H}_A$ , in other words

$$\mathcal{Q}_A(t) = \Delta \hat{H}_A. \quad (7.39)$$

Our main goal is to obtain the statistics of  $P(\mathcal{Q}_A(t))$  using the results of Section 7.1.

### 7.4.2 Initial states in the Simon form

We make a further restriction on the initial Gaussian states to obtain more clear results. As we intend to explore the effects of quantum correlations, we suppose that the initial joint state is in the normal Simon form (Eq. (4.116)). Therefore the joint system's initial covariance matrix is

$$\sigma_{AB} = \begin{pmatrix} a & 0 & c_+ & 0 \\ 0 & a & 0 & c_- \\ c_+ & 0 & b & 0 \\ 0 & c_- & 0 & b \end{pmatrix}, \quad (7.40)$$

where  $a$  and  $b$  are positive real numbers. Beyond the fact that any two-mode Gaussian state can be transformed by means of local unitaries in a state with a covariance matrix in the Simon form, this form also assumes that the local states are thermal, which will be useful to thermodynamic interpretations. The parameters  $a$  and  $b$  are

related to their local inverse of temperatures  $\beta_A$  and  $\beta_B$  by means of

$$a(b) = \frac{1}{2} \coth\left(\frac{\omega\beta_{A(B)}}{2}\right), \quad (7.41)$$

hence the parameters  $a$  and  $b$  are proportional to their system's temperature, i.e., if  $a > b$ , then the temperature of  $A$  is bigger than the temperature of  $B$  and vice-versa.<sup>10</sup>

We are going to focus on two important correlated two-mode states. First, the two-mode squeezed thermal state (TMST), its covariant matrix in Eq. (4.117), namely

$$\sigma_{\text{tmst}} = \begin{pmatrix} a & 0 & c & 0 \\ 0 & a & 0 & -c \\ c & 0 & b & 0 \\ 0 & -c & 0 & b \end{pmatrix}, \quad (7.42)$$

which is a Simon form with opposite correlation terms. Second, we shall use the state we call *two-mode thermal under beam splitter* (TSBS) state. It has the following covariance matrix

$$\sigma_{\text{tsbs}} = \begin{pmatrix} a & 0 & c & 0 \\ 0 & a & 0 & c \\ c & 0 & b & 0 \\ 0 & c & 0 & b \end{pmatrix}, \quad (7.43)$$

which is a covariance matrix in the Simon form in the case where the correlation terms are identical. The name chosen for this state comes simply from the fact that it is the result of the application of a beam splitter unitary in two uncorrelated local thermal states. This can be seen by the direct application of the unitary evolution in terms of the symplectic matrix of the beam splitter (see Eq. (6.8)) in the two-mode local thermal states.

The value of the correlation terms  $c$  in (7.43) can be positive or negative. Therefore, for further use, we shall call *TSBS positive state* the TSBS state for  $c > 0$  and

---

<sup>10</sup>This relation is a consequence of Eq. (C.35) and from Section C.13 discussion for the case of local Hamiltonians  $H_{A(B)}$  given by Eq. (7.36) and locally thermal states  $\rho_{A(B)} = e^{-\beta_{A(B)}H_{A(B)}}/Z_{A(B)}$ , where  $Z_{A(B)} = \text{Tr}\{e^{-\beta_{A(B)}H_{A(B)}}\}$ .

TSBS negative state the TSBS state for  $c < 0$ .

### 7.4.3 The heat average and correlations evolution

From Eq. (7.15), we can obtain the heat average with the formula

$$\langle \mathcal{Q}_A(t) \rangle = \langle U(t)^\dagger \hat{H}_A U(t) \rangle - \langle \hat{H}_A \rangle. \quad (7.44)$$

Since  $\langle \hat{H}_A \rangle = \frac{\omega}{2}(\langle \hat{q}_A^2 \rangle + \langle \hat{p}_A^2 \rangle)$  and the initial state has the covariance matrix given by Eq. (7.41), we obtain

$$\langle \hat{H}_A \rangle = \omega a. \quad (7.45)$$

Similarly, we have

$$\begin{aligned} \langle U^\dagger(t) \hat{H}_A U(t) \rangle &= \frac{\omega}{2} \left( (\langle \hat{q}_A^2 \rangle + \langle \hat{p}_A^2 \rangle) \cos^2(g) + (\langle \hat{q}_B^2 \rangle + \langle \hat{p}_B^2 \rangle) \sin^2(g) \right. \\ &\quad \left. + (\langle \hat{q}_A \hat{q}_B \rangle + \langle \hat{p}_A \hat{p}_B \rangle) \sin(2g) \right) \\ &= \frac{\omega}{2} \left( 2a \cos^2(g) + 2b \sin^2(g) + (c_+ + c_-) \sin(2g) \right). \end{aligned} \quad (7.46)$$

Hence, we obtain

$$\boxed{\langle \mathcal{Q}_A(t) \rangle = \omega \left( \sin^2(gt)(b - a) + \frac{1}{2} \sin(2gt)(c_+ + c_-) \right)}. \quad (7.47)$$

This result for the average pinpoints important aspects of the heat flow between two bosonic modes interacting via a beam splitter. The first term  $\omega \sin^2(gt)(b - a)$  indicates the ordinary heat flowing from the hot system to the cold system disregarding the initial correlations. As for the second term  $\frac{\omega}{2} \sin(2gt)(c_+ + c_-)$ , the effect of the correlations is completely manifest. The sign of the sum  $c_+ + c_-$  dictates the tendency of the correlations to reverse the heat flow or to increase the ordinary flow. Intriguingly, for a very usual state of correlated thermal two-mode states, namely, the two-mode squeezed thermal states, we have  $c_- = -c_+$  (see Eq. (7.42)) causing the effect of the correlations in the average heat flow to be null. However, the TSBS states are the ones that maximize the effect of the correlations in the heat flow. For the case of TSBS negative states, the reversing of the heat flow is maximally

achieved.

Additionally, we analyze the correlation quantifiers during the evolution of the system. For our results, the mutual information is computed according to the evolution of the covariance matrix using Eqs. (4.114), (4.115) and (3.20). The quantum discord is obtained by inverting Eqs. (4.131), (4.132), (4.133) and (4.134) numerically to obtain the parameters  $\tau$  and  $\eta$  and use Eq. (4.129) to the computation for each covariance matrix during the evolution. The quantity we call *classical correlation* ( $\mathcal{J}(A|B)$ ) is the difference between the mutual information and the quantum discord computed to each state  $\mathcal{J}(A|B) = \mathcal{I}(A : B) - \mathcal{D}(A|B)$ . From Eqs. (3.32), (3.33) and (3.34) we can interpret  $\mathcal{J}(A|B)$  as the maximum information one can obtain for the mode  $A$  with the outcomes of a quantum measurement in the mode  $B$ .

In Fig. 7.4, in the left-hand plot, we have the correlation quantifiers for an initial state in the TSBS negative state ( $c_+ = c_- = -1.0$ ). As described in [50–53], and analogously as founded in Ref. [54] for qubits, the mutual information, as well as the quantum discord, are completely *consumed* so that the heat flow inversion happens. After this correlation consumption, the correlations and the heat average oscillate due to the unitary nature of the interaction. It is important to point out that this is the first explicit computation for the heat flow inversion caused by initial correlations in the Gaussian bosonic case.

In the central plot of Fig. 7.4, we have an initially uncorrelated state ( $c_+ = c_- = 0$ ), the correlations are simply created during the evolution and start to oscillate with the unitary evolution. Unfortunately, if initially, we have a state with a covariance matrix in the Simon form, but we don't have  $c_- = c_+$ , the Beam-Splitter unitary evolution causes the local states not to be locally thermal during the evolution. This precludes the use of the method from Ref. [131] described in Subsection 4.8.3 to compute the quantum discord for two-mode Gaussian states, since it only considers locally thermal states. Hence, in the right-hand side plot of Fig. 7.4, we compute only the mutual information evolution as a quantifier of correlations, together with the heat average of the two-mode squeezed thermal state ( $c_+ = -c_- = 1.4$ ). In this case, we see a consumption of correlations although the correlations don't affect the



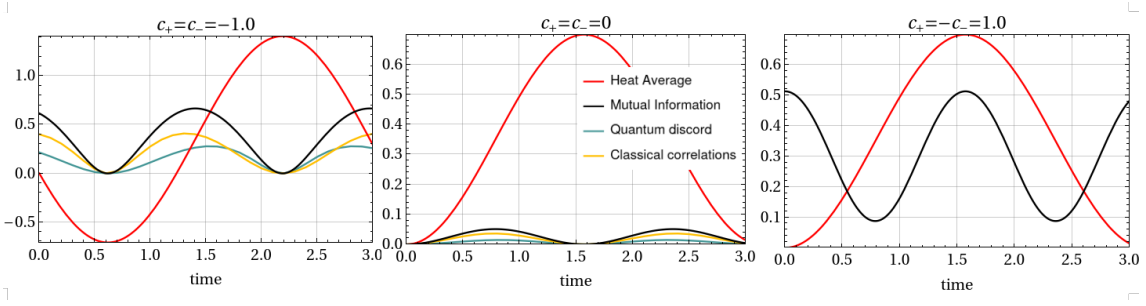


Figure 7.4: Heat average in units of  $\omega$  (red), mutual information (black), quantum discord (blue), and classical correlations (yellow) *versus* time of interaction. Each plot represents a different initial state with different values of  $c_+$  and  $c_-$  described above each plot, all the initial states are in the Simon form with  $a = 1.3$ ,  $b = 2.0$ .

heat flow. This is an indication that the *correlations may be consumed in order to affect higher moments of the heat*, instead of just affecting the average. The analysis of this specific case (for the two-mode squeezed thermal state with  $(c_+ = -c_- = 1.4)$ ) will strengthen this statement in the next subsection, when we expose the evolution of the variance.

#### 7.4.4 The evolution of the heat variance and correlations

Here we compute the variance of the heat distribution with the choice of the eigenensemble of the initial density matrix. Again, from Eq. (7.16), we have the second moment

$$\begin{aligned} \langle \mathcal{Q}_A^2(t) \rangle = & \sum_i \lambda_i \langle \lambda_i | \left( (U^\dagger(g, t) H_A U(g, t))^2 + H_A^2 \right) | \lambda_i \rangle \\ & - 2 \langle \lambda_i | H_A | \lambda_i \rangle \langle \lambda_i | U^\dagger(g, t) H_A U(g, t) | \lambda_i \rangle, \end{aligned} \quad (7.48)$$

where  $\{\lambda_i\}_i$  and  $\{|\lambda_i\rangle\}_i$  are the eigenvalues and eigenvectors of the initial density matrix  $\rho_{AB}(0)$ . Due to the complexity of computing the eigenvalues and eigenvectors of  $\rho_{AB}(0)$ , we compute the quantity above numerically.

The numerical computations are made supposing a finite Fock space, i.e., we consider in the trace computations all the Fock basis elements from the ground state  $|0\rangle$  to a higher energy state  $|N\rangle$  for each mode. The adequate value of  $N$  for a good approximation depends on the temperature of the state in question. The

higher the temperature of the state, the higher the states of the Fock basis need to be considered. For our computations, the number  $N = 25$  of the first Fock basis elements is sufficient for the convergence of the trace for its correct value. Given the initial state covariance matrix  $\sigma_{AB}$  (and supposing null first moments) we obtain its density matrix  $\rho_{AB}(0)$  by using Eq. (4.77) which is computed in the Fock basis with its first  $N = 25$  elements for each of the two modes. After obtaining the eigenvalues and eigenvectors of  $\rho_{AB}(0)$  in this finite Fock basis, we are able to compute  $\langle Q_A^2(t) \rangle$  from Eq. (7.48). Therefore, using also the results for the heat average, we can compute numerically the variance of the heat distributions.

From these computations, we obtain the plots of Fig. 7.5. For the three plots, representing different initial correlations quantifiers between the modes, we can observe that the variance peaks match the correlation minima while the variance local minima are often accompanied by the presence of correlations maxima. This strengthens our analysis at the end of the Subsection 7.2.1 when we concluded that the presence of correlations, for the qubits case, decreases the variance of the distribution. Here we observe the same behavior for the bosonic case. This indicates that this relation between the variance and correlations can be a more general behavior.

Furthermore, the right-hand side plot, in Fig. 7.5, is the case where the initial state is the two-mode squeezed thermal state with  $(c_+ = -c_- = 1.4)$ . Recalling the last Subsection, for this initial state, the correlations have no effect on the heat average flow, however, in this plot the variance seems to have a large influence due to the presence of correlations.<sup>11</sup> The increasing of the variance as the correlations decrease can be a marking that other moments of the heat distribution, rather than only the average, can consume correlations.

### 7.4.5 Profile of correlations in the initial state

Since we observed different behavior of the heat flow and of the heat variance for initially different states at the Simon form, we explore the content of the correlations for different states in the Simon form. In Fig. 7.6 we plot the mutual information

---

<sup>11</sup>Unfortunately, as stated in the last Subsection, for this case it is not possible to compute the quantum discord during the evolution using the method of the Subsection 4.8.3.

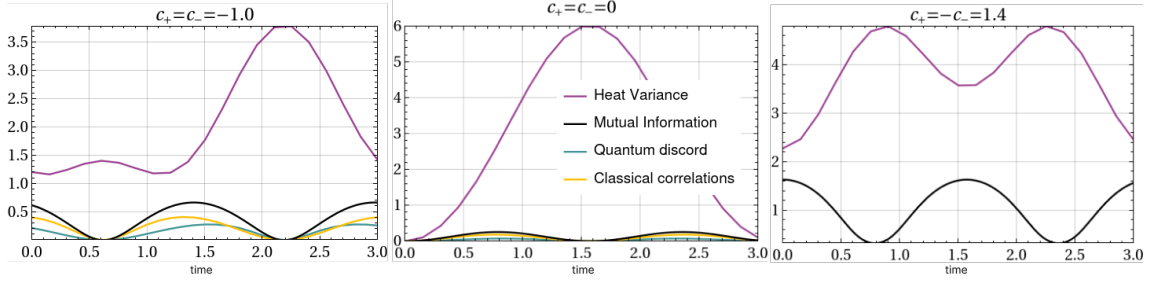


Figure 7.5: Heat variance in units of  $\omega^2$  (purple), mutual information (black), quantum discord (blue), and classical correlations (yellow) *versus* time of interaction. Each plot represents a different initial state, all the initial states are in the Simon form with  $a = 1.3$ ,  $b = 2.0$ , and the correlation terms are described above each plot. (For the case of  $c_+ = c_- = 0$ , we amplified the correlation values five times for a visible comparison in the plot.)

(representing the total correlation content) between the modes as well as the quantum discord and the classical correlations content between the modes for different values of  $c_+$  and  $c_-$  for fixed local temperatures  $a = 2$  and  $b = 10$ .

To prepare the plots we randomly peaked 100,000 points of  $r \in [1/10, 10]$  and  $\tau \in [\tau_{\min}, \tau_{\max}]$  where  $\tau_{\min}$  and  $\tau_{\max}$  are defined in the footnote of Page 85. This way, we create 100,000 Simon states with  $a = 2$ ,  $b = 10$  and  $c_+$ , and  $c_-$  given by the parametrization of Eqs. (4.133) and (4.134). With the covariance matrices, we compute the mutual information with the use of Eqs. (4.114), (4.115) and (3.20). Additionally, we use the values of  $a$ ,  $b$ ,  $r$  and  $\tau$  from each state to obtain the value of  $\eta$  (see footnote of Page 85) and finally, we use Eq. (4.129) to compute the quantum discord of each state.

We see from Fig. 7.6 that the mutual information is almost radially equally distributed for different values of  $c_+$  and  $c_-$ , i.e., the total correlations seem to increase as  $|c_+| + |c_-|$  increases. Differently, the quantum discord has not this radial pattern, it seems to decrease as  $c_-$  and  $c_+$  approaches to the  $c_+ = 0$  and  $c_- = 0$  axes. Also, the quantum discord increases substantially at the border regions with higher  $|c_-|$  and  $|c_+|$  and with  $|c_-| \approx |c_+|$ . These richer regions in quantum discord are correspondent to the TSBS states ( $c_- = c_+$ ) and two-mode squeezed thermal states  $c_- = -c_+$  and this can be a justification about why these initial states cause the higher correlations effects in the statistical moments of the heat. Curiously, the TSBS states regions are slightly richer in quantum discord than the two-mode

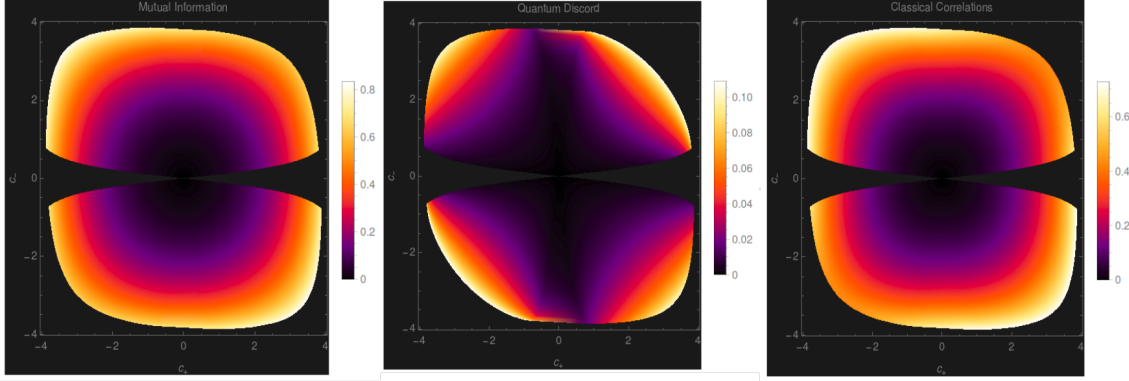


Figure 7.6: From left to right: mutual information, quantum discord, and classical information content as a function of  $c_+$  (horizontal axis) and  $c_-$  (vertical axis), for Simon states prepared with  $a = 2$  and  $b = 10$ .

squeezed thermal states, and the classical correlations are more present in two-mode squeezed thermal states than in TSBS states regions.

#### 7.4.6 Attempts to use coherent states ensembles

In order to be able to obtain analytical solutions for the heat distribution of Gaussian bosonic systems, we attempt to use the choice of coherent states ensemble to construct our QBN. With this choice, the initial density matrix has the following form

$$\rho_{AB}(0) = \int_{\mathbb{C}^2} d^2\alpha d^2\beta P(\alpha, \beta) |\alpha, \beta\rangle \langle \alpha, \beta|, \quad (7.49)$$

where  $P(\alpha, \beta) = W_1(\alpha, \beta)$  is the Glauber-Sudarshan P-function (see Eq. (4.47)) and  $|\alpha, \beta\rangle = |\alpha\rangle_A \otimes |\beta\rangle_B$  when  $|\alpha(\beta)\rangle_{A(B)}$  is a coherent state in  $A(B)$  with eigenvalues  $\alpha(\beta)$ .

We now have the caveat of determining the adequate function  $P_s$  of Eq. (7.4) in order to construct the heat probability distribution using Eq. (7.7). We now call the function  $P_s$  as the *seed probability*. The QBN developed in Sections 3.4 and 7.1 is the sum of successive products of conditional probabilities given the possible evolution of hidden layers states<sup>12</sup> times the seed probability (see Fig. 3.4 and Eq. (3.44)). The seed probability  $P_s$  could be understood as representing the *probability distribution* for the mixed initial state to be in each of the pure states of the initial

<sup>12</sup>We call *hidden layers* the set of states in the upper line of the graph in Fig. 3.4, which are the states which are not directly accessible but are the cause of the conditional probabilities.

hidden layer. However, as we shall see, the most suitable choice for representing the seed probability  $P_s$  for the case where the vectors of the ensemble choice of the initial density matrix ( $|\psi_s\rangle$ ) are coherent states  $|\alpha, \beta\rangle$  is the Glauber-Sudarshan P-function  $P(\alpha, \beta)$ , which is a *quasi-probability* distribution.

We can argue in favor of the last sentence above by supposing that we want our probability distribution to respect the marginalization conditions given in Eqs. (7.5) and (7.6). Let the probability distribution  $\mathcal{P}(a_0, a_t, b_0, b_t)$  of Eq. (7.4) for the choice of coherent states ensemble be of the form

$$\mathcal{P}(a_0, a_t, b_0, b_t) = \int_{\mathbb{C}^2} d^2\alpha d^2\beta f(\alpha, \beta) |\langle a_0, b_0 | \alpha, \beta \rangle|^2 |\langle a_t, b_t | U(t) | \alpha, \beta \rangle|^2. \quad (7.50)$$

We want to find the function  $f(\alpha, \beta)$  for the seed probability from imposing Eq. (7.6) to the probability distribution above.

Consider the sum

$$\begin{aligned} \sum_{a_0, b_0} \mathcal{P}(a_0, b_0, a_t, b_t) &= \int_{\mathbb{C}^2} d^2\alpha d^2\beta f(\alpha, \beta) |\langle a_t, b_t | U(t) | \alpha, \beta \rangle|^2 \\ &= \langle a_t, b_t | U(t) \left( \int_{\mathbb{C}^2} d^2\alpha d^2\beta f(\alpha, \beta) |\alpha, \beta\rangle \langle \alpha, \beta| \right) U^\dagger(t) | a_t, b_t \rangle, \end{aligned} \quad (7.51)$$

hence this sum is equal to  $\langle a_t, b_t | U(t) \rho_{AB}(0) U^\dagger(t) | a_t, b_t \rangle$  (in order to satisfy Eq. (7.5)) if and only if  $f(\alpha, \beta) = P(\alpha, \beta)$  (see Eq. (7.49)). The marginalization condition Eq. (7.5) is also satisfied by direct application of  $f(\alpha, \beta) = P(\alpha, \beta)$ .

One could guess that the most suitable function to play the role of  $f(\alpha, \beta)$  would be the Husimi Q-function  $Q(\alpha, \beta)$  since it is a valid probability distribution for every  $\alpha$  and  $\beta$ . However, this function represents the probability of obtaining outcomes  $\alpha$  and  $\beta$  for heterodyne measurements in  $A$  and  $B$ , and the seed probability need not assume that a measurement is indeed made. In fact, if we suppose in Eq. (7.51) that  $f(\alpha, \beta) = Q(\alpha, \beta)$ , then we have

$$\sum_{a_0, b_0} \mathcal{P}(a_0, b_0, a_t, b_t) = \langle a_t, b_t | U(t) \rho'_{AB} U^\dagger(t) | a_t, b_t \rangle, \quad (7.52)$$

where

$$\rho'_{AB} = \int_{\mathbb{C}^2} d^2\alpha d^2\beta Q(\alpha, \beta) |\alpha, \beta\rangle \langle\alpha, \beta|. \quad (7.53)$$

This density matrix is the result of performing the heterodyne measurement  $\{M_{\alpha, \beta} = \frac{1}{\pi} |\alpha, \beta\rangle \langle\alpha, \beta|\}_{\alpha, \beta}$  in  $\rho_{AB}(0)$  without revealing the outcome (see Appendix D, Section D.3). Therefore, the correct interpretation of the QBN probability distribution

$$\mathcal{P}_Q(a_0, a_t, b_0, b_t) = \int_{\mathbb{C}^2} d^2\alpha d^2\beta Q(\alpha, \beta) |\langle a_0, b_0 | \alpha, \beta \rangle|^2 |\langle a_t, b_t | U(t) | \alpha, \beta \rangle|^2, \quad (7.54)$$

is that this corresponds to the trajectory probability of the joint system after a heterodyne measurement  $\{M_{\alpha, \beta} = \frac{1}{\pi} |\alpha, \beta\rangle \langle\alpha, \beta|\}_{\alpha, \beta}$  is made in the initial state without revealing its outcome.

In conclusion, if we want QBN with the coherent states ensemble choice to respect correct marginalization conditions, the distribution *must* have the form

$$\mathcal{P}(a_0, a_t, b_0, b_t) = \int_{\mathbb{C}^2} d^2\alpha d^2\beta P(\alpha, \beta) |\langle a_0, b_0 | \alpha, \beta \rangle|^2 |\langle a_t, b_t | U(t) | \alpha, \beta \rangle|^2. \quad (7.55)$$

However, since  $P(\alpha, \beta)$  is a quasi-probability distribution, our QBN distribution  $\mathcal{P}(a_0, a_t, b_0, b_t)$ , in general, is not a probability distribution and therefore cannot be used to compute statistical moments in the usual manner.

The attempt to use the coherent state's ensemble led to the interesting situation that, if we wish to satisfy marginalization conditions, the distribution loses its original physical meaning. In future research, it can be promising to relate the distribution of Eq. (7.55) to quasi-probability definitions and results [145, 146].

# Chapter 8

## Conclusions and further perspectives

The main motivation of this thesis was to explore new effects of quantum correlations in two distinct situations.

The first project, relative to chapters 5 and 6, explored the effects of initial global correlations between the ancillae in the evolution and thermalization of a system that interacts locally with them in a collisional model setup. As a benchmark for comparison, we contrasted our results to well-known papers concerning collisional models and the asymptotic behavior of the system, leading us to a comparison with Refs. [18, 19], in which the model studied is very similar to our model explored in Chapter 5. The new component introduced in our studies (the initial ancillae correlations) revealed highly non-negligible effects, pushing the system towards different steady states and breaking the Homogenization proposed in [19]. These facts were numerically glimpsed in the qubit model and fully described for the bosonic modes case thanks to the very feasible description of Gaussian bosonic states. It was our initial intention to obtain the full description of the initial correlations effects in bosonic Gaussian modes and to construct a physical model capable of mimicking the initial correlations between the ancillae. Both goals were achieved and led us to the use of H-Graphs to prepare correlated bosonic modes. From Chapter 5 we can conclude that it is possible to create an environment with distance-dependent correlated ancillae with the use of H-graphs in qubits. We couldn't obtain analytical closed

expressions for preparing environments with the desired correlations, however, with numerical approaches it was possible to visualize non-trivial correlation patterns, as it is shown in Section 5.1. In Chapter 6, Section 6.3, we obtained a satisfactory method for such preparation of correlated ancillae for the Gaussian bosonic case, additionally it would be stimulating to suggest in detail a platform for physical implementation. This is a future work perspective and possibly a feasible candidate to implement in the context of waveguide-QED [103, 104]. Another alternative would be to recycle the ancillae and apply a periodic set of gates in them before they interact with the system to prepare the initial correlations between neighbors' ancillae. This “on the go” scheme of preparing correlations between ancillae can be applied, for the qubits case, can be implemented in recent quantum computing platforms. Additionally, the very structure of continuous variables graph-states itself [48], used in Section 6.3, is proposed under the possibility of optical preparation with offline squeezing plus interferometry [140, 141] or optical parametric oscillators [142].

The analytical results obtained in the Gaussian case raise a variety of inquiries. A special inquiry is about the underlying mechanisms of the pushing effects since there is still a lack of interpretation about how correlations can deviate the system towards the specific forms of Eqs. (6.26) and (6.34), for instance. One possible future research is to analyze this model from the perspective of Quantum Trajectories [8, 57, 147].

It is also important to remember that such kind of deviations can be present in a wide variety of collisional models rather than in the Homogenization context due to the generality of Eq. (6.24), and this could indicate the presence of such effects in a diversity of physical situations. For instance, one could consider not locally identical initial ancillae, but ancillae whose states fluctuate around an average. In this case, the steady state of the system without the initial ancillae correlations would be the average of the ancillae state, however, if we consider the initial correlations, the steady state would be pushed in the same way. Therefore, exploring the possibility of new environmental correlations inducing pushing in a system can be a fruitful direction for research.

A very relevant question to be asked is about the necessity for the ancillae cor-



relations to be of quantum nature. This is also a future work possibility that can be very challenging for qubits ancillae but feasible for bosonic systems with the use of continuous variables methods [14–16, 131]. Another possible exploration of the internal correlations of the ancillae with the use of our results is to analyze how the many-body *weaving* of the ancillae set can be changed with the collisions. This concept, proposed in [148], characterizes multipartite correlations and describes how correlations scale with the size of the many-body system.

Furthermore, Eqs. (6.26) and (6.34) give non-trivial results for thermodynamics. As already indicated in Section 6.2, we could have an initial local thermal system and ancillae (it could also be possible to have them in the same temperature), and Eqs. (6.26) and (6.34) indicate that, depending on the strength of the collision and on the ancillae initial correlations configuration, the system could get dramatically warmer or colder in the steady state. These predictions could result in a thermal machine or refrigerator in which correlations are consumed, rather than work. Therefore, a deeper study of this feature can give interesting insights into thermodynamics. Finally, a random distribution in the initial correlations of the ancillae could nullify or interfere with the pushing effect on the system. Further analysis of this subject could clarify this pushing effect in general physical systems.

In chapter 7, regarding the second project, we refer to the statistics of thermodynamic quantities using QBNs and our main search was to estimate an adequate probability distribution for the heat distribution which fully considered the effects of initial quantum correlations. We aimed to achieve this goal using QBNs initially proposed in Ref. [48]. In Chapter 7 we obtained, inspired by this main question, a general framework using QBNs to estimate probability distributions to describe observable variations (or *changes*) during a physical process. This framework was further reduced to the particular case for our studies of the heat distribution, but we can have a wide variety of applications due to the generality of the observable whose change can be explored. For instance, with this framework we are able to estimate the probability distribution variation of the number of particles (when the observable is the number operator) or work (in the presence of external time-dependent force on the Hamiltonian), being a possibly fruitful road for future research. The

characteristic function of such distribution obtained in Eq. (7.11), as well as the statistical moments resulting from it, takes under consideration the initial quantum coherences of the system to describe the full statistics of the changes and reduces to the TPM statistics for the case where there is no initial coherence in the eigenbasis of the initial observable in question. Additionally, this formalism is feasible to quantum fluctuation theorems [48] and has an experimental validation protocol based on the postselection of independent multiple copies [49]. Therefore, we expect that this formalism can be useful for further explorations of the statistics of thermodynamic quantities when one desires to consider entirely the effects of initial quantum correlations and quantum coherence.

Another important aspect observed from the result of the QBN characteristic function for the observable changes, obtained in Eq. (7.11), is its dependence on the choice of the ensemble to describe the initial covariance matrix. As a consequence, the statistical moments will also depend on this choice, with the notable exception of the average. Part of our analysis focuses on the behavior of the variance under this ensemble choice dependence since it is in our interest to understand which choice of initial ensemble causes in the probability distribution a smaller deviation from the average. In our analysis of the statistic of the heat exchange between two interacting qubits, we proved to agree with the results of Refs. [48, 54], we concluded that the probability distribution generated by the eigen-ensemble of the initial density matrix would minimize the variance in relation to any other ensemble choice. We made this affirmation as a conjecture, justified by the example explored in Section 7.2 and by the intuitive perspective, in which non-orthogonal ensembles would engender a larger variance distribution due to the indistinguishability of states. An ongoing research effort to prove analytically this statement or to discover counterexamples continues. And further research relating this feature to related papers as, for instance, Refs. [144, 149, 150] could illuminate this issue. This is related to the general question of how the ensemble choice affects the QBN probability distributions and which is the physical meaning of these different choices. The answer might be in relating the distributions to different measurement schemes. Hence, it can be worthwhile future research to relate our QBN probability distribution results concerning its

dependence on initial density matrices ensemble choice to different measurement schemes. This is done in Ref. [49] concerning the eigen-ensemble choice and a possible generalization can be explored.

Continuing to pursue our main goal in this second project, we focused on obtaining the statistics of the heat exchanged between two initially correlated Gaussian bosonic modes during a Beam Splitter interaction. We obtained the heat average for this case and observed that the heat average predicts a heat flow inversion caused by the initial correlations between the bosonic modes, analogous to the already experimentally proved qubits case [54]. This heat flow inversion cannot happen if the initial global state is the well-known two-mode squeezed thermal state, rather we observed that the heat flow inversion is maximally obtained for the case where the initial states are initially two local thermal states correlated by application of a Beam Splitter unitary (which we called TSBS states). However, it is still an open question and future query to interpret why an initial two-mode squeezed thermal state is unable to cause the heat flow inversion while the TSBS states can since both are rich in quantum correlations (quantum discord) and mutual information between the modes (see Subsection 7.4.5). Is there a feature or resource created during the preparation of the TSBS states which isn't present in a two-mode squeezed state?

As for our analysis of the variance for the heat exchange between two bosonic modes, we spotted that the variance decreases at the same time as the correlations (classical and quantum) are consumed for the heat flow inversion. Furthermore, the variance oscillates, achieving its maxima when the correlations are at their minima and its minima when the correlations reach their maxima. Therefore, this indicates that the presence of correlations decreases the variance. Since it was also observed for the qubits case, it might suggest that this fact is present in more general physical situations. Further investigations into the subject and interpretations can also be a theme for future research. A suggestion for such interpretation can be inspired by Ref. [143], which indicates that the presence of correlations can decrease the entropy of a system. If we suppose a similar reasoning for the entropy of the process, it might be possible that the correlations decrease the variance of the distribution.

Additionally, for the bosonic case where the initial joint state is a two-mode

squeezed thermal state, during the exchange of heat between the parties the correlations are consumed causing no effect on the heat average behavior. Instead, it causes an increasing effect on the variance of the heat distribution. This can be the first indication that correlations can be consumed to affect other heat distribution moments rather than the average.

Finally, regarding our attempt to use the coherent state ensemble choice to describe the bosonic QBN distribution, we concluded that the suitable seed probability distribution to the coherent-states ensemble is the Glauber-Sudarshan P-function, due to marginalization conditions. So the necessity of satisfying the marginalization conditions led our QBN distribution to lose its initial probabilistic interpretation. Therefore, the use of quasi-probabilities as seed probabilities still lacks better interpretations, and an ongoing research direction is to enlighten these results, relating it to other interpretations of quasi-probabilities [42, 145, 146, 151].

# Appendix A

## Some proofs and definitions in Open Quantum Systems and Collisional Models

### A.1 Some properties of purity

Given a density matrix  $\rho$ , we can make its spectral decomposition (since it is a hermitian operator)

$$\rho = \sum_k \lambda_k |\lambda_k\rangle \langle \lambda_k|, \quad (\text{A.1})$$

where  $\lambda_k$  and  $|\lambda_k\rangle$  are respectively the eigenvalues and eigenvectors of  $\rho$ . Notice that, from the semi positivity and normalization condition (Eqs. (2.4) and (2.5)), we obtain

$$\lambda_k \geq 0 \quad \text{and} \quad \sum_k \lambda_k = 1, \quad (\text{A.2})$$

which implies that we can treat  $\lambda_k$  as the probabilities. Now, computing the purity of  $\rho$ , we obtain

$$\mathcal{P}(\rho) = \text{Tr} \left\{ \sum_k \sum_l \lambda_k \lambda_l |\lambda_k\rangle \langle \lambda_k| \lambda_l \langle \lambda_l| \right\} = \sum_k \lambda_k^2 \leq 1, \quad (\text{A.3})$$

the above quantity is less or equal to 1 since it is a sum of probabilities squared and can be 1 *if and only if* all the probabilities are 0 except one  $\lambda_k$  which is 1, and in

this case, we arrive at a pure state.

Moreover, we can argue that the case where the purity is at its minimum is the situation where the state is more mixed. This is the case where we have no information that gives preference for the system to be in one state or another, so  $\lambda_k = 1/d$ ,  $\forall k$  (since  $\lambda_k$  represents the probability of the system being in the element of basis  $|\lambda_k\rangle$ ), where  $d$  is the dimension of the Hilbert space of the system. Consequently, we shall have

$$\mathcal{P}(\rho) = \sum_k \lambda_k^2 = \sum_k \frac{1}{d^2} = \frac{1}{d}, \quad (\text{A.4})$$

and thus we have the lower bound for  $\mathcal{P}(\rho)$ . This result can also be obtained by using Lagrange multipliers for minimizing  $\mathcal{P}(\rho)$  under the constraint of  $\rho$  normalization (Eq. (2.5)).

## A.2 The partial trace

If we treat a bipartite system  $AB$  in a Hilbert space  $\mathcal{H}_{AB} = \mathcal{H}_A \otimes \mathcal{H}_B$ , the partial trace comes from the idea of creating the adequate description for the subsystem  $A$  by summing the average effects of  $B$ . For accounting the effects of  $B$ , one can proceed as follows, suppose the most general linear operator  $\mathcal{O}$  that acts on  $\mathcal{H}_{AB}$

$$\mathcal{O} = \sum_k A_k \otimes B_k, \quad (\text{A.5})$$

where  $A_k$  and  $B_k$  are generic operators that act in  $\mathcal{H}_A$  and  $\mathcal{H}_B$  respectively. The partial trace with respect to  $B$  is defined to be *the trace of all the operators that act only on  $\mathcal{H}_B$  space*

$$\text{Tr}_B \mathcal{O} = \sum_k A_k \otimes \text{Tr}\{B_k\}, \quad (\text{A.6})$$

or, equivalently

$$\text{Tr}_B \mathcal{O} = \sum_k \sum_\alpha \langle \alpha |_B A_k \otimes B_k | \alpha \rangle_B, \quad (\text{A.7})$$

where  $\{|\alpha\rangle_B\}$  is some basis of  $\mathcal{H}_B$ . Evidently,  $\text{Tr}_B \mathcal{O}$  is not a number, but an operator acting on  $\mathcal{H}_A$  and

$$\text{Tr}\{\mathcal{O}\} = \text{Tr}_A\{\text{Tr}_B\{\mathcal{O}\}\}. \quad (\text{A.8})$$

Together with the definition of partial trace, we have the notion of *reduced density matrix* of a state  $\rho$  in  $AB$

$$\rho_A = \text{Tr}_B \rho, \quad (\text{A.9})$$

which describes the system that we would see if we only looked at  $A$  making an average of the effects of  $B$ . The intuition may come from the fact that if  $\mathcal{O}_A$  is an operator acting in  $\mathcal{H}_A$ , then

$$\langle \mathcal{O}_A \rangle = \text{Tr}\{\mathcal{O}_A \rho\} = \text{Tr}_A\{\mathcal{O}_A \text{Tr}_B\{\rho\}\} = \text{Tr}_A\{\mathcal{O}_A \rho_A\} = \text{Tr}\{\mathcal{O}_A \rho_A\}, \quad (\text{A.10})$$

where in the last equality we exchange  $\text{Tr}_A$  for the full trace  $\text{Tr}$  since all the operator inside the trace acts only on  $\mathcal{O}_A$ . The above equation means that  $\rho_A$  acts just like a density matrix should act for computing averages only on  $A$ .

### A.3 Interaction Picture

We shall make the description of this formalism just for completeness, here we are strictly following Ref. [91].

Notice that the von Neumann Equation (Eq. 2.11), just like Schrödinger's Equation, also describes a closed system evolving under a *time-dependent* Hamiltonian  $H(t)$ . So, given a quantum state  $\rho$  that evolves under such time-dependent Hamiltonian, we can define a new density matrix given by

$$\tilde{\rho} = S(t)\rho S^\dagger(t), \quad (\text{A.11})$$

where  $S(t)$  is an arbitrary time-dependent unitary.

The density matrix  $\tilde{\rho}$  is now a state that describes the system  $\rho$  in a *rotating*

frame and evolves according to a von Neumann equation

$$\boxed{\frac{d\tilde{\rho}}{dt} = -i[\tilde{H}(t), \tilde{\rho}]}, \quad (\text{A.12})$$

where

$$\boxed{\tilde{H}(t) = i\frac{dS(t)}{dt}S^\dagger(t) + S(t)H(t)S^\dagger(t)}. \quad (\text{A.13})$$

To prove Eqs. A.12 and A.13, we need only to differentiate  $\tilde{\rho}$  in function of  $t$

$$\begin{aligned} \frac{d\tilde{\rho}}{dt} &= \frac{dS(t)}{dt}\rho S^\dagger(t) + S(t)\frac{d\rho}{dt}S^\dagger(t) + S(t)\rho\frac{dS^\dagger(t)}{dt} \\ &= \frac{dS(t)}{dt}S^\dagger(t)\tilde{\rho} - iS(t)[H(t), \rho]S^\dagger(t) + \tilde{\rho}S(t)\frac{dS^\dagger(t)}{dt} \\ &= \frac{dS(t)}{dt}S^\dagger(t)\tilde{\rho} - i[S(t)H(t)S^\dagger(t), \tilde{\rho}] - \tilde{\rho}\frac{dS(t)}{dt}S^\dagger(t) \\ &= -i[S(t)H(t)S^\dagger(t) + i\frac{dS(t)}{dt}S^\dagger(t), \tilde{\rho}] = -i[\tilde{H}(t), \tilde{\rho}], \end{aligned}$$

where in the second equality we used the von Neumann Equation for  $\rho$ , and in the third equality we used that  $\frac{dS(t)}{dt}S^\dagger(t) = -S(t)\frac{dS^\dagger(t)}{dt}$  since  $\frac{d}{dt}(S(t)S^\dagger(t)) = 0$ .

The appropriate choice of  $S(t)$  can make a time-dependent Hamiltonian become time-independent and vice-versa. If we have a time-independent Hamiltonian that can be divided in

$$H = H_0 + V, \quad (\text{A.14})$$

then, if we chose

$$\boxed{S(t) = e^{iH_0t}}, \quad (\text{A.15})$$

we obtain

$$\tilde{H}(t) = e^{iH_0t}V e^{-iH_0t}. \quad (\text{A.16})$$

which means that we eliminate the direct dependence on the “free” Hamiltonian  $H_0$  on the but add a time dependence.

For the case where  $[H_0, V] = 0$ , we have, from the equation above

$$\boxed{\tilde{H}(t) = V}, \quad (\text{A.17})$$



which is a time-independent Hamiltonian, and means that the effective Hamiltonian will act just as the interaction Hamiltonian setting  $H_0 = 0$ . The assumption  $[H_0, V] = 0$  is valid for almost all of our cases of study in this thesis, and represents interactions that conserve the system's internal energy.

## A.4 Thermal states

Given a system with Hamiltonian  $H$  described by a density matrix  $\rho$ , we affirm that it is in a thermal state with temperature  $T$  when

$$\rho = \sum_i \frac{e^{-\beta E_i}}{Z} |E_i\rangle \langle E_i| = \frac{e^{-\beta H}}{Z}, \quad (\text{A.18})$$

where  $\beta = 1/T$ ,  $\{E_i\}_i$  and  $\{|E_i\rangle\}_i$  are, respectively, the sets of eigenvalues and eigenvectors of  $H$  and  $Z = \text{Tr}\{e^{-\beta H}\}$  is the *partition function*.

This is just the quantum version of the Gibbs distribution. Whereas, in classical physics, the probability distribution of a system in thermal equilibrium at temperature  $T$  is only dependent on its energy and is equal to

$$p(E_i) = \frac{e^{-\frac{1}{k_B T} E_i}}{Z}, \quad (\text{A.19})$$

where  $E_i$  is the energy of the system,  $k_B$  is the Boltzmann constant and  $Z = \sum_i e^{-\frac{1}{k_B T} E_i}$  (where the index  $i$  means “summing over all states for all possible energies  $E_i$ ”) is again the partition function. Finally, we just have that Eq. A.18 is

$$\rho = \sum_i p(E_i) |E_i\rangle \langle E_i|. \quad (\text{A.20})$$

For the case of a qubit, if we are dealing, for instance, with a standard Hamiltonian

$$H = E\sigma_z, \quad (\text{A.21})$$

with  $E > 0$ , then if  $|0\rangle$  and  $|1\rangle$  are the eigenvectors of  $\sigma_z$  (with eigenvalues  $-1$  and  $1$ , respectively), we shall have the same eigenvectors for  $H$  with eigenvalues  $-E$  and

$E$ , respectively. Hence, if the qubit is in a thermal state at temperature  $T$ , Eq. A.18 will result in

$$\rho = \begin{pmatrix} \frac{e^{\beta E}}{Z} & 0 \\ 0 & \frac{e^{-\beta E}}{Z} \end{pmatrix} = \begin{pmatrix} 1-p & 0 \\ 0 & p \end{pmatrix}, \quad (\text{A.22})$$

where  $\beta = 1/T$ ,  $Z = e^{\beta E}(1 + e^{-2\beta E})$  and  $p = \frac{1}{2}(1 - \tanh(\beta E))$ . Notice that  $0 \leq p \leq 1/2$  with the bounds achieved at  $\beta \rightarrow \infty$  and  $\beta \rightarrow 0$ , respectively.

## A.5 Proof of $\rho_{S,\text{rest}}^n \rightarrow 0$ and $\rho_{A,\text{rest}}^n \rightarrow 0$

This section of the Appendix is presented just for the completeness of the thesis. This was done following the results of Ref. [19].

For proving the properties above, it is sufficient to prove that  $\rho_S^n$  and  $\rho_A^n$  converge to  $\rho_A$ . The proof of these convergences can be made with the use of the Banach Theorem (see Ref. [152]). But to enunciate such a theorem, we must first define what is a contractive map.

Let  $\mathcal{S}$  be a space with a distance function  $D$ . A map  $T$  is called *contractive* if and only if, for any  $\rho$  and  $\eta$  that belong to  $\mathcal{S}$ , we have

$$D(T[\rho], T[\eta]) \leq kD(\rho, \eta), \quad \text{where } 0 \leq k < 1. \quad (\text{A.23})$$

The **Banach Theorem** states that, if a map  $T$  is contractive, then it has a fixed point  $\eta^* \in \mathcal{S}$  in which the interaction of the map converges to it, i.e.,  $\lim_{N \rightarrow \infty} T^N[\rho] = \eta^*$  for any  $\rho \in \mathcal{S}$ .

It is important to notice that if a map is contractive and has a fixed point (of course, this will always be true by the theorem stated above), then the fixed point will be unique. The proof is very simple: let  $\rho$  and  $\eta$  be two fixed points of a contractive map  $T$ , then it must be true that

$$D(T[\rho], T[\eta]) \leq kD(\rho, \eta) \Rightarrow D(\rho, \eta) \leq kD(\rho, \eta),$$

and the inequality above is true for some  $k$  where  $0 \leq k < 1$  if, and only if,  $\rho = \eta$ . Hence the Banach Theorem also implies the uniqueness of the fixed point of

a contractive map.

The space  $\mathcal{S}$  that we shall consider is the space of density matrices operators in the Hilbert space of the system  $\mathcal{H}_S$  while we want to show that the map  $\mathcal{E}$ , that makes the evolution of the system in the Homogenization case of Sec. 2.3.6, is contractive and has the fixed point  $\rho_A$ .

In order to show the above facts, we first parametrize our initial system's state as

$$\rho_S^0 = \frac{1}{2}\mathbf{I} + \vec{w} \cdot \vec{\sigma}, \quad (\text{A.24})$$

where  $\mathbf{I}$  is the identity operator,  $\vec{w}$  is a vector of real numbers with 3 components, with  $|\vec{w}| \leq 1/2$  and  $\vec{\sigma} = (\sigma_x, \sigma_y, \sigma_z)$  is the vector of Pauli matrices, it can be shown that every qubit density matrix can be parametrized in a Eq. (A.24) form (see Ref. [91]). We also parametrize the ancilla's initial state as

$$\rho_A = \frac{1}{2}\mathbf{I} + \vec{t} \cdot \vec{\sigma}. \quad (\text{A.25})$$

These parametrization permits us to represent  $\rho_S^0 = (1, w_x, w_y, w_z)$  and  $\rho_A = (1, t_1, t_2, t_3)$  as vectors in the operator basis  $\{\mathbf{I}/2, \sigma_x, \sigma_y, \sigma_z\}$  spanning the space of qubit density matrices.

Using this parametrizations and Eq. (2.50), we can write our map  $\mathcal{E}$  as

$$\begin{aligned} \mathcal{E}[\rho_S^0] &= \rho_S^1 = \frac{1}{2}\mathbf{I} + (s^2\vec{t} + c^2\vec{w}) \cdot \vec{\sigma} + ics[\vec{t} \cdot \vec{\sigma}, \vec{w} \cdot \vec{\sigma}] \\ &= \frac{1}{2}\mathbf{I} + [s^2\vec{t} + c^2\vec{w} - 2cs(\vec{t} \times \vec{w})] \cdot \vec{\sigma} = \frac{1}{2}\mathbf{I} + \vec{w}' \cdot \vec{\sigma}, \end{aligned} \quad (\text{A.26})$$

where we used that  $\sigma_k\sigma_l = \delta_{kl}\mathbf{I} + i\epsilon_{jkl}\sigma_j$  ( $\epsilon_{jkl}$  is the Levi-Civita symbol) in the third equality and we defined

$$w'_j = s^2t_j + (c^2\delta_{jl} - 2cs\epsilon_{jkl}t_k)w_l.$$

Now we can write Eq. (A.26) as a transformation  $\vec{w} \rightarrow \vec{w}'$  in the following way

$$\begin{pmatrix} 1 \\ w'_x \\ w'_y \\ w'_z \end{pmatrix} = \begin{pmatrix} 1 & 0 & 0 & 0 \\ s^2 t_x & c^2 & 2cst_z & -2cst_y \\ s^2 t_y & -2cst_z & c^2 & 2cst_x \\ s^2 t_z & 2cst_y & -2cst_x & c^2 \end{pmatrix} \begin{pmatrix} 1 \\ w_x \\ w_y \\ w_z \end{pmatrix}, \quad (\text{A.27})$$

the equation above can be rewritten as  $\mathcal{E}[\rho_S^0] = T\rho_S^0$ , with the vector representation of  $\rho_S^0$  and

$$T = \begin{pmatrix} 1 & \vec{0}^\top \\ s^2 \vec{t} & \mathbf{T} \end{pmatrix} \quad (\text{A.28})$$

where  $\vec{0}$  is the vector of 3 components with 0 in the entries. Finally, it is straightforward to prove that  $T\rho_A = \rho_A$  using Eqs. (A.27) and (A.28) and hence that  $\rho_A$  is a fixed point of  $\mathcal{E}$ .

Furthermore, to prove that  $\mathcal{E}$  is contrative, let us define  $\vec{v}$  such that  $\eta = \frac{1}{2}\mathbf{I} + \vec{v} \cdot \vec{\sigma}$  is a density matrix and  $\vec{r} = \vec{w} - \vec{v}$  and use the trace distance definition, so that

$$D(\rho, \eta) = \text{Tr} |(\vec{w} - \vec{v}) \cdot \vec{\sigma}| = \text{Tr} |\vec{r} \cdot \vec{\sigma}| = 2|\vec{r}|, \quad (\text{A.29})$$

where we used that the eigenvalues of  $\vec{r} \cdot \vec{\sigma}$  are  $\pm|\vec{r}|$ . Similarly, we obtain that

$$D(\mathcal{E}[\rho], \mathcal{E}[\eta]) = 2|\vec{r}'|, \quad (\text{A.30})$$

where

$$\begin{aligned} \vec{r}' &= \vec{w}' - \vec{v}' = s^2 \vec{t} + \mathbf{T}\vec{w} - s^2 \vec{t} - \mathbf{T}\vec{v} = \mathbf{T}(\vec{w} - \vec{v}) = \mathbf{T}\vec{r} \\ &= c^2 \vec{r} - 2cst \times \vec{r}, \end{aligned}$$

where we used Eqs. (A.27) and (A.28) in the last equality. The equation above implies that

$$|\vec{r}'|^2 = c^4 |\vec{r}|^2 + 4c^2 s^2 |\vec{t} \times \vec{r}|^2 = |\vec{r}|^2 c^2 (c^2 + 4s^2 |\vec{t}|^2 \sin^2 \beta),$$

where in the first equality we used that  $\vec{r}$  is orthogonal to  $\vec{t} \times \vec{r}$  and in the last equality we used that  $|\vec{t} \times \vec{r}| = |\vec{t}||\vec{r}|\sin\beta$ , for some  $0 \leq \beta \leq \pi$ . Now, since  $|\vec{t}|^2 \leq 1/4$ , we must have  $c^2 + 4s^2|\vec{t}|^2 \sin^2\beta \leq c^2 + s^2 \sin^2\beta \leq 1$  since  $\sin^2\beta \leq 1$ . Using this in the equation above, we obtain

$$|\vec{r}'| \leq |c||\vec{r}|.$$

Finally, combining the equation above with Eqs. (A.29) and (A.30), we obtain

$$D(\mathcal{E}[\rho], \mathcal{E}[\eta]) = 2|\vec{r}'| \leq 2|c||\vec{r}| = |c|D(\rho, \eta),$$

from which we obtain that  $\mathcal{E}$  is a contractive map if  $|c| < 1$  and thus it converges to its fixed point  $\rho_A$  due to Banach Theorem.

Turning the attention now to the ancillae evolution, we have from Eq. 2.53 that if we want to satisfy, for any  $\delta$ , the condition of Eq. (2.48), we must have a bound for the distance between the first collision and the original ancilla state  $D(\rho_A^1, \rho_A)$ . The condition of Eq. 2.48 implies that

$$D(\rho_A^1, \rho_A) \leq \delta. \tag{A.31}$$

Now, since  $\rho_A^1$  depends on the initial system state  $\rho_S^0$ , we must use the value of  $\rho_S^0$  that makes the greatest distance above. This is the case where the two states are pure and mutually orthogonal, i.e.,  $\vec{w} = -\vec{t}$  and  $|\vec{t}| = 1/2$ . Using this and Eq. (2.52) in the equation above, we obtain

$$2s^2 \text{Tr} |\vec{t} \cdot \vec{\sigma}| = 2s^2 \leq \delta,$$

and this implies Eq. (2.54). And since this assures that the distance between  $\rho_A^n$  and  $\rho_A$  is smaller than  $\delta$  for any  $n > 1$ , this completes the convergence of  $\rho_A^n$  to  $\rho_A$ .

# Appendix B

## Some proofs and definitions in Quantum Information

### B.1 Some useful equations

Given a function that can be expanded in the series of the form

$$f(x) = \sum_{i=0}^{\infty} a_i x^i, \quad (\text{B.1})$$

where  $a_i$  are complex numbers, and an operator  $A$  that can define  $f(A)$  such that

$$f(A) = \sum_{i=0}^{\infty} a_i A^i. \quad (\text{B.2})$$

If  $A$  can be diagonalized as

$$A = \sum_{\alpha} \lambda_{\alpha} |\lambda_{\alpha}\rangle \langle \lambda_{\alpha}|, \quad (\text{B.3})$$

where  $\{\lambda_\alpha\}_\alpha$  and  $\{|\lambda_\alpha\rangle\}_\alpha$  are respectively the eigenvalues and eigenvectors of  $A$ , then

$$\begin{aligned}
 f(A) &= \sum_{i=0}^{\infty} a_i \left( \sum_{\alpha} \lambda_{\alpha} |\lambda_{\alpha}\rangle \langle \lambda_{\alpha}| \right)^i \\
 &= \sum_{i=0}^{\infty} a_i \sum_{\alpha} \lambda_{\alpha}^i |\lambda_{\alpha}\rangle \langle \lambda_{\alpha}| \\
 &= \sum_{\alpha} \left( \sum_{i=0}^{\infty} a_i \lambda_{\alpha}^i \right) |\lambda_{\alpha}\rangle \langle \lambda_{\alpha}| \\
 &= \sum_{\alpha} f(\lambda_{\alpha}) |\lambda_{\alpha}\rangle \langle \lambda_{\alpha}|.
 \end{aligned}$$

Writing succinctly,

$$\boxed{f(A) = \sum_{\alpha} f(\lambda_{\alpha}) |\lambda_{\alpha}\rangle \langle \lambda_{\alpha}|.} \quad (\text{B.4})$$

## B.2 Proof of Eq. (3.10)

Being the density matrix  $\rho$  diagonalized as in Eq. (3.8) and given that the function  $x \log x$  can be Taylor expanded, we can use Eq. (B.4) to obtain

$$\rho \log \rho = \sum_i \lambda_i \log \lambda_i |\lambda_i\rangle \langle \lambda_i|, \quad (\text{B.5})$$

and hence we arrive at

$$-\text{Tr}(\rho \log \rho) = -\sum_i \lambda_i \log \lambda_i. \quad (\text{B.6})$$

# Appendix C

## Some proofs and definitions in Continuous Variables

### C.1 Notation for vectors and matrices of operators

Given two vector of operators  $\hat{\mathbf{a}}$  and  $\hat{\mathbf{b}}$ , we can build an operator

$$\hat{\mathbf{a}}^T \hat{\mathbf{b}} = \sum_j \hat{\mathbf{a}}_j \hat{\mathbf{b}}_j, \quad (\text{C.1})$$

and matrix of operators  $\hat{\mathbf{a}} \hat{\mathbf{b}}^T$  with components

$$(\hat{\mathbf{a}} \hat{\mathbf{b}}^T)_{jk} = \hat{\mathbf{a}}_j \hat{\mathbf{b}}_k. \quad (\text{C.2})$$

Since operators don't always commute, we have, in general,  $\hat{\mathbf{a}} \hat{\mathbf{a}}^T \neq (\hat{\mathbf{a}} \hat{\mathbf{a}}^T)^T$ , because the elements inside the vectors may not commute. Therefore, we can define the following commutators and anti-commutators

$$[\hat{\mathbf{a}}, \hat{\mathbf{a}}^T] = \hat{\mathbf{a}} \hat{\mathbf{a}}^T - (\hat{\mathbf{a}} \hat{\mathbf{a}}^T)^T, \quad (\text{C.3})$$

$$\{\hat{\mathbf{a}}, \hat{\mathbf{a}}^T\} = \hat{\mathbf{a}} \hat{\mathbf{a}}^T + (\hat{\mathbf{a}} \hat{\mathbf{a}}^T)^T, \quad (\text{C.4})$$



to express such differences. Combining both equations, we obtain

$$\{\hat{\mathbf{a}}, \hat{\mathbf{a}}^T\} + [\hat{\mathbf{a}}, \hat{\mathbf{a}}^T] = 2\hat{\mathbf{a}}\hat{\mathbf{a}}^T. \quad (\text{C.5})$$

We can also write

$$[\hat{\mathbf{a}}, \hat{\mathbf{a}}^T]_{jk} = \hat{\mathbf{a}}_j \hat{\mathbf{a}}_k - \hat{\mathbf{a}}_k \hat{\mathbf{a}}_j, \quad (\text{C.6})$$

$$\{\hat{\mathbf{a}}, \hat{\mathbf{a}}^T\}_{jk} = \hat{\mathbf{a}}_j \hat{\mathbf{a}}_k + \hat{\mathbf{a}}_k \hat{\mathbf{a}}_j. \quad (\text{C.7})$$

## C.2 The direct sum

Given two matrices  $N$  (with dimension  $n_1 \times n_2$ ) and  $M$  (with dimension  $m_1 \times m_2$ ), then the direct sum of both matrices is

$$N \oplus M = \begin{pmatrix} N & 0_{n_1 \times m_2} \\ 0_{m_1 \times n_2} & M, \end{pmatrix} \quad (\text{C.8})$$

where  $0_{n \times m}$  means a  $n \times m$  null matrix.

The notation  $\bigoplus_{n=1}^N A_n$  means the direct sum of the  $A_n$  matrices from 1 to  $N$

$$\bigoplus_{n=1}^N A_n = A_1 \oplus A_2 \oplus \cdots \oplus A_N. \quad (\text{C.9})$$

## C.3 General Gaussian integral

For further use, here we expose the well-known generalization of the Gaussian integral. Given a positive definite  $2n \times 2n$  matrix  $\mathbf{A}$  and a  $2n$ -dimensional vector  $\mathbf{b}$ , we have

$$\boxed{\int_{\mathbb{R}^{2n}} d\mathbf{r} e^{-\mathbf{r}^T \mathbf{A} \mathbf{r} + \mathbf{r}^T \mathbf{b}} = \frac{\pi^n}{\sqrt{\det \mathbf{A}}} e^{\frac{1}{4} \mathbf{b}^T \mathbf{A}^{-1} \mathbf{b}}.} \quad (\text{C.10})$$

## C.4 Proof of Eq. (4.18)

For proving this equation, we define a vector of operators  $\hat{f}(\mathbf{r}) = e^{-i\mathbf{r}^T \Omega \hat{\mathbf{r}}} \hat{\mathbf{r}} e^{i\mathbf{r}^T \Omega \hat{\mathbf{r}}}$ , from which we have  $\hat{f}(0) = \hat{\mathbf{r}}$ , where 0 here means a  $2n$  vector of 0s. Now, making

a Taylor expansion of  $\hat{f}(\mathbf{r})$  around  $\mathbf{r} = 0$ , we get

$$\hat{f}_k(\mathbf{r}) = \hat{f}_k(0) + \sum_j \mathbf{r}_j \left. \frac{\partial \hat{f}_k(\mathbf{r}')}{\partial \mathbf{r}'_j} \right|_{\mathbf{r}'=0} + \sum_{jl} \mathbf{r}_j \mathbf{r}_l \left. \frac{\partial^2 \hat{f}_k(\mathbf{r}')}{\partial \mathbf{r}'_j \partial \mathbf{r}'_l} \right|_{\mathbf{r}'=0} + \dots \quad (\text{C.11})$$

But

$$\begin{aligned} \left. \frac{\partial \hat{f}_k(\mathbf{r}')}{\partial \mathbf{r}'} \right|_{\mathbf{r}'=0} &= \left. \frac{\partial}{\partial \mathbf{r}'} \left( e^{-i \sum_{lm} \mathbf{r}'_l \Omega_{lm} \hat{\mathbf{r}}_m} \hat{\mathbf{r}}_k e^{\sum_{st} \mathbf{r}'_s \Omega_{st} \hat{\mathbf{r}}_t} \right) \right|_{\mathbf{r}'=0} \\ &= -i \sum_m \Omega_{jm} [\hat{\mathbf{r}}_m, \hat{\mathbf{r}}_k] \\ &= \sum_m \Omega_{jm} \Omega_{mk} \\ &= -\delta_{jk}, \end{aligned}$$

and it is easy to show that higher-order derivatives are 0. Using these results in Eq. (C.11), we obtain  $\hat{f}(\mathbf{r}) = \hat{\mathbf{r}} - \mathbf{r}$ .

## C.5 Proof of Eq. (4.26)

We have that, from the definition of  $|\alpha\rangle$  (Eq. (4.25))

$$\begin{aligned} \hat{a}_j |\alpha\rangle &= \hat{a}_j \hat{D}_\alpha |0\rangle \\ &= \alpha_j \hat{D}_\alpha |0\rangle \\ &= \alpha_j |\alpha\rangle, \end{aligned} \quad (\text{C.12})$$

where in the second equality we used the following result. From Eq. (4.24), we have

$$\begin{aligned} \hat{a}_j \hat{D}_\alpha |0\rangle &= \hat{D}_\alpha \hat{D}_\alpha^\dagger \hat{a}_j \hat{D}_\alpha |0\rangle \\ &= \hat{D}_\alpha (\hat{a}_j + \alpha_j) |0\rangle \\ &= \alpha_j \hat{D}_\alpha |0\rangle. \end{aligned} \quad (\text{C.13})$$

## C.6 Proof of the formula of the coherent state expanded in the Fock basis (Eq. (4.27))

We can assume that a coherent state can be expanded in the Fock basis as  $|\alpha\rangle = \sum_{m=0}^{\infty} c_m |m\rangle$  for some coefficients  $c_m$ , then

$$\begin{aligned}\hat{a}|\alpha\rangle &= \sum_{m=0}^{\infty} c_m \hat{a}|m\rangle \\ &= \sum_{m=0}^{\infty} c_m \sqrt{m} |m-1\rangle \\ &= \sum_{m=0}^{\infty} c_{m+1} \sqrt{m+1} |m\rangle \\ &= \alpha \sum_{m=0}^{\infty} c_m |m\rangle,\end{aligned}$$

since  $\alpha$  is the eigenvalue of  $\hat{a}$  for the eigenvector  $|\alpha\rangle$ . From the linear independence of the kets  $|m\rangle$ , we must have the recurrence equation

$$c_{m+1} \sqrt{m+1} = \alpha c_m,$$

whose solution is

$$c_m = A \frac{\alpha^m}{\sqrt{m!}},$$

where  $A$  is a constant to be determined by normalization. Then

$$\begin{aligned}\langle\alpha|\alpha\rangle &= \sum_{m=0}^{\infty} |c_m|^2 \\ &= |A|^2 \sum_{m=0}^{\infty} \frac{|\alpha|^{2m}}{m!} \\ &= |A|^2 e^{|\alpha|^2} \\ &= 1 \\ \implies A &= e^{-|\alpha|^2/2},\end{aligned}$$

so finally

$$|\alpha\rangle = \sum_{m=0}^{\infty} e^{-|\alpha|^2/2} \frac{\alpha^m}{\sqrt{m!}} |m\rangle. \quad (\text{C.14})$$

## C.7 Completeness relation for coherent states

Using the Fock basis decomposition (Eq. (4.27))

$$\begin{aligned}
 \frac{1}{\pi} \int_{\mathbb{C}} d^2\alpha |\alpha\rangle \langle\alpha| &= \frac{1}{\pi} \sum_{m,n=0}^{\infty} \int_{\mathbb{C}} d^2\alpha \frac{\alpha^m \alpha^{*n}}{\sqrt{m!n!}} e^{-|\alpha|^2} |m\rangle \langle n| \\
 &= \frac{1}{\pi} \sum_{m,n=0}^{\infty} \int_0^{\infty} d\hat{\rho} \int_0^{2\pi} d\phi e^{i(m-n)\phi} \frac{e^{-\hat{\rho}^2} \hat{\rho}^{m+n+1}}{\sqrt{m!n!}} |m\rangle \langle n| \\
 &= \sum_{m=0}^{\infty} 2 \int_0^{\infty} d\hat{\rho} \frac{e^{-\hat{\rho}^2} \hat{\rho}^{2m+1}}{m!} |m\rangle \langle m| \\
 &= \sum_{m=0}^{\infty} |m\rangle \langle m| \\
 &= \mathbf{I}, \tag{C.15}
 \end{aligned}$$

where in the second equality we used that  $\int_0^{2\pi} e^{i(m-n)\phi} d\phi = 2\pi\delta_{mn}$  and parametrized  $\alpha = \hat{\rho}e^{i\phi}$  and in the last equality we used the Gamma function  $\int_0^{\infty} e^{-\hat{\rho}^2} \hat{\rho}^{2m+1} d\hat{\rho} = m!/2$ .

## C.8 Proof of the Fourier-Weyl relation

From the completeness relation for coherent states, we can expand any bounded operator  $\hat{A}$  as

$$\hat{A} = \frac{1}{\pi^2} \int_{\mathbb{C}^2} d\alpha d\beta \langle\alpha| \hat{A} |\beta\rangle |\alpha\rangle \langle\beta|, \tag{C.16}$$

notice that if

$$|\alpha\rangle \langle\beta| = \frac{1}{\pi} \int_{\mathbb{C}} d^2\gamma \text{Tr}\{|\alpha\rangle \langle\beta| \hat{D}_\gamma\} \hat{D}_\gamma^\dagger, \tag{C.17}$$

the proof would be complete. So we shall demonstrate Eq. (C.17), applying  $\hat{D}_{-\alpha}$  from the left of Eq. (C.17) and  $\hat{D}_{\beta}$  from the right, we obtain

$$\begin{aligned}
 |0\rangle \langle 0| &= \frac{1}{\pi} \int_{\mathbb{C}} d^2\gamma \operatorname{Tr}\{|\alpha\rangle \langle\beta| \hat{D}_{\gamma}\} \hat{D}_{-\alpha} \hat{D}_{-\gamma} \hat{D}_{\beta} \\
 &= \frac{1}{\pi} \int_{\mathbb{C}} d^2\gamma \operatorname{Tr}\{|\alpha\rangle \langle\beta - \gamma|\} e^{\frac{1}{2}(\gamma\beta^* - \gamma^*\beta)} \hat{D}_{-\alpha} \hat{D}_{-\gamma} \hat{D}_{\beta} \\
 &= \frac{1}{\pi} \int_{\mathbb{C}} d^2\gamma \langle\beta - \gamma|\alpha\rangle e^{\frac{1}{2}(\gamma\beta^* - \gamma^*\beta)} \hat{D}_{-\alpha} \hat{D}_{-\gamma} \hat{D}_{\beta} \\
 &= \frac{1}{\pi} \int_{\mathbb{C}} d^2\gamma e^{-\frac{1}{2}|\beta - \alpha - \gamma|^2} \hat{D}_{\beta - \alpha - \gamma} \\
 &= \frac{1}{\pi} \int_{\mathbb{C}} d^2\gamma e^{-\frac{1}{2}|\gamma|^2} \hat{D}_{\gamma},
 \end{aligned} \tag{C.18}$$

where in the second equality we used Eq. 4.28, in the third equality we used Eq. 4.29, and at the last equality we made a change of variables. Thus we must prove that  $\frac{1}{\pi} \int_{\mathbb{C}} d^2\gamma e^{-\frac{1}{2}|\gamma|^2} \hat{D}_{\gamma} = |0\rangle \langle 0|$  in order to complete the proof. For this, notice that by applying it on a Fock basis vector  $|m\rangle$ , we have

$$\begin{aligned}
 \frac{1}{\pi} \int_{\mathbb{C}} d^2\gamma e^{-\frac{1}{2}|\gamma|^2} \hat{D}_{\gamma} |m\rangle &= \frac{1}{\pi} \int_{\mathbb{C}} d^2\gamma e^{-\frac{1}{2}|\gamma|^2} \hat{D}_{\gamma} \frac{\hat{a}^{\dagger m}}{\sqrt{m!}} |0\rangle \\
 &= \frac{1}{\pi} \int_{\mathbb{C}} d^2\gamma e^{-\frac{1}{2}|\gamma|^2} \hat{D}_{\gamma} \frac{\hat{a}^{\dagger m}}{\sqrt{m!}} \hat{D}_{\gamma}^{\dagger} \hat{D}_{\gamma} |0\rangle \\
 &= \frac{1}{\pi} \int_{\mathbb{C}} d^2\gamma e^{-\frac{1}{2}|\gamma|^2} \frac{(\hat{a}^{\dagger} - \gamma^*)^m}{\sqrt{m!}} |\gamma\rangle \\
 &= \int_{\mathbb{C}} \frac{d^2\gamma}{\pi} e^{-|\gamma|^2} \frac{(\hat{a}^{\dagger} - \gamma^*)^m}{\sqrt{m!}} \sum_{n=0}^{\infty} \frac{\gamma^n}{\sqrt{n!}} |n\rangle \\
 &= \sum_{n=0}^{\infty} \sum_{j=0}^m \int_{\mathbb{C}} \frac{d^2\gamma}{\pi} e^{-|\gamma|^2} \binom{m}{j} \frac{(-\gamma)^*{}^j \gamma^n}{\sqrt{m!n!}} \hat{a}^{\dagger(m-j)} |n\rangle \\
 &= \sum_{j=0}^m \binom{m}{j} (-1)^j |m\rangle \\
 &= \delta_{m0} |0\rangle,
 \end{aligned} \tag{C.19}$$

where in the third equality we used that  $\hat{D}_{\gamma} \hat{a}^{\dagger} \hat{D}_{\gamma}^{\dagger} = \hat{a}^{\dagger} - \gamma^*$ , in the fourth equality we used Eq. (4.27), in the sixth equality we used  $\frac{1}{\pi} \int_{\mathbb{C}} d^2\gamma e^{-|\gamma|^2} \gamma^*{}^j \gamma^n = n! \delta_{jn}$  and in the last step we used the fact that  $\sum_{j=0}^m \binom{m}{j} (-1)^j = (1-1)^m = \delta_{m0}$ . Finally, we have that Eq. (C.19) implies (C.18) which is equivalent to Eq. (C.17).

### C.9 Proof of Eq. (4.42)

Given the definitions of Eq. (4.41) and Eq. (4.21) and using that the one mode vector  $r' = (q', p')$ , we have

$$\begin{aligned}
 W(q, p) &= \frac{1}{\pi^2} \int_{\mathbb{R}} \int_{\mathbb{R}} dq' dp' e^{i(pq' - qp')} \chi(q', p') \\
 &= \frac{1}{2\pi^2} \int_{\mathbb{R}} \int_{\mathbb{R}} dq' dp' e^{i(pq' - qp')} \int_{\mathbb{R}} dx \langle x | \hat{D}_{-\frac{r'}{2}} \hat{\rho} \hat{D}_{-\frac{r'}{2}} | x \rangle \\
 &= \frac{1}{\pi^2} \int_{\mathbb{R}} \int_{\mathbb{R}} \int_{\mathbb{R}} dq' dp' dx e^{ipq'} e^{ip'(x-q)} \left\langle x - \frac{q'}{2} \left| \hat{\rho} \right| x + \frac{q'}{2} \right\rangle \\
 &= \frac{1}{\pi} \int_{\mathbb{R}} dq' e^{ipq'} \left\langle q - \frac{q'}{2} \left| \hat{\rho} \right| q + \frac{q'}{2} \right\rangle \\
 &= \frac{2}{\pi} \int_{\mathbb{R}} dq' e^{ipq'} \langle q - q' | \hat{\rho} | q + q' \rangle, \tag{C.20}
 \end{aligned}$$

where in the second equality we expanded the trace of the definition of  $\chi(q', p')$  (Eq. (4.38)) in terms of a first quadrature basis  $|x\rangle$ , we used the cyclic property of the trace and used that  $\hat{D}_{-r'} = \hat{D}_{-r'/2} \hat{D}_{-r'/2}$  and in the third equality we used that  $\hat{D}_{-r'/2} = e^{-\frac{i}{2}q'\hat{p}} e^{\frac{i}{2}p'\hat{q}} e^{\frac{i}{8}q'p'}$  and thus  $\hat{D}_{-r'/2} |x\rangle = |x + \frac{q'}{2}\rangle e^{\frac{i}{2}p'x} e^{\frac{i}{8}q'p'}$ .

### C.10 Proof of Eq. (4.47)

From applying the Weyl operator  $\hat{D}_\alpha$  from the left of Eq. (C.18) and its conjugate transpose operator from the right of this equation, we obtain

$$|\alpha\rangle \langle \alpha| = \frac{1}{\pi} \int_{\mathbb{C}} d^2\gamma e^{-\frac{1}{2}|\gamma|^2} e^{(\alpha\gamma^* - \alpha^*\gamma)} \hat{D}_{-\gamma}, \tag{C.21}$$

where we used Eq. (4.28) so that  $\hat{D}_\alpha \hat{D}_\gamma \hat{D}_{-\alpha} = e^{(\alpha\gamma^* - \alpha^*\gamma)} \hat{D}_\gamma$ . Using the equation above, we obtain

$$\begin{aligned}
 \int_{\mathbb{C}} d^2\alpha P(\alpha) |\alpha\rangle \langle\alpha| &= \frac{1}{\pi} \int_{\mathbb{C}} d^2\gamma e^{-\frac{1}{2}|\gamma|^2} \int_{\mathbb{C}} d^2\alpha e^{(\alpha\gamma^* - \alpha^*\gamma)} P(\alpha) \hat{D}_{-\gamma} \\
 &= \frac{1}{\pi} \int_{\mathbb{C}} d^2\gamma e^{-\frac{1}{2}|\gamma|^2} \chi_1(\gamma) \hat{D}_{-\gamma} \\
 &= \frac{1}{\pi} \int_{\mathbb{C}} d^2\gamma \chi_0(\gamma) \hat{D}_{-\gamma} \\
 &= \hat{\rho}, \tag{C.22}
 \end{aligned}$$

where in the second equality we used the inverse Fourier transform of  $P(\alpha)$  (since  $P(\alpha) = \int_{\mathbb{C}} d^2\beta e^{(\alpha\gamma^* - \alpha^*\gamma)} \chi_1(\beta)$  then its inverse will be  $\chi_1(\gamma) = \int_{\mathbb{C}} d^2\alpha e^{(\alpha\gamma^* - \alpha^*\gamma)} P(\alpha)$ ), in the third equality we used Eq. (4.44) to relate  $\chi_1(\alpha)$  to  $\chi_0(\alpha)$  and in the fourth equality we used the Fourier-Weyl relation (Eq. (4.35)).

## C.11 Proof of Eq. (4.49)

Using the Fourier Weyl relation, (Eq. (4.35)) we obtain

$$\begin{aligned}
 \frac{1}{\pi} \langle\alpha| \hat{\rho} |\alpha\rangle &= \frac{1}{\pi^2} \int_{\mathbb{C}} d^2\beta \chi_0(\beta) \langle\alpha| \hat{D}_{-\beta} |\alpha\rangle \\
 &= \frac{1}{\pi^2} \int_{\mathbb{C}} d^2\beta e^{\frac{1}{2}(\alpha\beta^* - \alpha^*\beta)} \chi_0(\beta) \langle\alpha|\alpha - \beta\rangle \\
 &= \frac{1}{\pi^2} \int_{\mathbb{C}} d^2\beta e^{(\alpha\beta^* - \alpha^*\beta)} \chi_0(\beta) e^{-\frac{|\beta|^2}{2}} \\
 &= W_{-1}(\alpha), \tag{C.23}
 \end{aligned}$$

where in the second equality we used Eq. (4.28) to obtain  $\hat{D}_{-\beta} |\alpha\rangle = \hat{D}_{\alpha-\beta} |0\rangle e^{\frac{1}{2}(\alpha\beta^* - \alpha^*\beta)} = |\alpha - \beta\rangle e^{\frac{1}{2}(\alpha\beta^* - \alpha^*\beta)}$  and in the third equality we used Eq. (4.29).

## C.12 Proof of the Robertson-Schrödinger relation (Eq. (4.58))

In order to obtain the formula, first consider the following  $2n \times 2n$  complex matrix

$$\tau = 2 \operatorname{Tr} [(\hat{\mathbf{r}} - \bar{\mathbf{r}})(\hat{\mathbf{r}} - \bar{\mathbf{r}})^\dagger \hat{\rho}]. \quad (\text{C.24})$$

We can show that this operator is positive semi-definite in the following way. Suppose  $v \in \mathbb{C}^{2n}$ , then we have

$$\begin{aligned} v^\dagger \tau v &= 2v^\dagger \operatorname{Tr} [(\hat{\mathbf{r}} - \bar{\mathbf{r}})(\hat{\mathbf{r}} - \bar{\mathbf{r}})^\dagger \hat{\rho}] v \\ &= 2 \operatorname{Tr} [v^\dagger (\hat{\mathbf{r}} - \bar{\mathbf{r}})(\hat{\mathbf{r}} - \bar{\mathbf{r}})^\dagger v \hat{\rho}] \\ &= 2 \operatorname{Tr} [\hat{\mathcal{O}} \hat{\mathcal{O}}^\dagger \hat{\rho}] \\ &\geq 0, \end{aligned} \quad (\text{C.25})$$

where  $\mathcal{O} = v^\dagger (\hat{\mathbf{r}} - \bar{\mathbf{r}})$ . In the second equality, we used Eqs. (C.1) and (C.2) which imply

$$\begin{aligned} v^\dagger \operatorname{Tr} [(\hat{\mathbf{r}} - \bar{\mathbf{r}})(\hat{\mathbf{r}} - \bar{\mathbf{r}})^\dagger \hat{\rho}] v &= \sum_{jk} v_j \operatorname{Tr} [(\hat{\mathbf{r}} - \bar{\mathbf{r}})_j (\hat{\mathbf{r}} - \bar{\mathbf{r}})_k \hat{\rho}] v_k \\ &= \operatorname{Tr} \left[ \sum_{jk} v_j (\hat{\mathbf{r}} - \bar{\mathbf{r}})_j (\hat{\mathbf{r}} - \bar{\mathbf{r}})_k v_k \hat{\rho} \right] \\ &= \operatorname{Tr} [v^\dagger (\hat{\mathbf{r}} - \bar{\mathbf{r}})(\hat{\mathbf{r}} - \bar{\mathbf{r}})^\dagger v \hat{\rho}], \end{aligned}$$

and in the last step of Eq. (C.25), we used the fact that for every operator  $\mathcal{O}$ ,  $\mathcal{O}\mathcal{O}^\dagger$  is positive semidefinite and  $\hat{\rho}$  is also semidefinite, hence  $\mathcal{O}\mathcal{O}^\dagger \hat{\rho}$  is positive semidefinite. This concludes the proof that  $\tau \geq 0$ . Now, from Eq. (C.5) and from  $\tau \geq 0$ , we have



that

$$\begin{aligned}
 \tau &= 2 \operatorname{Tr} [(\hat{\mathbf{r}} - \bar{\mathbf{r}})(\hat{\mathbf{r}} - \bar{\mathbf{r}})^\dagger \hat{\rho}] \\
 &= \operatorname{Tr} [\{(\hat{\mathbf{r}} - \bar{\mathbf{r}}), (\hat{\mathbf{r}} - \bar{\mathbf{r}})^\dagger\} \hat{\rho}] + \operatorname{Tr} [[(\hat{\mathbf{r}} - \bar{\mathbf{r}}), (\bar{\mathbf{r}} - \bar{\mathbf{r}})^\dagger] \hat{\rho}] \\
 &= \operatorname{Tr} [\{(\hat{\mathbf{r}} - \bar{\mathbf{r}}), (\hat{\mathbf{r}} - \bar{\mathbf{r}})^\dagger\} \hat{\rho}] + \operatorname{Tr} [[\hat{\mathbf{r}}, \bar{\mathbf{r}}^\dagger] \hat{\rho}] \\
 &= 2\sigma + i\Omega \\
 &\geq 0,
 \end{aligned} \tag{C.26}$$

where in the third equality we used Eqs. (4.56) and (4.11). Finally, we obtain

$$\boxed{\sigma + \frac{i\Omega}{2} \geq 0.} \tag{C.27}$$

### C.13 Density matrix and covariance matrix of free Gaussian bosonic modes

If we have a Gaussian state of  $N$  free bosonic modes, then it will have the form

$$\hat{\rho}_{\text{free}} = \frac{e^{-\hat{\mathbf{r}}^\top \Lambda \hat{\mathbf{r}}}}{Z}, \tag{C.28}$$

where  $\Lambda = \operatorname{diag}(\lambda_1, \lambda_2, \dots, \lambda_N)$ ,  $\lambda_j > 0$ ,  $\forall j$  and  $Z = \operatorname{Tr} (e^{-\hat{\mathbf{r}}^\top \Lambda \hat{\mathbf{r}}})$ . Since the modes are non-interacting, we have

$$\hat{\rho}_{\text{free}} = \bigotimes_{j=1}^n \frac{e^{-\frac{\lambda_j}{2}(\hat{q}_j^2 + \hat{p}_j^2)}}{Z_j}, \tag{C.29}$$

where  $Z_j = \operatorname{Tr} \left( e^{-\frac{\lambda_j}{2}(\hat{q}_j^2 + \hat{p}_j^2)} \right)$ . Computing explicitly and using the geometric series, we obtain

$$\begin{aligned}
 Z_j &= \sum_{n_j=0}^{\infty} e^{-\lambda_j(n_j+1/2)} \\
 &= \frac{e^{-\lambda_j/2}}{1 - e^{-\lambda_j}}.
 \end{aligned} \tag{C.30}$$

Consequently, the density matrix will be

$$\begin{aligned}
 \hat{\rho}_{\text{free}} &= \bigotimes_{j=1}^n \frac{e^{-\frac{\lambda_j}{2}(\hat{q}_j^2 + \hat{p}_j^2)}}{Z_j} \\
 &= \bigotimes_{j=1}^n \sum_{n_j=0}^{\infty} \frac{e^{-\lambda_j(n_j+1/2)}}{Z_j} |n_j\rangle \langle n_j| \\
 &= \bigotimes_{j=1}^n \left(1 - e^{-\lambda_j}\right) \sum_{n_j=0}^{\infty} e^{-\lambda_j n_j} |n_j\rangle \langle n_j|
 \end{aligned} \tag{C.31}$$

For a mode  $j$ , we have a well-known average, called the *Bose-Einstein* distribution

$$\boxed{\bar{n}_j = \langle \hat{a}_j^\dagger \hat{a}_j \rangle = \frac{1}{e^{\lambda_j} - 1}.} \tag{C.32}$$

We can rewrite the density matrix of free bosonic modes in terms of the Bose-Einstein distribution

$$\boxed{\hat{\rho}_{\text{free}} = \bigotimes_{j=1}^n \frac{1}{1 + \bar{n}_j} \sum_{n_j=0}^{\infty} \left(\frac{\bar{n}_j}{\bar{n}_j + 1}\right)^{n_j} |n_j\rangle \langle n_j|.} \tag{C.33}$$

From Eq. (4.3) we have that, for a mode  $j$ ,

$$\langle \hat{q}_j^2 \rangle = \langle \hat{p}_j^2 \rangle = \langle a_j^\dagger a_j \rangle + 1/2, \tag{C.34}$$

and hence, using Eq. (C.32), we have

$$\langle \hat{q}_j^2 \rangle = \langle \hat{p}_j^2 \rangle = \frac{1}{2} \coth(\lambda_j/2). \tag{C.35}$$

For this state  $\langle q_j \rangle = \langle p_j \rangle = 0$ ,  $\forall j$ , so the covariance matrix will be

$$\begin{aligned}
 \sigma_{ij} &= \frac{1}{2} \langle \{\hat{\mathbf{r}}_i, \hat{\mathbf{r}}_j\} \rangle \\
 &= \frac{1}{2} \coth(\lambda_j/2) \delta_{ij}
 \end{aligned} \tag{C.36}$$

which means

$$\boxed{\sigma = \frac{1}{2} \coth\left(\frac{\Lambda}{2}\right).} \tag{C.37}$$

This can also be rewritten as

$$\sigma = \bigoplus_{j=1}^n \nu_j \begin{pmatrix} 1 & 0 \\ 0 & 1 \end{pmatrix}, \quad (\text{C.38})$$

where  $\nu_j = \frac{1}{2} \coth\left(\frac{\lambda_j}{2}\right)$ .

Notice that from Eqs. (C.34) and (C.35) we can describe the diagonal covariance matrix elements in terms of the Bose-Einstein distributions

$$\nu_j = \bar{n}_j + \frac{1}{2}. \quad (\text{C.39})$$

Finally, we can write the density matrix in terms of the diagonal elements of the covariance matrix

$$\hat{\rho}_{\text{free}} = \bigotimes_{j=1}^n \frac{1}{\nu_j + 1/2} \sum_{n_j=0}^{\infty} \left( \frac{\nu_j - 1/2}{\nu_j + 1/2} \right)^{n_j} |n_j\rangle \langle n_j|. \quad (\text{C.40})$$

## C.14 Obtaining symplectic eigenvalues

According to the Williamson's theorem (Eq. (4.78)), given a positive definite matrix  $M$ , there is a symplectic matrix  $S$  such that

$$M = SDS^T, \quad (\text{C.41})$$

where

$$D = D_n \otimes \mathbb{I}_2, \quad \text{with } D_n = \text{diag}(d_1, d_2, \dots, d_n), \quad (\text{C.42})$$

with  $d_j > 0, \forall j$ .

Notice that the matrix  $i\Omega M$  is hermitian, hence it can be diagonalized as

$$i\Omega M = BAB^\dagger, \quad (\text{C.43})$$

where  $\Lambda$  is a diagonal matrix of eigenvalues and  $B$  is a unitary matrix with eigen-

vectors as columns. Using the properties of the symplectic matrix  $S$  and of the symplectic form  $\Omega$ , we can relate  $\Lambda$  to the symplectic eigenvalues, this can be done as follows. From Eq. (C.42) we obtain

$$\begin{aligned}
 i\Omega M &= i\Omega S D S^\top \\
 &= i\Omega S (D_n \otimes \mathbb{I}_2) S^\top \\
 &= iS^{-\top}(\Omega)(D_n \otimes \mathbb{I}_2) S^\top \\
 &= iS^{-\top}(\mathbb{I}_n \otimes \Omega_1)(D_n \otimes \mathbb{I}_2) S^\top \\
 &= iS^{-\top}(D_n \otimes \Omega_1) S^\top \\
 &= S^{-\top}(D_n \otimes i\Omega_1) S^\top
 \end{aligned} \tag{C.44}$$

where in the third equality, we used  $\Omega S = S^{-\top} \Omega$ .<sup>1</sup>

Finally, notice that

$$i\Omega_1 = -U_2 \sigma_z U_2^\dagger, \tag{C.45}$$

where  $U_2 = \frac{1}{\sqrt{2}} \begin{pmatrix} 1 & 1 \\ i & -i \end{pmatrix}$ . The formula above can be shown by direct evaluation, and applying it in Eq. (C.44), it follows that

$$i\Omega M = S^{-\top}(\mathbb{I}_n \otimes U_2)(D_n \otimes (-\sigma_z))(\mathbb{I}_n \otimes U_2^\dagger) S^\top, \tag{C.46}$$

which is in the form of Eq. (C.43). Identifying the unitary  $B = S^{-\top}(\mathbb{I}_n \otimes U_2)$  and  $\Lambda = D_n \otimes (-\sigma_z)$  we conclude that we can obtain the symplectic eigenvalues (the diagonal elements of  $D_n$ ) by computing the eigenvalues of  $i\Omega M$  and taking their absolute values (since the eigenvalues of  $i\Omega M$  come in pairs of plus and minus the diagonal elements of  $D_n$ ).

---

<sup>1</sup>This is a consequence of the fact that if  $S$  is a symplectic matrix,  $S^\top$  also is symplectic (this can be seen by taking the transpose of Eq. (4.76) and using that  $\Omega^\top = -\Omega$ ). Using this fact, we have that  $S^\top \Omega S = \Omega$  and applying  $S^{-\top}$  from the left hand side, we obtain  $\Omega S = S^{-\top} \Omega$ .

## C.15 Justifying the existence of a Hamiltonian matrix corresponding to any symplectic matrix

We want to prove that, given a matrix  $S \in S_{p_{2n, \mathbb{R}}}$  with strictly positive eigenvalues, then there exists a real and symmetric matrix  $H$  such that  $S = e^{\Omega H}$ . Furthermore, there exists a unitary  $\hat{S}$  such that

$$S\hat{\mathbf{r}} = \hat{S}^\dagger \hat{\mathbf{r}} \hat{S}, \quad (\text{C.47})$$

for any  $2n$  vector of canonical operators  $\hat{\mathbf{r}}$ .

Given  $S \in S_{p_{2n, \mathbb{R}}}$  with strictly positive eigenvalues, we can define the following matrix

$$H = \Omega^\top \log S. \quad (\text{C.48})$$

By construction,  $H$  has positive elements. For proving that  $H$  is symmetric, notice that

$$\begin{aligned} H^\top &= \log(S^\top) \Omega \\ &= \Omega \Omega^\top \log(S^\top) \Omega \\ &= \Omega \log(\Omega^\top S^\top \Omega) \\ &= \Omega \log(S^{-1}) \\ &= -\Omega \log(S) \\ &= \Omega^\top \log(S) \\ &= H, \end{aligned} \quad (\text{C.49})$$

where repeatedly used that  $-\Omega = \Omega^\top = \Omega^{-1}$  and in the fourth equality we used the fact that  $\Omega S = S^{-\top} \Omega$  (which is proved in the previous section of this Appendix) which implies  $S = \Omega^\top S^{-\top} \Omega \Rightarrow \Omega^\top S^{-1} \Omega$ . Since we have that  $H$ , given by Eq. (C.48), is real and symmetric, then we have  $S = e^{\Omega H}$  and, by the construction of

Eq. (4.65), there must be a unitary  $\hat{S} = e^{-\frac{1}{2}\hat{\mathbf{r}}^\dagger H \hat{\mathbf{r}}}$  such that

$$S\hat{\mathbf{r}} = \hat{S}^\dagger \hat{\mathbf{r}} \hat{S}. \quad (\text{C.50})$$

## C.16 Proof for the parametrization of Eq. (4.77)

We can start the proof as follows. Since  $\hat{\rho}_G$  is a Gaussian state, then (see Eqs. (4.52) and (4.53)) it can be described as

$$\hat{\rho}_G = \frac{e^{-\frac{1}{2}(\hat{\mathbf{r}}-\bar{\mathbf{r}})^\text{T} M (\hat{\mathbf{r}}-\bar{\mathbf{r}})}}{Z}, \quad (\text{C.51})$$

where  $M$  is a positive definite matrix and  $Z$  is a normalization constant. From Williamson's Theorem, we can diagonalize  $M$  with the use of a symplectic matrix  $S$ . Defining a new valid vector of canonical operators  $\hat{\mathbf{Y}} = S(\hat{\mathbf{r}} - \bar{\mathbf{r}})$  and using Eq. (4.78), we can rewrite the Gaussian state as

$$\hat{\rho}_G = \frac{e^{-\frac{1}{2}\hat{\mathbf{Y}}^\text{T} D \hat{\mathbf{Y}}}}{Z}. \quad (\text{C.52})$$

Since  $D$  is a diagonal matrix, the state  $\hat{\rho}_G$  in the equation above represents a set of free non-interacting harmonic oscillators described by the canonical operators in  $\hat{\mathbf{Y}}$ . The covariance matrix of non-interacting harmonic oscillators has the simple form of (see Eq. (C.37), and the whole Section for a proof)

$$\begin{aligned} \tilde{\sigma} &= \frac{1}{2} \langle \hat{\mathbf{Y}}, \hat{\mathbf{Y}}^\text{T} \rangle \\ &= \frac{1}{2} \coth\left(\frac{D}{2}\right). \end{aligned} \quad (\text{C.53})$$

Now, consider the following relations

$$\begin{aligned}
 \sigma &= \frac{1}{2} \langle \{(\hat{\mathbf{r}} - \bar{\mathbf{r}}), (\hat{\mathbf{r}} - \bar{\mathbf{r}})^\top\} \rangle \\
 &= \frac{1}{2} \langle \{S^{-1} \hat{\mathbf{Y}}, \hat{\mathbf{Y}}^\top S^{-\top}\} \rangle \\
 &= \frac{1}{2} S^{-1} \langle \{\hat{\mathbf{Y}}, \hat{\mathbf{Y}}^\top\} \rangle S^{-\top} \\
 &= S^{-1} \tilde{\sigma} S^{-\top} \\
 &= \frac{1}{2} S^{-1} \coth\left(\frac{D}{2}\right) S^{-\top}. \tag{C.54}
 \end{aligned}$$

We can use the equation above to obtain the relation between  $M$  and  $\sigma$ . With the use of Eq. (C.46), we have

$$\coth\left(\frac{i\Omega M}{2}\right) = S^{-1} (\mathbb{I}_n \otimes U_2) \coth\left(\frac{D_n \otimes (-\sigma_z)}{2}\right) (\mathbb{I}_n \otimes U_2^\dagger) S, \tag{C.55}$$

where  $U_2 = \begin{pmatrix} 1 & 1 \\ i & -i \end{pmatrix}$  and  $D_n = \text{diag}(d_1, d_2, \dots, d_n)$  such that  $D = D_n \otimes \mathbb{I}_2$ . Using the fact that  $\coth(\bullet)$  is an odd function, we have that  $\coth\left(\frac{D_n \otimes (-\sigma_z)}{2}\right) = \coth(D_n/2) \otimes (-\sigma_z)$ , and hence

$$\begin{aligned}
 \coth\left(\frac{i\Omega M}{2}\right) &= S^{-1} (\mathbb{I}_n \otimes U_2) (\coth(D_n/2) \otimes (-\sigma_z)) (\mathbb{I}_n \otimes U_2^\dagger) S \\
 &= S^{-1} \coth(D_n/2) \otimes (i\Omega_1) S \\
 &= S^{-1} (\coth(D_n/2) \otimes \mathbb{I}_2) (\mathbb{I}_n \otimes i\Omega_1) S \\
 &= S^{-1} (\coth(D/2) i\Omega) S \\
 &= S^{-1} (\coth(D/2) S^{-\top} i\Omega) \\
 &= 2\sigma i\Omega, \tag{C.56}
 \end{aligned}$$

where in the second equality we used Eq. (C.45), in the fifth equality we used that  $S^{-\top} \Omega = \Omega S$  (with is proved in the previous section of this Appendix), and in the last equality we used Eq. (C.54).

Applying  $i\Omega$  in both sides of Eq. (C.56), and using that  $(i\Omega)^2 = \mathbb{I}$ , we obtain

$$i\Omega \coth\left(\frac{i\Omega M}{2}\right) i\Omega = 2i\Omega\sigma. \quad (\text{C.57})$$

Since  $i\Omega$  is unitary, the equation above can be rewritten as

$$2i\Omega\sigma = \coth\left(\frac{Mi\Omega}{2}\right), \quad (\text{C.58})$$

inverting this result we finally obtain

$$M = 2\text{arccoth}(2i\Omega\sigma)i\Omega. \quad (\text{C.59})$$

## C.17 Proof that the commutator between any second order operators is a second order operator

Given two generic second order operators  $\hat{\mathcal{O}}_1 = \frac{1}{2} \sum_{jk} O_{1jk} \hat{\mathbf{r}}_j \hat{\mathbf{r}}_k + \sum_j \mu_{1j} \hat{\mathbf{r}}_j$  and  $\hat{\mathcal{O}}_2 = \frac{1}{2} \sum_{jk} O_{2jk} \hat{\mathbf{r}}_j \hat{\mathbf{r}}_k + \sum_j \mu_{2j} \hat{\mathbf{r}}_j$ , the commutator between them will be

$$\begin{aligned} [\mathcal{O}_1, \mathcal{O}_2] &= \frac{1}{4} \sum_{jklm} O_{1jk} O_{2lm} [\hat{\mathbf{r}}_j \hat{\mathbf{r}}_k, \hat{\mathbf{r}}_l \hat{\mathbf{r}}_m] + \frac{1}{2} \sum_{jkl} O_{1jk} \mu_{2l} [\hat{\mathbf{r}}_j \hat{\mathbf{r}}_k, \hat{\mathbf{r}}_l] \\ &\quad + \frac{1}{2} \sum_{jlm} O_{2lm} \mu_{1j} [\hat{\mathbf{r}}_j, \hat{\mathbf{r}}_l \hat{\mathbf{r}}_m] + \sum_{jm} \mu_{1j} \mu_{2m} [\hat{\mathbf{r}}_j, \hat{\mathbf{r}}_m]. \end{aligned} \quad (\text{C.60})$$

In order to show that the above commutator is at most of the second order, we start by noticing that

$$\begin{aligned} [\hat{\mathbf{r}}_j \hat{\mathbf{r}}_k, \hat{\mathbf{r}}_l \hat{\mathbf{r}}_m] &= \hat{\mathbf{r}}_j [\hat{\mathbf{r}}_k, \hat{\mathbf{r}}_l] \hat{\mathbf{r}}_m + [\hat{\mathbf{r}}_j, \hat{\mathbf{r}}_l] \hat{\mathbf{r}}_k \hat{\mathbf{r}}_m + \hat{\mathbf{r}}_l \hat{\mathbf{r}}_j [\hat{\mathbf{r}}_k, \hat{\mathbf{r}}_m] + \hat{\mathbf{r}}_l [\hat{\mathbf{r}}_j, \hat{\mathbf{r}}_m] \hat{\mathbf{r}}_k \\ &= i\hat{\mathbf{r}}_j \hat{\mathbf{r}}_m \Omega_{kl} + i\hat{\mathbf{r}}_k \hat{\mathbf{r}}_m \Omega_{jl} + i\hat{\mathbf{r}}_l \hat{\mathbf{r}}_j \Omega_{km} + i\hat{\mathbf{r}}_l \hat{\mathbf{r}}_k \Omega_{jm}, \end{aligned} \quad (\text{C.61})$$

where in the first equality we used that  $[AB, CD] = A[B, C]D + [A, C]BD + CA[B, D] + C[A, D]B$  and in the second equality we used Eq. (4.11). The above commutator is thus at most of the second-order on canonical operators, and using



again Eq. (4.11) we can similarly show that  $[\hat{r}_j \hat{r}_k, \hat{r}_l]$ ,  $[\hat{r}_j, \hat{r}_l \hat{r}_m]$  and  $[\hat{r}_j, \hat{r}_m]$  are all at most second order operators. Hence, we conclude that the commutator of two generic second-order Hamiltonians in Eq. (C.60) is a second-order operator, as we intended.

## C.18 Proof of Eq. (4.114)

Analyzing a mode  $j$ , notice that

$$\begin{aligned}
 \mathbf{S}(\hat{\rho}_{\text{free}_j}) &= -\text{Tr} \left[ \hat{\rho}_{\text{free}_j} \log(\hat{\rho}_{\text{free}_j}) \right] \\
 &= -\text{Tr} \left[ \hat{\rho}_{\text{free}_j} \log \left( \frac{1}{\nu_j + 1/2} \sum_{n_j=0}^{\infty} \left( \frac{\nu_j - 1/2}{\nu_j + 1/2} \right)^{n_j} |n_j\rangle \langle n_j| \right) \right] \\
 &= -\text{Tr} \left[ \hat{\rho}_{\text{free}_j} \log \left( \sum_{n_j=0}^{\infty} \left( \frac{\nu_j - 1/2}{\nu_j + 1/2} \right)^{n_j} |n_j\rangle \langle n_j| \right) \right] \\
 &\quad + \text{Tr} \left[ \hat{\rho}_{\text{free}_j} \log(\nu_j + 1/2) \right] \\
 &= -\text{Tr} \left[ \hat{\rho}_{\text{free}_j} \sum_{n_j=0}^{\infty} \log \left( \left( \frac{\nu_j - 1/2}{\nu_j + 1/2} \right)^{n_j} \right) |n_j\rangle \langle n_j| \right] + \log(\nu_j + 1/2) \\
 &= -\text{Tr} \left[ \hat{\rho}_{\text{free}_j} \sum_{n_j=0}^{\infty} n_j \log \left( \frac{\nu_j - 1/2}{\nu_j + 1/2} \right) |n_j\rangle \langle n_j| \right] + \log(\nu_j + 1/2) \\
 &= -\log \left( \frac{\nu_j - 1/2}{\nu_j + 1/2} \right) \text{Tr} \left[ \hat{\rho}_{\text{free}_j} \sum_{n_j=0}^{\infty} n_j |n_j\rangle \langle n_j| \right] + \log(\nu_j + 1/2) \\
 &= -\log \left( \frac{\nu_j - 1/2}{\nu_j + 1/2} \right) \text{Tr} \left[ \hat{\rho}_{\text{free}_j} \hat{n}_j \right] + \log(\nu_j + 1/2) \\
 &= -\log \left( \frac{\nu_j - 1/2}{\nu_j + 1/2} \right) \bar{n}_j + \log(\nu_j + 1/2) \\
 &= -\log \left( \frac{\nu_j - 1/2}{\nu_j + 1/2} \right) (\nu_j - 1/2) + \log(\nu_j + 1/2) \\
 &= (\nu_j + 1/2) \log(\nu_j + 1/2) - (\nu_j - 1/2) \log(\nu_j - 1/2). \tag{C.62}
 \end{aligned}$$

The equation above, together with Eq. (4.113) justifies Eqs. (4.114) and (4.115). In the Equation above, we used that  $\log(\sum_n (c_n) |n\rangle \langle n|) = \sum_n \log(c_n) |n\rangle \langle n|$  (for any positive  $c_n$ ) in the forth equality, and we used Eq. (C.39) in the ninth equality.

## C.19 Proof of Simon normal form statement

The statement says that any covariance matrix representing a two-mode Gaussian state can be reduced, by local single-mode symplectic transformation, to the following form

$$\sigma_S = \begin{pmatrix} a & 0 & c_+ & 0 \\ 0 & a & 0 & c_- \\ c_+ & 0 & b & 0 \\ 0 & c_- & 0 & b \end{pmatrix}, \quad (\text{C.63})$$

with  $a$  and  $b$  positive real numbers, and  $c_+$  and  $c_-$  real numbers satisfying the Bona-fide conditions.

For the proof, suppose that  $\sigma$  is a generic covariance matrix of a two-mode state. Williamson's theorem (Eq. (4.78)) states that any single-mode covariance matrix can be diagonalized by means of a single-mode symplectic transformation into  $x\mathbb{I}$ , where  $x > 0$ . Consequently, there exist symplectic transformations  $S_a$  acting in the first mode and  $S_b$  acting in the second mode, such that

$$S_b^\top S_a^\top \sigma S_a S_b = \begin{pmatrix} a\mathbb{I} & C \\ C^\top & b\mathbb{I} \end{pmatrix}, \quad (\text{C.64})$$

where  $a$  and  $b$  are positive real numbers and  $C$  is a  $2 \times 2$  real matrix. Since  $a\mathbb{I}$  and  $b\mathbb{I}$  are invariant under transformations that are orthogonal and symplectic, we can apply the orthogonal and symplectic transformations needed to diagonalize the off-diagonal block-matrix  $C$ , according to the *Singular Value Decomposition* (SVD).<sup>2</sup>

## C.20 Proof that $S(\mathcal{E}(|\alpha\rangle\langle\alpha|)) = S(\mathcal{E}(|0\rangle\langle 0|))$ for any Gaussian channel $\mathcal{E}$

The covariance matrix of any coherent state  $|\alpha\rangle\langle\alpha|$  and the vacuum  $|0\rangle\langle 0|$  has the same value, namely  $\mathbb{I}/2$ , their only difference exists in their first moments.

From the results of Section 4.7, and as it was shown in Eqs. (4.67) and (4.72), the

---

<sup>2</sup>See such version of the SVD in Chapter 5 of Ref. [14].

evolution of the first moments and of the covariance matrix for a Gaussian state are decoupled during all the Stinespring dilation process. Since any quantum channel can be expressed by a Stinespring dilation, we conclude that any Gaussian channel evolution must have a decoupled behavior between the covariance matrix and the first moments. Consequently, if the input of two states with the same covariance matrix are inputs to a quantum channel, their outputs will also have the same covariance matrix.

Therefore, the outputs of  $\mathcal{E}(|\alpha\rangle\langle\alpha|) = \mathcal{E}(|0\rangle\langle 0|)$  will have the same covariance matrix. Finally, since the entropy of a Gaussian state only depends on its covariance matrix (Eqs. (4.114) and (4.115)), we conclude that their entropy will be the same.

## C.21 Computations to obtain Eq. (4.129)

For obtaining Eq. (4.129), we must compute  $\mathbf{S}(\hat{\rho}_{AB})$ ,  $\mathbf{S}(\hat{\rho}_B)$  and  $\mathbf{S}(\mathcal{E}(|0\rangle\langle 0|))$ .

The entropies  $\mathbf{S}(\hat{\rho}_{AB}) = g(\nu_-) + g(\nu_+)$  and  $\mathbf{S}(\hat{\rho}_B) = g(\beta)$  are direct consequences of Eq. (4.114) and from the fact that the local covariance matrix of  $\hat{\rho}_B$  is already in its diagonal form.

The entropy of  $\mathcal{E}(|0\rangle\langle 0|)$  can be obtained from the fact that the covariance matrix of the vacuum is  $\sigma_{\text{vac}} = \mathbb{I}/2$  and its evolution through the phase-insensitive Gaussian channel  $\mathcal{E}$  is given by Eq. (4.119). Hence, the evolved covariance matrix will be  $\mathbb{I}_2(\tau + \eta)/2$ , which has only the symplectic eigenvalues  $(\tau + \eta)/2$ , and the result follows from Eq. (4.114).

## C.22 Two-mode squeezed thermal state, EPR state, and friends

Here we give examples of how to construct the Simon form of the two-mode squeezed thermal state, EPR state, and other kinds of local thermal states from canonical operations acting in initial thermal states.

### C.22.1 Two-mode squeezed thermal state

Given two bosonic modes  $A$  and  $B$ , the *Two-mode squeezing* operator (for further applications of the two-mode squeezing, see Refs. [55, 121, 122]) is a unitary operator defined as

$$\hat{S}_{ts}(\xi) = e^{\xi^* \hat{a} \hat{b} - \xi \hat{a}^\dagger \hat{b}^\dagger}, \quad (\text{C.65})$$

where  $\hat{a}(\hat{b})$  is the annihilator operator and  $\hat{a}^\dagger(\hat{b}^\dagger)$  is the creation operator acting in the mode  $A(B)$ . For a real parameter  $r$ , it has the form

$$\hat{S}_{ts}(\xi)(r) = e^{r(\hat{a} \hat{b} - \hat{a}^\dagger \hat{b}^\dagger)}. \quad (\text{C.66})$$

The Hamiltonian matrix that generates this operator is

$$H_{ts}(r) = r \begin{pmatrix} 0 & 0 & 0 & 1 \\ 0 & 0 & 1 & 0 \\ 0 & 1 & 0 & 0 \\ 1 & 0 & 0 & 0 \end{pmatrix}. \quad (\text{C.67})$$

Therefore the correspondent symplectic matrix is

$$\begin{aligned} S_{ts}(r) &= e^{\Omega H_{ts}(r)} \\ &= \begin{pmatrix} \cosh(r) & 0 & \sinh(r) & 0 \\ 0 & \cosh(r) & 0 & -\sinh(r) \\ \sinh(r) & 0 & \cosh(r) & 0 \\ 0 & -\sinh(r) & 0 & \cosh(r) \end{pmatrix}. \end{aligned} \quad (\text{C.68})$$

From Eq. (C.37), we have that the thermal state of two bosonic modes  $A$  and  $B$  with local Hamiltonians  $H_{A(B)} = \omega \left( \hat{a}^\dagger(\hat{b}^\dagger) \hat{a}(\hat{b}) + \frac{1}{2} \right)$  is

$$\sigma_{AB}^{\text{th}} = \begin{pmatrix} \bar{n}_A + 1/2 & 0 & 0 & 0 \\ 0 & \bar{n}_A + 1/2 & 0 & 0 \\ 0 & 0 & \bar{n}_B + 1/2 & 0 \\ 0 & 0 & 0 & \bar{n}_B + 1/2 \end{pmatrix}, \quad (\text{C.69})$$

where  $\bar{n}_A + 1/2 = \frac{1}{2} \coth\left(\frac{\omega\beta_A}{2}\right)$  and  $\beta_{A(B)}$  is the inverse of the temperature of  $A(B)$ . Hence, the *two-mode squeezed thermal state* is just the two-mode squeezed applied in this thermal state

$$\begin{aligned}\sigma_{AB}^{\text{TMST}} &= S_{ts}(r)\sigma_{AB}^{\text{th}}S_{ts}^\top \\ &= \begin{pmatrix} \mathbf{a} & 0 & c & 0 \\ 0 & \mathbf{a} & 0 & -c \\ c & 0 & \mathbf{b} & 0 \\ 0 & -c & 0 & \mathbf{b} \end{pmatrix},\end{aligned}\tag{C.70}$$

where  $\mathbf{a} = \left(\bar{n}_A + \frac{1}{2}\right) \cosh^2(r) + \left(\bar{n}_B + \frac{1}{2}\right) \sinh^2(r)$ ,  $\mathbf{b} = \left(\bar{n}_B + \frac{1}{2}\right) \cosh^2(r) + \left(\bar{n}_A + \frac{1}{2}\right) \sinh^2(r)$  and  $c = \frac{1}{2}(1 + \bar{n}_A + \bar{n}_B) \sinh(2r)$ .

### C.22.2 EPR state

The EPR state is defined as the two-mode squeezed operator applied in the vacuum. The vacuum is equivalent to a thermal state at 0 temperature, thus a two-mode vacuum state has covariance matrix  $\sigma_{AB}^{\text{vac}} = \frac{1}{2}\mathbb{I}_4$ . Therefore, the EPR covariance matrix for a squeezing operator  $\hat{S}_{ts}(r)$  is

$$\begin{aligned}\sigma_{EPR} &= \frac{1}{2}S_{ts}(r)S_{ts}^\top(r) \\ &= \begin{pmatrix} \beta & 0 & \sqrt{\beta^2 - 1} & 0 \\ 0 & \beta & 0 & -\sqrt{\beta^2 - 1} \\ \sqrt{\beta^2 - 1} & 0 & \beta & 0 \\ 0 & -\sqrt{\beta^2 - 1} & 0 & \beta \end{pmatrix},\end{aligned}\tag{C.71}$$

where  $\beta = \frac{1}{2} \cosh(2r)$ . If we change the sign of  $r$ , i.e.,  $r \rightarrow -r$ , then the off-diagonal terms of the matrix switch sign.

# Appendix D

## Some proofs and definitions in Obtaining Observables Variations Using QBNs

### D.1 Proof of Eq. (7.20)

With the use of Eqs. (7.17) and (7.18) we have

$$\mathcal{P}_{\text{TPM}}(a_0, a_t) = \sum_{b_t, b, b_1} \langle a_t, b_t | U(t) | a_0, b \rangle \langle a_0, b | \rho_{AB}(0) | a_0, b' \rangle \langle a_0, b' | U^\dagger(t) | a_t, b_t \rangle, \quad (\text{D.1})$$

where we just used that  $\mathbb{I}_B = \sum_b |b\rangle \langle b|$ , for the basis  $\{|b\rangle\}_b$  and  $\{|b'\rangle\}_{b'}$  of  $B$ .

Let the characteristic function for the shift probability of Eq. (7.19) be

$$G_{\mathcal{O}_{A\text{TPM}}}(k) = \int_{-\infty}^{\infty} (d\Delta a) e^{ik\Delta a} p_{\text{TPM}}(\Delta\mathcal{O}_A = \Delta a), \quad (\text{D.2})$$

from which we have

$$G_{\mathcal{O}_{A\text{TPM}}}(k) = \sum_{a_0, a_t} e^{ik(a_t - a_0)} \mathcal{P}_{\text{TPM}}(a_0, a_t). \quad (\text{D.3})$$

Appendix D. Some proofs and definitions in Obtaining Observables Variations  
Using QBNs

---

Applying Eq. (D.1) in this characteristic function, we obtain

$$\begin{aligned}
G_{\mathcal{O}_{\text{ATPM}}}(k) &= \sum_{b_t, b, b', a_0, a_t} \langle b_t, a_t | U(t) e^{-ik a_0} | a_0, b \rangle \langle a_0, b | \rho_{AB}(0) | a_0, b' \rangle \langle a_0, b' | U^\dagger(t) e^{ik a_t} | a_t, b_t \rangle \\
&= \sum_{b_t, b, b', a_0, a_t} \langle b_t, a_t | U(t) e^{-ik \mathcal{O}_A(0)} | a_0, b \rangle \langle a_0, b | \rho_{AB}(0) | a_0, b' \rangle \langle a_0, b' | U^\dagger(t) e^{ik \mathcal{O}_A(t)} | a_t, b_t \rangle \\
&= \sum_{b_t, a_0, a_t} \langle b_t, a_t | U(t) e^{-ik \mathcal{O}_A(0)} | a_0 \rangle \langle a_0 | \rho_{AB}(0) | a_0 \rangle \langle a_0 | U^\dagger(t) e^{ik \mathcal{O}_A(t)} | a_t, b_t \rangle \\
&= \text{Tr} \left\{ U(t) e^{-ik \mathcal{O}_A(0)} \left( \sum_{a_0} | a_0 \rangle \langle a_0 | \rho_{AB}(0) | a_0 \rangle \langle a_0 | \right) U^\dagger(t) e^{ik \mathcal{O}_A(t)} \right\} \\
&= \text{Tr} \left\{ e^{-ik \mathcal{O}_A(0)} \mathcal{D}_{\mathcal{O}_A(0)}(\rho_{AB}(0)) U^\dagger(t) e^{ik \mathcal{O}_A(t)} U(t) \right\} \\
&= \text{Tr} \left\{ e^{ik U^\dagger(t) \mathcal{O}_A(t) U(t)} e^{-ik \mathcal{O}_A(0)} \mathcal{D}_{\mathcal{O}_A(0)}(\rho_{AB}(0)) \right\},
\end{aligned} \tag{D.4}$$

which is the desired equation, where  $\mathcal{D}_{\mathcal{O}_A(0)}(\bullet) = \sum_{a_0} | a_0 \rangle \langle a_0 | \bullet | a_0 \rangle \langle a_0 |$ .

## D.2 Matrices for generating ensembles in Subsection 7.3.1

The matrices used to generate the different ensembles of  $\rho_{AB}^0$  with the use of Eq. (7.34) in Subsection 7.3.1 are the following

$$\begin{aligned}
 M_1 &= \begin{pmatrix} 0 & 0 & 1 \\ 0 & -\frac{\sqrt{3}}{2} & 0 \\ \frac{\sqrt{3}}{2} & -\frac{1}{4} & 0 \\ \frac{1}{2} & \frac{\sqrt{3}}{4} & 0 \end{pmatrix}, \quad M_2 = \begin{pmatrix} 0 & 1 & 0 \\ 0 & 0 & -\frac{1}{2} \\ \frac{\sqrt{3}}{2} & 0 & \frac{\sqrt{3}}{4} \\ \frac{1}{2} & 0 & -\frac{3}{4} \end{pmatrix}, \\
 M_3 &= \frac{1}{\sqrt{3}} \begin{pmatrix} 0 & 1 & 1 \\ 1 & 0 & 1 \\ 1 & -1 & 0 \\ 1 & 1 & -1 \end{pmatrix}, \quad M_4 = \frac{1}{\sqrt{3}} \begin{pmatrix} 0 & 1 & 1 \\ 1 & 0 & -1 \\ 1 & -1 & 1 \\ 1 & 1 & 0 \end{pmatrix}, \\
 M_5 &= \begin{pmatrix} 0 & 0 & 1 \\ -\frac{1}{2} & -\frac{\sqrt{3}}{2} & 0 \\ \frac{\sqrt{3}}{4} & -\frac{1}{4} & 0 \\ -\frac{3}{4} & \frac{\sqrt{3}}{4} & 0 \end{pmatrix}, \quad M_6 = \begin{pmatrix} 0 & 1 & 0 \\ 0 & 0 & 1 \\ 1 & 0 & 0 \end{pmatrix}, \\
 M_7 &= \begin{pmatrix} 0 & \cos(0.1) & \sin(0.1) \\ 0 & \sin(0.1) & -\cos(0.1) \\ 1 & 0 & 0 \end{pmatrix} \quad \text{and} \quad M_8 = \begin{pmatrix} 0 & \cos\left(\frac{\pi}{4}\right) & \sin\left(\frac{\pi}{4}\right) \\ 0 & \sin\left(\frac{\pi}{4}\right) & -\cos\left(\frac{\pi}{4}\right) \\ 1 & 0 & 0 \end{pmatrix}.
 \end{aligned}$$

## D.3 The QBN generated by post-measurements

Suppose we have an observable  $\mathcal{O}_C$  acting on the joint Hilbert space of  $A$  and  $B$  described in the setup of Section 7.1. Given the eigenvalues  $\{|c_i\rangle\}_i$  and eigenvectors  $\{|c_i\rangle\}_i$  of  $\mathcal{O}_C$ , we can define the projective measurement  $\{M_i = |c_i\rangle\langle c_i|\}_i$ . Then, if such projective measurement is made in the initial joint state  $\rho_{AB}(0)$  but the outcome



is not revealed, the state is uploaded to the average of all possible backactions

$$\begin{aligned}
 \rho'_{AB} &= \sum_i P_{c_i} \frac{M_i \rho_{AB}(0) M_i^\dagger}{P_{c_i}} \\
 &= \sum_i M_i \rho_{AB}(0) M_i^\dagger \\
 &= \sum_i P_{c_i} |c_i\rangle \langle c_i|, \tag{D.5}
 \end{aligned}$$

where  $P_{c_i} = \text{Tr}\{M_i \rho_{AB}(0) M_i^\dagger\} = \langle c_i | \rho_{AB}(0) | c_i \rangle$  is the probability of the measure to have the outcome  $c_i$ . Hence, the probability distribution generated by

$$\mathcal{P}_{\mathcal{O}_C}(a_0, b_0, a_t, b_t) = \sum_i P_{c_i} |\langle a_0, b_0 | c_i \rangle|^2 |\langle a_t, b_t | U(t) | c_i \rangle|^2, \tag{D.6}$$

is with the seed probability  $P_{c_i}$  the QBN generated by the post-measured density matrix  $\rho'_{AB}$ .

This is exactly the case of Eq. (7.54), where the seed probability  $P_{c_i}$  is the Husimi Q-function  $Q(\alpha, \beta)$ , representing the probability of having an outcome  $(\alpha, \beta)$  for the projective measurement  $\{\frac{1}{\pi} M_{\alpha, \beta} |\alpha, \beta\rangle \langle \alpha, \beta| \}_{\alpha, \beta}$  and the kets  $|c_i\rangle$  are coherent states  $|\alpha, \beta\rangle$ . Thus the matrix

$$\begin{aligned}
 \rho'_{AB} &= \sum_i P_{c_i} |c_i\rangle \langle c_i| \\
 &= \int_{\mathbb{C}^2} d^2\alpha d^2\beta Q(\alpha, \beta) |\alpha, \beta\rangle \langle \alpha, \beta|, \tag{D.7}
 \end{aligned}$$

is the density matrix after a heterodyne measurement is made without the outcome being revealed. This interpretation explains the result of Eq. (7.52), i.e.,  $\mathcal{P}_{\mathcal{O}_C}(a_t, b_t) = \langle a_t, b_t | U(t) \rho'_{AB} U^\dagger(t) | a_t, b_t \rangle$ .

# Bibliography

- [1] M. A. Nielsen and I. L. Chuang, *Quantum Computation and Quantum Information: 10th Anniversary Edition*. Cambridge University Press, 2010. DOI: [10.1017/CB09780511976667](https://doi.org/10.1017/CB09780511976667).
- [2] J. Preskill, *Course information for physics 219/computer science 219 quantum computation*.
- [3] R. Horodecki, “Quantum information,” *Acta Physica Polonica A*, vol. 139, no. 3, pp. 197–2018, Mar. 2021, ISSN: 0587-4246. DOI: [10.12693/aphyspola.139.197](https://doi.org/10.12693/aphyspola.139.197).
- [4] R. S. Ingarden, “Quantum information theory,” *Reports on Mathematical Physics*, vol. 10, no. 1, pp. 43–72, 1976, ISSN: 0034-4877. DOI: [https://doi.org/10.1016/0034-4877\(76\)90005-7](https://doi.org/10.1016/0034-4877(76)90005-7).
- [5] I. H. Deutsch, “Harnessing the power of the second quantum revolution,” *PRX Quantum*, vol. 1, p. 020101, 2 Nov. 2020. DOI: [10.1103/PRXQuantum.1.020101](https://doi.org/10.1103/PRXQuantum.1.020101).
- [6] L. Jaeger, *The Second Quantum Revolution: From Entanglement to Quantum Computing and Other Super-Technologies*. Springer, 2018, ISBN: 9783319988252.
- [7] T. D. Ladd, F. Jelezko, R. Laflamme, Y. Nakamura, C. Monroe, and J. L. O’Brien, “Quantum computers,” *Nature*, vol. 464, no. 7285, pp. 45–53, Mar. 2010. DOI: [10.1038/nature08812](https://doi.org/10.1038/nature08812).
- [8] H. Wiseman and G. Milburn, *Quantum Measurement and Control*. Cambridge University Press, 2010, ISBN: 9780521804424.
- [9] A. Einstein, B. Podolsky, and N. Rosen, “Can quantum-mechanical description of physical reality be considered complete?” *Phys. Rev.*, vol. 47, pp. 777–780, 10 May 1935. DOI: [10.1103/PhysRev.47.777](https://doi.org/10.1103/PhysRev.47.777).
- [10] E. Schrödinger, “Discussion of probability relations between separated systems,” *Mathematical Proceedings of the Cambridge Philosophical Society*, vol. 31, no. 4, pp. 555–563, 1935. DOI: [10.1017/S0305004100013554](https://doi.org/10.1017/S0305004100013554).
- [11] N. Bohr, “Can quantum-mechanical description of physical reality be considered complete?” *Phys. Rev.*, vol. 48, pp. 696–702, 8 Oct. 1935. DOI: [10.1103/PhysRev.48.696](https://doi.org/10.1103/PhysRev.48.696).
- [12] J. S. Bell, “On the einstein podolsky rosen paradox,” *Physics Physique Fizika*, vol. 1, pp. 195–200, 3 Nov. 1964. DOI: [10.1103/PhysicsPhysiqueFizika.1.195](https://doi.org/10.1103/PhysicsPhysiqueFizika.1.195).

- [13] *Scientific background on the nobel prize in physics 2022*, <https://www.nobelprize.org/uploads/2022/10/advanced-physicsprize2022-3.pdf>, Accessed: 2023-04-11.
- [14] A. Serafini, *Quantum Continuous Variables: A Primer of Theoretical Methods*. CRC Press, Taylor & Francis Group, 2017, ISBN: 9781482246346.
- [15] M. Wilde, *Quantum Information Theory*. Cambridge University Press, 2017, ISBN: 9781316813300.
- [16] C. Weedbrook *et al.*, “Gaussian quantum information,” *Reviews of Modern Physics*, vol. 84, no. 2, pp. 621–669, May 2012. DOI: [10.1103/revmodphys.84.621](https://doi.org/10.1103/revmodphys.84.621).
- [17] J. Rau, “Relaxation phenomena in spin and harmonic oscillator systems,” *Phys. Rev.*, vol. 129, pp. 1880–1888, 4 Feb. 1963. DOI: [10.1103/PhysRev.129.1880](https://doi.org/10.1103/PhysRev.129.1880).
- [18] V. Scarani, M. Ziman, P. Stelmachovic, N. Gisin, and V. Buzek, “Thermalizing quantum machines: Dissipation and entanglement,” *Phys. Rev. Lett.*, vol. 88, p. 097905, 9 Feb. 2002. DOI: [10.1103/PhysRevLett.88.097905](https://doi.org/10.1103/PhysRevLett.88.097905).
- [19] M. Ziman, P. Stelmachovic, V. Buzek, M. Hillery, V. Scarani, and N. Gisin, “Diluting quantum information: An analysis of information transfer in system-reservoir interactions,” *Phys. Rev. A*, vol. 65, p. 042105, 4 Mar. 2002. DOI: [10.1103/PhysRevA.65.042105](https://doi.org/10.1103/PhysRevA.65.042105).
- [20] S. Campbell and B. Vacchini, *Collision models in open system dynamics: A versatile tool for deeper insights?* 2021. arXiv: [2102.05735 \[quant-ph\]](https://arxiv.org/abs/2102.05735).
- [21] F. Ciccarello, S. Lorenzo, V. Giovannetti, and G. M. Palma, “Quantum collision models: Open system dynamics from repeated interactions,” *Physics Reports*, vol. 954, pp. 1–70, Apr. 2022. DOI: [10.1016/j.physrep.2022.01.001](https://doi.org/10.1016/j.physrep.2022.01.001).
- [22] J. Goold, M. Huber, A. Riera, L. del Rio, and P. Skrzypczyk, “The role of quantum information in thermodynamics: a topical review,” *Journal of Physics A: Mathematical and Theoretical*, vol. 49, no. 14, p. 143001, Feb. 2016. DOI: [10.1088/1751-8113/49/14/143001](https://doi.org/10.1088/1751-8113/49/14/143001).
- [23] S. Vinjanampathy and J. Anders, “Quantum thermodynamics,” *Contemporary Physics*, vol. 57, no. 4, pp. 545–579, Jul. 2016. DOI: [10.1080/00107514.2016.1201896](https://doi.org/10.1080/00107514.2016.1201896).
- [24] F. Binder, L. Correa, C. Gogolin, J. Anders, and G. Adesso, *Thermodynamics in the Quantum Regime: Fundamental Aspects and New Directions* (Fundamental Theories of Physics). Springer International Publishing, 2019, ISBN: 9783319990460.
- [25] S. Deffner and S. Campbell, *Quantum thermodynamics: An introduction to the thermodynamics of quantum information*, 2019. DOI: [10.48550/ARXIV.1907.01596](https://doi.org/10.48550/ARXIV.1907.01596).
- [26] L. Szilard, “Über die entropieverminderung in einem thermodynamischen system bei eingriffen intelligenter wesen,” *Zeitschrift für Physik*, vol. 53, pp. 840–856, 1929.

- [27] M. B. Plenio and V. Vitelli, “The physics of forgetting: Landauer’s erasure principle and information theory,” *Contemporary Physics*, vol. 42, no. 1, pp. 25–60, Jan. 2001. DOI: [10.1080/00107510010018916](https://doi.org/10.1080/00107510010018916).
- [28] C. H. Bennett, *Notes on landauer’s principle, reversible computation and maxwell’s demon*, 2003. arXiv: [physics/0210005](https://arxiv.org/abs/physics/0210005) [[physics.class-ph](https://arxiv.org/abs/physics/0210005)].
- [29] S. Bhattacharjee and A. Dutta, “Quantum thermal machines and batteries,” *The European Physical Journal B*, vol. 94, no. 12, Dec. 2021. DOI: [10.1140/epjb/s10051-021-00235-3](https://doi.org/10.1140/epjb/s10051-021-00235-3).
- [30] “Quantum thermodynamics and quantum coherence engines,” *TURKISH JOURNAL OF PHYSICS*, vol. 44, no. 5, Oct. 2020. DOI: [10.3906/fiz-2009-12](https://doi.org/10.3906/fiz-2009-12).
- [31] M. Campisi and R. Fazio, “The power of a critical heat engine,” *Nature Communications*, vol. 7, no. 1, Jun. 2016. DOI: [10.1038/ncomms11895](https://doi.org/10.1038/ncomms11895).
- [32] M. P. Woods, N. H. Y. Ng, and S. Wehner, “The maximum efficiency of nano heat engines depends on more than temperature,” *Quantum*, vol. 3, p. 177, Aug. 2019. DOI: [10.22331/q-2019-08-19-177](https://doi.org/10.22331/q-2019-08-19-177).
- [33] P. Talkner, E. Lutz, and P. Hänggi, “Fluctuation theorems: Work is not an observable,” *Physical Review E*, vol. 75, no. 5, May 2007. DOI: [10.1103/physreve.75.050102](https://doi.org/10.1103/physreve.75.050102).
- [34] M. Esposito, U. Harbola, and S. Mukamel, “Nonequilibrium fluctuations, fluctuation theorems, and counting statistics in quantum systems,” *Reviews of Modern Physics*, vol. 81, no. 4, pp. 1665–1702, Dec. 2009. DOI: [10.1103/revmodphys.81.1665](https://doi.org/10.1103/revmodphys.81.1665).
- [35] M. Campisi, P. Hänggi, and P. Talkner, “Colloquium: Quantum fluctuation relations: Foundations and applications,” *Reviews of Modern Physics*, vol. 83, no. 3, pp. 771–791, Jul. 2011. DOI: [10.1103/revmodphys.83.771](https://doi.org/10.1103/revmodphys.83.771).
- [36] A. E. Allahverdyan and T. M. Nieuwenhuizen, “Fluctuations of work from quantum subensembles: The case against quantum work-fluctuation theorems,” *Phys. Rev. E*, vol. 71, p. 066 102, 6 Jun. 2005. DOI: [10.1103/PhysRevE.71.066102](https://doi.org/10.1103/PhysRevE.71.066102).
- [37] A. Engel and R. Nolte, “Jarzynski equation for a simple quantum system: Comparing two definitions of work,” *Europhysics Letters (EPL)*, vol. 79, no. 1, p. 10 003, Jun. 2007. DOI: [10.1209/0295-5075/79/10003](https://doi.org/10.1209/0295-5075/79/10003).
- [38] G. E. Crooks, “Entropy production fluctuation theorem and the nonequilibrium work relation for free energy differences,” *Physical Review E*, vol. 60, no. 3, pp. 2721–2726, Sep. 1999. DOI: [10.1103/physreve.60.2721](https://doi.org/10.1103/physreve.60.2721).
- [39] C. Jarzynski, “Nonequilibrium equality for free energy differences,” *Phys. Rev. Lett.*, vol. 78, pp. 2690–2693, 14 Apr. 1997. DOI: [10.1103/PhysRevLett.78.2690](https://doi.org/10.1103/PhysRevLett.78.2690).
- [40] H. Tasaki, *Jarzynski relations for quantum systems and some applications*, 2000. DOI: [10.48550/ARXIV.COND-MAT/0009244](https://doi.org/10.48550/ARXIV.COND-MAT/0009244).

- [41] A. E. Allahverdyan, “Nonequilibrium quantum fluctuations of work,” *Physical Review E*, vol. 90, no. 3, Sep. 2014. DOI: [10.1103/physreve.90.032137](https://doi.org/10.1103/physreve.90.032137).
- [42] M. Lostaglio, “Quantum fluctuation theorems, contextuality, and work quasiprobabilities,” *Physical Review Letters*, vol. 120, no. 4, Jan. 2018. DOI: [10.1103/physrevlett.120.040602](https://doi.org/10.1103/physrevlett.120.040602).
- [43] A. Darwiche, *Modeling and Reasoning with Bayesian Networks*. Cambridge University Press, 2009, ISBN: 9780521884389.
- [44] T. Nielsen and F. JENSEN, *Bayesian Networks and Decision Graphs* (Information Science and Statistics). Springer New York, 2007, ISBN: 9780387682815.
- [45] R. Neapolitan and R. Neapolitan, *Learning Bayesian Networks* (Artificial Intelligence). Pearson Prentice Hall, 2004, ISBN: 9780130125347.
- [46] R. Neapolitan, *Probabilistic Reasoning in Expert Systems: Theory and Algorithms*. CreateSpace Independent Publishing Platform, 2012, ISBN: 9781477452547.
- [47] J. Pearl, “Bayesian networks: A model of self-activated memory for evidential reasoning,” in *Proceedings of the 7th conference of the Cognitive Science Society, University of California, Irvine, CA, USA*, 1985, pp. 15–17.
- [48] K. Micadei, G. T. Landi, and E. Lutz, “Quantum fluctuation theorems beyond two-point measurements,” *Physical Review Letters*, vol. 124, no. 9, Mar. 2020. DOI: [10.1103/physrevlett.124.090602](https://doi.org/10.1103/physrevlett.124.090602).
- [49] K. Micadei, G. T. Landi, and E. Lutz, *Extracting bayesian networks from multiple copies of a quantum system*, 2021. arXiv: [2103.14570](https://arxiv.org/abs/2103.14570) [quant-ph].
- [50] M. H. Partovi, “Entanglement versus stosszahlansatz: Disappearance of the thermodynamic arrow in a high-correlation environment,” *Physical review. E, Statistical, nonlinear, and soft matter physics*, vol. 77, p. 021110, Mar. 2008. DOI: [10.1103/PhysRevE.77.021110](https://doi.org/10.1103/PhysRevE.77.021110).
- [51] S. Jevtic, D. Jennings, and T. Rudolph, “Maximally and minimally correlated states attainable within a closed evolving system,” *Physical Review Letters*, vol. 108, no. 11, Mar. 2012. DOI: [10.1103/physrevlett.108.110403](https://doi.org/10.1103/physrevlett.108.110403).
- [52] D. Jennings and T. Rudolph, “Entanglement and the thermodynamic arrow of time,” *Physical Review E*, vol. 81, no. 6, Jun. 2010. DOI: [10.1103/physreve.81.061130](https://doi.org/10.1103/physreve.81.061130).
- [53] M. N. Bera, A. Riera, M. Lewenstein, and A. Winter, “Generalized laws of thermodynamics in the presence of correlations,” *Nature Communications*, vol. 8, no. 1, Dec. 2017. DOI: [10.1038/s41467-017-02370-x](https://doi.org/10.1038/s41467-017-02370-x).
- [54] K. Micadei *et al.*, “Reversing the direction of heat flow using quantum correlations,” *Nature Communications*, vol. 10, no. 1, Jun. 2019. DOI: [10.1038/s41467-019-10333-7](https://doi.org/10.1038/s41467-019-10333-7).
- [55] M. Scully and M. Zubairy, *Quantum Optics*. Cambridge University Press, 1997, ISBN: 9780521435956.
- [56] R. Loudon, *The Quantum Theory of Light*. OUP Oxford, 2000, ISBN: 9780191589782.

- [57] H. Breuer, P. Breuer, F. Petruccione, and S. Petruccione, *The Theory of Open Quantum Systems*. Oxford University Press, 2002, ISBN: 9780198520634.
- [58] C. Gardiner, P. Zoller, and P. Zoller, *Quantum Noise: A Handbook of Markovian and Non-Markovian Quantum Stochastic Methods with Applications to Quantum Optics* (Springer Series in Synergetics). Springer, 2004, ISBN: 9783540223016.
- [59] D. A. Lidar, *Lecture notes on the theory of open quantum systems*, 2019. DOI: [10.48550/ARXIV.1902.00967](https://doi.org/10.48550/ARXIV.1902.00967).
- [60] T. Tome and M. De Oliveira, *Dinamica Estocastica E Irreversibilidade*. EDUSP, ISBN: 9788531414800.
- [61] S. Salinas, *Introducao a Fisica Estatistica Vol. 09*. EDUSP, 1997, ISBN: 9788531403866.
- [62] K. Huang, *Statistical Mechanics*. Wiley, 1987, ISBN: 9780471815181.
- [63] P. Strasberg, G. Schaller, T. Brandes, and M. Esposito, “Quantum and information thermodynamics: A unifying framework based on repeated interactions,” *Physical Review X*, vol. 7, no. 2, Apr. 2017. DOI: [10.1103/physrevx.7.021003](https://doi.org/10.1103/physrevx.7.021003).
- [64] H. R. Brown and W. Myrvold, *Boltzmann’s h-theorem, its limitations, and the birth of (fully) statistical mechanics*, 2008. DOI: [10.48550/ARXIV.0809.1304](https://doi.org/10.48550/ARXIV.0809.1304).
- [65] C. M. Caves, “Quantum mechanics of measurements distributed in time. a path-integral formulation,” *Phys. Rev. D*, vol. 33, pp. 1643–1665, 6 Mar. 1986. DOI: [10.1103/PhysRevD.33.1643](https://doi.org/10.1103/PhysRevD.33.1643).
- [66] C. M. Caves, “Quantum mechanics of measurements distributed in time. ii. connections among formulations,” *Phys. Rev. D*, vol. 35, pp. 1815–1830, 6 Mar. 1987. DOI: [10.1103/PhysRevD.35.1815](https://doi.org/10.1103/PhysRevD.35.1815).
- [67] C. M. Caves and G. J. Milburn, “Quantum-mechanical model for continuous position measurements,” *Phys. Rev. A*, vol. 36, pp. 5543–5555, 12 Dec. 1987. DOI: [10.1103/PhysRevA.36.5543](https://doi.org/10.1103/PhysRevA.36.5543).
- [68] P. Filipowicz, J. Javanainen, and P. Meystre, “Theory of a microscopic maser,” *Phys. Rev. A*, vol. 34, pp. 3077–3087, 4 Oct. 1986. DOI: [10.1103/PhysRevA.34.3077](https://doi.org/10.1103/PhysRevA.34.3077).
- [69] P. Filipowicz, J. Javanainen, and P. Meystre, “Quantum and semiclassical steady states of a kicked cavity mode,” *J. Opt. Soc. Am. B*, vol. 3, no. 6, pp. 906–910, Jun. 1986. DOI: [10.1364/JOSAB.3.000906](https://doi.org/10.1364/JOSAB.3.000906).
- [70] P. Filipowicz, J. Javanainen, and P. Meystre, “The microscopic maser,” *Optics Communications*, vol. 58, no. 5, pp. 327–330, 1986, ISSN: 0030-4018. DOI: [https://doi.org/10.1016/0030-4018\(86\)90237-3](https://doi.org/10.1016/0030-4018(86)90237-3).
- [71] M. Ziman and V. Bužek, “All (qubit) decoherences: Complete characterization and physical implementation,” *Physical Review A*, vol. 72, no. 2, Aug. 2005. DOI: [10.1103/physreva.72.022110](https://doi.org/10.1103/physreva.72.022110).
- [72] F. Ciccarello and V. Giovannetti, “A quantum non-markovian collision model: Incoherent swap case,” *Physica Scripta*, vol. T153, p. 014010, Mar. 2013, ISSN: 1402-4896. DOI: [10.1088/0031-8949/2013/t153/014010](https://doi.org/10.1088/0031-8949/2013/t153/014010).

- [73] T. Rybár, S. N. Filippov, M. Ziman, and V. Bužek, “Simulation of indivisible qubit channels in collision models,” *Journal of Physics B: Atomic, Molecular and Optical Physics*, vol. 45, no. 15, p. 154 006, Jul. 2012. DOI: [10.1088/0953-4075/45/15/154006](https://doi.org/10.1088/0953-4075/45/15/154006).
- [74] N. K. Bernardes, A. R. R. Carvalho, C. H. Monken, and M. F. Santos, “Environmental correlations and markovian to non-Markovian transitions in collisional models,” *Physical Review A*, vol. 90, no. 3, Sep. 2014, ISSN: 1094-1622. DOI: [10.1103/physreva.90.032111](https://doi.org/10.1103/physreva.90.032111).
- [75] N. K. Bernardes, A. R. R. Carvalho, C. H. Monken, and M. F. Santos, “Coarse graining a non-Markovian collisional model,” *Physical Review A*, vol. 95, no. 3, Mar. 2017, ISSN: 2469-9934. DOI: [10.1103/physreva.95.032117](https://doi.org/10.1103/physreva.95.032117).
- [76] E. Mascarenhas and I. de Vega, “Quantum critical probing and simulation of colored quantum noise,” *Physical Review A*, vol. 96, no. 6, Dec. 2017, ISSN: 2469-9934. DOI: [10.1103/physreva.96.062117](https://doi.org/10.1103/physreva.96.062117).
- [77] Z.-X. Man, Y.-J. Xia, and R. Lo Franco, “Temperature effects on quantum non-markovianity via collision models,” *Physical Review A*, vol. 97, no. 6, Jun. 2018, ISSN: 2469-9934. DOI: [10.1103/physreva.97.062104](https://doi.org/10.1103/physreva.97.062104).
- [78] P. Liuzzo-Scorpo, W. Roga, L. A. M. Souza, N. K. Bernardes, and G. Adesso, “Non-markovianity hierarchy of gaussian processes and quantum amplification,” *Physical Review Letters*, vol. 118, no. 5, Jan. 2017, ISSN: 1079-7114. DOI: [10.1103/physrevlett.118.050401](https://doi.org/10.1103/physrevlett.118.050401).
- [79] F. L. Rodrigues, G. D. Chiara, M. Paternostro, and G. T. Landi, “Thermodynamics of weakly coherent collisional models,” *Physical Review Letters*, vol. 123, no. 14, Oct. 2019. DOI: [10.1103/physrevlett.123.140601](https://doi.org/10.1103/physrevlett.123.140601).
- [80] O. A. D. Molitor and G. T. Landi, “Stroboscopic two-stroke quantum heat engines,” *Physical Review A*, vol. 102, no. 4, Oct. 2020. DOI: [10.1103/physreva.102.042217](https://doi.org/10.1103/physreva.102.042217).
- [81] F. Ciccarello, G. M. Palma, and V. Giovannetti, “Collision-model-based approach to non-markovian quantum dynamics,” *Physical Review A*, vol. 87, no. 4, Apr. 2013, ISSN: 1094-1622. DOI: [10.1103/physreva.87.040103](https://doi.org/10.1103/physreva.87.040103).
- [82] R. McCloskey and M. Paternostro, “Non-markovianity and system-environment correlations in a microscopic collision model,” *Physical Review A*, vol. 89, no. 5, May 2014, ISSN: 1094-1622. DOI: [10.1103/physreva.89.052120](https://doi.org/10.1103/physreva.89.052120).
- [83] B. Çakmak, M. Pezzutto, M. Paternostro, and Ö. E. Müstecaplıoğlu, “Non-markovianity, coherence, and system-environment correlations in a long-range collision model,” *Physical Review A*, vol. 96, no. 2, Aug. 2017, ISSN: 2469-9934. DOI: [10.1103/physreva.96.022109](https://doi.org/10.1103/physreva.96.022109).
- [84] S. Kretschmer, K. Luoma, and W. T. Strunz, “Collision model for non-Markovian quantum dynamics,” *Physical Review A*, vol. 94, no. 1, Jul. 2016, ISSN: 2469-9934. DOI: [10.1103/physreva.94.012106](https://doi.org/10.1103/physreva.94.012106).

- [85] S. Campbell, F. Ciccarello, G. M. Palma, and B. Vacchini, “System-environment correlations and markovian embedding of quantum non-markovian dynamics,” *Physical Review A*, vol. 98, no. 1, Jul. 2018, ISSN: 2469-9934. DOI: [10.1103/physreva.98.012142](https://doi.org/10.1103/physreva.98.012142).
- [86] S. Lorenzo, F. Ciccarello, and G. M. Palma, “Composite quantum collision models,” *Physical Review A*, vol. 96, no. 3, Sep. 2017, ISSN: 2469-9934. DOI: [10.1103/physreva.96.032107](https://doi.org/10.1103/physreva.96.032107).
- [87] J. Jin and C.-s. Yu, “Non-Markovianity in the collision model with environmental block,” *New Journal of Physics*, vol. 20, no. 5, p. 053 026, May 2018, ISSN: 1367-2630. DOI: [10.1088/1367-2630/aac0cb](https://doi.org/10.1088/1367-2630/aac0cb).
- [88] R. R. Camasca and G. T. Landi, “Memory kernel and divisibility of gaussian collisional models,” *Physical Review A*, vol. 103, no. 2, Feb. 2021, ISSN: 2469-9934. DOI: [10.1103/physreva.103.022202](https://doi.org/10.1103/physreva.103.022202).
- [89] J. v. Neumann, “Wahrscheinlichkeitstheoretischer aufbau der quantenmechanik,” *Nachrichten von der Gesellschaft der Wissenschaften zu Göttingen, Mathematisch-Physikalische Klasse*, vol. 1927, pp. 245–272, 1927.
- [90] K. Kraus, “General state changes in quantum theory,” *Annals of Physics*, vol. 64, no. 2, pp. 311–335, 1971, ISSN: 0003-4916. DOI: [https://doi.org/10.1016/0003-4916\(71\)90108-4](https://doi.org/10.1016/0003-4916(71)90108-4).
- [91] G. T. Landi, *Quantum information and quantum noise*.
- [92] I. de Vega and D. Alonso, “Dynamics of non-markovian open quantum systems,” *Rev. Mod. Phys.*, vol. 89, p. 015 001, 1 Jan. 2017. DOI: [10.1103/RevModPhys.89.015001](https://doi.org/10.1103/RevModPhys.89.015001).
- [93] D. Chruscinski, “On time-local generators of quantum evolution,” *Open Systems and Information Dynamics*, vol. 21, no. 01n02, p. 1 440 004, Mar. 2014. DOI: [10.1142/s1230161214400046](https://doi.org/10.1142/s1230161214400046).
- [94] A. Rivas, S. F. Huelga, and M. B. Plenio, “Quantum non-markovianity: Characterization, quantification and detection,” *Reports on Progress in Physics*, vol. 77, no. 9, p. 094 001, Aug. 2014. DOI: [10.1088/0034-4885/77/9/094001](https://doi.org/10.1088/0034-4885/77/9/094001).
- [95] M. Lostaglio, “An introductory review of the resource theory approach to thermodynamics,” *Reports on Progress in Physics*, vol. 82, no. 11, p. 114 001, Oct. 2019. DOI: [10.1088/1361-6633/ab46e5](https://doi.org/10.1088/1361-6633/ab46e5).
- [96] N. E. Comar and G. T. Landi, “Correlations breaking homogenization,” *Physical Review A*, vol. 104, no. 3, Sep. 2021. DOI: [10.1103/physreva.104.032217](https://doi.org/10.1103/physreva.104.032217).
- [97] F. Ciccarello, *Stochastic versus periodic quantum collision models*, 2022. DOI: [10.48550/ARXIV.2208.04353](https://doi.org/10.48550/ARXIV.2208.04353).
- [98] S. Haroche and J. Raimond, *Exploring the Quantum: Atoms, Cavities, and Photons* (Oxford Graduate Texts). OUP Oxford, 2013, ISBN: 9780199680313.
- [99] B.-G. Englert and G. Morigi, “Five lectures on dissipative master equations,” in *Coherent Evolution in Noisy Environments*, Springer Berlin Heidelberg, 2002, pp. 55–106. DOI: [10.1007/3-540-45855-7\\_2](https://doi.org/10.1007/3-540-45855-7_2).



- [100] H.-J. Briegel and B.-G. Englert, “Macroscopic dynamics of a maser with non-poissonian injection statistics,” *Phys. Rev. A*, vol. 52, pp. 2361–2375, 3 Sep. 1995. DOI: [10.1103/PhysRevA.52.2361](https://doi.org/10.1103/PhysRevA.52.2361).
- [101] S. N. Filippov, J. Piilo, S. Maniscalco, and M. Ziman, “Divisibility of quantum dynamical maps and collision models,” *Physical Review A*, vol. 96, no. 3, Sep. 2017. DOI: [10.1103/physreva.96.032111](https://doi.org/10.1103/physreva.96.032111).
- [102] M. Cattaneo, G. D. Chiara, S. Maniscalco, R. Zambrini, and G. L. Giorgi, “Collision models can efficiently simulate any multipartite markovian quantum dynamics,” *Physical Review Letters*, vol. 126, no. 13, Apr. 2021. DOI: [10.1103/physrevlett.126.130403](https://doi.org/10.1103/physrevlett.126.130403).
- [103] D. Cilluffo, A. Carollo, S. Lorenzo, J. A. Gross, G. M. Palma, and F. Ciccarello, “Collisional picture of quantum optics with giant emitters,” *Physical Review Research*, vol. 2, no. 4, Oct. 2020. DOI: [10.1103/physrevresearch.2.043070](https://doi.org/10.1103/physrevresearch.2.043070).
- [104] F. Ciccarello, “Collision models in quantum optics,” *Quantum Measurements and Quantum Metrology*, vol. 4, Dec. 2017. DOI: [10.1515/qmetro-2017-0007](https://doi.org/10.1515/qmetro-2017-0007).
- [105] J. P. Dowling and G. J. Milburn, *Quantum technology: The second quantum revolution*, 2002. DOI: [10.48550/ARXIV.QUANT-PH/0206091](https://doi.org/10.48550/ARXIV.QUANT-PH/0206091).
- [106] W. H. Zurek, “Decoherence, einselection, and the quantum origins of the classical,” *Reviews of Modern Physics*, vol. 75, no. 3, pp. 715–775, May 2003. DOI: [10.1103/revmodphys.75.715](https://doi.org/10.1103/revmodphys.75.715).
- [107] M. Schlosshauer, “Decoherence, the measurement problem, and interpretations of quantum mechanics,” *Reviews of Modern Physics*, vol. 76, no. 4, pp. 1267–1305, Feb. 2005. DOI: [10.1103/revmodphys.76.1267](https://doi.org/10.1103/revmodphys.76.1267).
- [108] E. Jaynes and G. Bretthorst, *Probability Theory: The Logic of Science*. Cambridge University Press, 2006.
- [109] C. E. Shannon, “A mathematical theory of communication,” *The Bell System Technical Journal*, vol. 27, pp. 379–423, 1948.
- [110] K. Modi, A. Brodutch, H. Cable, T. Paterek, and V. Vedral, “The classical-quantum boundary for correlations: Discord and related measures,” *Reviews of Modern Physics*, vol. 84, no. 4, pp. 1655–1707, Nov. 2012. DOI: [10.1103/revmodphys.84.1655](https://doi.org/10.1103/revmodphys.84.1655).
- [111] R. Horodecki, P. Horodecki, M. Horodecki, and K. Horodecki, “Quantum entanglement,” *Reviews of Modern Physics*, vol. 81, no. 2, pp. 865–942, Jun. 2009, ISSN: 1539-0756. DOI: [10.1103/revmodphys.81.865](https://doi.org/10.1103/revmodphys.81.865).
- [112] L. Henderson and V. Vedral, “Classical, quantum and total correlations,” *Journal of Physics A: Mathematical and General*, vol. 34, no. 35, pp. 6899–6905, Aug. 2001. DOI: [10.1088/0305-4470/34/35/315](https://doi.org/10.1088/0305-4470/34/35/315).
- [113] W. Zurek, “Einselection and decoherence from an information theory perspective,” *Annalen der Physik*, vol. 512, no. 11-12, pp. 855–864, Nov. 2000. DOI: [10.1002/andp.200051211-1204](https://doi.org/10.1002/andp.200051211-1204).

- [114] H. Ollivier and W. H. Zurek, “Quantum discord: A measure of the quantumness of correlations,” *Physical Review Letters*, vol. 88, no. 1, Dec. 2001. DOI: [10.1103/physrevlett.88.017901](https://doi.org/10.1103/physrevlett.88.017901).
- [115] K. Micadei *et al.*, “Experimental validation of fully quantum fluctuation theorems using dynamic bayesian networks,” *Physical Review Letters*, vol. 127, no. 18, Oct. 2021. DOI: [10.1103/physrevlett.127.180603](https://doi.org/10.1103/physrevlett.127.180603).
- [116] K. Micadei, G. T. Landi, and E. Lutz, *Extracting bayesian networks from multiple copies of a quantum system*, 2021. DOI: [10.48550/ARXIV.2103.14570](https://doi.org/10.48550/ARXIV.2103.14570).
- [117] P. Kaye, P. Mosca, I. Kaye, R. Laflamme, M. Mosca, and I. Mosca, *An Introduction to Quantum Computing* (An Introduction to Quantum Computing). OUP Oxford, 2007, ISBN: 9780198570004.
- [118] M. Gu, C. Weedbrook, N. C. Menicucci, T. C. Ralph, and P. van Loock, “Quantum computing with continuous-variable clusters,” *Physical Review A*, vol. 79, no. 6, Jun. 2009, ISSN: 1094-1622. DOI: [10.1103/physreva.79.062318](https://doi.org/10.1103/physreva.79.062318).
- [119] A. Altland and B. Simons, *Condensed Matter Field Theory* (Cambridge books online). Cambridge University Press, 2010, ISBN: 9780521769754.
- [120] R. Shankar, *Quantum Field Theory and Condensed Matter: An Introduction* (Cambridge monographs on mathematical physics). Cambridge University Press, 2017, ISBN: 9781108363464.
- [121] P. Meystre and M. Sargent, *Elements of Quantum Optics* (SpringerLink: Springer e-Books). Springer Berlin Heidelberg, 2007, ISBN: 9783540742111.
- [122] D. Walls and G. Milburn, *Quantum Optics*. Springer Berlin Heidelberg, 2010, ISBN: 9783642066764.
- [123] K. E. Cahill and R. J. Glauber, “Density operators and quasiprobability distributions,” *Phys. Rev.*, vol. 177, pp. 1882–1902, 5 Jan. 1969. DOI: [10.1103/PhysRev.177.1882](https://doi.org/10.1103/PhysRev.177.1882).
- [124] K. Ikramov, “On the symplectic eigenvalues of positive definite matrices,” *Moscow University Computational Mathematics and Cybernetics*, vol. 42, pp. 1–4, Jan. 2018. DOI: [10.3103/S0278641918010041](https://doi.org/10.3103/S0278641918010041).
- [125] F. Nicacio, “Williamson theorem in classical, quantum, and statistical physics,” *American Journal of Physics*, vol. 89, no. 12, pp. 1139–1151, Dec. 2021. DOI: [10.1119/10.0005944](https://doi.org/10.1119/10.0005944).
- [126] R. Bhatia and T. Jain, “On symplectic eigenvalues of positive definite matrices,” *Journal of Mathematical Physics*, vol. 56, no. 11, p. 112201, Nov. 2015. DOI: [10.1063/1.4935852](https://doi.org/10.1063/1.4935852).
- [127] V. Arnold, K. Vogtmann, and A. Weinstein, *Mathematical Methods of Classical Mechanics* (Graduate Texts in Mathematics). Springer New York, 2013, ISBN: 9781475716931.
- [128] M. Wilde, *Gaussian quantum information—phys 7895*.

- [129] A. Holevo, “One-mode quantum gaussian channels: Structure and quantum capacity,” *Problems of Information Transmission*, vol. 43, pp. 1–11, Mar. 2007. DOI: [10.1134/S0032946007010012](https://doi.org/10.1134/S0032946007010012).
- [130] G. Adesso, S. Ragy, and A. R. Lee, “Continuous variable quantum information: Gaussian states and beyond,” *Open Systems &amp; mathsemicolon Information Dynamics*, vol. 21, no. 01n02, p. 1440001, Mar. 2014. DOI: [10.1142/s1230161214400010](https://doi.org/10.1142/s1230161214400010).
- [131] S. Pirandola, G. Spedalieri, S. L. Braunstein, N. J. Cerf, and S. Lloyd, “Optimality of gaussian discord,” *Physical Review Letters*, vol. 113, no. 14, Oct. 2014. DOI: [10.1103/physrevlett.113.140405](https://doi.org/10.1103/physrevlett.113.140405).
- [132] A. Mari, V. Giovannetti, and A. S. Holevo, “Quantum state majorization at the output of bosonic gaussian channels,” *Nature Communications*, vol. 5, no. 1, May 2014. DOI: [10.1038/ncomms4826](https://doi.org/10.1038/ncomms4826).
- [133] V. Giovannetti, R. Garcia-Patron, N. J. Cerf, and A. S. Holevo, “Ultimate classical communication rates of quantum optical channels,” *Nature Photonics*, vol. 8, no. 10, pp. 796–800, Sep. 2014. DOI: [10.1038/nphoton.2014.216](https://doi.org/10.1038/nphoton.2014.216).
- [134] G. Pantaleoni, B. Q. Baragiola, and N. C. Menicucci, *Subsystem analysis of continuous-variable resource states*, 2021. arXiv: [2102.10500](https://arxiv.org/abs/2102.10500) [quant-ph].
- [135] M. Hein, J. Eisert, and H. J. Briegel, “Multiparty entanglement in graph states,” *Phys. Rev. A*, vol. 69, p. 062311, 6 Jun. 2004. DOI: [10.1103/PhysRevA.69.062311](https://doi.org/10.1103/PhysRevA.69.062311).
- [136] L. Aolita, A. J. Roncaglia, A. Ferraro, and A. Acín, “Gapped Two-Body hamiltonian for Continuous-Variable quantum computation,” *Physical Review Letters*, vol. 106, no. 9, Feb. 2011, ISSN: 1079-7114. DOI: [10.1103/physrevlett.106.090501](https://doi.org/10.1103/physrevlett.106.090501).
- [137] N. C. Menicucci, S. T. Flammia, and P. van Loock, “Graphical calculus for gaussian pure states,” *Physical Review A*, vol. 83, no. 4, Apr. 2011, ISSN: 1094-1622. DOI: [10.1103/physreva.83.042335](https://doi.org/10.1103/physreva.83.042335).
- [138] O. Pfister, “Continuous-variable quantum computing in the quantum optical frequency comb,” *Journal of Physics B: Atomic, Molecular and Optical Physics*, vol. 53, no. 1, p. 012001, Nov. 2019. DOI: [10.1088/1361-6455/ab526f](https://doi.org/10.1088/1361-6455/ab526f).
- [139] R. M. Gray, *Toeplitz and circulant matrices: A review*.
- [140] P. van Loock, C. Weedbrook, and M. Gu, “Building gaussian cluster states by linear optics,” *Physical Review A*, vol. 76, no. 3, Sep. 2007. DOI: [10.1103/physreva.76.032321](https://doi.org/10.1103/physreva.76.032321).
- [141] S. L. Braunstein, “Squeezing as an irreducible resource,” *Physical Review A*, vol. 71, no. 5, May 2005. DOI: [10.1103/physreva.71.055801](https://doi.org/10.1103/physreva.71.055801).
- [142] N. C. Menicucci, S. T. Flammia, H. Zaidi, and O. Pfister, “Ultracompact generation of continuous-variable cluster states,” *Phys. Rev. A*, vol. 76, p. 010302, 1 Jul. 2007. DOI: [10.1103/PhysRevA.76.010302](https://doi.org/10.1103/PhysRevA.76.010302).

- [143] S. Lloyd, “Use of mutual information to decrease entropy: Implications for the second law of thermodynamics,” *Phys. Rev. A*, vol. 39, pp. 5378–5386, 10 May 1989. DOI: [10.1103/PhysRevA.39.5378](https://doi.org/10.1103/PhysRevA.39.5378).
- [144] L. P. Hughston, R. Jozsa, and W. K. Wootters, “A complete classification of quantum ensembles having a given density matrix,” *Physics Letters A*, vol. 183, no. 1, pp. 14–18, 1993, ISSN: 0375-9601. DOI: [https://doi.org/10.1016/0375-9601\(93\)90880-9](https://doi.org/10.1016/0375-9601(93)90880-9).
- [145] M. Lostaglio, A. Belenchia, A. Levy, S. Hernández-Gómez, N. Fabbri, and S. Gherardini, *Kirkwood-dirac quasiprobability approach to quantum fluctuations: Theoretical and experimental perspectives*, 2022. arXiv: [2206.11783](https://arxiv.org/abs/2206.11783) [quant-ph].
- [146] P. P. Hofer, “Quasi-probability distributions for observables in dynamic systems,” *Quantum*, vol. 1, p. 32, Oct. 2017. DOI: [10.22331/q-2017-10-12-32](https://doi.org/10.22331/q-2017-10-12-32).
- [147] A. J. Daley, “Quantum trajectories and open many-body quantum systems,” *Advances in Physics*, vol. 63, no. 2, pp. 77–149, Mar. 2014. DOI: [10.1080/00018732.2014.933502](https://doi.org/10.1080/00018732.2014.933502).
- [148] D. Girolami, T. Tufarelli, and C. E. Susa, “Quantifying genuine multipartite correlations and their pattern complexity,” *Physical Review Letters*, vol. 119, no. 14, Oct. 2017. DOI: [10.1103/physrevlett.119.140505](https://doi.org/10.1103/physrevlett.119.140505).
- [149] T. Theurer, N. Killoran, D. Egloff, and M. Plenio, “Resource theory of superposition,” *Physical Review Letters*, vol. 119, no. 23, Dec. 2017. DOI: [10.1103/physrevlett.119.230401](https://doi.org/10.1103/physrevlett.119.230401).
- [150] K. A. Kirkpatrick, *The schrodinger-hjw theorem*, 2005. arXiv: [quant-ph/0305068](https://arxiv.org/abs/quant-ph/0305068) [quant-ph].
- [151] A. Levy and M. Lostaglio, “Quasiprobability distribution for heat fluctuations in the quantum regime,” *PRX Quantum*, vol. 1, no. 1, Sep. 2020. DOI: [10.1103/prxquantum.1.010309](https://doi.org/10.1103/prxquantum.1.010309).
- [152] M. Reed, B. Simon, A. P. (Londyn), and A. P. (Londyn)., *I: Functional Analysis* (Methods of Modern Mathematical Physics). Elsevier Science, 1980, ISBN: 9780125850506.